University of Glasgow

University of Strathclyde Glasgow

BioMedEng25

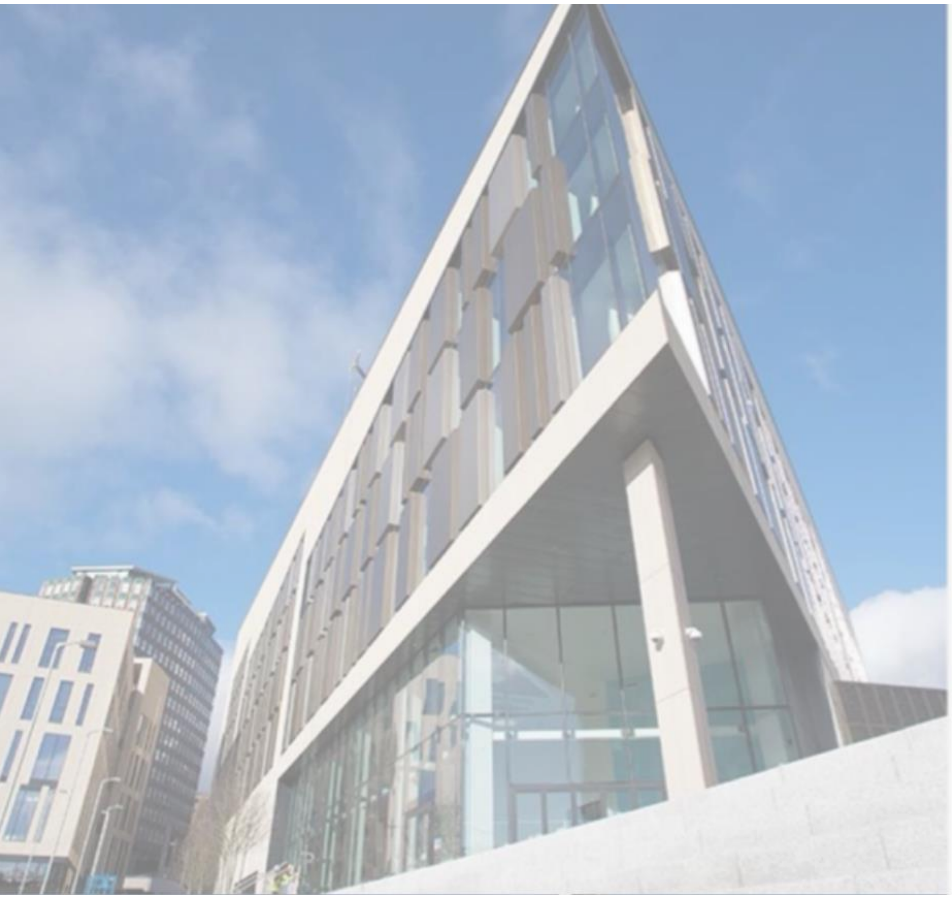

4th & 5th September 2025

biomedeng.org/biomedeng25

Contents

Welcome

On behalf of the local organising committee, the Universities of Strathclyde and Glasgow, and the Trustees and Council members of the Association of Biomedical Engineers, Medical Engineers and Bioengineers, we wish you all a warm welcome to the Technology and Innovation Centre, at the University of Strathclyde, for **BioMedEng25**.

There is an App with all the required information to fully engage with the conference, and you should have an email giving you information on how to access it. If you don't, please come to the reception desk at the conference for us to help you. If you need any other assistance, please look out for our willing band of volunteers who can help you regarding the scientific and social programme.

We have managed to keep the registration costs as low as possible, by the generosity of our sponsors. Please take time out to visit their stalls during the event. Also, ANSYS and Thermofisher are putting on free workshops for conference delegates, so please consider these when you are working out what to attend.

On the Thursday night, starting from 18:30, the conference will be dining and dancing the night away in traditional Scottish style with a Ceilidh (pronounced kay-lee). It will be great to see as many of you there as possible.

Thank you for coming and we hope you enjoy the conference!

Helen Mulvana and Phil Riches
Co-chairs of BioMedEng25

University of Glasgow

University of Strathclyde Glasgow

BioMedEng25

is sponsored by

TERUMO AORTIC

Ansys

MDMC
Medical Device Manufacturing Centre
Scottish Enterprise

ThermoFisher SCIENTIFIC

IET The Institution of Engineering and Technology

Seluna
Advancing Clinical Diagnostics

IPEM
Institute of Physics and Engineering in Medicine

Wonderful Scientific

materialise
innovators you can count on

BioReJen

NETZSCH
Proven Excellence.

DANU

frontiers

Conference Venue

Technology and Innovation Centre (TIC)

99 George St,
Glasgow, G1 1RD

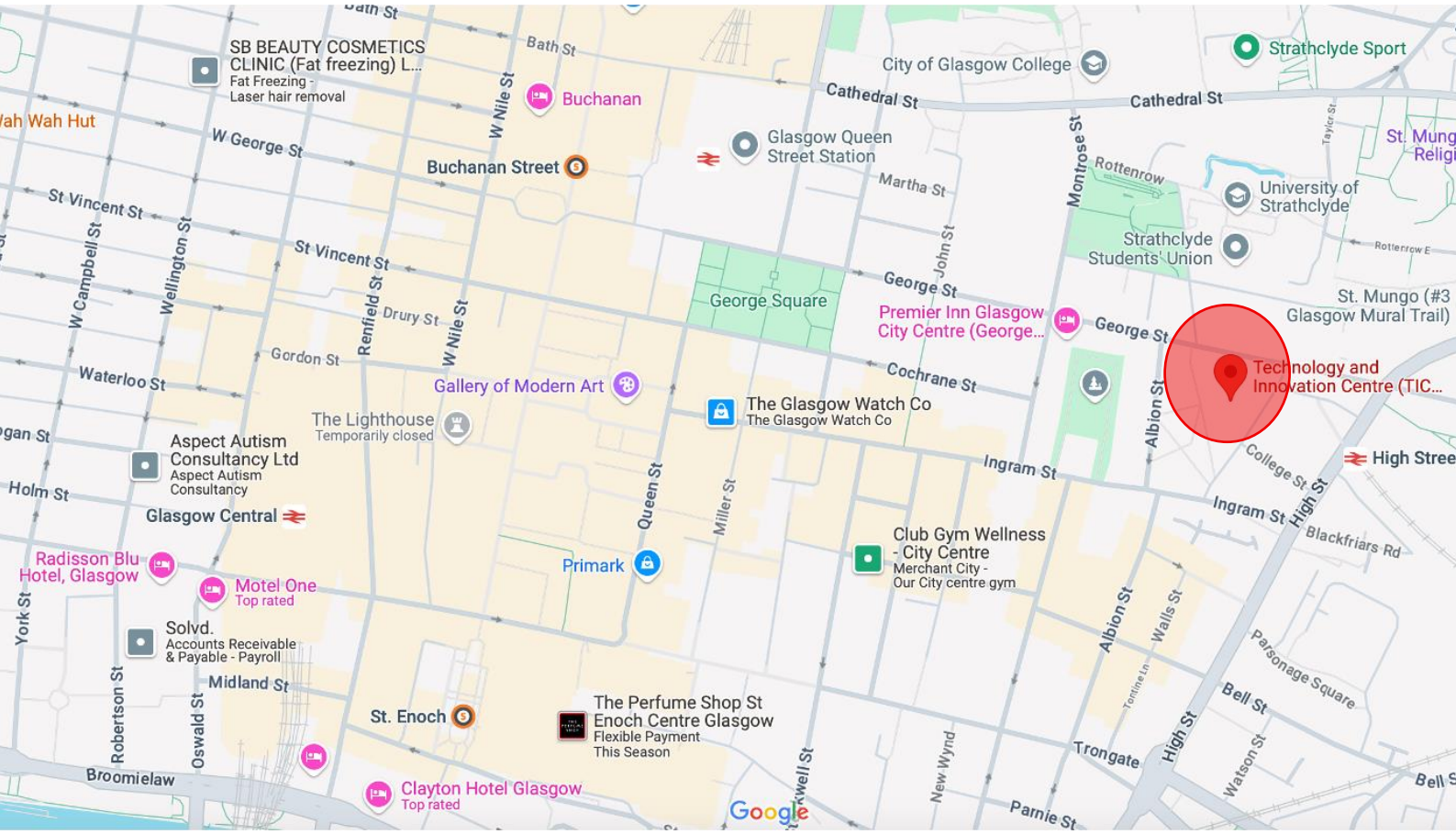

Drinks, Dinner & Ceilidh Venue

Strathclyde Students' Union
51 Richmond Street,
Glasgow, G1 1XU

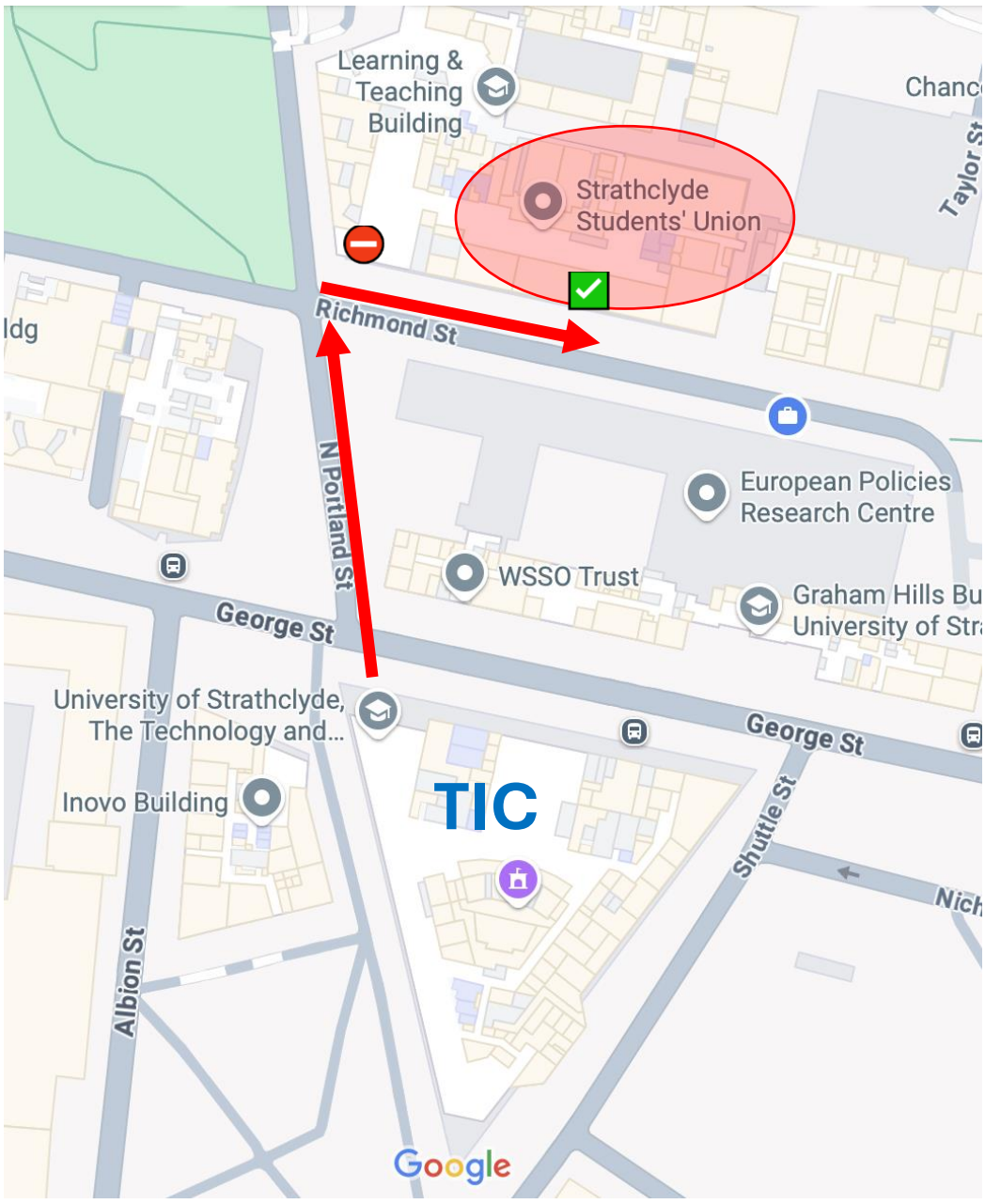

TIC LEVEL 2

Level 1 Auditorium

TIC LEVEL 2

Entrance Exit
Auditorium B/C
Auditorium A
Posters
Lunch + Coffee
Sponsors

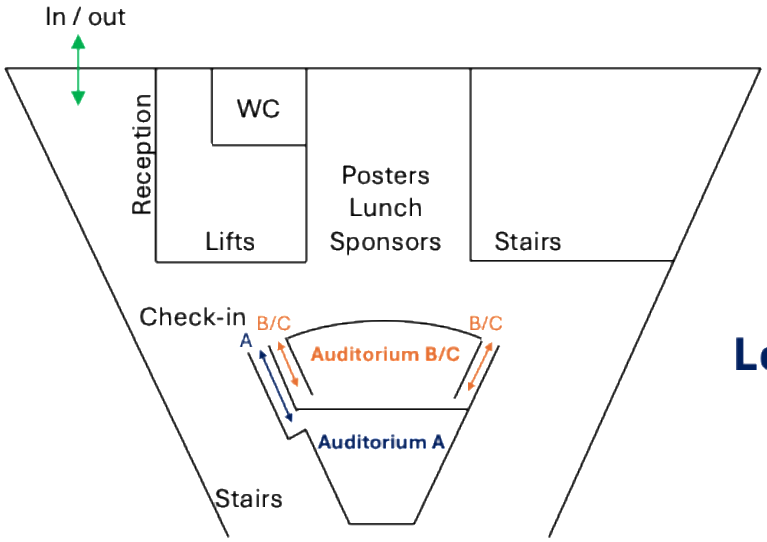

Level 2

TIC LEVEL 3

Auditorium B/C
Room 4/5
Room 6/7
Coffee

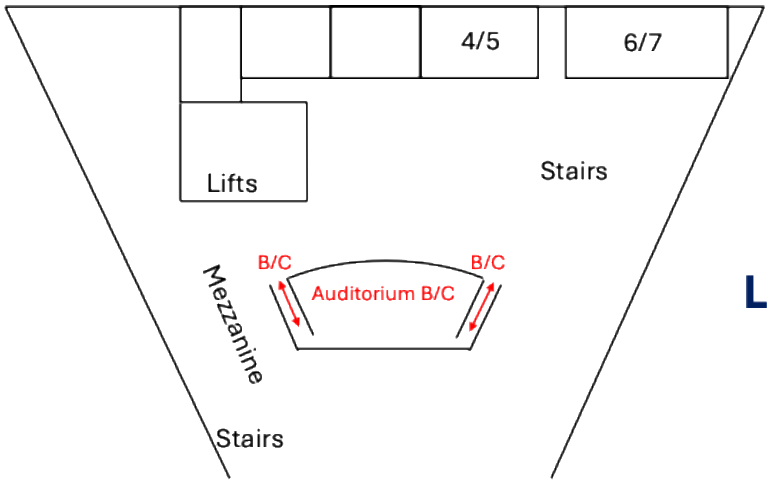

Level 3

BioMedEng25

Programme Outline

Day One

Time	Foyers and Mezzanine Levels 2 & 3	Auditorium A Level 2	Auditorium BC Levels 2 and 3	Auditorium Level 1	Room 4/5 level 3	Room 6/7 level 3
08:00 to 09:00	Registration & Coffee/Tea					
09:00 to 09:40			Welcome Addresses			
09:40 to 10:30			Plenary Prof Keith Mathieson			
10:30 - 11	Tea/Coffee					
11.00 to 12:00		Cardiovascular mechanics 1	Tissue Engineering 1 - Biomaterials	Biomechanics 1 Orthopaedic and Skeletal Biomechanics		Workshop: Digital Health and co-creation
12.00 to 13:00	Lunch + Posters (even posters)					
13:00 to 13:30			Keynote Prof Adriana Tavares			
13.30 to 14:30		Cardiovascular mechanics 2	Tissue Engineering 2 - Vascular and Cardiovascular	Biomechanics 2 Skin & Soft Tissue mechanics	Engineering Innovations in Clinical Diagnostics &	Workshop: Thermofisher (Deep Learning and Image
14:30 to 15:00	Tea/Coffee					
15:00 to 15:30			Keynote Prof Jon Cooper			
15.30 to 16:30		Cardiovascular mechanics 3	Tissue Engineering 3 - MSK and Orth. Tissue	Prosthetics & Orthotics	Women's Health	Workshop: ANSYS
10 mins	Break					
16.40 to 17:40		Cardiovascular mechanics 4	Tissue Engineering 4	Biomechanics 3	AI-Driven Insights in Biomedical Engineering	Workshop: ECR
Close						
18:30 to 19:00	Drinks (Students' Union, 51 Richmond Street)					
19:00 -	Conference Dinner & Ceilidh (Students' Union, 51 Richmond Street)					

Day Two

Time	Foyers and Mezzanine Levels 2 & 3	Auditorium A Level 2	Auditorium BC Levels 2 and 3	Auditorium Level 1	Room 4/5 level 3	Room 6/7 level 3
08:30 to 09:00	Registration & Coffee/Tea					
09:00 to 09:30			Plenary Prof Will Shu			
09.30 to 10:30		Biomedical Imaging 1	Rehabilitation 1	Biosensing 1 - Biomarkers		Clinical and Surgical Engineering
10:30 - 11	Tea/Coffee					
11.00 to 12:00		Biomedical Imaging 2	Rehabilitation 2	Inclusive Design		Emerging Tools, Interfaces, and Systems
12.00 to 13:00	Lunch + Posters (odd posters)					
13:00 to 13:30			Keynote Prof M. Kersaudy-Kerhoas			
13.30 to 14:20		Biomedical Imaging 3	Rehabilitation 3	Biosensing 2 - Devices		Trustees Meeting
14:20 to 15:00	Tea/Coffee					BioMedEng AGM
15:00 to 15:50			Plenary Prof Praminda Caleb Solly			
16:00 to 16:30			Awards, BioMedEng26, Closing			
Close						

BioMedEng25

Plenary & Keynote Speakers

Plenary Speakers

We are pleased to announce the two plenary speakers for BioMedEng25 as being

- Professor Praminda Caleb-Solly, University off Nottingham, and
- Professor Keith Mathieson, University of Strathclyde.

Keynote Speakers

In addition to our Plenary speakers, we have four keynote speakers in the scientific programme. Our keynote speakers are:

- Prof. Jonathan Cooper, University of Glasgow
- Prof Maiwenn Kersaudy-Kerhoas, Heriot-Watt University
- Prof. Will Shu, University of Strathclyde
- Prof. Adriana Tavares, University of Edinburgh

Please see below for biographies of all our invited speakers. The abstracts of their talks are in the detailed programme.

Prof. Praminda Caleb-Solly

Professor Praminda Caleb-Solly specialises in assistive robotics and intelligent sensing. She is currently Professor of Embodied Intelligence at the University of Nottingham, where she leads the Cyber-physical Health and Assistive Robotics Technologies (**CHART**) research group.

She holds a BEng in Electronic Systems Engineering, an MSc in Biomedical Instrumentation Engineering, and a PhD in Interactive Evolutionary Computation. Prior to joining the University of Nottingham in September 2021, Professor Caleb-Solly was a Professor of Assistive Robotics and Intelligent Health Technologies at the Bristol Robotics Laboratory, University of the West of England (UWE), where she led the Robotics Engineering and Computing for Health Research Group and served as Associate Head of Department for Research and Scholarship.

From 2014 to 2018, she was Head of Electronics and Computer Systems at Designability, a not-for-profit organisation specialising in assistive technology design. Her research portfolio includes projects funded by Innovate UK, EPSRC, NIHR, AHRC, and the European Commission, focusing on the design and evaluation of socially and physically assistive robotics, and Internet of Things (IoT) sensor-based intelligent technology. Her work aims to assist people with disabilities and long-term conditions, as well as their caregivers, by supporting activities of daily living.

Professor Caleb-Solly is also the Academic Lead for the University of Nottingham at the National Rehabilitation Centre (**NRC**), contributing her expertise to advance rehabilitation research and innovation. Additionally, she co-founder and director of **Robotics for Good**, a Community Interest Company dedicated to deploying intelligent robotics and smart technology solutions that empower individuals in their daily lives.

Her academic contributions encompass machine learning and human-robot interaction, and she has co-authored the UK-Robotics and Autonomous Systems White Paper on Robotics in Social Care. She has also provided evidence to the UK House of Lords' Science and Technology Committee inquiry into Ageing: Science, Technology, and Healthy Living. Furthermore, Professor Caleb-Solly serves as a member of the British Standards Institute's Technical Committees on Robotics and Ethics for Robots and Autonomous Systems, and co-chairs the IEEE Robotics and Automation Society Technical Committee for Robot Ethics.

Prof. Keith Mathieson

Professor Keith Mathieson is a distinguished physicist specialising in neural interfaces and neurophotonics. Earning his BSc and PhD degrees in Physics from the University of Glasgow in 1997 and 2001, he was elected a Fellow of the Royal Society of Edinburgh in 2024.

He holds a Royal Academy of Engineering Chair in Emerging Technologies at the University of Strathclyde, a prestigious 10-year appointment extending until 2029. His research centres on developing advanced brain-interfacing technologies, working with neuroscientists to further our understanding of neural circuits and their alterations due to neurological disorders. This has led to systems that can help restore function. In particular, he has been working on retinal implant technologies to restore vision to patients with degenerative retinal conditions. His publication record includes pioneering

work on photovoltaic retinal prostheses and optogenetic control using high-density neural probes.

Professor Mathieson recently formed the **Strathclyde Neurotechnology Centre**, a pioneering centre drawing together engineers, physicists, neuroscientists and AI specialists focussed on developing advanced neural interface technology. This has been supported by funding from the Royal Academy of Engineering, the Wolfson Foundation and alumni donors.

Prof. Jonathan Cooper

Professor Jonathan Mark Cooper, FREng, FRSE, holds the Wolfson Chair of Bioengineering at the University of Glasgow and is renowned for his contributions to biomedical diagnostics and microfluidics, with a track record of spin-out and translation into industry including for example Scotetch and Nebuflow Ltd.

One aspect of his current work focusses on aspects of community based diagnostics and digital health using blockchain secure connected mobile phone based platforms with an AI decision support tools to enable healthcare workers and government ministries to monitor the prevalence of infectious disease in remote rural village communities in East Africa. More recently, working with Google, these same systems have been adapted and used in urban settings in Africa, combining meteorological and pollution data, with electronic health records to explore the impact of our changing climate on non-communicable diseases such as asthma, COPD, cardiovascular disease and mental health.

In recognition of his contributions to engineering and science, Professor Cooper was elected a Fellow of the Royal Society of Edinburgh in 2001 and a Fellow of the Royal Academy of Engineering in 2004.

Prof. Maïwenn Kersaudy-Kerhoas

Professor Maïwenn Kersaudy-Kerhoas is a distinguished expert in microfluidic engineering, currently serving as a Full Professor at Heriot-Watt University's Institute of Biological Chemistry, Biophysics and Bioengineering in Edinburgh. She also holds an honorary fellowship in Infection Medicine at the University of Edinburgh.

Her research focuses on developing innovative microfluidic tools for rapid sample preparation, particularly in the extraction of circulating nucleic acids (cfDNA, RNA, miRNA) for applications in non-invasive prenatal testing, cancer diagnostics, and infectious disease detection. She emphasizes sustainable, cost-effective manufacturing processes for polymer-based microfluidic components, aiming to replace petroleum-derived products with renewable alternatives.

In 2013, Professor Kersaudy-Kerhoas was awarded a five-year Royal Academy of Engineering Research Fellowship to advance microfluidic systems for prenatal diagnostics. She later secured a £1.3 million EPSRC Healthcare Technology Challenge Award to develop total pre-analytical systems for cfDNA extraction at the point-of-need. This led to the creation of CNASafe, an automated platform and patented fluidic cartridge for cfDNA extraction, currently under clinical pilot for identifying sepsis-causing pathogens.

Prof. Will Shu

Professor Will Shu is a leading figure in biomedical engineering, currently serving as the Hay Chair in Biomedical Engineering and Director of Research in the Department of Biomedical Engineering at the University of Strathclyde in Glasgow. He earned his PhD in Electrical Engineering and Nanoscience from the University of Cambridge, where he also completed postdoctoral research. Prior to joining Strathclyde, he held academic positions at Heriot-Watt University, advancing from Lecturer to Reader in Biomedical Microengineering between 2007 and 2016.

Professor Shu's research focuses on 3D biofabrication, bioprinting, biosensors, and microsystems, with applications in regenerative medicine. He led pioneering work demonstrating the first bioprinting of human embryonic and induced pluripotent stem cells, contributing to the development of animal-free drug testing and 3D-printed organs.

In 2024, his team introduced the PRINCESS method (PRINting Cell Embedded Sacrificial Strategy), enabling the creation of microvasculature structures as small as 70 micrometres using DNA hydrogel biolubricants. This innovation holds promise for reducing animal testing by providing more accurate human tissue models for drug screening.

Beyond academia, Professor Shu is the founder and director of OrganLike, a company developing 3D-printed human tissue models for surgical training and research. He has held a visiting position at Stanford University and is an emeritus member of the Royal Society of Edinburgh's Young Academy. His professional contributions include serving on the editorial board of the IOP Biofabrication Journal and as a board director of the International Society for Biofabrication.

Prof Adriana Tavares

Professor Adriana Tavares is a leading expert in translational molecular imaging at the University of Edinburgh, where she holds a Personal Chair in the Deanery of Clinical

Sciences. She also serves as the Head of the Preclinical PET Facility within the Centre for Cardiovascular Science and is affiliated with Edinburgh Imaging.

Her research focuses on the development of novel PET radiotracers and advanced image analysis techniques to enhance disease diagnosis, prognosis, and treatment monitoring. Her team is particularly engaged in creating molecular imaging biomarkers and kinetic modeling tools for whole-body PET studies.

At the University of Edinburgh, she established the “PET is Wonderful” initiative, aimed at fostering collaboration and innovation in PET imaging research. She is an active member of the European Society of Molecular Imaging (ESMI) and co-chairs its STANDARD group. Additionally, she contributes to the Scottish Imaging Network: A Platform for Scientific Excellence (SINAPSE) and co-leads the UK PET Network’s preclinical subgroup.

Professor Tavares has secured significant research funding, including a £1.93 million MRC award for developing the TSPO PET radiotracer [18F]LW223, aimed at detecting regional tissue inflammation. Her extensive publication record and leadership in the field underscore her commitment to advancing molecular imaging technologies for improved healthcare outcomes.

BioMedEng25

Workshops

Workshop	**Thursday 5th September, Room 6/7: 11:00 to 12:00**
Digital Health and Co-creation Workshop Lead by Prof. Will Shu University of Strathclyde	Discover how collaboration between patients, clinicians, researchers, and technologists is reshaping the future of healthcare. This workshop explores practical examples for co-creating digital health solutions that are not only innovative but also meaningful, inclusive, and sustainable. Join us to share perspectives, prototype ideas, and reimagine how digital tools can truly help in addressing people's health needs.

Workshop	**Thursday 5th September, Room 6/7: 13:30 to 14:30**
ThermoFisher SCIENTIFIC	To be introduced at the Welcome talk

Workshop	**Thursday 5th September, Room 6/7: 15:30 to 16:30**
Ansys	To be introduced at the Welcome talk

Workshop	**Thursday 5th September, Room 6/7: 16:40 to close**

ECR Workshop
 	
Organised by the BioMedEng ECR working group
	• Alasdair Stewart & Kirsten Watson
	  ○ Faculty Engineering Librarians (Strathclyde Library team)
	• Dr John Armstrong
	  ○ Research Associate (Continuous Manufacturing and Advanced Crystallisation)
	• Janette Hughes
	  ○ Director of Planning & Performance (Digital Health & Care Innovation Centre)

BioMedEng25

Programme Detail

Day One
09:40 to 10:30

Plenary	**Auditorium B/C: 09:40 to 10:30 Session chair: Phil Riches / Helen Mulvana**
Prof. Keith Mathieson: University of Strathclyde An Optoelectronic retinal prosthesis to restore vision to patients with macular degeneration	Degenerative retinal diseases, such as age-related macular degeneration, are amongst the leading causes of untreatable blindness in the world. They cause the loss of the 'image capturing' photoreceptor layer, while neurons in the 'image-processing' inner retinal layers are relatively well preserved. Electronic retinal prostheses seek to restore sight by electrically stimulating the surviving neurons. Here, I will present the results from a collaboration with Stanford University on the development of a photovoltaic subretinal prosthesis. The implant consists of silicon photodiodes in a pixelated format that receive power and data directly through pulsed near-infrared illumination and electrically stimulate neurons. This wireless approach simplifies implantation of the device and increases the achievable resolution. Results from in vitro and in vivo studies, in animal models of retinal degeneration, have shown that retinal stimulation is produced with millisecond pulse durations and threshold peak irradiances of 0.2–5 mW/mm2. Neural responses were elicited with pixel dimensions as small as 20-micron diameter, demonstrating the possibility of a fully integrated photovoltaic retinal prosthesis with high pixel density. Network-mediated retinal stimulation is highly localized, measured through visual acuity experiments in blind rats. Furthermore, the device preserves many features of natural vision, including flicker fusion, adaptation to static images and transient responses to changes in luminance. The system is now licensed to Science Corporation who have just completed a 38-patient clinical trial. Patients with advance AMD were implanted with the device (PRIMA) and reached a restored visual acuity of around 20/460, which approaches the limit of pixel dimensions in the implanted device (100 microns) and can be improved by magnifying the projected infra-red images. This demonstrates a link between device resolution and restored visual acuity in the patient, important for the development of future higher resolution systems.

Day One
11:00 to 12:00

Biomechanics 1 - Orthopaedic and Skeletal Biomechanics	**Level 1 Auditorium: 11:00 to 12:00 Session chair: Dr Phil Riches**
Dr Rosti Readioff	Mechanics of the human knee joint menisci from in vivo dynamic dual-plane fluoroscopy
George Allison	Investigating the effect of marrow properties on bone strength in paediatric femora
Mr Jaasiel Edwards	External Fixator Mechanics - A Quantitative Investigation of the Influences of Pin, Rod and Distance Factors on External Fixator Stiffness.
Dr Aikta Sharma	Female tibial architecture confers resistance to load-induced epiphyseal strain in the STR/Ort model of osteoarthritis

Cardiovascular mechanics 1	**Auditorium A: 11:00 to 12:00 Session chair: Prof Sotiros Korossis**
Mr. Bojin Marinov	Exploring Collagen Degradation and Mechanical Properties in Degenerative Versus Bicuspid Aortic Valve Aneurysmal Tissue
Dr Riaz Akhtar	Micromechanical heterogeneity in abdominal aortic aneurysms is associated with rupture risk
Dr Ankush Aggarwal	Biomechanics of human aorta: spatial and demographical variations
Orla Conlon	Exploring the Influence of Particle Size on Contact Pressure Between Drug-Coated Balloons and Arterial Walls.
Claire Rosnel	Image-Driven Computational Modelling of Aortic Biomechanics in Paediatric Patients with Marfan Syndrome

Tissue Engineering 1 - Biomaterials	**Auditorium B/C: 11:00 to 12:00 Session chair: Dr Vanessa Hearnden**
Dr Carsten Schulte	A Tour de Force through Cellular Nanoscale Mechanobiology in (Patho)Physiology, and how biomedical engineering can pave a way
Miss Zarina Issabekova	Tuneable microgels for guiding cellular response in tissue repair
Mr Pietro Riccio	Fluidgel-Based PEGDA Platforms Functionalised with Wnt3a and Romosozumab for Regenerative Therapeutics: Development and Cytotoxicity Assessment on Human Mesenchymal Stem Cells
Dr Jenny Shepherd	Perivascular biodegradable mesh for the controlled delivery of the corticosteroid dexamethasone for treatment of vein graft diseases
Shweta Thapa	Hybrid Scaffold Fabrication Using 3D Printing and Direct Electrospin Writing for Patient-Specific Bone Implants
Miss Justine Clarke	Engineering the next generation of biologically active vascular grafts

Day One
13:00 to 13:30

Keynote	**Auditorium B/C: 13:00 to 13:30 Session chair: Dr Helen Mulvana**
Prof. Adriana Tavares University of Edinburgh Positron Emission Tomography imaging – kinetic modelling, network analysis and other engineering methods to understand human (patho)physiology.	Non-invasive Positron Emission Tomography (PET) imaging is a powerful technique for in vivo quantification of specific molecular processes. It has served as a valuable biomarker for understanding the development and progression of a variety of diseases, as well as a companion biomarker in drug discovery programmes. Sophisticated methods of analysis of PET datasets are needed to deliver the full potential of this technique and obtain multiple parameters of interest from a given PET image. Kinetic modelling and network analysis are important engineering methods to extract multiple features of interest from human PET datasets. This presentation will provide a brief overview of PET imaging and its applications, as well as described the latest advances in kinetic modelling, network analysis and other relevant methods of analysis of PET data.

Day One
13:30 to 14:30

Biomechanics 2 - Skin & Soft Tissue mechanics	**Level 1 Auditorium: 13:30 to 14:30 Session chair: Dr Ahktar Riaz**
Niloofar Sedighi	Investigating the viability of 3D-printed foaming Thermoplastic Polyurethane (TPU) as an alternative to traditional materials for pressure relief applications
Dr Ciara Durcan	Mechanical and microstructural differences between colorectal cancer and normal colon tissue using a mouse model
Mrs Angie Katherine Molina-Oviedo	Towards constructing a physiologically stratified skin model including a vascularization channel
Mr Venkata Sai Mahesh Peddapeta	Modelling early inflammatory and matrix-degrading dynamics in haemophilic cartilage damage
Miss Sahar Sattar	Assessing facial pressures: novel impact analysis of oronasal continuous positive airway pressure masks

Cardiovascular mechanics 2	**Auditorium A: 13:30 to 14:30 Session chair: Dr Asimina Kazakidi**
Dr Sean McGinty	Drug-coated balloons: computational modelling of deployment,drug delivery and retention
Mr Giorgos Troulliotis	In-Silico Cardiac Model of a Patient Undergoing Transcatheter Mitral Valve Replacement with Tendyne™
Mr Filippos Vlontakis	Patient-specific Modelling of the Left Ventricle – Quantification of Myocardial Fiber Angle Uncertainty in Passive Loading
Mr Shiting Huang	Effect of lung resection surgery on the cardiovascular system: a computational modelling study
Dr Hao Gao	Mathematical modelling of growth and remodelling of the right ventricle caused by valvular regurgitation

Engineering Innovations in Clinical Diagnostics & Therapeutic Devices	**Conference Room 4/5: 13:30 to 14:30 Session chair: Dr Helen Mulvana**
Mr Delu Zheng	Mechanical ventilation phantom for evaluating a sensor-equipped endotracheal tube
Dr Jinghua Tang	A Comprehensive Risk Model for Evaluating Deep Tissue Injury in Diabetic Foot Ulcers
Xindi Huang	Prediction of Epileptic Seizures using GAN-based Approach to EEG Signal Augmentation
Mr Joseph Kinney	Dual-modality optical and ultrasonic imaging using lead-free, transparent, single crystal ultrasonic transducers for inline clinical dermoscopy

Tissue Engineering 2 - Vascular and Cardiovascular Tissue	**Auditorium B/C: 13:30 to 14:30 Session chair: Dr Chris McCormick**
Dr Abiola Basirat Bakare	Physicochemical and mechanical properties of electrospun polycaprolactone composite grafts integrated with silver nanoparticles for vascular applications
Miss Chi Kuan (lydia) Lei	3D Bioprinting Nanofiber-Reinforced Vascular Branches
Ms Nevena Slavova	Tissue Engineered Vascular Grafts
Dr Faraz Fazal	Biofabrication of bi-layered vascular grafts for bypass surgeries.
Mr Dominic Muzikiza	Rotationally Seeded and Bioreactor-Cultured Vascular Grafts Fabricated from UV-Cured Methacrylated PGS HIPEs
Miss Rosanna Hood	Decalcifying and antibacterial bilayer grafts for vascular tissue engineering

Day One
15:00 to 15:30

Keynote	**Auditorium B/C: 15:00 to 15:30 Session chair: Prof. Arjan Buis**
Prof Jonathan Cooper University of Glasgow Digital Integration for Diagnostic Decision Support enabling Connected Digital Health	We describe our work over the last decade with government ministries, charities and NGOs in East Africa, linking new diagnostic systems through mobile communications into regional and national electronic health records. We focus our research in rural, underserved community settings, developing new systems that combine rapid low-cost diagnostic testing with blockchain secured communication, deep-learning and diagnostic decision support to enable secure, privacy-preserved connected and integrated healthcare. We also show how, in future, these same tools may be linked with meteorological information to show how climate change is influencing the range and incidence of both non-communicable and infectious disease.

Day One
15:30 to 16:30

Cardiovascular mechanics 3	**Auditorium A: 15:30 to 16:30 Session chair: Dr Sean McGinty**
Dr Igor Khovanov	Framework for analysing cardio-respiratory synchronisation
Mr Joshua Preston	Determining aortic wall nanomechanical properties in neonatal patients with coarctation of the aorta
Miss Juliane Loges	Designing functionalised human arterial in vitro models
Mr Kenneth Macleod	Development of a novel wire-form magnesium based bioabsorbable vascular scaffold for the treatment of peripheral artery disease
Laure Vidal-Roussel	Biology and Biomechanics for angiogenesis: hand in hand to unveil the possibilities of tissue engineering
Mrs. Ratna Lestari Budiani	Evaluating Respiratory Sinus Arrhythmia and Mutual Correlation Coefficient Metrics for Cardiorespiratory Coupling across Breathing Patterns

Prosthetics & Orthotics	**Level 1 Auditorium: 15:30 to 16:30 Session chair: Prof Arjan Buis**
Mr Mark Wolstenholme	Look where you walk – can predictive controllers offer improvements for lower limb prosthetics?
Ms Renad Albasri	Evidence Limitations on the Use of AFOs Following Stroke: A Systematic Review
Miss Laura Antezana Merida	Post-mortem tissue viability in a perfused rat model: a feasibility study
Isna Riski Safira	Stress shielding in end-bearing socket prosthetic in comparison to osseointegration prosthetic
Miss Lois Galletly	Design requirements for above-knee adjustable socket design, considering male and female users' needs

Tissue Engineering 3 - Musculoskeletal and Orthopaedic Tissue	**Auditorium B/C: 15:30 to 16:30 Session chair: Dr Nicola Green**
Dr Jennifer Paxton	Anatomically guided manufacture of multicomponent scaffolds for calcaneofibular ligament replacement
Miss Emily Dewhurst	Incorporating a synthetic mucus hydrogel within a colonic in vitro model
Miss Ilona Bognar	3D Tissue Engineered Models of Osteogenesis Imperfecta
Dr Rosalia Cuahtecontzi Delint	Nanovibration driven chondrogenesis
Mr Jianping Zhang	Deer Antler - Derived Scaffold for Repair of Bone Defect

Women's Health	**Conference Room 4/5: 15:30 to 16:30 Session chair: Dr Encarna Micó Amigo**
Dr Vanessa Hearnden	Integrating Women's Health into Biomedical Engineering Curricula
Mr Muhammad Faizan Basil	An Inclusive Webapp to Enable Preventive Interventions for Girls and Women affected by Female Genital Mutilation and Cutting
Ms Ella Boswell	Point-of-care Cassette for nucleic acid-based HPV diagnosis.
Dr Amisha Desai	Biomechanics of Uterine Scaffolds: Supporting Innovation in Women's Healthcare

Day One
16:40 to 17:40

AI-Driven Insights in Biomedical Engineering	**Conference Room 4/5: 16:40 to 17:30 Session chair: Dr Shufan Yang**
Dr Antonio Fratini	Evaluating nnUNet for Automated Cardiac CT Segmentation in Paediatric Congenital Heart Disease
Mr Ezzaldin Alkooheji	Data-Driven Interactive Visualisation Platform for Paediatric Intensive Care Using the PIC Database
Mr. Philip Graemer	Comparative Evaluation of Deep Learning Architectures for Automated Cell Image Classification Toward Industrial Biotech Applications
Miss Narjes Meselmani	Machine Learning Enhanced Impedance Probe For Real-time Monitoring of Perfusion In Free Flaps Post Micro reconstructive Surgeries

Biomechanics 3	**Level 1 Auditorium: 16:40 to 17:30 Session chair: Dr Marlene Mengoni**
Miss Alissa Parmenter	TomoSAXS enables quantification of nano- to whole-joint-scale structure and mechanics in the intervertebral disc
Dr Marta Peña Fernández	Synchrotron x-ray radiation induced damage in bone during in situ μCT experiments
Prof Yuhang Chen	Micromechanics in Human Prostate: A Histology-Based Computational Homogenisation Approach
Dr. Subrata Mondal	Patient-Specific Cervical Spine Finite Element Modeling to Advance the Understanding and Treatment of Degenerative Cervical Myelopathy
Mr Vahid Darvishi	From Ventricular Enlargement to White Matter Injury: A Biomechanical Perspective on Normal Pressure Hydrocephalus

Cardiovascular mechanics 4	**Auditorium A: 16:40 to 17:30 Session chair: Dr Hao Gao**
Dr Sathish Kumar Marimuthu	Finite element modelling and validation of stent-induced growth and remodelling in aneurysmal aortas
Mr Ammar Al-Areqi	Quantifying haemodynamic forces across the cerebral microvasculature using a computational modelling approach
Ms Emer Burke O'Leary	Development of a skeletonization algorithm for segmentation of disconnected and collapsed blood vessel networks
Dr Shufan Yang	Modelling diseased prosthetic valve leaflets for redo-tavi simulations

Tissue Engineering 4	**Auditorium B/C: 16:40 to 17:30 Session chair: Dr Jennifer Paxton**
Dr Tania Mendonca	The Mitotic Chromosome Periphery: A Fluid Coat That Mediates Chromosome Mechanics
Mr Juan Grano De Oro Fernandez	Development of Electroconductive Polymer fibres by Pressurised Gyration for Cardiac Tissue Engineering Applications.
Mrs Noor Jibawi	Biopolymers for Cardiac Patches Application
Dr Rachel Furmidge	Tissue-engineered oral mucosal models and electrical impedance spectroscopy for rapid and early diagnosis of oral cancer

Day Two
09:00 to 09:30

Keynote	**Auditorium B/C: 09:00 to 09:30 Session chair: Phil Riches**
Prof. Will Shu University of Strathclyde From Organ Printing to the Future of Surgery	This talk will give a brief overview of the rapidly developing field of 3D bioprinting and biofabrication, particularly in the applications of fabricating synthetic organs for in vitro models, surgical training and surgical simulation. The future challenges and opportunities in surgery will be discussed.

Day Two
09:30 to 10:30

Biomedical Imaging 1	**Auditorium A: 09:30 to 10:30 Session chair: Dr Jinghua Tang**
Mx Arlo Feechan	An Open-Source Tool for Accurate Determination of Polar Moment of Inertia in Bone from micro-Computed Topography
Mr Rory Bennett	3D Prostate Reconstruction from Surface-Based Ultrasound Scans
Mr Rory Bennett	Real-Time Prostate Detection in Surface-Based Ultrasound Scans
Mr Alan Mollins	Prototype development for hyperspectral imaging of glioblastoma samples using the OpenFlexure 3D-printed microscope
Miss Izabela Nowakowska	Use of Stereo-DIC on Surgical Images to Substitute Palpation in Minimally Invasive Surgery
Prof Peter Lee	Glomeruli to Whole Organ Modelling of Blood Flow in the Human Kidney

Biosensing 1 - Biomarkers	**Level 1 Auditorium: 09:30 to 10:30 Session chair: Dr Parastoo Hashemi**
Assem Aimaganova	Development of a Transparent Patient Severity Score Using Biomarker Profiles and Age with Applications to Limited Datasets
Miss Bowen Wang	Near-infrared fluorescent glutathione capped gold nanoclusters: impact of synthesis conditions and hairpinDNA functionalization
Dr Parastoo Hashemi	Fast Scan Cyclic Voltammetry as a Translational Tool for Neuroscience
Miss Alexandra Dobrea	A novel microfluidic-enabled tool for enhancing the performance of electrochemical biosensors at research level
Amrutha Sankar	Fluorescent gold nanoprobes for biomarker RNA detection

Clinical and Surgical Engineering	Conference Room 6/7: 09:30 to 10:30 Session chair: Dr Ankush Aggarwahl
Dr Neeraj Kavan Chakshu	User Centric Design Study for the Development of Digital Twins for Sepsis Diagnosis and Management
Miss Natalia Poprawa	Evaluating Suture Performance in Abdominal Wall Closure: A Simulation-Based Approach
Mr. Mahesh Kumar Ola	A database to fix the inconsistency in clinically reported human airway dimensions
Dr Lisa Asciak	3D-printed mechanically-realistic synthetic kidney models towards digital twin-assisted surgery.
Mr Zhaoyuan Cui	Effect of Supporting Surface on Chest Compressions During CPR: A Finite Element Study

Rehabilitation 1 - Neuromuscular Control, Movement and Rehabilitation	Auditorium B/C: 09:30 to 10:30 Session chair: Prof. Aleksandra Vuckovic
Miss Claire Docherty	A biomechanical comparison of athlete agility performance under mental and physical fatigue
Mr Omer Kursad Katirci	Walking With a Stimulated Hip: Exploring the Role of Gluteus Medius FES in Gait
Miss Hannah Little	The Assessment of Muscular and Kinematic Asymmetry Following a Transtibial Amputation
Ms Anna Paton	Clinically-relevant lower limb joint angle reconstruction from arbitrary 2D images of gait.
Mr Alistair Cooper	Radar-Based Classification of Knee Osteoarthritis Rehabilitation Exercises Using Deep Learning

Day Two
11:00 to 12:00

Biomedical Imaging 2	Auditorium A: 11:00 to 12:00 Session chair: Dr Giuseppe di Caprio
Dr Theresa Urban	Resolving micron-scale features within a whole head using HiP-CT
Dr. Edoardo Occhipinti	Skeletonization to Assess Cardiac Vasculature Segmentation in Hierarchical Phase-Contrast Tomography
Dr Matthieu Chourrout	Cohort analysis of the high-resolution atlases of whole ex vivo brains with hierarchical phase-contrast tomography (HiP-CT) and NextBrain
Joseph Brunet	Near-cellular to Whole Organ Quantitative Mapping of the Human Heart Using Hierarchical Phase-Contrast Tomography
Mr Eric Wanjau	Towards the use of Hierarchical Phase-Contrast Tomography (HiP-CT) as a ground truth reference for validating Diffusion-weighted Magnetic Resonance Imaging (dMRI).
Mr Sumudith Jayasuriya	Establishing a Contrast-Enhanced Micro-Computed Tomography Protocol for Visualizing Rodent Growth Plates

Emerging Tools, Interfaces, and Systems	**Conference Room 6/7: 11:00 to 12:00 Session chair: Dr Andy Kerr**
Mr Graham Henderson	Evaluating the use of smart glasses as a display screen for environmental control system users
Miss Beatriz Gonzalez Carmona	Enhancing Myoelectric Prosthetic Response Through Sex-Differentiated Forearm EMG Analysis
Mr Alex Domniteanu	Do sound spatialisation engines affect sound localisation abilities in normal-hearing human participants?
Mrs Jules Arya	Measuring effort in listening through tactile response times
Professor Elisa Budyn	Human in vitro systems to study skeletal biology and advance animal-free research.
Dr Lauren Forsyth	Game development of a stability-based leaping activity for rehabilitative use

Inclusive Design	**Level 1 Auditorium: 11:00 to 12:00 Session chair: Dr Viktorija Makarovaite**
Mr Lukasz Regulski	Development of a Dual-Lever Rowing Ergometer and Novel Trunk Stability Metrics for Objective Assessment in SCI Rehabilitation
Ireen James	Re-engineering stump skin to improve load bearing capacity
Dr Scott Black	Validation study of machine-learning algorithms to interpret paediatric sleep studies and diagnose sleep apnoea from retrospective PSG & CRSS data
Dr Nour Ghadban	Comparative Analysis of Handcrafted and Deep Learning Features for Radar-Based ECG Reconstruction: Advancing Inclusive Non-Contact Cardiovascular Monitoring
Dr Rashedul Hoque	Implementation of pressure monitoring and a risk algorithm to evaluate pre- and post- interventions in the community
Mr Emanuele Carriero	Design of A Base-Model Forearm Prosthetic: A Versatile System for Partial and Near-Elbow Amputations

Rehabilitation 2 - Advances in Wearable Sensors	**Auditorium B/C: 11:00 to 12:00 Session chair: Dr David Hamilton**
Mr. Hesam Boroomand	Effect of Shoe-Mounted IMU Sensor Positions on Toe Clearance Estimation
Dr Lauren Forsyth	Assessment of Wearable Technologies for Monitoring TKA Recovery
Abbie Nagle	Gaming rehabilitation for ankle injuries: a feasibility study using the DANU Sports smart sock
Dr Samuel Smith	The validity of IMU-derived kinematics after 7 hours of use for long-term monitoring of military personnel musculoskeletal health.
Pritika Ganguly	Optical Fibre-Based MRI-Compatible Knee Sensor for Osteoarthritis
Muhammad Iqbal Nugraha	Wearable Soft Sensor for Capturing Multiple Degrees of Freedom Movement

Day Two
13:00 to 13:30

Keynote	**Auditorium B/C: 13:00 to 13:30 Session chair: Dr Mairi Sandison**
Prof Maïwenn Kersaudy-Kerhoas Heriot-Watt University Diagnostics for a complex world: Engineering Performance, Sustainability and Equity at the Point of Care	This keynote will explore how microfluidic engineering can bridge critical gaps in healthcare delivery through the case studies of devices for circulating nucleic acid markers isolation with applications from cancer to infectious disease identification and transplant surgery. Drawing from interdisciplinary research and global collaborations, the talk will highlight two blind spots—waste associated to diagnostics and inequities in device deployment — that have complex and multifaceted impact on populations.

Day Two
13:30 to 14:20

Biomedical Imaging 3	**Auditorium A: 13:30 to 14:20 Session chair: Dr Haotian Chen**
Dr Thierry Lefebvre	Enabling Co-localised Multi-scale Analysis of Hierarchical Phase-Contrast Computed Tomography of Intact Human Organs through Image Co-registration
Dr Thierry Lefebvre	Early radiation therapy response assessment using multi-scale photoacoustic imaging
Mr Andrew Keenlyside	Reframing Connectomics as a Problem of Distributed Graph Networks in Synchrotron Imaging of the Human Brain
Miss Dai Chen	Improving blood vessel segmentation via noise reduction using Noise2Inverse: Case study on a HiP-CT Kidney X-ray tomogram
Dr Yang Zhou	Cross-modality Registration of 3D Hierarchical Phase-Contrast Tomography and 2D Histology

Biosensing 2 - Devices, modelling & POC	**Level 1 Auditorium: 13:30 to 14:20 Session chair: Prof Natasha Khovanova**
Dr Bettina Bohl	Engineering human stem cell-derived neuronal networks to study serotonergic neurotransmission
Mrs Magdalena Urban	Development of a modelling environment and its application to blood-brain barrier (BBB) investigation
Professor Natalia Khovanova	Continuous Glucose Monitoring as an Educational Tool for Prediabetes
Claire Gould	A novel blood filtration method for detection of Salmonella enterica serovar Typhi via loop-mediated isothermal amplification in a point-of-care device

Mr Georgios Ziakas	Spatial variation in mechanical stimulation within 2D and 3D organ-on-a-chip models.

Rehabilitation 3 - Neurological Disorders	**Auditorium B/C: 13:30 to 14:20 Session chair: Dr Lisa Alcock**
Miss Claire Wilkinson	Habitual turning behaviour over 7 days in a participant with Parkinson's disease: A case study
Mr Daniel Nicoll	Investigating stride variation in curvilinear walking gait across Parkinson's disease and older adult cohorts in a supervised clinical test
Ms Ekgari Kasawala	Wearable-Based Activity Recognition for Older Adults: Leveraging Comfort and Flexibility in Daily Health Monitoring
Dr Chloe Hinchliffe	Predicting Parkinson's Disease Severity from Gait with Federated Learning: Challenges to Overcome
Mr Mohammadreza Sedghi	Application of wearable devices in rest-activity assessment in neurodegenerative disease

Day Two
15:00 to 15:50

Plenary	**Auditorium B/C: 13:00 to 13:30 Session chair: Dr Andy Kerr**
Prof Praminda Caleb-Solly University of Nottingham Beyond Sensing – Adaptive Embodied AI and Digital Twins for Safe and Personalised Assistive Robotics	Assistive and rehabilitation robots offer the potential to deliver more frequent, flexible, and proactive support, enabling people to better manage their well-being and rehabilitation with greater independence. Their ability to reliably sense and respond to changes in a person's physical, cognitive, and sensory state, and their environment, underpins their ability to function autonomously. In this plenary, Prof Praminda Caleb-Solly will explore how intelligent sensing, embodied AI, and digital twin technologies can be used to create and maintain a dynamic, multi-dimensional personal health profile, enabling personalised, anticipatory support that evolves with the person. However, as autonomy grows, so do the risks. Intelligent behaviour can unintentionally compromise safety, particularly if human limitations such as cognitive overload, reduced situational awareness, or communication challenges are not adequately considered. Drawing on her interdisciplinary research, Prof Caleb-Solly will highlight the importance of integrating human factors into risk assessment and system design. She will discuss methodologies such as Systems Theoretic Process Analysis (STPA), ethical hazard analysis, and inclusive benchmarking as part of a roadmap toward safe, accountable, and user-aware assistive robotics.

BioMedEng25

Oral Presentations

Abstracts

Investigating the effect of marrow properties on bone strength in paediatric femora

Allison G[1,2], Almutairi S[3], Offiah A[2,3], Li X[1,2]
[1]School of Mechanical, Aerospace & Civil Engineering, University of Sheffield, [2]INSIGNEO Institute, University of Sheffield, [3]School of Medicine and Population Health, University of Sheffield

The current computed tomography to strength (CT2S) pipeline represents the whole bone through properties estimated from Hounsfield units. However, this does not accurately capture the material properties of bone marrow. The aim of this study is therefore to: (a) propose a methodology to incorporate marrow and (b) investigate the effect on bone strength prediction. The study utilised scans from 29 post-mortem children (0-3 years) performed at Sheffield Children's Hospital. The methodology followed the CT2S pipeline [1] but used new marrow compartment and elemental boundary constraints. A custom script produced the finite element model input file with heterogeneous materials for bone and a homogeneous core for marrow. The marrow was assumed as linear elastic isotropic, with a modulus of 24.7 kPa and v of 0.49 [2]. Two model types were produced. MOD1 is the standard heterogenous process for CT2S. MOD2 is the new methodology. Four-point-bending simulations were conducted at 36 angles (10^o intervals) in ANSYS. A Wilcoxon test revealed a significant difference between methodologies ($p<0.001$). There was an average difference of 17.90%±0.066, in critical moment between MOD1 and MOD2. Regression results between critical moment and weight generated comparable values with 0.967 and 0.974 for MOD1 and MOD2. In this study, a more accurate representation of marrow produced a non-negligible difference without substantially increasing the simulation time. This shows that marrow is an important inclusion in the established CT2S pipeline, to more accurately predict bone strength.

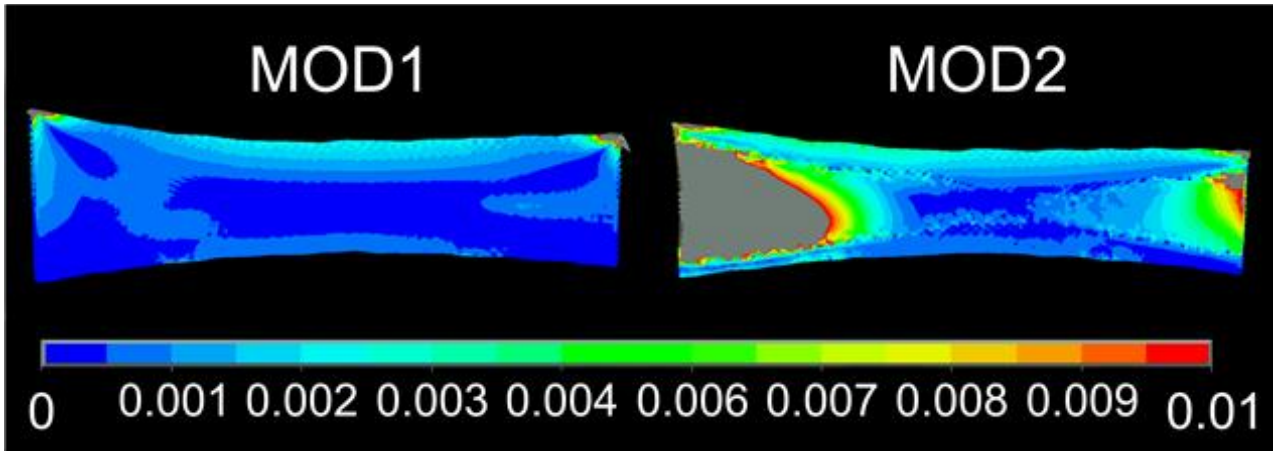

Cross-sectional contour plot of first principal strain distribution for a 2-week-old, showing much higher strains in the marrow in MOD2.

[1] Viceconti et al. Current Osteoporosis Reports, Vol. 16.
[2] Jansen et al. Journal of the Mechanical Behavior of Biomedical Materials, Vol 50.

Biomechanical Comparison of the Annulus Fibrosus Between Rats and Mini Pigs

Chen J[1], Parmenter A[1,2], Sharma A[1], Brunet J[1,3], Zwingenberger S[4], Raina D[5], Bele E[1], Urban T[1,3], Dejea I Velardo H[3], Marussi S[2], Pitsillides A[6], Lee P[1,2]
[1]University College London, [2]Research Complex at Harwell, [3]European Synchrotron Radiation Facility, [4]Technical University Dresden, [5]Lund University, [6]Royal Veterinary College

Lower back pain is a leading cause of disability and socioeconomic burden worldwide, which has prompted widespread use of animal models such as rats and pigs to investigate the underpinning intervertebral disc degeneration [1–3]. The biomechanical comparability between species, and to the human spine, remains unclear. Prior studies identified interspecies differences in annulus fibrosus (AF) architecture [4], but these were constrained by static imaging modalities, usually destructive, and a limited field of view. Building on our previous work in rats using in situ synchrotron X-ray computed tomography (sCT) combined with Digital Volume Correlation (DVC) [5], this study extends the methodology to mini pig lumbar segments. Uniaxial compression was combined with sCT imaging of intact lumbar at the BM18 beamline of the European Synchrotron, followed by fibre orientation analysis and 3D strain mapping. A bottom-up multiscale finite element model, incorporating representative volume elements (RVE), was implemented and validated against DVC-derived strain fields. This revealed that the mini pig AF exhibited regional heterogeneity, with concentrated first and third principal strains in a ‘transitional zone’ associated with abrupt changes in fibre orientation. Compared to rats, mini pigs displayed less curvature, a reversed inner AF orientation, and predominantly tensile strain patterns. Upscaling of RVE-derived material properties to lamellar-level models, with integration into whole-organ simulations, is ongoing. These findings suggest that local orientation discontinuities, rather than absolute fibre angle or lamellar thickness, are critical in shaping AF biomechanics. This work offers a framework for evaluating the translational relevance of animal models in intervertebral disc research.

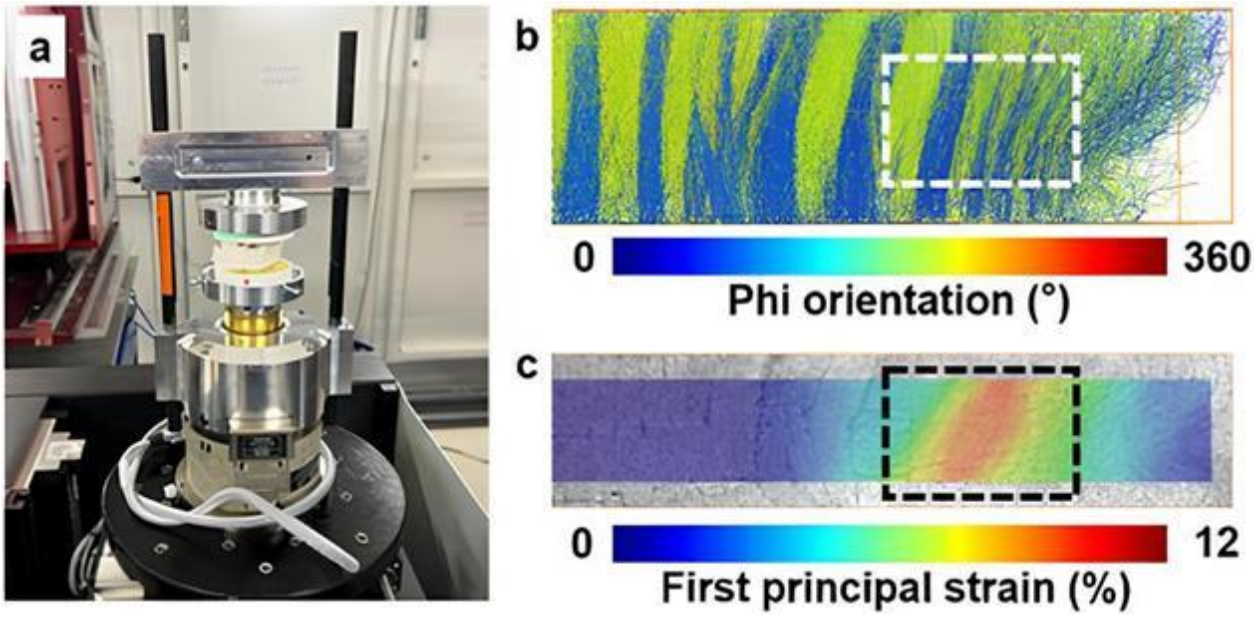

(a) Mini pig lumbar mounted on mechanical tester; (b) Orientation and (c) strain mapping of AF. Dashed lines: ‘transitional zone’.

[1] Hartvigsen et al., 2018, The Lancet, 391(10137):2356-2367. [2] Mogil et al., 2009, Nat Rev Neurosci, 10(4):283-294. [3] Shi et al., 2018, J Orthop Res, 36(5):1305-1312. [4] Raza et al., 2021, Eur Spine J, 30:3450–3456. [5] Disney et al., 2022, Acta Biomater, 138:361-374.

Female tibial architecture confers resistance to load-induced epiphyseal strain in the STR/Ort model of osteoarthritis

Sharma A[1,2], Bourne L[3], Evans L[3,4], Parmenter A[1,2], Brunet J[1], Marussi S[1,2], Madi K[5], Staines K[3], Pitsillides A[4], Lee P[1,2]
[1]University College London, [2]Research Complex at Harwell, [3]University of Brighton, [4]Royal Veterinary College, [5]3Dmagination

Osteoarthritis (OA) is a degenerative joint disease with greater worldwide prevalence and severity in women than men[1,2]. The contributions of local epiphyseal biomechanics in divergent OA phenotypes remain poorly understood. Herein, we employed synchrotron X-ray computed tomography (sCT) and digital volume correlation (DVC) to measure biomechanical strains in whole epiphyses in-situ in the sexually dimorphic STR/Ort model of OA[3] in male and female mice. Intact knee joints from 10-week-old male (N=4, OA-prone) and female (N=3) STR/Ort and healthy parental CBA mice underwent physiological in-situ compression (Deben CT500). sCT images (1.45µm/voxel, BM05-beamline) were acquired at the European Synchrotron following stepwise displacement-controlled loading with strain magnitudes at the tibial epiphysis resolved using DVC[4] (Avizo 3D). Microarchitectural and geometrical analyses of tibiae were performed using microCT (4.98µm/voxel). DVC revealed low load-induced compressive strains across articular and growth plate in CBA epiphyses in both sexes. Conversely, load-induced compressive strain patterns were markedly greater in magnitudes ($P<0.0001$) localised to the lateral epiphysis in males. MicroCT revealed female tibiae possess greater trabecular BV/TV (CBA=$P<0.05$; STR/Ort=$P<0.001$) and mineral density (CBA=$P<0.01$; STR/Ort=$P<0.0001$) than males due to thicker and more connected trabeculae ($P<0.0001$). In contrast, male STR/Ort tibial cortices had greater predicted resistance to torsion and eccentricity than female CBA and STR/Ort mice. Tibial microarchitecture and geometry in female STR/Ort mice prevent detrimental epiphyseal strain accumulation at articular regions to protect against joint failure. In OA-prone males, however, high compressive strains accumulate in articular regions, with reduced distal strain transfer potentially resulting in compensatory pathological changes to tibial structure.

[1] Faber et al., 2024, Front Endocrinol, 2024 Oct 4:15:1445468.
[2] Segal et al., 2024, Osteoarthritis Cartilage, 2024;32(9):1045-53
[3] Javaheri et al., 2018, Osteoarthritis Cartilage, 2018 Jun;26(6):807-817.
[4] Madi et al., 2020, Nat Biomed Eng 2020, Mar;4(3):343-354.

Mechanics of the human knee joint menisci from in vivo dynamic dual-plane fluoroscopy

Readioff R[1], Surbeck R[2], Ortigas-Vásquez A[2,3], Hamed Hosseini Nasab S[2], R. Taylor W[2]
[1]University Of Liverpool, [2]Laboratory for Movement Biomechanics, [3]Research & Development, Aesculap AG

Knee joint menisci are fibrocartilaginous structures between the femoral condyle and tibial plateau, critical for load distribution [1]. Prior research largely focused on in vitro mechanics, limiting understanding of meniscal behaviour in vivo [2]. This study investigates menisci kinematics during the stance phase of gait cycles using experimental, imaging, and computational methods.

Following ethics approval, dynamic dual-plane fluoroscopy and biomechanics data were collected from a healthy participant. A finite element (FE) model of the right knee was developed from photon-counting CT and 7-tesla MRI, with material properties assigned according to previous work [3]. Meniscal roots were modelled as continuum solids sharing the menisci's modulus, and cruciate and collateral ligaments were tied [4]. Experimental gait data defined and validated the model's boundary and loading conditions. A parametric analysis assessed knee kinematic impacts on meniscal mechanics during level walking across eight simulation cases (Figure 1a).

Peak resultant displacement was greater in the medial menisci at a midpoint along the superior edge, with the largest displacement noted at ~10% of the gait cycle in both menisci (Figure 1b&c). However, elsewhere, the lateral meniscus often exhibited greater displacement. In the FE7 case, the lateral meniscus displaced anterolaterally by up to 7.6 mm at ~20% of the gait cycle, while the medial meniscus displaced posterolaterally up to 3.8 mm (Figure 1d&e).

Findings indicate knee kinematics influence meniscal displacement more than axial loads, particularly during abduction/adduction and tibial rotation. Meniscal injury prevention should therefore prioritise knee kinematics over weight-bearing.

Acknowledgements: Project funded by EPSRC (EP/Y002415/1).

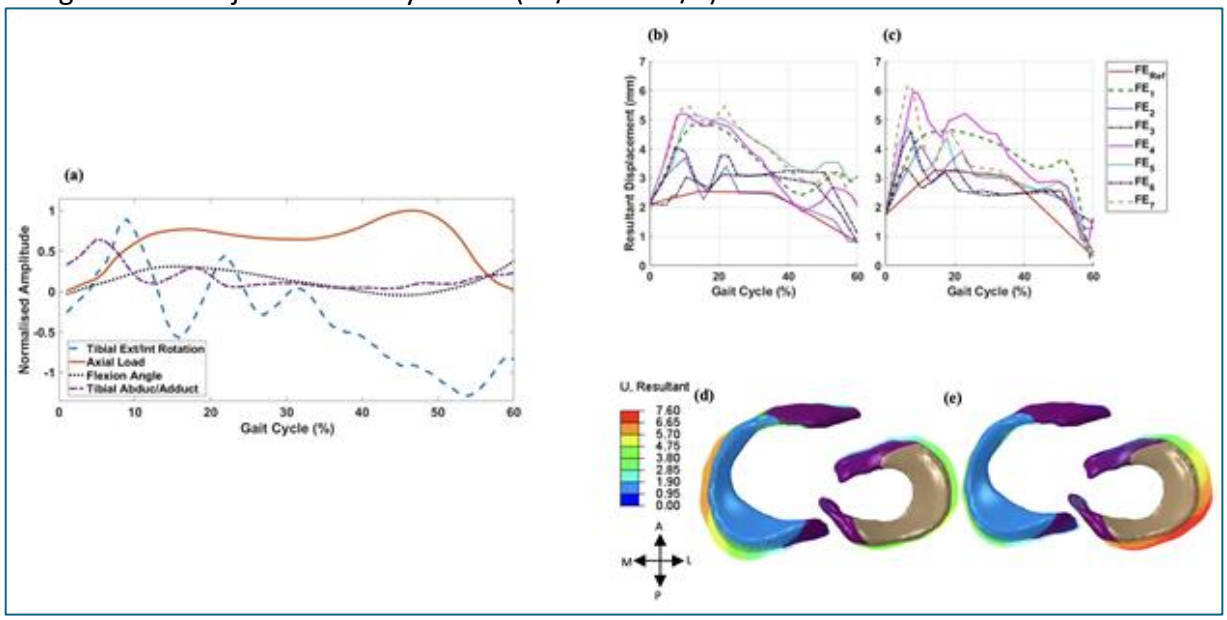

(a) Knee kinematics during stance, menisci displacements ((b) lateral and (c) medial) at (d) 10% and (e) 20% gait cycle.

[1] Fox et al. Sports Health 4, 340–351 (2012).
[2] Liu et al. PLOS ONE 15, e0238785 (2020).
[3] Yao et al. Biomech Model Mechanobiol. 23, (2024).
[4] Peters et al. Front Bioeng Biotechnol. 10:954837 (2022).

External Fixator Mechanics - A Quantitative Investigation of the Influences of Pin, Rod and Distance Factors on External Fixator Stiffness.

Edwards J[1], Chappell M[1], Kumar V[2], Dharmrajan A[3], Upadhyay P[4]
[1]School of Engineering, University Of Warwick, [2]Manchester Royal Infirmary, [3]Queen Elizabeth Grammar School, [4]George Eliot Hospital

External fixators are medical devices used in orthopaedic surgeries to stabilise fractures. Fixators comprise several modular components, including pins and rods. These are combined such that the fixator's overall mechanical properties (e.g. stiffness) are influenced by alterations to the individual components. Since fixators are attached to fractured bones, variations in stiffness caused by changing, for instance, pin position, can modify the stiffness of the entire fixator-bone construct, which plays a crucial role in fracture healing [1]. The ability to modulate mechanical properties by adjusting individual components is exploited during fixator installation to optimise stiffness. However, many quantitative aspects of the relationships between component properties and stiffness are not known precisely. Studies which enhance understanding of these relationships are therefore invaluable to orthopaedic surgeons. This study quantified the impacts of pin-to-pin separation, rod-to-bone separation, the number of connecting rods and pin diameter on fixator stiffness. Mechanical bending and compression tests were performed on fixator constructs with an ElectroForce 3510 rig within the University of Warwick Metrology Laboratory. Constructs incorporated realistic synthetic Sawbones as surrogates for cadaveric bones [2]. Results indicated that pin diameter was the most influential factor in bending, since using 5 mm diameter pins instead of 4 mm pins increased stiffness by 62.1%. In compression, pin separation was the most impactful, with its reduction from 66 mm to 22 mm increasing stiffness by 20.7%. Adding one transverse rod enhanced bending and compressive stiffnesses by 16.4% and 5.0% respectively, whilst incorporating two rods improved them by 15.3% and 15.9% respectively.

[1] P.L.N. Fernando et al., "An engineering review of external fixators", 2021, Med. Eng. Phys., vol. 98, pp. 91–103.
[2] L. Cristofolini et al., "Mechanical validation of whole bone composite femur models", 1996, J. Biomech., vol. 29, no.4, pp. 525-535.

Exploring the Influence of Particle Size on Contact Pressure Between Drug-Coated Balloons and Arterial Walls.

Conlon O[1], McGinty S[1], Aggarwal A[1], Penta R[1]
[1]University Of Glasgow

Drug-coated balloon (DCB) deployment has become a common treatment for obstructive coronary artery disease in recent years. However, there is still a lack of understanding as to how to optimise DCB coating properties to enhance drug delivery. It is now acknowledged that transfer of the DCB coating to the arterial wall is a key mechanism of DCB drug delivery. Recent literature indicates that the microstructure of the DCB coating influences arterial contact pressure and, therefore, coating transfer and retention [1]. However, these works utilised simple contact models, which have limitations.

In this work, we present results comparing contact pressures obtained from different DCB coating particle morphologies, and additionally compare the results of simple contact models, based on Hertz's law [2], with higher fidelity finite element simulations. These simulations investigate the contact pressure for a range of particle geometries and material properties of both the particles and the arterial wall to identify the conditions under which the accuracy of the simple mathematical models begin to deteriorate. The ultimate goal is to find the balance between model complexity and accuracy with a view to optimising DCB design to ensure successful treatment and recovery in patients.

[1] G. H. Chang et al., 2019, Sci. Rep., vol. 9, no. 1, pp. 6839.
[2] J. Escuer et al., 2022, Int. J. Pharm., vol. 620, 121742.

Micromechanical heterogeneity in abdominal aortic aneurysms is associated with rupture risk

Akhtar R[1], Hossack M[1,2], Maerivoet A[1], Bjallmark A[3], Torella F[2], Field M[4], Madine J[1]
[1]University Of Liverpool, [2]Liverpool University Hospitals, [3]Jönköping University, [4]Liverpool Heart and Chest Hospital

Abdominal aortic aneurysms (AAA) are common, especially in men, and associated with a high mortality when ruptured. Clinical guidance for surgical repair is based on the maximum aortic diameter (>5.5 cm in men or 5 cm in women) but this is a poor indicator of clinical risk. Here, we examined micromechanical and biochemical properties of tissue excised from 21 patients undergoing repair for degenerative AAA using nanoindentation and biochemical assays (collagen elastin and glycosaminoglycans (GAGs)). AAA tissue properties were compared with peak wall stress (PWS), peak wall rupture risk (PWRR) localised rupture risk index (RRI) and wall stress (WS) determined from patient-specific finite element (FE) models, and also with abdominal aortic calcification scoring obtained from CT scans. A heteroscedastic relationship was found in all samples; AAA patients with the highest median stiffness exhibited the largest interquartile range (IQR). Correlative analysis showed that the elastic modulus (E) was related to RRI but a complex, interplay of tissue properties contributed to overall PWRR. Abdominal aortic calcification was found to be inversely correlated with PWRR. Random forest modelling demonstrated that RRI is most influenced by E, GAG and collagen. In conclusion, micromechanical properties and calcification may be useful for patient-specific rupture risk prediction.

Biomechanics of human aorta: spatial and demographical variations

Aggarwal A[1,2], Mills M[1,2], Byun J[1,2]
[1]James Watt School of Engineering, University Of Glasgow, [2]Glasgow Computational Engineering Centre, University of Glasgow

Biomechanics of the aorta, our main blood vessel that carries blood from the left ventricle to the entire body, plays a key role in the disease development and long-term outcome post treatment. However, it is currently not fully understood and not taken into account in clinical decision making. One challenge in incorporating biomechanics as a clinical tool is its variation: spatial and across the population. The properties of the aortic root, ascending aorta, and descending aorta are known to be different. Moreover, these properties vary substantially from person to person, even in the healthy state. While utilising patient-specific properties can be desirable for precision-medicine, there are limitations to the information in the in-vivo data, such as MRI or ultrasound.
In this study, we present an analysis based on a large dataset and look at how the demographics correlate with the aortic properties. Specifically, we use deep-learning based automatic segmentation and Gaussian-mixture model fitting to determine the distribution of aortic area, distensibility, and demographical factors -- for both males and females, separately. We find that age is a major determinant in the aortic properties, followed by the blood pressure and body surface area. We also infer the biomechanical properties using Markov Chain Monte Carlo simulation. Lastly, we determine the factors most correlated with an abnormal growth of the aortic diameter -- a common disease called aneurysm. The results highlight the diversity in biomechanics and how taking them into account can improve the diagnosis and treatment of cardiovascular diseases.

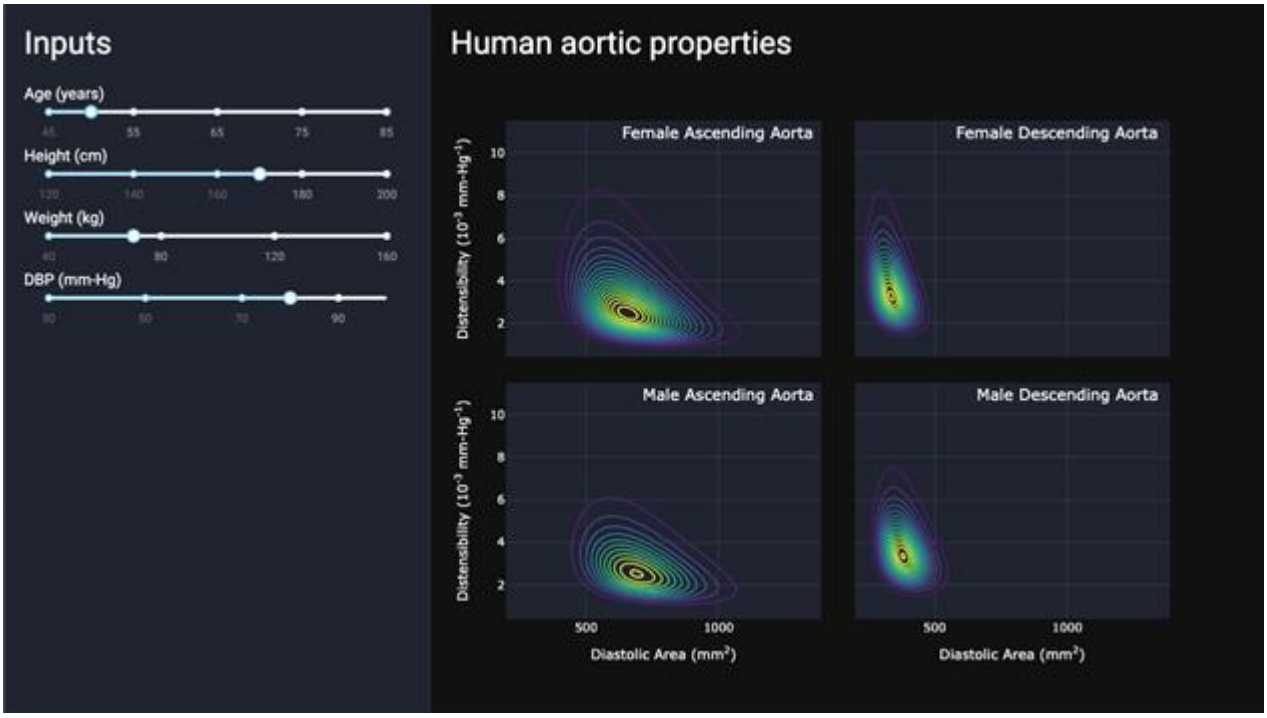

Probability distribution of the human aortic properties (area and distensibility) of males and females show large variations and differences.

Exploring Collagen Degradation and Mechanical Properties in Degenerative Versus Bicuspid Aortic Valve Aneurysmal Tissue

Marinov B[1], Akhtar R[1], Madine J[1], Field M[2]
[1]University Of Liverpool, [2]Liverpool Hearth and Chest hospital
Health and Life Sciences, University of Liverpool, L3 5RB.

Congenital heart conditions such as bicuspid aortic valve (BAV) disease are associated with increased risk of aortic diseases such as thoracic aortic aneurysms (TAA). Previous work has shown that despite the presence of a similar diameter aneurysm to idiopathic degenerative aneurysms (DA), BAV patients appear to have a more structurally intact dilated aorta with stiffer tissue and compact elastin fibres. Here, we sought to determine ultrastructural and nanomechanical changes in the collagen fibrils of TAA tissue from BAV and compare these to DA patients.

Aortic wall tissues were obtained from 10 BAV patients. Additionally, 10 DA samples were collected. The tissues were cryosectioned to 5 µm and imaged with atomic force microscopy (AFM). The morphology of the outer, middle and inner layers of the tissue were examined with a silicon nitride tip with 8 nm radius. Collagen fibril organisation and mechanical properties were determined with the PeakForce QNM modality. Abundant collagen fibrils were identified in both groups. In the BAV group the collagen fibrils seemed unidirectionally oriented and had conserved morphology (G and H). On the contrary, in DA tissue the collagen fibrils were disorganised, and their morphology was disrupted. In addition, the middle layer of DA tissue was observed to have a reduced stiffness compared to BAV tissue with high statistical significance. In addition CHP staining analysis revealed the higher rate of collagen degradation in TAV-DA.

[1] Y. H. Chim et al., J. Thorac. Cardiovasc. Surg., vol. 160, no. 6, pp. e239–e257, 2020.
[2] Bede Pittenger et al, ‘Quantitative mechanical property mapping at the nanoscale with PeakForce QNM’,2010.
[3] G. Goudot et al., Front. Physiol., vol. 10, p. 299, Apr. 2019.

Image-Driven Computational Modelling of Aortic Biomechanics in Paediatric Patients with Marfan Syndrome

Rosnel C[1], Sivera R[2], Schievano S[2], Capelli C[2], Aggarwal A[1]
[1]Glasgow Computational Engineering Centre, University of Glasgow, [2]Institute of Cardiovascular Science, University College London

Marfan Syndrome (MFS) is a connective tissue disorder that weakens the aortic tissue, increasing the risks of aneurysm, dissection and rupture [1]. Although current surgical guidelines rely on aortic root diameter, growing evidence suggests that biomechanical metrics may better predict aneurysmal progression [2,3]. In this longitudinal study, we propose a complete workflow from MRI imaging to a patient-specific finite element analysis, and we investigate the correlation between peak wall stress/strain at baseline with aortic growth at follow-up.

A 3D static MRI scan is used to build the patient-specific geometry, while 2D+t MRI scans provide boundary conditions. Material parameters are estimated via an inverse modelling approach by matching simulated cross-sections to 2D+t MRI contours. A statistical analysis investigates the correlation between mechanical response and aortic growth at follow-up.

Our results reinforce the clinical importance of biomechanics in paediatric MFS, a population often underrepresented in research. Our inverse modelling approach provides a purely image-based material parameter estimation for diseased connective tissue. We observed a significant correlation between peak wall stress/strain and aortic root growth, confirming established clinical knowledge on the root usually being the first site of aneurysm formation in MFS. Additionally, from an image reconstruction perspective, our framework demonstrates how biomechanics can enhance 3D dynamic reconstruction from low-resolution 2D MRI datasets. Together, these findings support more personalised risk assessment and monitoring strategies for Marfan patients.

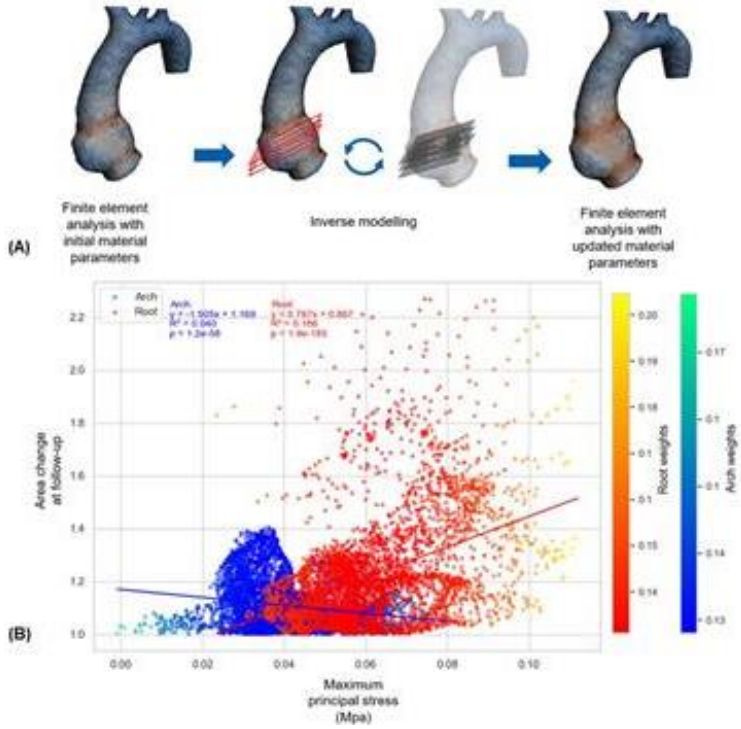

(A) Inverse modelling workflow. (B) Aortic growth vs. principal stress with weighted linear regression using kernel density estimation.

[1] Mockrin, 1996, Molecular Genetics & Gene Therapy of Cardiovascular Diseases, 1st ed. Taylor & Francis
[2] Singh et al., 2021, J Am Heart Assoc, 10:e019772
[3] Rosnel et al., 2024, BMMB, 23(6), 2043-2061

Biventricular Myocardium Passive Property of Repaired Tetralogy of Fallot

Li W[1], Guan D, Gao H
[1]School of Mathematics & Statistics, University Of Glasgow

Tetralogy of Fallot (ToF) is one of right ventricle (RV) related congenital malformations. Pulmonary regurgitation (PR) is the most common residual hemodynamic lesion following repaired TOF. PR promotes RV dilation and dysfunction and ultimately RV failure. In this study, cine cardiac MR images and clinical data of four adult repaired ToF patients taken at the ages of 30 years (±10.3 years) and 32.7 years (±10.0 years) post-repair were processed along with six healthy controls. Patient-specific RV-LV geometries were reconstructed from MR images for both the repaired ToF patients and healthy controls, layered myofibre architecture is implemented using a rule-based method, anisotropic hyperepalstic strain energy function is used to describe the passive properties of myocardium. Material properties of the myocardium for the RV and the LV are inversely determined by matching MRI measured RV and LV cavity volumes and the ejection fraction using a multi-step optimization approach. It is shown that the ejection fractions of ToF patients and healthy are in good agreement with clinical measurements (<2%). The RV of ToF patients have stiffer passive property than healthy subjects which may be due to RV free wall hypertrophy under persistent PR. For a specific subject either healthy or rToF, the right ventricle seems stiffer than the left ventricle, suggesting RV has different mechanical behaviours compared to LV. The significant different passive property in the RV of rTOF could play a vital role in assessment of RV intrinsic pump function, a potential biomarker to determine optimal timing for PVR.

Hybrid Scaffold Fabrication Using 3D Printing and Direct Electrospin Writing for Patient-Specific Bone Implants

Thapa S[1], Twigg P[2]
[1]University Of Bradford, [2]University Of Bradford

This study presents a hybrid scaffold fabrication approach combining 3D printing and Direct Electrospin Writing (DEW) to develop patient-specific bone implants with enhanced mechanical and bioactive properties. Polycaprolactone (PCL), a biodegradable polymer with a slow degradation rate of 2–4 years, was selected to provide structural support during bone regeneration. To overcome its limited osteoconductivity, PCL scaffolds were surface-modified with electrospun hydroxyapatite (HA) and PCL nanofibers to improve cellular adhesion and proliferation.
Patient-specific knee scaffolds were created from MRI scans, converted into 3D models, and analyzed using Finite Element Analysis under physiological loads of 700N and 1500N. Scaffolds with 50% and 100% infill densities were fabricated and compared mechanically to a control scaffold made of titanium alloy Ti-6Al-4V. While the titanium scaffold maintained superior stability, the 100% infill PCL variant demonstrated improved load-bearing capacity over the 50% infill scaffold.
Surface coatings were applied using DEW, and Scanning Electron Microscopy revealed that HA nanofibers, with an average diameter of 0.713 µm, exhibited more uniform distribution than PCL nanofibers. This enhanced the scaffold's biomimetic characteristics. However, challenges such as uneven nanofiber deposition due to voltage instability and complex scaffold geometry were identified, highlighting areas for refinement.
This work underscores the potential of hybrid fabrication techniques to create customized bone implants that meet both mechanical and biological demands. Ongoing efforts are focused on optimizing nanofiber deposition, conducting long-term mechanical evaluations, and validating scaffold performance through in vivo studies for clinical readiness.

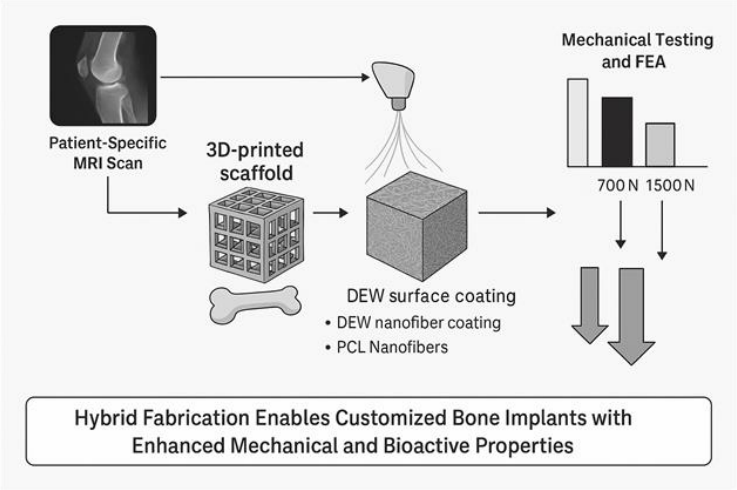

Flowchart illustrating a hybrid fabrication process for customized bone implants using MRI, 3D printing, and DEW nanofiber coating

[1] Kazemi M, Dabiri Y, etc. Recent advances in computational mechanics of the human knee joint. Epub 2013 Feb 19.PMCID: PMC3590578. [2] Venugopal, J., Low, S., Choon, A.T., Kumar, A.B. and Ramakrishna, S. (2008), Electrospun-modified nanofibrous scaffolds for the mineralization of osteoblast cells. J. Biomed. Mater. Res., 85A: 408-417

A Tour de Force through Cellular Nanoscale Mechanobiology in (Patho)Physiology, and how biomedical engineering can pave a way

Schulte C[1,2], Chighizola M[2,3], Fowler D[1], Feenie F[1], Holuigue H[2], Dini T[2,3], D'Urso M[2,4], Marchesi S[3], Marcotti S[5], Borghi F[2], Piazzoni C[2], Kurniawan N[4], Stramer B[5], Scita G[2,3], Jackson M[7], Lenardi C[2], Milani P[2], Diaferia G[6], Ferrai C[8], Podestà A[2]
[1]University Of Strathclyde, [2]Università degli Studi di Milano, [3]The FIRC Institute of Molecular Oncology (IFOM), [4]Eindhoven University of Technology, [5]King's College London, [6]European Institute of Oncology (IEO), [7]University of Glasgow, [8]University of Goettingen

Albeit it is an acknowledged concept nowadays that mechanosensing/transduction strongly affect cellular behaviour in health and disease, there is an urgent need to better understand the intricate underlying force-based cell/microenvironment dialogue down to the nanoscale. Biomedical engineering, and in particular biomaterials fabrication, are essential to get a grasp of mechanotransduction.

By integrating versatile interdisciplinary approaches (such as micro/nanotopgraphical biomaterials, advanced bioimaging, adhesion force spectroscopy, omics, and bioinformatics-driven analysis of genomic patient data), we dissect 1) integrin-mediated and nanotopography-sensitive events at the cell/microenvironment interface, and 2) their effect on cellular responses in various health and disease contexts, such neuronal and murine embryonic stem cell differentiation, as well as brain tumours.

We found, e.g., a strong impact of the nanotopography and the glycocalyx, a pericullar sugar coat attached to lipids and proteins, on force loading-related processes that affect mechanotransduction and cellular responses. The glycocalyx configuration influences the way the cell perceives its nanotopographical cues, which we imagine as a kind of 3D QR code [1, and unpublished]. We furthermore established a proof-of-principle approach that enables the measurement of force loading during cellular interaction with native, complex extracellular matrix at the piconewton range by atomic force microscopy-based force spectroscopy. These measurements showed the dependency of adhesion force dynamics from the compositional and biophysical cues in native ECM [2].
These findings highlight the relevance of nanoscale force-related mechanotransductive processes in pathophysiological situations, and the importance of the ECM nanoarchitecture and glycocalyx therein, which has implications for the understanding of cellular perception of biomedical materials.

[1] Chighizola et al. 2022 Journal of Nanobiotechnology, doi: 10.1186/s12951-022-01585-5
[2] Holuigue et al. 2023 Nanoscale, doi: 10.1039/D3NR01568H

Engineering the next generation of biologically active vascular grafts

Clarke J[1], Boumpouli M[2], Salmeron-Sanchez M[1], Paterson N[2], Berry C[1]
[1]University Of Glasgow, [2]Terumo Aortic

Cardiovascular diseases (CVDs) are the leading cause of death globally.[1] The use of synthetic Polyethylene Terephthalate (PET) vascular grafts has shown great promise in treating CVDs however, they are still at risk of developing acute thrombosis and intimal hyperplasia over time.[2,3] Mesenchymal stromal cell (MSC) derived extracellular vesicles (EVs) will be investigated as a biologically active graft coating to promote endothelialisation and limit blood clot formation. MSCs were primed in normal (21% O2) and hypoxic (1% and 5% O2) culture to generate MSC-EVs with enhanced angiogenic factors.[4] The EVs were characterised by size, concentration and antibodies. Then EV cargo was assessed for potential angiogenic effects using a tube formation assay and cytokine analysis. PET graft samples were prepared with a proprietary coating to facilitate EV binding via integrins.[5] Whole blood interaction was recorded at initial, 30min and 2hr timepoints with agitation, to observe surface activation of the coagulation cascade. Normal and hypoxic MSC-EVs had a similar size and concentration, with 5% hypoxic EVs exhibiting more angiogenic factors. MSC-EVs successfully adhered to the graft material, with its woven topography manipulating EV distribution across the surface. The bioactive coating reduced platelet adhesion in comparison to the uncoated PET graft. Overall, the bioactive coating shows promise to improve graft longevity through the proprietary coatings anti-thrombotic potential alongside the hypoxic EVs promoting endothelialisation, therefore resulting in better graft integration within the injured blood vessel. Future work will involve assessing platelet factor response to determine coating activation under static and flow conditions.

[1] World Health Organization, “Cardiovascular diseases (CVDs).” Accessed: Nov. 28, 2022. https://www.who.int/news-room/fact-sheets/detail/cardiovascular-diseases-(cvds)
[2] T. Pennel and P. Zilla, Tissue-Engineered Vascular Grafts, 3–34, 2020.
[3] K. Yoshizawa et al. J Neurointerventional Surgery, 2022.
[4] C. Almeria et al., Front Bioeng Biotechnol, vol.7, Oct. 2019
[5] M. Cantini et al. Biomaterials, 2020.

Tuneable microgels for guiding cellular response in tissue repair

Issabekova Z[1,2], Oliver-Cervelló L[1,2], Williams J[3], Chen Y[2], Cantini M[1,2], Gonzalez-Garcia C[1,2]
[1]Centre for the Cellular Microenvironment, University Of Glasgow, [2]Biomedical Engineering Division, University of Glasgow, [3]Biomedical Engineering Division, University of Strathclyde

Orthopaedic conditions, including non-union bone and cartilage tissue defects, require innovative, minimally invasive treatments using injectable systems for tissue regeneration. Promising strategies for bone and cartilage repair include the controlled delivery of therapeutic proteins, such as growth factors, and the use of biomimetic scaffolds that recapitulate the properties of the native extracellular matrix (ECM) [1,2]. Injectable microgels with precisely controlled biomechanical properties and protein release profiles can be developed for minimally invasive administration at the defect site. These microgels can be produced by using microfluidics techniques, which allows for high-throughput production of size-controlled and monodisperse microparticles. Natural collagen- (COL) and synthetic poly(ethylene) glycol (PEG)-based scaffolds are promising biomaterial candidates for the bone and cartilage tissue repair [3]. The aim of this project is to develop robust natural and synthetic microgel platforms for the sustained protein delivery at low dosages and modulation of cellular response, achieved by designing COL- and PEG-based microgels, via droplet-based flow-focussing microfluidics, with tuneable mechanical properties and degradation rates. COL and PEG-MAL microgels were successfully synthesised within a microfluidic device, and FITC-BSA was effectively encapsulated in both microgels and bulk hydrogels. Mechanical properties were characterised via rheology and AFM. Protein release was evaluated over 21 days, showing an initial burst followed by a sustained release of the GF. The GF encapsulation within microgels embedded in a bulk hydrogel enhanced sustained release compared to the direct encapsulation in the bulk hydrogel alone. The microgels supported MSCs viability and proliferation and promoted MSCs differentiation in vitro.

(1) Oliveira et al., 2021, Int. J. Mol. Sci., 22(2), 903.
(2) Wang et al., 2024, Materials Today Bio, Vol 24, 100948.
(3) Sarrigiannidis et al., 2021, Materials Today Bio, Vol 10, 100098.

Perivascular biodegradable mesh for the controlled delivery of the corticosteroid dexamethasone for treatment of vein graft diseases

Shepherd J[1], Kasi S[1]
[1]University Of Leicester

The long saphenous vein (LSV) sees common use in coronary artery bypass grafts (CABG). Utilising a thin-walled vein to bypass blood flow within a thick-walled arterial system triggers a cascade of events that contribute to blockage of the vein (1). Zakkar et al observed alleviation of these effects by pre-treating LSV with 10uM of dexamethasone, a corticosteroid for 30 minutes. Hence, we proposed a unidirectional, biocompatible and hemocompatible collagen conduit to deliver dexamethasone over a longer time period in order to promote better success rates in CABG (2).

Collagen slurry of various weight percent was prepared by swelling type 1 insoluble collagen in 0.05M acetic acid before homogenisation. Desired drug concentrations were incorporated into the slurry, it was then degassed and poured into rectangular silicone moulds. Lyophillisation was used to form highly porous collagen sheets which were wrapped and adhered to produce cylindrical conduits. Air-drying of collagen slurry produced non porous collagen films which were adhered to collagen conduits to encourage unidirectional drug release.

Scanning electron microscopy (SEM) images showed good integration between the non-porous collagen film and porous drug loaded collagen sheets as shown in fig. (1). The integration remained the same after 31 days of degradation study. UV spectroscopy of the release medium for drug release study showed prolonged drug release without burst response.

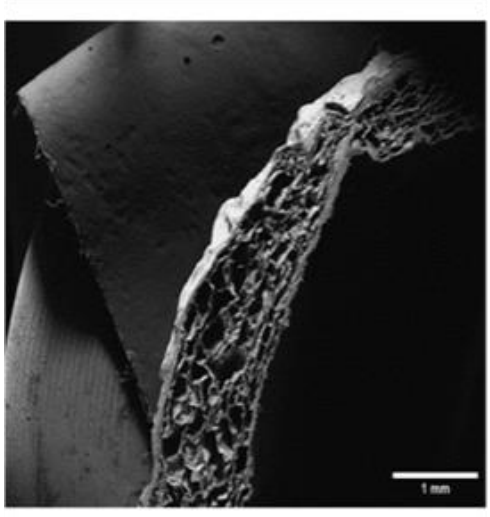

SEM image showing integration between non porous film and porous drug containing sheet

1. Diodato and Chedrawy, 2014, 10.1155/2014/726158.
2. Zakkar et al., 2011,https://doi.org/10.1161/circulationaha.110.979542

Fluidgel-Based PEGDA Platforms Functionalised with Wnt3a and Romosozumab for Regenerative Therapeutics: Development and Cytotoxicity Assessment on Human Mesenchymal Stem Cells

Riccio P[1], Rotherham M[1], Moakes R[1], El Haj A[1]
[1]Healthcare Technology Institute, Institute of Translational Medicine, School of Chemical Engineering, University of Birmingham, Birmingham, UK.

Osteoporosis and osteoarthritis are widespread degenerative diseases characterised by the progressive loss of bone and cartilage integrity, leading to significant morbidity worldwide. The Wnt signalling pathway has emerged as a promising therapeutic target due to its central role in skeletal tissue regeneration.

We previously employed Wnt3a, a glycoprotein of the Wnt family that promotes intracellular polarisation during mitosis and guides asymmetric cell division, to develop biomaterials for bone repair that demonstrated excellent regenerative potential both in vitro and in vivo [1, 2].

In this study, we investigate a synthetic, injectable biomaterial (SyMGel) based on poly(ethylene glycol) diacrylate (PEGDA), fabricated through shear-induced photopolymerisation. This fluid gel forms discrete microparticles that can be post-functionalised via Michael-type addition reactions [3].

SyMGels were functionalised with either Wnt3a or Romosozumab, a clinically approved monoclonal antibody that enhances Wnt signalling by inhibiting sclerostin, though its systemic administration is associated with potential side effects. These functionalised platforms were designed to deliver localised therapeutic stimulation to support osteochondral regeneration.

Human stem cells derived from patients with bone pathologies were used to assess the system's bioactivity. Cytocompatibility was evaluated through viability assays, morphological analysis, alkaline phosphatase activity, and osteogenic gene expression measured by RT-PCR.

Initial findings indicate that PEGDA-based SyMGels support high stem cell viability and exhibit no significant cytotoxicity. Functionalisation with Wnt3a or Romosozumab enhanced cell aggregation and proliferation, producing results comparable to positive controls and superior to unmodified gels, highlighting the therapeutic potential of the platform.

[1] Okuchi, Y., et al., Nature Materials, 2021. 20(1): p. 108-118.
[2] Lowndes, M., et al., Stem Cell Reports, 2016. 7(1): p. 126-37.
[3] Foster, N.C., et al., Advanced Healthcare Materials, 2021. 10(16): p. 2100622.

Mechanical and microstructural differences between colorectal cancer and normal colon tissue using a mouse model

Durcan C[1], Rajasekaran V[2], Miedzybrodzka E[2], Farrington S[2], Reuben R[1], MacPherson B[1], Hand D[1], Chen Y[1]
[1]Heriot-Watt University, [2]University of Edinburgh

Numerous studies have shown that tumours originating from soft tissues are significantly stiffer than the normal tissue surrounding them [1,2]. High grade or stage cancer tissue can be as high as 13-15 times stiffer than the adjacent normal soft tissue [1,2]. Further insight into the origins and mechanisms of this stiffness increase could advance understanding of the mechanical implications of tumour growth, and be used for diagnostic, monitoring or surgical devices [3,4]. Despite colorectal cancer (CRC) being the second deadliest cancer worldwide, there is very little research investigating the macromechanical properties of CRC, particularly regarding its corresponding microstructural origins. Mouse models are commonly used to investigate the mechanisms of cancer and potential pharmacological interventions [5]; however, to the best of the authors' knowledge, no study has been published regarding the macromechanical properties of CRC grown in mice. Here, we use a mouse model (genotypes: WildType and Shroom2Knockout) to perform indentation experiments on mouse CRC and normal colon tissue using the MicroTester LT (CellScale, Ontario, Canada). Microstructural analysis of the mouse tissue was also carried out to explore the origin of the stiffness measurements. Elastic modulus results, according to mouse genotype, can be seen in the Figure for the proximal and distal normal tissue and CRC. These findings are comparable to those of Kawano et al. [2] who performed indentation experiments on human CRC, implying that mouse CRC models can be used to represent human CRC for applications such as the development of mechanical-based diagnostic or surgical medical devices [3,4].

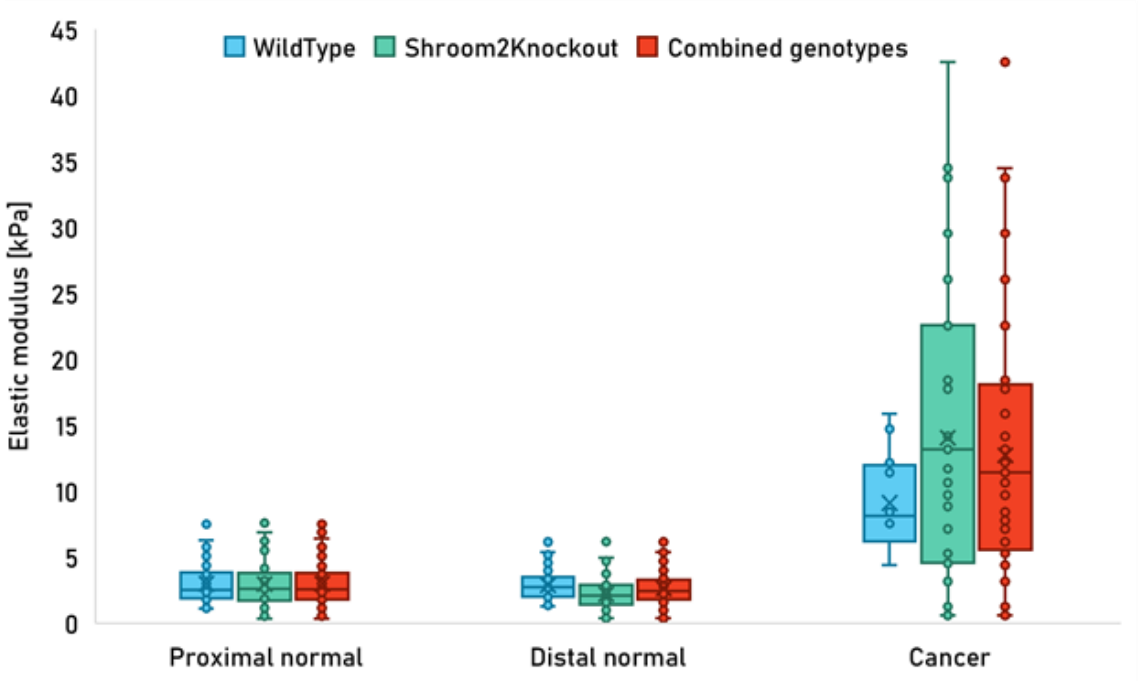

Figure: Elastic moduli of proximal and distal normal colon tissue and CRC retrieved from mice injected with intestinal tumour cells.

[1] Samani et al., 2007. Phys. Med. Biol., 52(6), 1565. [2] Kawano et al., 2015. Cancer Sci., 106(9), 1232-1239. [3] Tian et al., 2024. Eur. J. Mech. A/Solids, 103, 105148. [4] Yan et al., 2021. IEEE Robot. Autom. Lett., 6(2), 1707-1714. [5] Brás et al., 2022. Cancers, 14(8), 1945.

Investigating the viability of 3D-printed foaming Thermoplastic Polyurethane (TPU) as an alternative to traditional materials for pressure relief applications

Sedighi N[1], Pallari J[2], Hendry G[1], Barn R[1]
[1]Department of Podiatry and Radiography, School of Health and Life Sciences, Glasgow Caledonian University, [2]Taika 3D Oy

TPU foams are used across a wide range of applications due to their highly tuneable mechanical properties. When combined with additive manufacturing, foaming TPU allows creation of lightweight, cost-effective products with complex geometries and personalised designs, while reducing material consumption, presenting a promising alternative to conventional foam. This study explores the potential of using 3D-printed TPU parts with an integrated foaming agents as an alternative to conventional cushioning foams, using a novel filament, designed to foam at specific temperatures. The effect of the following printing parameters on foaming behaviour and hardness were evaluated: temperature (210–260°C), speed (10–50 mm/s), flow rate (50–100%), layer height (0.15mm–0.30mm), infill patterns (gyroid, 3D honeycomb, crosshatch), density (10–60%), and orientation (XY vs YX). Uniaxial compression tests assessed compressive performance. Results showed that temperature had the greatest influence on hardness, with maximum foaming at 240°C, resulting in ~30% reduction in hardness. Among infill patterns, crosshatch consistently produced higher hardness values than gyroid or 3D honeycomb at equivalent infill densities. Compression tests showed that 3D honeycomb pattern produced better compressive strength compared to the other patterns, while gyroid and crosshatch performed similarly. Print orientation influenced both compressive strength and hardness, with parts printed on the XY axis showing improved compressive performance and higher hardness values. Results indicate that this approach can produce parts with shore hardness ranging from 22A to 82A, consistent with conventional pressure-relief materials such as wheelchair cushions (40A–50A) [1], insoles (25A–55A) [2], and midsoles (25A–66A) [3], highlighting its potential for a variety of applications.

[1] B. Wieczorek et al., 2024, Materials, 17(3), 641.
[2] H.B. Menz et al., 2021, J Foot Ankle Res 14, 63.
[3] J.M Gerrard et al., 2020, J Foot Ankle Res 13, 35.

Assessing facial pressures: novel impact analysis of oronasal continuous positive airway pressure masks

Sattar S[1], Pritchard T[1], Dorrington P[1], Newton W[1], Thompson J[1]
[1]Swansea University

Obstructive sleep apnea (OSA) is a respiratory condition where individuals experience airway occlusion during sleep [1]. Continuous positive airway pressure (CPAP) therapy is commonly used to alleviate OSA symptoms. However, adherence and tolerance to CPAP therapy remains low despite its high treatment efficacy [1]. This study investigates methods of optimizing CPAP and improving adherence by analyzing the fit of oronasal masks to improve mask comfort.
Influenced by a previous study conducted by Savoldi et al. [2], a novel experimental approach was developed to determine contact pressures produced by an oronasal CPAP mask. A pressure-sensitive, head rig was constructed using FlexiForce pressure sensors embedded within a hyperplastic silicone rubber face phantom, obtained from a 3D scan.
To obtain quantifiable results, a load-controlled experimental method was designed. Orientated in a fixed downward position, half of the head phantom and headgear straps were attached to a mechanical testing system where a controlled tensile load was applied. Surface and embedded pressure sensor readings from eight facial locations were recorded at incrementally controlled loads. The pressure-sensitive human head phantom successfully exhibits improved realism and clear distinction between applied tensile loads, where the load-controlled conditions are reliably reproduced. This novel experimental approach may be followed for the testing of other CPAP masks. Additionally, further development to the head phantom may result in the representation of different population groups according to gender, age and ethnicity. A greater range of facial features prominent within underrepresented groups would produce more inclusive testing conditions for CPAP mask fitness and performance.

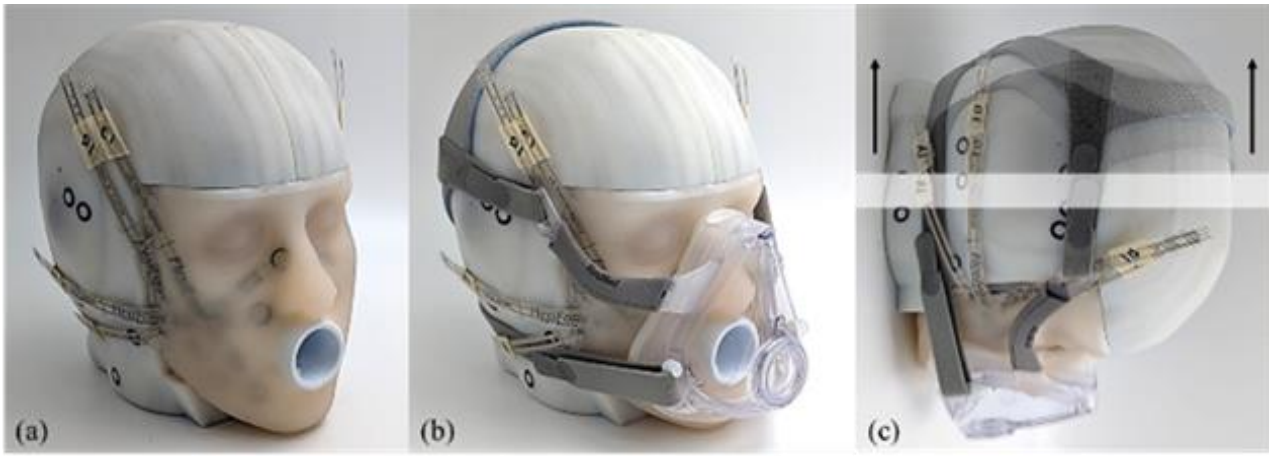

(a) head phantom with embedded pressure sensors visible; (b) phantom with ResMed mask attached; (c) orientation of phantom during experiment.

[1] J. M. Slowik et al., 2025, StatPearls [Internet], StatPearls Publishing, Treasure Island (FL), updated Mar. 4, 2025. Available: https://www.ncbi.nlm.nih.gov/books/NBK459252/
[2] F. Savoldi et al., 2022, J. Mech. Behav. Biomed. Mater., vol. 132, 105272

Modelling early inflammatory and matrix-degrading dynamics in haemophilic cartilage damage

Peddapeta V[1], Fermor H[1], de Boer G[1], Mengoni M[1]
[1]University of Leeds

Haemophilic arthropathy results from recurrent joint bleeds that trigger inflammatory cascades and matrix degradation, leading to progressive cartilage damage. To investigate the early molecular responses following blood exposure, a systems-level ordinary differential equation (ODE)-based network model was developed, containing 32 interacting species, including inflammatory cytokines, matrix degrading enzymes, and key extracellular matrix components. Regulatory and degradative interactions were modelled using mass action kinetics and Hill functions to capture nonlinear feedback and enzyme–substrate dynamics. Model parameters were estimated from literature-reported dissociation constants, half-lives, and enzymatic rates. The model was initialized at physiological steady-state concentrations to represent baseline tissue homeostasis, and a pathological simulation was performed by exposing the system to constant blood components for 4 days, replicating experimental haemarthrosis conditions [1–3]. The simulation predicted marked inflammatory activation: pro-inflammatory cytokines increased by 60–80%, matrix degrading enzymes rose by 100–200%, while anti-inflammatory cytokines levels decreased. By day 4, these resulted in a 21% loss in glycosaminoglycans and a 20% reduction in collagen II content, with elevated cytokine levels corresponding to tissue degradation, consistent with experimental observations [1–3] from blood exposure models of haemarthrosis-induced cartilage damage. The individual impact of each biological species on tissue degradation was analysed to identify key molecular drivers of matrix loss. This mechanistic framework highlights the cumulative inflammatory signalling over the 4-day exposure period, with IL-1β and TNF-α driving upregulation of matrix-degrading enzymes and accelerating matrix loss. By mapping molecular interactions and their temporal dynamics during blood exposure, the model provides insight into critical regulatory nodes.

[1] Swärd, P. et al., 2012, Osteoarthritis and Cartilage, 20, 1302–1308.
[2] Van Meegeren, M. E. R. et al., 2013, Rheumatology, 52, 1563–1571.
[3] Tsuchida, A. I. et al., 2014, Arthritis Res Ther, 16, 441.

Towards constructing a physiologically stratified skin model including a vascularization channel

Alonso-Martinez M[1], Molina-Oviedo A[1], Sorrentino I[1], Arevalo-Nuñez de Arenas E[1], Medraño-Fernandez I[1]
[1]Universidad Carlos III De Madrid

Organotypic skin 3D-cultures using immortalized cells aim to produce standardized models for studying tissue biology or serve as platforms for pharma and drug testing. However, current in vitro systems lack structural complexity and some of the fundamental components of native skin[1]. Specifically, resident immune cells and nurturing internal vessels are absent in the dermis[2], while isogenic cell lines build deficient epidermis formed by few layers of flattened cells. To address this issue, we have developed a protocol based on prior conditioning of cultured immortalized keratinocyte monolayers that favors a progenitor-like phenotype in the founding cells of the construct. Our procedure, consisting of a single bolus pretreatment with 2µg/ml L-ascorbic acid 2-phosphate provided under controlled presence of Ca^{2+} ions, results in a physiologically stratified dermo-epithelial equivalent that adequately disposes relevant markers of native skin across layers and shows the reconstitution of fundamental communication axes needed to accurately complete the re-epithelialization phase. As a preliminary step to introduce the vascular and immune compartments, we have designed a device that creates a microfluidic channel in our improved skin model. By introducing a mold filled with alginate that can be dissolved on-demand inside the culturing transwell, this insert will allow us to perfuse first endothelial cells and then monocytes, ultimately recreating a functional capillary inside the dermis. Thus, we have produced an effective bilayered 3D-skin that can be readily used for many applications while we are paving the way for more advanced studies concerning immune cell recruitment and bioartificial sustaining of the engineered tissue.

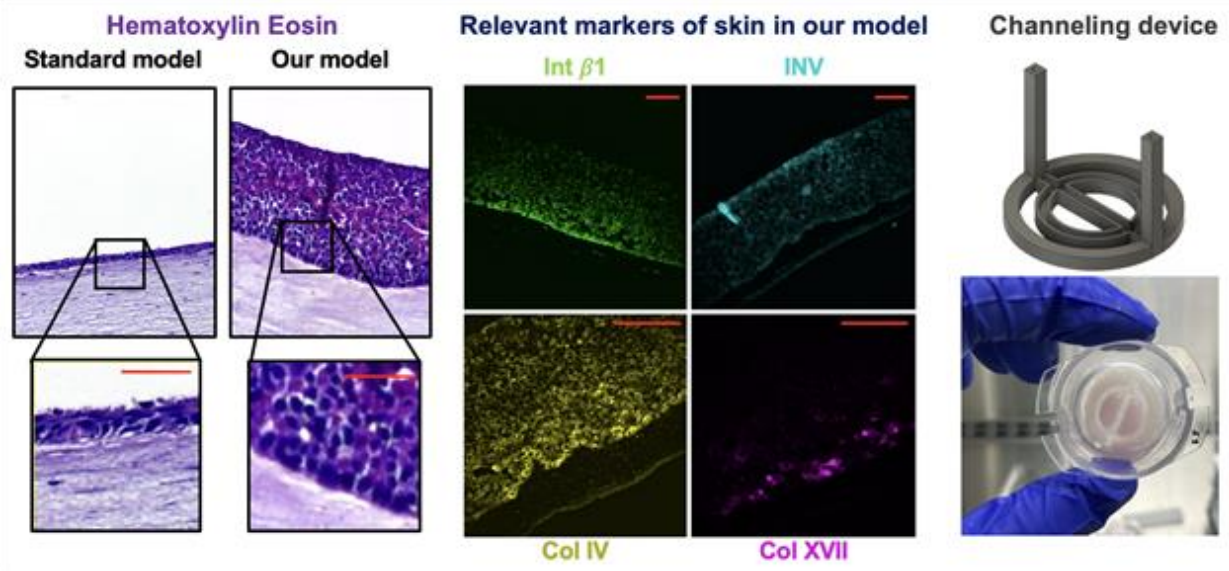

Figure:Standard HaCaT-model vs. our improved skin-model differentiated for at least 3weeks and design of device that creates a microfluidic channel.

[1] W.H. Yap et al., 2021, J. Biosci, vol. 46, no. 86.
[2] H. Shahin et al., 2020, Burns & trauma, vol. 8:tkaa022

In-Silico Cardiac Model of a Patient Undergoing Transcatheter Mitral Valve Replacement with Tendyne™

Troulliotis G[1,3], Mirsadraee S[2,3], Duncan A[2,4], Xu X[3], Gandaglia A[5], Vlontakis F[1], Versteeg H[1], Korossis S[1,6]
[1]Loughborough University, [2]Royal Brompton and Harefield Hospital, [3]Imperial College, [4]King's College, [5]Biocompatibility Innovation SLR, [6]Hannover Medical School

Transcatheter mitral valve replacement (TMVR) has recently emerged as a viable alternative to treat mitral valve regurgitation (MR) [1]. Tendyne™ with its unique tether and apical pad design (Figure 1A) has been shown to eliminate MR and minimize paravalvular leakage [1]. This study developed a virtual TMVR model based on a validated, pre-operative patient-specific cardiac model. The model was used to examine post-operative biomechanics and organ-implant interaction.
Pre-operative computed tomography (CT) and echocardiography data of a patient who underwent TMVR with Tendyne™, were used to construct a cardiac finite element model coupled with cardiovascular circulation. The preoperative model (PO) was parameterized and validated against in-vivo data. TMVR was simulated by eliminating MR and stretching the apical tether through the fixed apical puncture site (Figure 1B) to a peak tension of 15N [1]. Traditional mitral valve replacement (MVR) was simulated by eliminating MR only.
TMVR predicted a larger decrease in end-diastolic (ED) volume compared to MVR (30mL vs. 10mL) and ED average von-Mises stress of 6.06kPa, compared to 9.59kPa and 7.48kPa for the PO and MVR models, respectively (Figure 1C). Preliminary results suggested that the tethered design of Tendyne™, apart from eliminating MR, could support the myocardium reducing stress, potentially leading to favourable remodelling.
An in-silico patient-specific model of Tendyne™ TMVR, was created using preoperative data. The results demonstrated the important future role of biomechanical cardiac models in the design of novel treatments and personalized medicine.

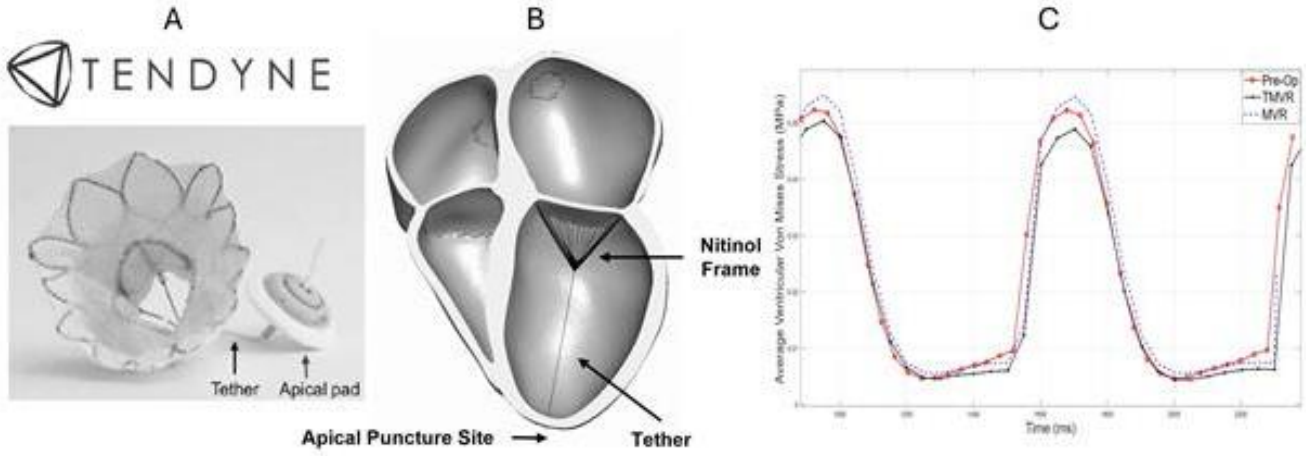

Figure:
A)Tendyne™TMVR adopted from [1].
B)TMVR FE model showing apical puncture site, tether and nitinol frame.
C)Average ventricular von-Mises stress comparison.

[1]Fukui, M. et al. JACC: Cardiovascular Interventions 2020;13(17), 2038–2048

Patient-specific Modelling of the Left Ventricle – Quantification of Myocardial Fiber Angle Uncertainty in Passive Loading

Vlontakis F[1], Troulliotis G[1], Versteeg H[1], Korossis S[1]
[1]Loughborough University

Patient-specific computational cardiac models contain uncertainties due to low-resolution clinical imaging and lack of experimental mechanical and histological data. These uncertainties affect accuracy and robustness of patient-specific models, whilst they can be assessed through uncertainty quantification techniques[1]. This study assessed the effect of uncertainty in local myocardial fiber orientation on left ventricle stiffness.
A synthetic ventricular model was developed using a Holzapfel-Ogden (HO) passive anisotropic hyperelastic material model and subjected to passive loading. The principal anisotropy directions for each element were determined using the Laplace-Dirichlet method, assigning the fiber, sheet and sheet-normal myocardial directions deterministically. Noise was introduced as a random fiber angle field that was described by a squared exponential covariance function. Using the Karhunen-Loeve theorem to decompose the random field and Polynomial Chaos Expansion (PCE), the statistical distribution of ventricular volumes at end-diastolic pressure was generated for 3 cases with varying fiber correlation lengths.
The PCE for each case could accurately predict the behavior of the system, with root mean square errors (RMSE) below 21% of the StDev for all 3 cases. However, as the correlation length decreased, more sampling points were required for the PCE. Smaller lengths had less tendency to overestimate myocardial stiffness, since they emulate physiological organization more closely.
The preliminary results indicated that fiber angle field uncertainty influences the predicted ventricular compliance significantly. This finding needs to be further investigated in the context of patient-specific modelling during the whole cardiac cycle, where material model personalization is compliance-based.

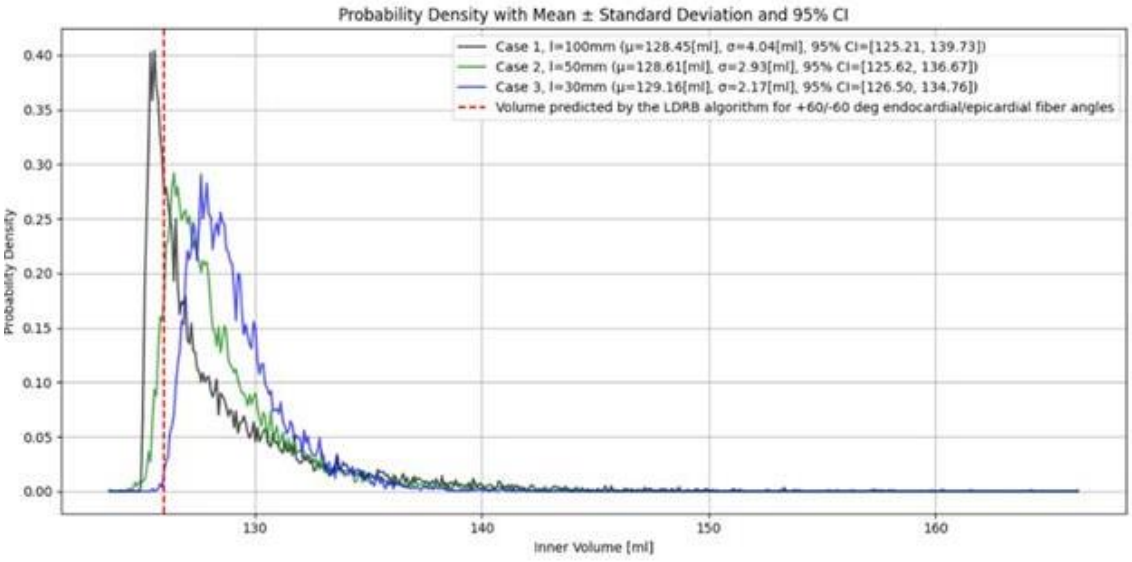

Figure:Probability densities by Monte Carlo Sampling of PCE for 100mm, 50mm and 10mm correlation lengths. RMSE (%StDev):8%, 17%, 21%, respectively.

[1] Eck, V., et al. International Journal for Numerical Methods in Biomedical Engineering 2016; 32, n/a.

Mathematical modelling of growth and remodelling of the right ventricle caused by valvular regurgitation

Gao H[1], Guan D[2]
[1]School of Mathematics and Statistics, University of Glasgow, [2]School of control science and engineering

Modelling of cardiac function is currently revolutionising patient management of heart disease to achieve optimal individual health decisions [1]. However, few studies have focused on modelling right ventricular (RV) physiology and biomechanics despite its equal importance as the left heart. RV dysfunction is the principal determinant of adverse outcomes in patients with chronic valvular regurgitation. Both pulmonary valve (PV) and tricuspid valve (TV) regurgitation will lead to adverse growth and remodelling in the right ventricle, causing RV dilation and ultimately RV pump function failure if untreated. To the best of our knowledge, no computational RV model has been developed to incorporate TV and PV regurgitation, and its functional and structural adaptation in the long term. In this study, we will report a bi-ventricular model by focusing on RV biomechanics, a proof-of-concept study to assess and predict RV dysfunction due to PV and TV regurgitation using a kinematic growth and remodelling framework [2]. The results show that this model can capture the main characteristics of cardiac functions under TV and PV regurgitation, such as increased RV filling volume, increased RV pressure, increased RV stroke work, and the bulged septum towards LV. It can also model RV dilation and thickening with the presence of TV and RV regurgitation. Personalised RV biomechanics models, once validated, have the potential to be integrated into clinical workflow for optimal patient management with RV dysfunction.

[1] C. Rodero, et al., 2023. Advancing clinical translation of cardiac biomechanics models: a comprehensive review, applications and future pathways. Frontiers in physics, 11, 1306210.
[2] D. Guan, et al., 2023. An updated Lagrangian constrained mixture model of pathological cardiac growth and remodelling. Acta Biomaterialia, 166, 375-399.

Drug-coated balloons: computational modelling of deployment, drug delivery and retention

McGinty S[1], Fensterseifer Schmidt A[1], Aggarwal A[1], McCormick C[2], Oldroyd K[1]
[1]University Of Glasgow, [2]University of Strathclyde

Drug-coated balloons (DCB) are becoming an increasingly attractive alternative to stents for the treatment of obstructive arterial disease. The key advantage of DCB is their temporary nature: they are deployed for a period of 1-3 minutes, then removed leaving nothing behind. This holds many potential benefits including a reduction in use of dual anti-platelet therapy; versatility in challenging lesions and; the provision of more options to the clinical team in cases where a repeat revascularisation is required. Despite the apparent advantages of DCB, surprisingly little is understood about how their design and use may be optimised to achieve controlled, efficacious drug delivery and retention in the arterial wall. Computational modelling and simulation offers a unique platform for understanding this problem, particularly due to the inability to monitor local drug delivery and tissue retention in humans in-vivo. A major limitation of existing models is that they all consider the drug source as either a constant source or an influx boundary condition. A further limitation is that none of these models directly considered the influence of structural or soft tissue mechanics (resulting from DCB deployment) on drug delivery and retention. In this work, we address the aforementioned shortcomings of existing state-of-the-art approaches by presenting an original computational framework, calibrated against in-vitro experimental data, that simultaneously accounts for the effects of DCB deployment, drug delivery and retention in tissue. This approach enables the calculation of key indicators of device safety and efficacy, which we compare against available in-vivo data.

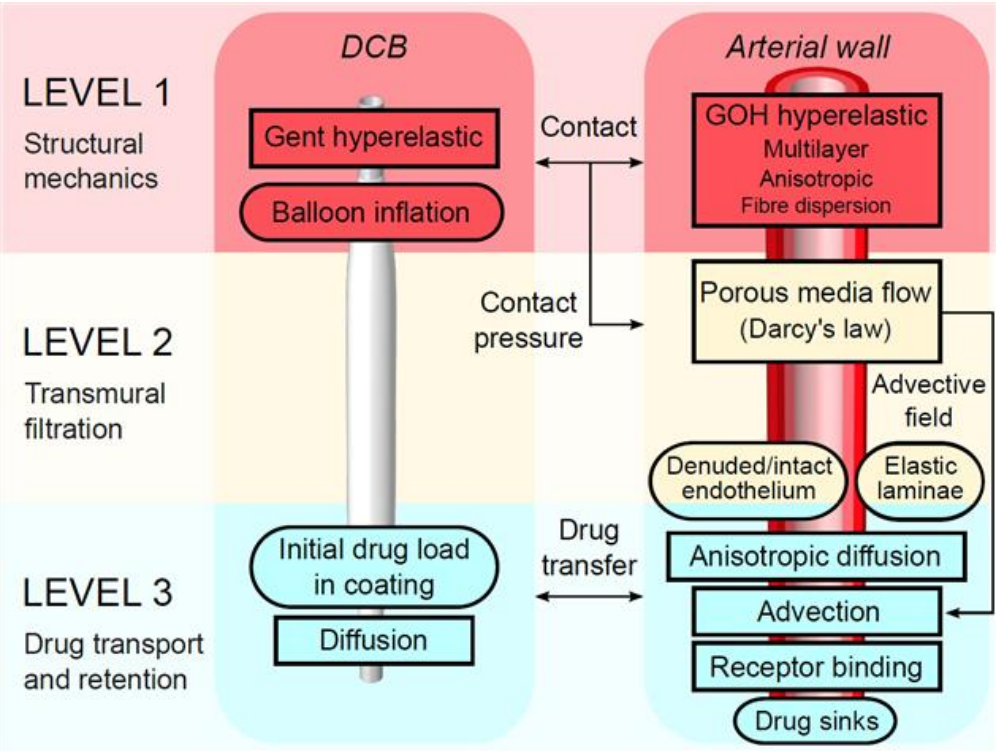

Schematic representation of the multiphysics computational model describing drug-coated balloon deployment, drug delivery and retention in arterial tissue.

Effect of lung resection surgery on the cardiovascular system: a computational modelling study

Huang S[1], Good R[1,2], McCall P[1,2], McGinty S[1], Shelley B[1,2], Aggarwal A[1]
[1]University of Glasgow, [2]NHS Golden Jubilee

Lung cancer, a common and life-threatening disease, is most effectively treated by lung resection. However, patients often experience reduced exercise capacity and shortness of breath postoperatively. These symptoms were initially attributed to impaired lung function. Yet, subsequent studies found that impaired cardiac function, especially right ventricular (RV) dysfunction, plays a key role [1]. Changes in afterload and RV contractility have been hypothesised as possible mechanisms underlying the RV dysfunction [2]. However, isolating these hypotheses in clinical studies remains challenging. To better understand RV dysfunction and symptoms following lung resection, we developed a lumped parameter model. RV contractility and afterload were adjusted in the model to test volume and pressure response in the cardiovascular systems. Both mechanisms caused RV dysfunction and similar trends (except for three pressure values that showed divergent changes, Fig.1). Furthermore, because invasive in-vivo measurements are difficult, the resulting small sample size of clinical datasets limits the analysis of RV dysfunction. Leveraging a detailed clinical dataset, we used a Markov Chain Monte Carlo (MCMC) method to generate synthetic virtual patient data (VPD) representative of the clinical observations. Based on the VPD and using logistic regression, we developed novel risk factors predictive of the RV dysfunction. This is the first computational study on this topic. By evaluating different mechanisms and applying statistical methods to predict RV dysfunction risk, the model aims to clarify its underlying causes. In the future, these results will help clinicians anticipate surgery-related complications, inform patients prior to lung surgery and take steps to improve outcomes.

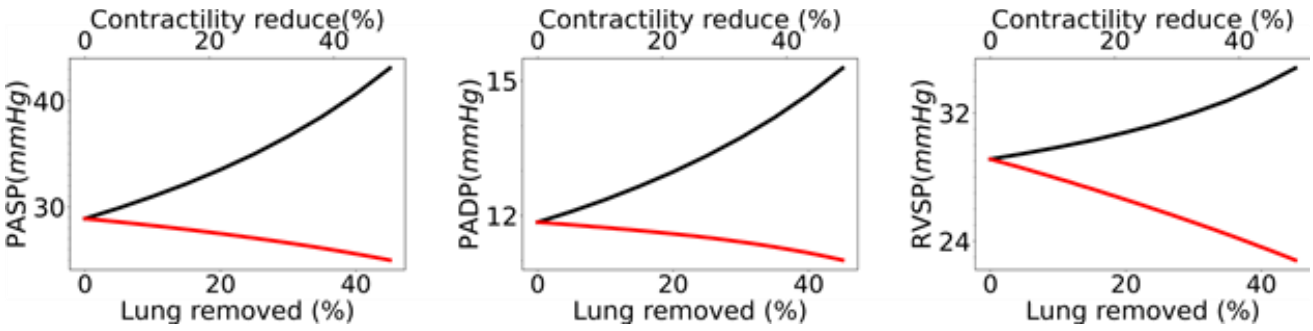

Figure 1: The changes in three pressure values based on the two hypotheses show opposite trends

[1] R. Larsen K et al.,1997, Ann. Thorac. Surg, 64: 960–4
[2] Shelley B et al., 2023, Br. J. Anaesth, 130: e66–79

Engineering Innovations in Clinical Diagnostics & Therapeutic Devices, Conference Room 4/5, September 4, 2025, 13:30 - 14:30

Prediction of Epileptic Seizures using GAN-based Approach to EEG Signal Augmentation

Huang X[1], Meng H[1], Li Z[2]
[1]Brunel University of London, [2]Chongqing University of Posts and Telecommunications

Epilepsy is a chronic neurological disorder affecting over 50 million people worldwide. Electroencephalogram (EEG) signals are widely used for seizure detection due to their high temporal resolution, low cost, and non-invasiveness [1]. However, early detection of seizures by EEG faces several challenges, including the limited duration of EEG seizure datasets and the presence of low signal-to-noise ratio in non-invasive EEG recordings. Deep Learning techniques such as Generative Adversarial Networks (GANs) and Convolutional Neural Networks (CNNs) are being employed to address these issues. GANs allow for the unsupervised learning of real dataset distributions, enabling the generator to augment the original dataset and improve the accuracy of EEG signal prediction. CNNs have been modified to identify EEG signals from different dimensions in the time-frequency graph, yielding improved performance of seizure prediction models [2]. Despite this, issues such as poor data quality and limited generalisability persist. To address these limitations, this study proposes a Combinational Generative Adversarial Network (CGAN), which integrates Deep Convolutional GAN and Conditional GAN to generate class-specific EEG data. The expanded dataset is evaluated by the CNN model to compare the performance of the expanded dataset with previous works. Through the Leave-One-Seizure- Out Cross-Validation method, the average Area Under the Curve (AUC) is 0.876 when the training epoch equals 50 and the augmentation rate equals 60%. The result of AUC is greater than the previous works shows the expanded dataset generated by the CGAN has similar features to the original data and can contribute to the seizure prediction task.

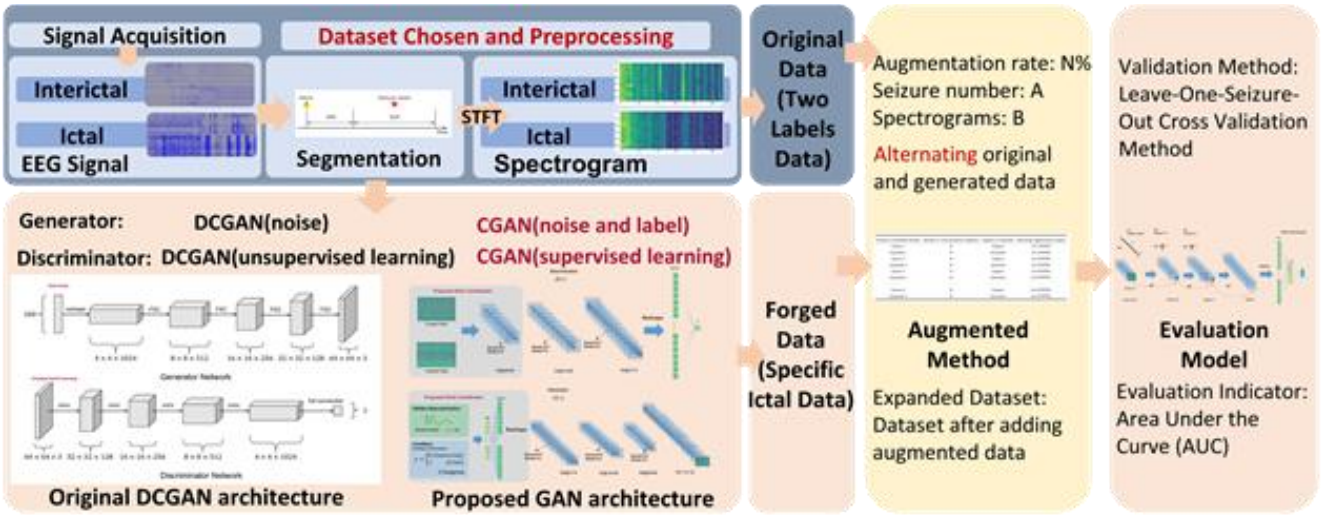

This is the whole procedure of CGAN model contains dataset chosen and preprocessing, CGAN architecture, augmented method and evluation model.

[1] Luis Fernando Nicolas-Alonso and Jaime Gomez-Gil, “Brain computer interfaces, a review,” sensors, vol. 12, no. 2, pp. 1211–1279, 2012.
[2] Truong et al., 2018. Convolutional neural networks for seizure prediction using intracranial and scalp electroencephalogram. Neural Networks 105, 104–111.

Engineering Innovations in Clinical Diagnostics & Therapeutic Devices, Conference Room 4/5, September 4, 2025, 13:30 - 14:30

Stochastic modelling of inhibitory efficacy of HIV-1 therapeutic interfering particles

Sazonov I[1], Savinkov R[2], Grebennikov D[2], Bocharov G[2], Meyerhans A[3,4]
[1]Swansea University, [2]Marchuk Institute of Numerical Mathematics of the RAS, [3]ICREA, Pg. Lluis Companys 23, [4]Infection Biology Laboratory, Universitat Pompeu Fabra

Efficient control of the HIV-1 infection relies on use of highly active antiretroviral therapy. However, it is only curative and requires a continuous administration of the drug. Application of engineered HIV-1 defective interfering particles characterized by ablation of key protein expression suggested a therapeutic potential referred to as TIPs. Recent animal model study in nonhuman primates has reported a substantial reduction of the HIV-1 viral loads after a single intravenous injection of TIPs [1]. However, a quantitative view of intracellular replication for HIV-1 in the presence of TIPs is still missing. In our study we develop a stochastic numerical model to study various aspects of the interference of TIPs with HIV-1 replication with the defense response of an infected CD4+ T cell. The model of infection process in a cell is formulated as a Markov Chain employing the algorithm proposed by Gillespie [2] based on Monte Carlo method. To accelerate the computation, a hybrid approach has been proposed and implemented with possibility of automatic switching of dynamics of highly populated components to deterministic one and back to stochastic dynamics if the abundance becomes low during the computation [3,4]. This approach allows performing numerous computations and obtaining reliable statistical results for different combination of initial numbers of free virions (MOI), and TIPs, and extracellular interferon-I. The total number of mature virions released by infected cell, the TIP Inhibitory Factor and probability of infection to extinct have been computed. Significant reduction of total viral progeny in presence of TIPs has been shown.

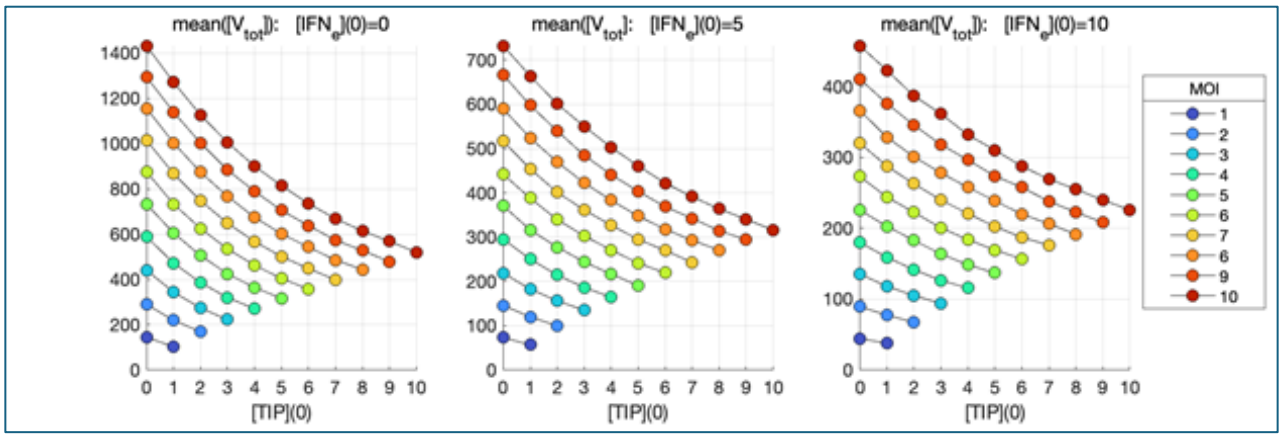

Mean value of the total number of released virions versus initial number of TIPs for different MOI and extracellular IFN.

[1] F.N.N. Pitchai et al., 2024, Science, vol. 385.
[2] D. Gillespie, 2007, Annu Rev Phys Chem., vol. 58, pp. 35-55.
[3] I. Sazonov et al., 2023, Viruses 2023, vol. 15.
[4] M. Locke et al., 2024, Mathematics, vol. 1.

Engineering Innovations in Clinical Diagnostics & Therapeutic Devices, Conference Room 4/5, September 4, 2025, 13:30 - 14:30

Dual-modality optical and ultrasonic imaging using lead-free, transparent, single crystal ultrasonic transducers for inline clinical dermoscopy

Kinney J[1], Lam K[1], Gyöngy M[2]
[1]University Of Glasgow, [2]Dermus

Transparent ultrasonic transducers have primarily been developed to enable inline optoacoustic imaging. Their optical transparency also makes them ideal for simultaneous conventional optical imaging, supporting dual-modality systems. While ultrasound excels at imaging deep tissue structures, it lacks detailed surface information. Integrating optical surface information with ultrasound depth data provides a more comprehensive diagnostic view particularly beneficial in dermatology. In collaboration with an industrial partner, we aim to explore the integration of transparent transducers and optical imaging for clinical use.

To achieve the goal, ~30-MHz transparent ultrasonic transducers were developed for inline dual-modality imaging. A novel imaging setup was developed; a compact optical camera is positioned behind the transducer. This configuration integrates simultaneous acquisition of ultrasound and dermascopy-like video, capturing both structural and superficial information in parallel. The system performs 2D imaging by mechanically scanning the single-element transducer across the target, while the co-axially aligned camera records video inline with the ultrasound beam. This setup eliminates the need for acoustic mirrors or water columns that are commonly required to align optical and acoustic fields, simplifying hardware design and significantly reducing potential image registration errors.

Preliminary scans were performed on standard test objects, including steel blocks with drilled holes, International Electrotechnical Commission tissue phantoms, and human skin. The results confirm that the transducer is sufficiently transparent to allow the camera placed behind it to capture clear, inline video of the target area. To facilitate multimodal analysis, custom software was developed to enable synchronous playback and frame-by-frame comparison of ultrasound and video data.

Mechanical ventilation phantom for evaluating a sensor-equipped endotracheal tube

Zheng D[1], Agbiki T[1], Correia R[1,2], Korposh S[1,2], Gadsby B[2], He C[1], Hayes-Gill B[1,2], Morgan S[1,2]
[1]Optics and Photonics Research Group, Faculty of Engineering, University of Nottingham, [2]Medical Photonics Limited

Ventilator-associated pneumonia (VAP) affects up to 20% of mechanically ventilated patients, increases the duration of intensive care stay and raises mortality rate by 30% [1]. Leakage of orogastric secretions past the cuff of endotracheal tubes (ETT) is one of the main causative factors of VAP [2]. The current test method (International Standard for Anaesthetic and Respiratory Equipment, EN ISO 5361:2023) recommends using a transparent cylinder for simulating the trachea when measuring fluid leakage. Furthermore, this test setup does not include the ventilator, which may affect fluid leakage. There is a need for better phantoms to evaluate fluid leakage during ventilation. The phantom developed in this research is used to evaluate a sensor-equipped ETT [3] which contains auto-inflation of the cuff and photoplethysmography (PPG). Three system configurations were evaluated 1) only a transparent cylinder, 2) adding the ventilator and lung, 3) adding cuff auto-inflation. 1) had the highest mean leakage rate (mean and SD:328.6±18.78mL/h). A notable decrease was observed in test 2) (236.9±7.78ml/h), and a further decrease in test 3) (194.5±9.62ml/h), demonstrating the benefits of automatic cuff inflation for reducing leakage past the cuff. We conclude that a more realistic simulation of mechanical ventilation enables a better assessment of cuff leakage rates. This can provide valuable insights on the influence of ventilation on leakage, and aid manufacturers in optimising ETT design. The system can also be used in conjunction with the 'iTraXS' smart ETT [3] for measuring PPG signals using the hand wrapped around the transparent cylinder to simulate tracheal PPG.

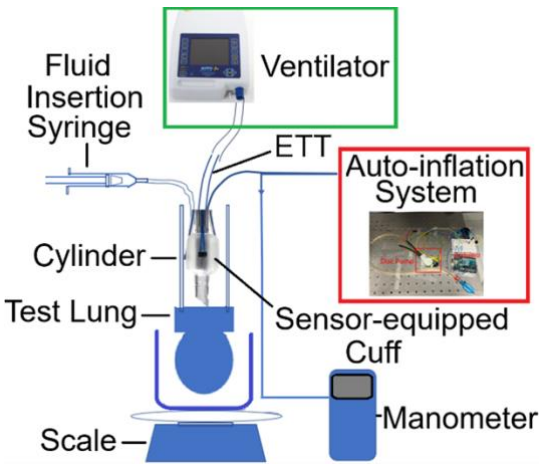

Figure 1: The experimental set-up diagram of cuff leakage test

[1] T. Agbiki et al., 2024, BJA Open, vol. 10, art.100290.
[2] S. Gopal et al., 2015, EJCTS, vol. 47, no. 3, pp. e92–e96.
[3] R. Correia et al., 2021, Biomed. Opt. Express, vol. 13, no. 1, pp. 48-64.

Engineering Innovations in Clinical Diagnostics & Therapeutic Devices, Conference Room 4/5, September 4, 2025, 13:30 - 14:30

A Comprehensive Risk Model for Evaluating Deep Tissue Injury in Diabetic Foot Ulcers

Tang J[1], Zhang J[1], Jiang L[1]
[1]School of Engineering, Faculty of Engineering and Physical Sciences, University of Southampton

Diabetic foot ulcers (DFUs) affect approximately 25% of people with diabetes (PWD) in their lifetime. Sensory loss in PWDs increases the risk of developing hard-to-heal deep tissue injury (DTI) at bony prominent sites, i.e. heel, metatarsal heads (MH) and hallux (Fig.1a). To date, DTI risk analysis has been mostly relied on lab-based ex-vivo data [1] and Finite Element Analysis. Additionally, no model currently exists to objectively assess real-time DTI risk based on dynamic plantar load/unload characteristics during walking. This study presents a novel analytical approach which integrates load transfer with a DTI model [2], whereby DTI is marked by the physiological response of real tissue e.g. blood occlusion, reflecting ulceration aetiology. Dynamic pressure experienced at heel, MH and hallux [3] (Fig.1b), combined with representative tissue elasticities from healthy and PWDs, were used to evaluate the load transfer to the tissue adjacent to bony areas. The transferred loads were subsequently used in the DTI model (Eq.1 and Eq. 2) to generate quantitative measures (R) for tissue injures, which is proportionally associated with DTI risks. Fig.1c illustrates the R values and thus the DFU-DTI risk increases over a gait cycle. An increase of peak R is observed across at all sites for PWDs especially at MHs (37%, Fig.1d). Detailed results for effects of duration, load/unload frequency, physical activities to risk scores will also be presented. Potential applications in real-time deep tissue injury risk monitoring in daily living will be discussed.

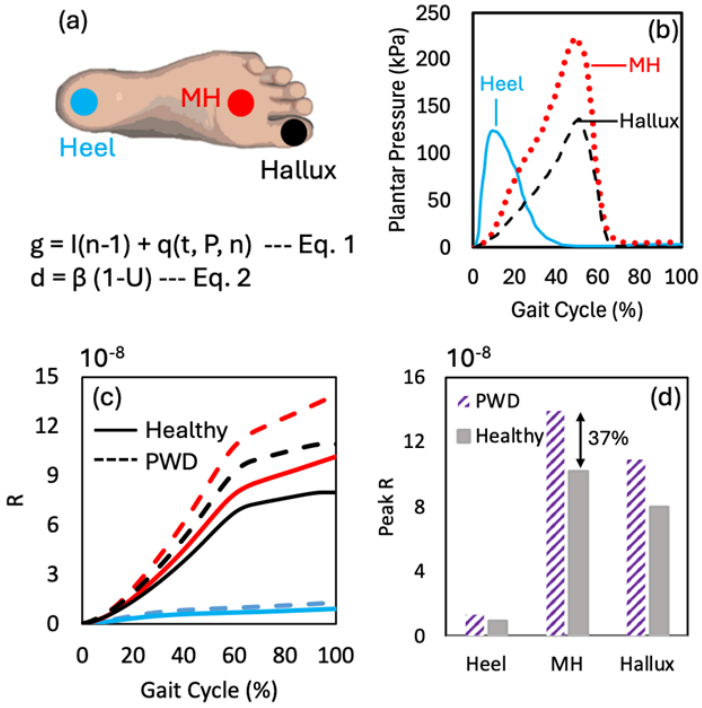

Figure 1: (a) DFU-prone sites. (b) Pressure profiles, (c) R values and (d) peak R values over a gait cycle.

[1] A. Gefen et al., 2008, J. Biomech., vol. 41, no. 9, pp. 2003-2012. [2] B. Osuagwu et al., 2023, BMC Biomed. Eng., vol. 5, no. 1, pp. 8-20. [3] G. Warren et al., 2004, Gait Posture, vol. 19, no. 1, pp. 91-100.

Decalcifying and antibacterial bilayer grafts for vascular tissue engineering

Hood R[1]
[1]University Of Sheffield

The number of people living with cardiovascular disease (CVD) has doubled to an estimated 640 million people globally since 1993 [1]. Saphenous vein autografts remain the gold standard for vascular replacement, but for patients lacking implantable vessels synthetic, bioinert alternatives based on non-biodegradable polymers are used. These often fail at smaller diameters due to thrombus formation and compliance mismatch [2]. Citric acid, a naturally occurring reagent in the Krebs cycle, has the potential to reduce post operative infections and both atherosclerotic calcium deposits and thrombus formation through the chelation of calcium ions in solution [3], [4]. Here previously developed poly(glycerol sebacate) (PGS) was functionalised with different ratios of citric acid (5-10 mol%). The resulting polymers were characterised before analysis into the effect of composition on the mechanical properties and biocompatibility. Degradation and citrate elution of the material has been studied, confirming favourable properties for the graft. The outer layer has been synthesised from porous polyHIPE scaffolds of PGS-methacrylate and optimised for ideal pore size and interconnectivity. Human dermal fibroblasts were cultured for 28 days, and a comparison of cell proliferation and infiltration was completed. This highlighted the best compositions to have pore diameters greater than 30 microns and interconnects larger than 10 microns. Development of an extended culture period and subsequent decellularisation protocol will be completed in order to maintain the high levels of obtained ECM and remove any immunogenic material ready for implantation into the patient.

[1] M. Lindstrom, 2022, J Am Coll Cardiol, vol. 80, no. 25, pp. 2372-2425
[2] M. Naegeli, 2022, Circ. Res., vol. 131, no. 1, pp109-126
[3] L-C Su, 2014,Front Bioeng Biotechnol, vol 2, pp 23
[4] L. Machado-Silveiro et al, 2004, Int Endod J, vol 37, no 6, pp 365-369.

3D Bioprinting Nanofiber-Reinforced Vascular Branches

Lei C[1], Koutsos V[1], Callanan A[2], Radacsi N[1,2,3]
[1]School of Engineering, Institute For Materials And Processes, The University of Edinburgh, [2]School of Engineering, Institute for Bioengineering, The University of Edinburgh, [3]Centre for Cardiovascular Science, The Queen's Medical Research Institute (QMRI), University of Edinburgh

A hybrid biofabrication approach combining embedded 3D bioprinting and electrospinning was used to create bifurcated vasculature. A bifurcated graft is essential during open surgical repair when the aorto-iliac part of the vasculature is diseased.[1] However, fabricating a tissue-engineered vascular graft (TEVG) that closely mimics the native blood vessel network presents significant challenges, namely replicating the complex multi-layered structure of the native vessels, and TEVGs are prone to complications such as thrombosis and intimal hyperplasia.[2] An embedded bioprinting method was utilised, employing a support bath including Freeform Reversible Embedding Hydrogels (FRESH) and agarose, in which a bifurcated gelatine-based hydrogel structure is printed. Preliminary results showed that achieving uniform nanofiber deposition onto bifurcated structures via conventional electrospinning is challenging, short nanofibers were instead incorporated inside the hydrogel matrix prior to bioprinting. Trial runs showed that the composite hydrogel exhibited improved mechanical properties compared to the nanofiber-free hydrogel. Future work will focus on optimising the mechanical performance of the printed constructs. Hence, this approach has the potential to serve as a starting point for the biofabrication of complex tissue structures, like vascular branches and soft organs.

[1] S. Li et al., 2016, Biomicrofluidics, vol. 10, no. 6, pp. 064102.
[2] R. Xiong et al., 2015, Biofabrication, vol. 7, no. 4, pp. 045011.

Rotationally Seeded and Bioreactor-Cultured Vascular Grafts Fabricated from UV-Cured Methacrylated PGS HIPEs

Muzikiza D[1], Green N[1], Claeyssens F[1]
[1]University Of Sheffield.

Cardiovascular diseases (CVDs) are the number one cause of mortality across the globe [1]. Synthetic vascular grafts and autologous vessels are the current standard treatment for CVDs, with the former often limited in terms of availability and the latter prone to thrombosis and intimal hyperplasia [1][2]. Tissue engineered vascular grafts (TEVGs) offer an alternative to the above mentioned methods. However, current TEVGs performance and clinical translation has been unsatisfactory due to issues associated with compliance mismatch [2]. This study aims to fabricate a compliant, ECM-rich and off-the-shelf vascular graft from methacrylated Poly (glycerol sebacate) through rotational seeding and bioreactor conditioning under flow conditions.

Tubular scaffolds were fabricated using methacrylated poly(glycerol sebacate) (PGS) high internal phase emulsions (polyHiPEs). The emulsion was polymerized under UV light within a custom-designed mold to produce the scaffolds. Human fibroblast cells (BJ-5ta) were seeded onto both the luminal and abluminal surfaces of the scaffolds using a rotational seeding device designed for uniform cell distribution. Histological analysis indicated that the cells successfully infiltrated the scaffold. The seeded scaffolds will be cultured within a custom-designed 3D-printed bioreactor to subject the cells to flow-induced mechanical stimulation. Subsequently, extracellular matrix (ECM) protein levels will be quantified using ELISA to evaluate the influence of mechanical cues on ECM production. Finally, the engineered vascular grafts will be decellularized to render them non-immunogenic and suitable for future in vivo applications.

Preliminary histological analysis suggests effective cellular penetration into the scaffold. Mechanical stimulation should enhance this and upregulate ECM protein expression.

[1] S. Pashneh-Tala et al.,2016, “The tissue-engineered vascular graft - Past, present, and future,” Tissue Eng. - Part B Rev., vol. 22, no. 1, pp. 68–100.
[2] J.S.Soares et al.,2022. Engineered tissue vascular grafts: are we there yet?. Applications in Engineering Science, 12, p.100114.

Physicochemical and mechanical properties of electrospun polycaprolactone composite grafts integrated with silver nanoparticles for vascular applications

Bakare A[1], Konar S[1], Onarinde B[1], Tucker N[1], Jaganathan S[2]
[1]University Of Lincoln, [2]University of Leicester

Electrospinning is a versatile technique for the fabrication of nanofibres with potential for tissue engineering using materials such as polycaprolactone (PCL). PCL nanocomposites have been used in various applications, such as vascular tissue repair and regeneration, and as a blend or coating with other composites or nanoparticles in biomedical devices. In this study, vascular grafts were fabricated from PCL blended with silver (Ag2O) nanoparticles (AgNP). AgNP was prepared with three different leaf extract formulations: silver oxide with nettle grass (Urtica dioica) (N), perennial ryegrass (Lolium perenne) (R), and a 1:1 mixture of both extracts (NR). The extracts (AgNP-N, AgNP-R, and AgNP-NR) were oven-dried and characterised using SEM-EDX, FTIR, and UV-Vis. The nanoparticles produced different nanoparticle morphologies. The AgNP with the best results (AGNP-R) was further incorporated into PCL to fabricate electrospun vascular grafts in three different ratios (9:0, 8:1, and 7:2). SEM characterisation of the electrospun fibres revealed a reduced fibre diameter with bead-free fibres with diameter inversely proportional to AgNP content. The mechanical strength and thermal stability of the nanocomposites were higher than those of the pristine PCL. This is due to the strong interfacial interaction between the PCL matrix and the nanofillers. The composites had a lower contact angle with demineralised water than pristine PCL fibre. Hence, the electrospun PCL/AgNP demonstrates promise for applications in tissue engineering. These composites will be characterised for hemocompatibility and antibacterial properties, including bacteriophage addition—results to be reported elsewhere.

Tissue Engineering 2 - Vascular and Cardiovascular Tissue, Auditorium B/C, September 4, 2025, 13:30 - 14:30

Biofabrication of bi-layered vascular grafts for bypass surgeries.

Fazal F[1], Hadoke P[1], Melchels F[2], Macrae V[1], Radacsi N[1]
[1]The University Of Edinburgh, [2]The University of South Australia

Patient-specific Small-diameter vascular conduits for the treatment of cardiovascular diseases are in high demand. Bioprinting is an attractive technique to fabricate vascular grafts for bypass surgeries, however, the mechanical performance of cell-laden hydrogels is a major challenge. Here, we present a hybrid approach to fabricate a bi-layered vascular constructs. The inner electrospun fibre layer offered an active surface for endothelial cells to grow and proliferate. The smooth muscles cells loaded gelatin methacryloyl hydrogel was then printed using a vertical additive lathe printing system. The cell survival rates of ECs and SMCs at week 2 and week 4 were found to be greater than 80%, along with the substantial amount of collagen deposition after 4 weeks of cell culture. Hence, the presented method could be used to biofabricate a vascular graft for the treatment of cardiovascular disease.

Tissue Engineered Vascular Grafts

Slavova N[1,2], Claeyssens F[1], Green N[1]
[1]University of Sheffield, [2]University of Manchester

Cardiovascular diseases are often a result of atherosclerosis that leads to vessels stenosis. The current gold-standard treatment is a coronary bypass surgery where the occluded vessel is bypassed using an autologous saphenous vein (SV) [1]. However, autologous grafts are associated with donor side morbidity, poor quality/durability and lack of availability. Synthetic grafts are routinely used for large vessel grafting in patients who are not candidates for autologous grafting, but poor patency and thrombosis limit their use for small-diameter applications (<6mm) [2,3]. To address these limitations, we propose a decellularised tissue-engineered vascular graft combining porous biocompatible polymer and extracellular matrix deposited by immortalised fibroblasts. High-internal phase emulsions were synthesised from poly(glycerol sebacate)-methacrylate (PGS-M) polymer. Injection moulding was used to generate 3.8 mm PGS-M grafts. We show that immortalised human fibroblasts readily infiltrate grafts with a median pore size of 30 microns, ranging between 10-100 microns and readily deposit collagen and additional ECM proteins over a 3-week culture period. PGS-M grafts were sterilised using medical grade ethylene oxide (EtO). We show that EtO sterilisation has no effect on the graft properties, and they are conducive of cell growth and proliferation. Macromolecular crowding of culture media with carrageenan or polyvinylpyrrolidone to enhance collagen production is promising, but we showed a cell-type specificity where collagen production was increased in primary fibroblasts but not in immortalised fibroblasts. The generation of small-diameter cell-laden PGS-M grafts with good ECM deposition enables the next stages of the project – graft decellularisation and mechanical testing being the next focus.

[1] G. A. Roth, G. et. al. Am. Coll. Cardiol., 2020, 76, 2982–3021.
[2] S. Pashneh-Tala, S. MacNeil and F. Claeyssens, Tissue Eng. Part B Rev., 2016, 22, 68–100.
[3] M. S. Conte, J. Vasc. Surg., 2013, 57, 8S–13S.

Framework for analysing cardio-respiratory synchronization

Khovanov I[1], Khovanova N[1]
[1]University Of Warwick

Despite active research into cardio-respiratory synchronisation, its use in clinical diagnosis and monitoring remains limited to a few specific examples[1]. Beginning with a modelling perspective, we clarify the relationship between synchronisation and modulation, with the latter being closely related to the respiratory sinus arrhythmia (RSA) effect. We then examine experimental findings to explain the influence of breathing rate and variability on the synchronisation manifestation.

Notably, a 1:1 ratio between breathing and heart rates[2,3] is associated with cardio-respiratory coordination, where a specific phase relationship between the respiratory signal and heart rate is observed. However, under spontaneous breathing conditions, the RSA effect tends to obscure this phase relationship, and the natural variability in breathing complicates signal analysis. Introducing controlled breathing reveals a more complex picture of cardio-respiratory interaction, where adaptation to the experimental environment becomes a key factor. Nonetheless, reduced breathing variability is associated with longer episodes of synchronisation.

Time series analysis of different breathing patterns for the same subject showed that both synchronisation and the RSA effect are subject-dependent and influenced by the individual's level of physical fitness. However, for some participants, the reproducibility of the derived metrics was inconsistent, suggesting that heart rate variability measures should be incorporated into synchronisation analysis to more accurately assess autonomic regulation.

By integrating these findings, the study suggests a framework for analysing cardio-respiratory synchronisation, combining synchronisation with other metrics of cardio-respiratory interaction, along with heart rate and breathing variabilities. The proposed framework has potential applications in diagnosing and monitoring individual cardio-respiratory function.

[1] D. A. Kenwright, et al., 2015, Anaesthesia, vol. 70, pp. 1356-1368.
[2] I.A. Khovanov et al, 2022, Communications in Nonlinear Science and Numerical Simulation, vol. 105, 106071.
[3] S. Perry et al, 2019, Scientific Reports, vol. 9: 1545.

Evaluating Respiratory Sinus Arrhythmia and Mutual Correlation Coefficient Metrics for Cardiorespiratory Coupling across Breathing Patterns

Budiani R[1], Khovanov I[2]
[1]The University of Warwick, [2]The University of Warwick

Cardiorespiratory coupling indicates autonomic regulation and serves as a significant tool for clinical monitoring and diagnosis [1] [2]. The complexity and non-stationarity of physiological signals present challenges in the development of robust coupling indicators. We initially analyzed simulated cardiorespiratory signals generated by a unidirectional Van der Pol oscillator [3], assessing two coupling indicators: Respiratory Sinus Arrhythmia (RSA) and Mutual Correlation Coefficient (MCC). The insights derived from these modeled signals were subsequently applied to physiological data obtained from healthy subjects who were participating in various controlled breathing patterns.

The results indicate that RSA increases linearly with slower breathing rates. MCC generated a value indicating the presence of coupling. Furthermore, both RSA and MCC demonstrated decreased variability under controlled breathing conditions, underscoring their reliability in standardized assessments. Our analysis showed that utilizing only the highest MCC from a one-minute window provides RSA values comparable to those calculated throughout the entire duration. This indicates that RSA may be accurately evaluated using shorter time durations.

The complementary strengths of RSA and MCC were apparent: RSA demonstrated clear, linear relationships with respiratory intervals, whereas MCC indicated stable interaction magnitudes across various breathing patterns. Our modeling approach clarified the physiological interpretation of RSA and MCC, confirming their combined application as indicators for assessing cardiorespiratory coupling. The findings suggest potential clinical applications for non-invasive monitoring, enabling early diagnosis and continuous evaluation of autonomic health.

[1] C. D. Da Silva et al., 2023, Respir. Physiol. Neurobiol., vol. 311.
[2] W. Wongdhamma et al., 2013, in Proc. IEEE Int. Conf. Autom. Sci. Eng., pp. 605–610.
[3] J.-M. Ginoux et al., 2012, Chaos, vol. 22, no. 2, pp. 1-40.

Determining aortic wall nanomechanical properties in neonatal patients with coarctation of the aorta

Preston J[1,2,5], Lip G[1,5], Lotto A[3,5], Akhtar R[4,5]
[1]Department of Cardiovascular and Metabolic Medicine, Institute of Life Course and Medical Sciences, University of Liverpool, [2]Research Department, Liverpool Heart and Chest Hospital, [3]Alder Hey Children's Hospital, [4]Department of Materials Design and Manufacturing Engineering University of Liverpool, [5]Liverpool Centre for Cardiovascular Science

Coarctation of the aorta (CoA) is a congenital heart defect, typically presented as a narrowing of the descending aorta, leading to an obstruction of blood flow [1]. CoA patients are diagnosed and treated as neonates through surgical repair. However, even after successful repair, these patients often experience a higher mortality rate than healthy age and gender matched controls, due to the presence of complications related to persitent hypertension [2]. This study aims to utilise atomic force microscopy (AFM) to characterise the nanomechanical properties of the aortic wall in CoA patients following childhood correction.
Aortic samples were collected from neonatal CoA patients undergoing surgical repair at Alder Hey Children's Hospital. These samples were divided into three regions: the coarctation site, and regions proximal and distal to the coarctation site. AFM was conducted on a Bruker Multimode AFM using a Si pyramidal tip with a nominal 8 nm radius. Imaging was conducted utilising the Peakforce QNM modality. AFM images demonstrated abundant collagen fibrils in the neonatal aorta. However, the collagen fibrils appeared more disorganised in the coarctation site compared to proximal and distal samples (Figure 1). The coarctation site also demonstrated a greater mean elastic modulus of 2994.6MPa compared to both the proximal (2727.1MPa) and distal (2725.8MPa) groups. The increased elastic modulus and greater disorganisation of collagen fibrils in the coarctation site may indicate changes in extracellular matrix (ECM) composition as a result of CoA, highlighting potential therapeutic targets in the ECM for further research.

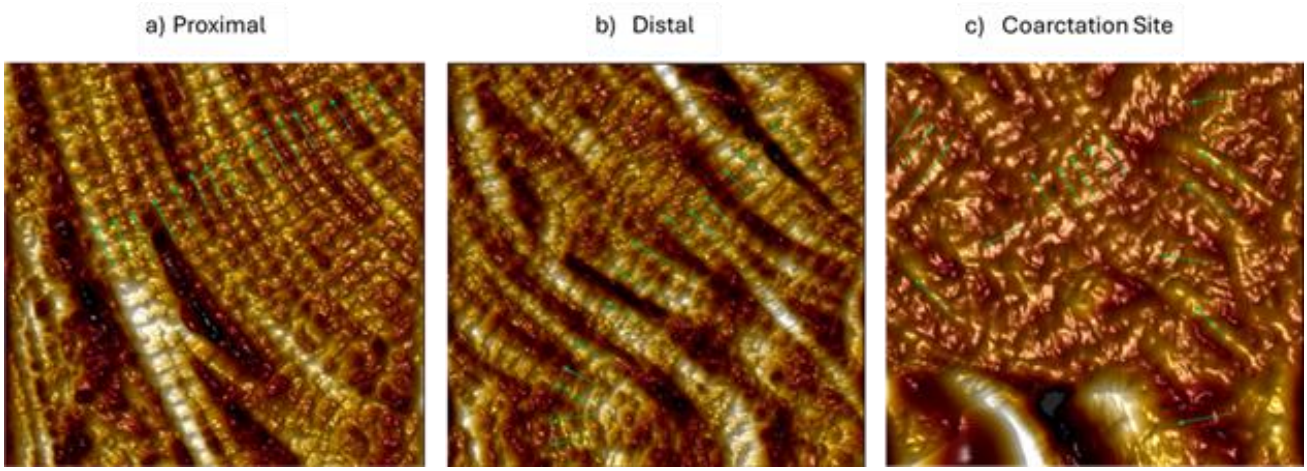

1.5µm AFM images of collagen fibrils in the aortic wall of a CoA patient. Arrows highlight collagen fibril directionality.

[1] Rosenthal, E. et al., 2005, Heart, 91(11), 1495-1502.
[2] Lee, MGY. et al., 2019, Heart, 105, 1190-1196.

Development of a novel wire-form magnesium based bioabsorbable vascular scaffold for the treatment of peripheral artery disease

Macleod K[1], Nash D[1], MacLeod C[2], Steckel M[2]
[1]The University Of Strathclyde, [2]Lumenology Ltd.

Bioabsorbable vascular scaffolds (BVS) are an emerging technology which seek to address an unmet clinical need for effective treatment of peripheral artery disease (PAD). PAD is primarily caused by atherosclerosis, which narrows and damages the arteries, and is commonly treated with drug eluting stents (DES). While effective for treating the coronary arteries, permanent DES are less suitable for PAD lesions, particularly below-the-knee (BTK), due to early re-occlusion and stent breakages.[1]
Temporary BVS are a potential solution for the treatment of BTK arteries. A BVS must provide acute structural support, equivalent to DES, to widen and allow the artery to heal but subsequently be safely absorbed, removing the long-term complications associated with DES. The relatively poor mechanical properties of available bioabsorbable materials, compared to the those applied in DES, has limited the success of BVS technology to date. Consequently, new alloys and novel approaches to device design are required to advance BVS technology.
A novel wire-form BVS device (Figure: 1a), manufactured from a cold drawn Mg-Li-Y alloy wire, is proposed to overcome the limitations of previous BVS devices. This work investigates how the alloy composition and processing routes applied during device manufacture can be optimised to tailor the microstructure of the Mg alloy wire to maximise device mechanical performance. Through minimising the number of secondary phase particles and controlling the deformation mechanisms activated during forming the microstructure of the BVS device can be optimised (Figure: 1b+c). Consequently, the device exhibits comparable mechanical performance to current DES during benchtop testing.

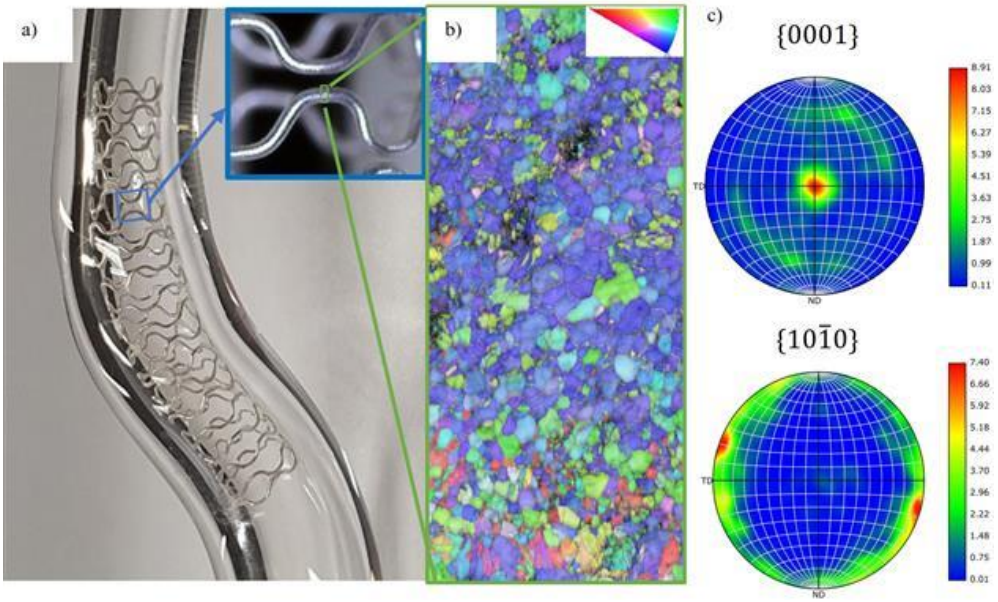

Figure: 1 a) BVS device b) Inverse pole figure (IPF) map of optimised microstructure c) Pole figures for IPF map

[1] Matsuoka, Emi et al. (2022). Cardiovascular intervention and therapeutics. vol. 37 pp. 145-157

Biology and Biomechanics for angiogenesis: hand in hand to unveil the possibilities of tissue engineering

Vidal--Roussel L[1], Walker M[2], Tassieri M[2], Schulte C[2], Vassalli M[2], Shu W[1], Wu J[1]
[1]University Of Strathclyde, [2]University of Glasgow

The major challenges in new drug development are the low translational efficiency (<10%), soaring costs (>$5 billion/drug) and ethical concerns regarding animal welfare. The emergence of bioengineering promises to offer new strategies to create non-animal models using human cell lines to address these shortcomings. Absence of vascularisation is one of the main bottlenecks to obtaining fully functional bioengineered tissues. The passive diffusion limit for oxygen and nutrients in biological tissues is ~200 µm. Providing a dense and functional microvascular network is key to the formation of larger healthy constructs. Current microfabrication technologies allow to engineer passive tubular networks in hydrogel matrices, but they lack the dynamic functionality of in vivo capillaries. If biochemical cues and their gradients' impact on microvascular tubule self-assembly have been thoroughly investigated, the importance of local mechanical properties in scaffolds has often been overlooked. Exploring the impact of local mechanical properties in 3D matrices is one of the next main axes of progress for tissue engineering, and being able to intertwine engineering and biological-based knowledge and techniques will be crucial.

In this study, we use a simple, non-inflammatory collagen-based 3D system to study the impact of local mechanical property gradients on HUVECs' self-assembly and lumenisation. We focused on cross-validating imaging-based observations on properties of the tubules across the system, like morphology or cytoskeleton distribution with biomechanical data obtained through rheological measurements, nano-indentation and optical micro rheology to depict a comprehensive and robust picture of angiogenic behaviours in mechanically heterogeneous matrices, by comparison to homogeneous matrices.

Designing functionalised human arterial in vitro models

Loges J[1], Sandison M[1], McCormick C[1], Wu J[1]
[1]University Of Strathclyde

Cardiovascular diseases are the leading cause of death worldwide, accounting for 32% of all deaths.[1] Medial arterial calcification (MAC) is a disease that is commonly connected to increasing age, diabetes and chronic kidney disease and severely heightens the risks for heart attacks and strokes. During MAC Smooth Muscles Cells (SMCs) within the arterial wall undergo phenotypical changes to osteoblast-like cells.[2] However, current in vitro research models display inaccuracies while mimicking the native cell environment for most arterial models. As the exact pathogenesis of MAC is not yet fully understood, the development of an accurate in vitro model is crucial for further research. Electrospun gelatine membranes are utilised as a scaffold, providing a flexible cell seeding environment with easily controllable properties such as Young's Modulus (YM) and conductivity. Furthermore, it allows for control over cell orientation through variability in fibre orientation.[3] Aligned SMCs on a flexible seeding surface (YM=0.9MPa, YM of human femoral artery=0.8MPa) show a higher degree of calcification compared to randomly orientated SMCs on commonly used cell culture plastics (YM=1GPa). Due to better cell attachment, SMCs on membranes are less likely to detach while undergoing calcification, allowing for a more extensive drug treatment to simulate MAC in vitro. Those differences further highlight the importance of creating an accurate cell environment when disease modelling.

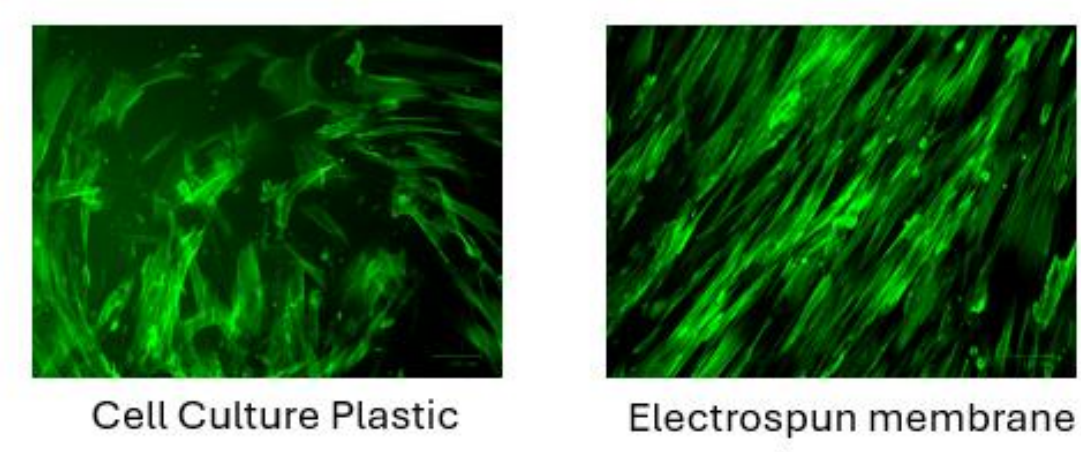

Figure: HUASMCs stained with Phalloidin on common Cell culture Plastic vs electrospun membrane.

1. World Health Organization 2021 [cited 2025)
2. Faleeva, M., et al., Regulating Extracellular Matrix Circulation Research, 2024. 134(3): p. 307-324.
3. Rickel, A.P., et al., Mater Sci Eng C Mater Biol Appl, 2021. 129: p. 112373.

Post-mortem tissue viability in a perfused rat model: a feasibility study

Antezana Merida L[1], Buis A[1], Wu J[1]
[1]University Of Strathclyde

Deep Tissue Injuries (DTIs) often develop in prosthetic and wheelchair users due to sustained or repetitive loading of soft tissues. These injuries typically originate in deep muscle layers and can be difficult to detect before irreversible damage occurs. Prior in vitro studies by Sargent et al. showed that applying transverse forces to isolated rat muscle can induce early signs of tissue damage, though the lack of perfusion in these models limits their physiological relevance [1]. To address this, the present study investigates post-mortem skeletal muscle viability using a whole-body Sprague-Dawley rat model perfused with heparinised bovine blood. Circulation is maintained via the carotid artery and jugular vein using a modified organ perfusion system. Parameters including flow rate, arterial pressure, temperature, oxygen saturation (SpO_2), and partial oxygen pressure (pO_2) are monitored continuously to assess tissue condition over time. Inspired by recent work in post-mortem extracorporeal perfusion [2], this model enables assessment of muscle under conditions that more closely resemble those in vivo, without involving live animals at this stage. While mechanical loading is not applied at this stage, the outcomes will help define the time window during which post-mortem tissue remains viable for future testing. This model contributes to the development of experimental platforms for studying mechanically induced soft tissue damage under physiologically relevant conditions.

[1] S. Marisa et al. “An ex vivo animal model to study the effect of transverse mechanical loading on skeletal muscle.” Communications biology vol. 7,1 302. 9 Mar. 2024
[2] D. Matthias Manfred et al. "Post-Mortem Extracorporeal Membrane Oxygenation Perfusion Rat Model: A Feasibility Study" Animals 13, no. 22:3532. 2023

Look where you walk – can predictive controllers offer improvements for lower limb prosthetics?

Wolstenholme M[1], Ellison P[1]
[1]University Of York

Biomimetic lower limb prostheses have been of increasing research interest due to their potential mechanical and user-comfort advantages over existing commercial devices. They present additional challenges, however, in their control, owing to their increased complexity and high degree of non-linearity. Model Predictive Controllers (MPCs) have gained increasing popularity because of their optimal-control nature and ability to handle input and state constraints, and thanks to increasing computational power they have recently been successfully applied to robotic applications including bipedal robots. However, to date they have not been applied to prosthetic devices despite their potential advantages.

In this paper, we investigate the efficacy of MPCs applied to biomimetic lower limb prosthetic devices. Firstly, we present the design process for a nonlinear MPC for a biomimetic knee rig, including implementation of offset free tracking. We then present the controllers performance under various challenges, including step, ramp, sine wave, and realistic gait-based reference signals. A traditional gain-scheduled PID controller is developed for comparison based on the previous work in [1]. The MPC showed faster settling time than the PID on the step input, as well as improvements in terms of the integral of time-weighted squared error (ITSE) for ramp and sine wave input for frequencies of 0.1-0.4Hz. In the gait cycle test, the MPC showed lower overshoot at transition between swing and stance phase.

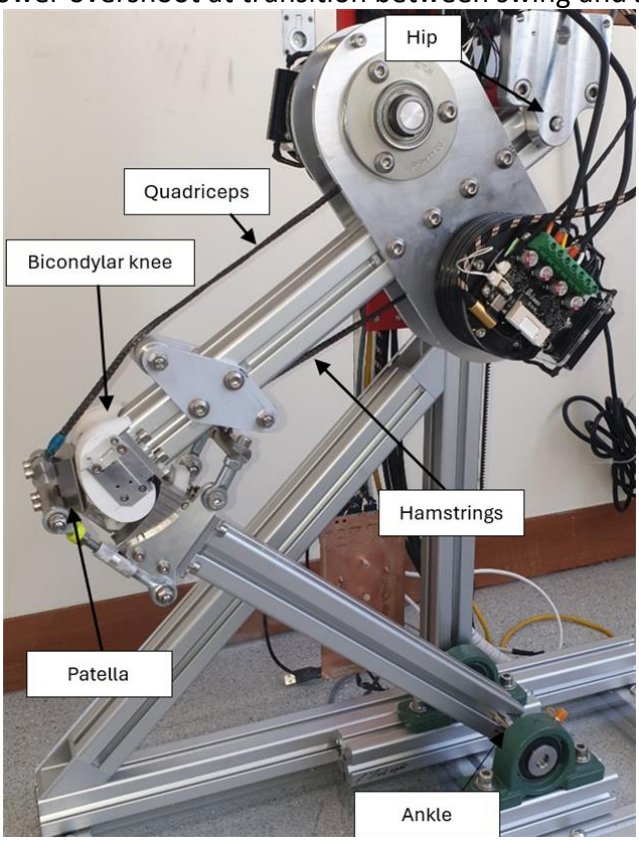

Bicondylar knee rig with patellofemoral joint and driven quadriceps and hamstrings

[1] F. Russel, ‘A complete robotic knee as a tool for better understanding of joint dynamics’, PhD Thesis, Imperial College of Science, Technology and Medicine, London, 2020.

Evidence Limitations on the Use of AFOs Following Stroke: A Systematic Review

Albasri R[1], Cox C[1], Kerr A[1]
[1]University Of Strathclyde

The clinical and research implications of studies investigating the effects of ankle-foot orthoses (AFOs) following stroke are limited by poor study design and inadequate reporting of participant characteristics and AFO specifications. There is a lack of research highlighting these limitations, and no established guidelines exist for study design and reporting quality in AFO studies. This study aims to identify common limitations in the literature and establish guidelines to improve future research design and reporting. An electronic search was conducted across key databases to identify relevant articles based on a pre-specified eligibility criterion. A customised checklist was developed to evaluate study design, participant characteristics, and AFO specification, enabling a systematic and comprehensive evaluation of quality and reporting standards. 92 studies met the inclusion criteria. The overall quality of evidence was low, with only 14.8% of studies being randomised controlled trials, 37% provided no justification for sample size, such as a power calculation and 70.4% providing insufficient justification for the validity and reliability of measurement systems. Key participant information was often missing, with 77.8% of studies not reporting lower limb muscle power or range of motion. AFO specification reporting was also limited, with 83.3% not detailing material and thickness, 66.7% not specifying AFO tuning, and 11.1% not identifying the type of AFO used. These limitations impede the translation of research into patient care and hinder evidence-based practice in stroke rehabilitation. Adhering to the proposed guidelines will enhance reporting, improve clinical decision-making, and ultimately patient outcomes.

Design requirements for above-knee adjustable socket design, considering male and female users' needs

Galletly L[1], Clark A[1], Bull A[1]
[1]Imperial College London

One of the most reported reasons for prosthesis dissatisfaction and abandonment is socket discomfort, which can be caused by fluctuations in socket fit due to residual limb size changes, both within-day and between days. One solution to these short to medium-term size changes is adjustable-size sockets, currently marketed for both above-knee and below-knee users. Despite a higher level of dissatisfaction and abandonment among above-knee prosthesis users [1] and female users [2], the majority of prosthetics research, particularly around socket comfort and residual limb size changes, still focuses on below-knee limb absence, and research participant cohorts are predominantly male. Furthermore, when asked about their experiences with prosthetics services, something highlighted by female prosthesis users was that they felt that prosthetic limbs were designed for male bodies, and did not accommodate the needs of female bodies [3]. Therefore, a set of design requirements has been developed, based on the literature, measurements of residual limb size fluctuations in male and female above-knee prosthesis users, and discussions with clinicians and users, to collate both technical and user requirements for above-knee adjustable socket design, particularly with female bodies in mind as well as male bodies. Appropriate validation tests were then identified for each requirement. These technical requirements will help to both design and test sockets to ensure they are appropriate for both male and female use.

[1] K.P. MacCallum et al., 2021, Ann, Vasc. Surg., vol. 71, pp. 331-337.
[2] K. Lehavot et al., 2022, J Gen Intern Med, vol. 37, no. 3, pp. 799-805.
[3] C.J.B. Randolph et al., 2016, Mil Med, vol. 181.

Stress shielding in end-bearing socket prosthetic in comparison to osseointegration prosthetic

Safira I[1], Masouros S[1], Bull A[1]
[1]Imperial College London

Osseointegration has emerged as an alternative to socket prostheses for transfemoral amputees, aiming to mitigate soft tissue complications. However, osseointegration is associated with adverse outcomes due to stress shielding, where the titanium implant absorbs mechanical loads typically transferred through the bone, leading to a deteriorated bone condition. Previous finite element studies have proposed optimized osseointegration designs (ie. material and geometry) [1] tailored to individual transfemoral amputee characteristics (ie. sex and stump length) [2] to minimize stress shielding; however, it remains unclear whether these improvements lead to better bone health compared to socket prostheses. Few studies have compared stress shielding in OI with that of conventional socket prosthetic. Therefore, this study employs finite-element simulations to predict femoral stress distributions in transfemoral amputee (Figure 1) under equivalent conditions for osseointegration system, an end-bearing socket prosthetic system, and in comparison with healthy system. Results demonstrated that maximum von Misses stress in the proximal femur was higher in healthy model (σ1= 36.55MPa), followed by osseointegration model (σ2= 13.17MPa) and end-bearing socket model (σ3= 12.53MPa). Meanwhile, maximum von Misses stress at the implant region for healthy, osseointegration, and end-bearing socket model are σ1= 24.15MPa, σ2= 10.64MPa, σ3= 11.82MPa. These findings indicate that osseointegration outperform the conventional socket prosthetic proximally, but stress shielding at the implant region remains a concern.

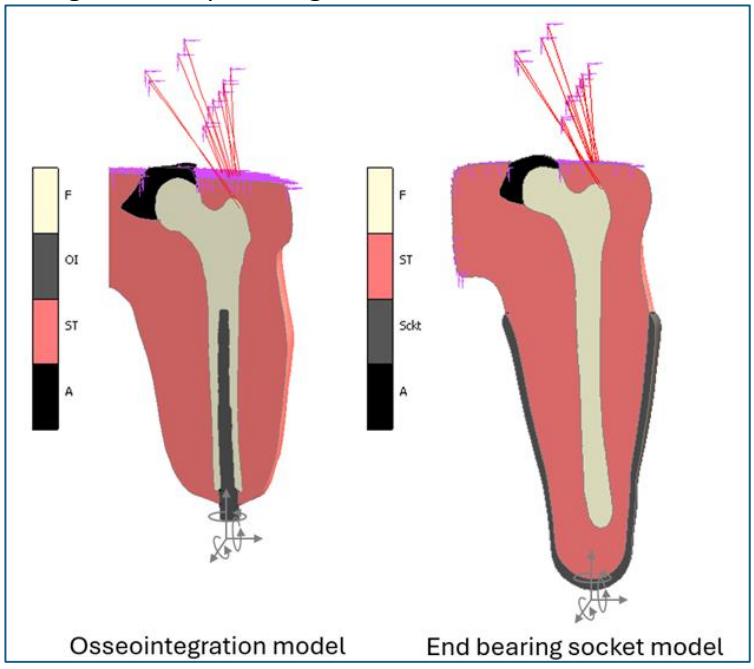

Figure 1: Transfemoral amputee with osseointegration system, an end-bearing socket prosthetic system

[1] Prochor, P., et al., 2020, Acta Bioeng. Biomech., vol. 22, no. 2, pp.1-24.
[2] McGuire, T., et al., 2025, Med. Eng. Phys., pp.104304.

Incorporating a synthetic mucus hydrogel within a colonic in vitro model

Dewhurst E[1], Berberolli S[1], Moura I[1], Davis Birch W[1], Buckley A[1], Culmer P[1], Kapur N[1]
[1]University Of Leeds

The gastrointestinal (GI) tract is host to a consortium of microbes existing within different niches, including luminal and mucosal communities. Mucosal biofilms within the colon play a key role in triggering inflammatory mechanisms through direct contact with host cells or via microbially produced metabolites [1, 2]. However, given the difficulties studying these communities in situ, our understanding of biofilms remains limited. Therefore, we propose a platform that can accurately replicate these mucosal biofilms in vitro. Structures to support biofilm growth were developed to integrate into a clinically reflective in vitro model of the human colon, the MiGut. Prior to placement within the MiGut, two of the four structures were coated with a synthetic hydrogel designed to mimic the mucosal layer within the GI tract. Two MiGut models were inoculated with human faeces (10% w/v) and samples were collected on days 4, 7, and 10 for DNA extraction and real-time quantitative PCR analysis. Biofilm samples were also removed for scanning electron microscopy (SEM). At early time points, biofilm populations from structures with the synthetic mucus present had an increased abundance of Akkermansia muciniphila, Enterococcus and Enterobacteriaceae compared to uncoated. SEM revealed visible biofilm on both uncoated and coated structures; over the observed time points, biofilm formation progressed from isolated regions to covering the entire surface. These results show that the addition of a synthetic mucus hydrogel allows for biofilm growth and alters the microbial composition to more accurately replicate in vivo conditions, with an increased abundance of mucin-degrading populations [3].

[1] Motta, J. P., et al, 2021, Nat Rev Gastroenterol Hepatol, vol. 18, no. 5, pp. 314-334.
[2] Tailford, L. E., et al, 2015, Front Genet, vol. 6, no. 81.
[3] Glover, J. S., et al, 2022, Sci Rep, vol. 12, no. 8456.

3D Tissue Engineered Models of Osteogenesis Imperfecta

Bognar I[1,2], Balasubramanian M[3], Green N[1,2], Trikic M[1], Reilly G[1,2]
[1]School of Chemical, Materials and Biological Engineering, University of Sheffield, [2] INISGNEO Institute for in silico Medicine, University of Sheffield, [3]School of Medicine and Population Health, University of Sheffield

Osteogenesis Imperfecta (OI) is a genetic disorder resulting in defective type I collagen synthesis, causing brittle bones and a heightened risk of fractures. It affects approximately 1 in 15,000 people worldwide. In vitro studies of OI face significant challenges. Patient-derived osteoblasts require invasive biopsies, exhibit high patient-specific variability, while also being prone to de-differentiation and genetic instability. Additionally, monolayer cultures fail to replicate the structural and mechanical characteristics of native 3D bone tissue, limiting their utility for studying collagen I-containing extracellular matrix (ECM), the primary outcome of interest in OI research. Our previous work demonstrated that fibroblast-derived ECM from OI patients exhibit distinct structural differences compared to healthy donors when cultured in 3D [1].

This study seeks to use a similar approach and overcome these limitations by culturing immortalised human mesenchymal stem cells (hMSCs) engineered with CRISPR/Cas9 (still in development) to mimic the genetic, molecular, and biochemical features of OI. The cells are to be cultured on electrospun polycaprolactone scaffolds, which provide a 3D environment supportive of osteogenic differentiation and bone-like ECM deposition. This ECM then may be observed via light sheet and second harmonic generation microscopy. Through these methods we hope to observe and accurately compare diseased ECM next to a strictly matched healthy control.
By offering a reproducible and scalable platform, this model has the potential to advance understanding of OI pathophysiology, facilitate drug development, and support therapeutic innovation for this debilitating disorder.

[1] Y. Cebe et al., 2022, Tissue Eng. Part A, vol. 28, no. S1, pp. S-1–S-654.

Anatomically guided manufacture of multicomponent scaffolds for calcaneofibular ligament replacement

Paxton J[1,2], Mok S[1,2], Grant R[3], Radacsi N[3,4,5], Simpson H[6,7]
[1]Anatomy@Edinburgh, Edinburgh Medical School, University Of Edinburgh, [2]Centre for Discovery Brain Sciences, Biomedical Sciences, University of Edinburgh, [3]School of Engineering, Institute for Bioengineering, University of Edinburgh, [4]School of Engineering, Institute for Materials & Processes, University of Edinburgh, [5]Centre for Cardiovascular Science, The Queen's Medical Research Institute, University of Edinburgh, [6]Centre for Inflammation Research, University of Edinburgh, [7]Academic Centre for Healthy Ageing, Barts Health NHS Trust, Queen Mary University

The calcaneofibular ligament (CFL) of the lateral ankle ligamentous complex is frequently injured, particularly at the enthesis, where complex structure and mechanical stress complicate healing [1,2]. As a result of poor surgical outcomes, tissue-engineered repair strategies are increasingly explored. This study aims to (1) develop anatomically accurate bone-ligament scaffolds incorporating the enthesis, based on CFL morphometrics, and (2) evaluate their ability to support cell adhesion and proliferation for CFL regeneration. CFL scaffold blueprints were created using CAD software (Shapr3D, Tinkercad) based on anatomical morphometrics. Brushite cement mimicked bone, while random and aligned polylactic acid electrospun fibres replicated ligament structure. Cell adhesion and proliferation were assessed using differentiated rat osteoblasts and rat tendon fibroblasts, with SEM and confocal imaging used to examine cell distribution. A CFL bone-ligament model was developed using precise anatomical morphometrics (Figure 1). Brushite scaffolds showed 54% porosity, comparable to native trabecular bone [3]. Electrospun fibres (1.3–3.4 µm) replicated native collagen alignment. The scaffolds were biocompatible, with no cytotoxicity or attachment issues. Imaging showed widespread cell distribution, including within pores, and quantitative analysis confirmed proliferation over time. This study presents the successful development of an anatomically accurate CFL bone-ligament scaffold, with brushite cement mimicking bone porosity and electrospun fibres replicating ligament architecture. Cell studies confirmed biocompatibility and support for osteoblast and fibroblast growth, highlighting potential for ligament repair. Future work will establish a co-culture system to model the enthesis and assess tissue integration through histology, immunohistochemistry, and mechanical testing.

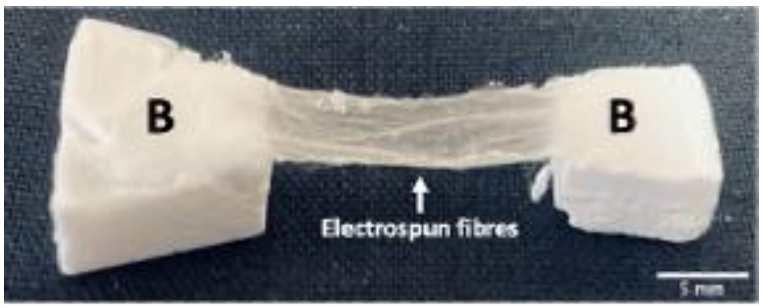

Anatomically accurate CFL bone-ligament scaffold. Electrospun fibres embedded in brushite cement mimicking the attachment of the CFL. B: Brushite cement

[1]Noguchi, H. 2019. Location and morphology of acute lateral ligament injury of the ankle. American Orthopaedic Foot & Ankle Society Meeting. [2]Li, Q et al., 2024. Prevalence and injury patterns of CFL injury in chronic lateral ankle instability: An observational cross-sectional study using ultrasound. J Foot Ankle Surg, 63:27-32.

Nanovibration driven chondrogenesis

Cuahtecontzi Delint R[1], Rigou I[1], Day G[1], Cantini M[1], Tsimbouri P[1], Childs P[2], Salmeron-Sanchez M[1], Dalby M[1]
[1]University Of Glasgow, [2]University of Strathclyde

Cartilage is avascular and so suffers poor healing and unattended cartilage damage results in osteoarthritis (OA), the most prevalent chronic pathology of joints. OA costs the UK £13B pa including indirect costs such as days lost from work; which makes novel strategies for OA a research priority.(1)

Current therapies such as autologous chondrocyte implantation (ACI) or matrix-assisted ACI (MACI) have been a focus on cartilage regeneration for >25 years. Success is limited as cultured chondrocytes from human mesenchymal stromal cells (hMSCs) require TGFb to regain phenotype, resulting in deep cartilage (collagen X-rich) rather than hyaline cartilage (collagen II-rich) phenotype in culture, therefore approaches to substitute TGFb in the clinic are needed.

The Centre for Cell Microenvironment have used nanovbration as a mechanotransduction cue to differentiate hMSCs into bone cells. Here, we want to direct the differentiation of hMSCs into chondrocytes that produce matrix rich in collagen II, the hyaline phenotype. The hMSCs are seeded as a dense micro-mass on the well plate to mimic 3D conditions, and the level of chondrogenesis measured at the gene and protein level to find SRY-box transcriptor factor (SOX9), collagen II, collagen X, and aggrecan, along with histological staining.

The obtained results so far have shown the possibility of using nanovibration to direct chondrogenesis at 21 days in a donor and age dependent manner. More studies are being carried out to optimise the system.

Funded by EPSRC

(1) Eldridge Sci Trans Med 2020. (2) Tsimbouri Nat Biomed eng 2017.

Deer Antler - Derived Scaffold for Repair of Bone Defect

Zhang J[1]
[1]University College Of London

Patients who have bone abnormalities or fractures may experience major health problems. Extracellular matrix (ECM) is known to be an efficient and promoting component and structure to facilitate the process of critical-sized bone regeneration, which has been actively investigated for clinical therapies using bio-scaffolds. It is difficult to repair defects completely in adult mammals because they cannot regrow complex tissues and organs. This criterion is broken by the totally bony growth of deer antler, which offers an unique opportunity to investigate cutting-edge strategies for quick bone regeneration. Here, an ECM bone matrix scaffold is built by taking use of the antlers' structural, biochemical, and biophysical properties. It is decellularized deer antler to obtain an ECM bone matrix scaffold. The ECM bone matrix promotes BMSCs proliferation to repair bone defect. In addition, the ECM bone matrix regulates the polarization of macrophage into M2 by targeting MRS1 gene and activating Akt/PI3k pathway to impact immunomodulation. And M2 macrophage further promotes new-born BMSC to differentiate toward osteoblast to repair bone defects. In vivo, the ECM bone matrix scaffold triggers rapid bone formation in different animal models. These findings provide practical insights to develop a therapeutic intervention for treating severe bone defects.

Measuring ultrasound-induced vibrations on cell substrates for bone healing using laser Doppler vibrometry

Orthodoxou A[1], Lucas M[1], Mulvana H[1]
[1]University Of Glasgow

Low-intensity pulsed ultrasound has shown promise in promoting bone healing, but the precise mechanical stimuli experienced by cells during treatment remain poorly defined. While many in vitro studies attribute biological responses to ultrasound stimulation, the specific displacements at the cell substrate interface are rarely quantified or characterized. This study uses laser Doppler vibrometry to measure the vibrational displacement of cell culture substrates exposed to therapeutic ultrasound, aiming to better understand the mechanical environment relevant to regenerative healing processes.

A custom setup was used to scan substrates immersed in water and exposed to ultrasound at clinically relevant parameters. Fast Fourier transform analysis was performed on time-resolved velocity data from over 300 spatial points to quantify vibration amplitudes and frequency components across the sample surface.

Results revealed non-uniform vibration fields across the substrate with displacement amplitudes in the nanometer range being the highest at the centre of the beam and decreasing as we move away, as expected from hydrophone field mapping measurements. A dominant frequency of 1 MHz was consistently observed, alongside bands at multiples of the pulse repetition frequency. These findings offer quantitative insight into the mechanical cues potentially sensed by adherent cells during ultrasound-induced bone healing. This work provides the foundation for correlating mechanical stimuli with biological outcomes and supports more targeted design of in vitro experiments and ultrasound protocols in bone tissue engineering.

Integrating Women's Health into Biomedical Engineering Curricula

Hearnden V[1,2], Martinez J[1]
[1]School of Chemical, Materials and Biological Engineering, University of Sheffield, [2]INSIGNEO Institute, University of Sheffield

Sex disparities in healthcare outcomes are extensively documented, highlighting the need for more inclusive biomedical engineering innovations. Currently, undergraduate curricula in biomedical engineering often lack comprehensive content focused on women's health, resulting in limited preparation for addressing sex-specific challenges. This study aimed to explore the perceptions of students and educators at one UK institution regarding the importance and integration of women's health within biomedical engineering education.

The study, approved by the University of Sheffield Research Ethics Committee, utilised a mixed-methods, cross-sectional approach. Responses were collected from 35 participants—32 students and 3 educators—to assess how women's health is presently incorporated into the undergraduate curriculum. Qualitative insights were obtained through open-ended questions, interviews, and a focus group, with analysis conducted via thematic coding.

Findings revealed that the majority (91.4%) of respondents thought the current curriculum addressed sex-specific health differences "poorly" or "not at all". Conversely, 97.1% recognised women's health topics as "important" or "very important" within the context of biomedical engineering. Reasons cited by students for their interest in women's health included increasing understanding and awareness, enhancing future career prospects, promoting inclusivity in medical technology design, and personal interest.

Identified barriers to integrating women's health topics into the curriculum included limited space within the existing program, perceived low prioritisation of the subject, and institutional resource constraints. Overall, this study highlights a gap between student interest and curriculum content, and these findings will be used to inform the development of women's health related curricula for biomedical engineering students in the future.

An Inclusive Webapp to Enable Preventive Interventions for Girls and Women affected by Female Genital Mutilation and Cutting

Basil M[1], Mattireddy S[1], Channiwala A, Callaghan S[1], Levine D[1], Kaul H[1]
[1]University Of Leicester

Female Genital Mutilation and Cutting (FGM/C) affects >400,000 girls/women in the US. Survivors experience urinary problems, vaginal/pelvic pain, painful intercourse, and mental ill health. Planning and deploying effective, sustainable, and affordable solutions is not possible because relevant authorities cannot draw on the available high-quality data.

To address this issue, we developed a webapp enabling geospatial visualisation of an existing FGM/C database and added features to accelerate localised interventions. The webapp is based on a database [1] that includes FGM/C prevalence at national, state, county and public use micro area levels. Data was visualised geospatially via Mapbox [2]. To enable localised interventions, we combined the FGM/C data with proximity information for nearby hospitals, private and public schools.

We made the webapp inclusive in three ways. First, our design enabled intuitive navigation, wide accessibility, and inclusive functionality. Second, we built the webapp iteratively with stakeholders. Third, we enabled visualisation of data on females from multiethnic backgrounds associated by ancestry or place of birth with 26 countries of origin.

Our users include state-level coalitions, health service planners, and federal law enforcement agencies in the US. Organisations are using the webapp to develop preventive interventions, including training of teachers/medics, community engagement, legislation advocacy, etc. Our users agreed that the webapp is easy to navigate, inclusive, accessible and effective.

Our webapp makes risk and prevalence data actionable for the first time thus supporting stakeholders to better protect vulnerable populations and support survivors. It represents a step-change in how we approach the health challenges of FGM/C.

[1] S. Callaghan, Female Gential Mutilation (FGM/C) in the United States. A study of the prevalence, distribution, and impact of FGM/C in the US, 2015-2019, Center for Open Science, 2023.
[2] Mapbox, “Mapbox,” 2025. [Online]. Available: https://www.mapbox.com/. [Accessed 2025].

Biomechanics of Uterine Scaffolds: Supporting Innovation in Women's Healthcare

Desai A[1], Hugo J[1], Jennings L[1]
[1]University Of Leeds

Uterine tissue regeneration offers a promising approach for patients with intrauterine adhesions or post-cancer damage, where current treatments often fail to restore full function [1]. Uterine transplantation is limited by donor availability and immunosuppression requirements, highlighting the need for scaffold-based alternatives that restore native tissue function.

This study assessed the mechanical properties of biological and synthetic materials for uterine scaffold development. Biological groups included porcine and ovine cellular uterus (native controls), porcine cellular bladder (potential alternative base scaffold source), and porcine and ovine uterus fixed with 0.6% glutaraldehyde (GA). Synthetic materials comprised Gelacell™ PLGA and thermoplastic polyurethane (TPU). Uniaxial tensile testing was performed in axial (A) and circumferential (C) directions for biological ($n \geq 8$) and synthetic ($n \geq 12$) specimens. Biological tissues were tested hydrated at 37°C, while synthetic materials were tested dry at 20°C. Modulus was derived from the collagen-dominated region for biological tissues and the linear elastic region for synthetic materials. Ultimate tensile strength (UTS) and failure strain were reported where measurable. Data were analysed using one-way ANOVA and Tukey's post hoc test ($p<0.05$).

GA fixation significantly reduced axial UTS in ovine uterus compared to cellular controls ($p< 0.001$). Porcine cellular bladder showed mechanical properties within the range of native uterus, indicating potential as a biological scaffold [Table 1]. PLGA displayed higher stiffness in the circumferential direction than axial ($p=0.017$). TPU showed high extensibility but lacked the triphasic stress-strain profile of compliant uterine tissue.

These results support further investigation of these materials for uterine scaffold applications, including biocompatibility and regenerative potential.

Group Name and Specimen Tested Directions (A= axial and C=Circumferential)	Thickness	Ultimate Tensile Stress (UTS)	Modulus	Failure Strain
	Mm	MPa	MPa	%
Cellular Control Groups				
Porcine Cellular Uterus (A)	1.47 ± 0.37	0.50 ± 0.24	2.46 ± 1.98	66.76 ± 49.78
Porcine Cellular Uterus (C)	1.42 ± 0.30	0.56 ± 0.24	2.07 ± 0.97	45.48 ± 12.59
Ovine Cellular Uterus (A)	1.89 ± 0.52	1.10 ± 0.49	2.80 ± 1.27	88.31 ± 20.67
Ovine Cellular Uterus (C)	1.76 ± 0.42	0.32 ± 0.11	0.92 ± 0.36	43.45 ± 34.82
Biological Scaffold Groups				
Porcine Cellular Bladder (A)	1.46 ± 0.24	0.95 ± 0.22	0.63 ± 0.20	176.06 ± 28.85
Porcine Cellular Bladder (C)	1.36 ± 0.16	1.18 ± 0.32	1.18 ± 0.49	154.95 ± 35.35
Porcine Uterus 0.6% GA Fixed (A)	4.14 ± 0.82	0.40 ± 0.14	1.19 ± 0.37	73.63 ± 28.04
Porcine Uterus 0.6% GA Fixed (C)	4.46 ± 0.79	0.40 ± 0.20	1.41 ± 0.79	49.15 ± 10.89
Ovine Uterus 0.6% GA Fixed (A)	4.64 ± 1.56	0.28 ± 0.23	0.59 ± 0.38	69.09 ± 15.49
Ovine Uterus 0.6% GA Fixed (C)	4.47 ± 1.10	0.25 ± 0.13	0.81 ± 0.46	47.21 ± 19.48
Synthetic Scaffold Groups				
Gelacell™ PLGA (A)	0.16 ± 0.00	0.12 ± 0.01	0.31 ± 0.02	57.75 ± 2.74
Gelacell™ PLGA (C)	0.16 ± 0.00	0.26 ± 0.06	2.68 ± 1.03	16.61 ±16.47
Thermoplastic Polyurethane (TPU)	1.58 ± 0.01	—**	10. 1.25	—**
-**Not acquired				

Table 1: Mechanical Properties of Native cellular, Fixed, and Synthetic Materials (Mean ± 95% Confidence Limits)

[1] Z. Wei et al., 2022, iScience, vol. 25, no. 12, pp. 105657.

Point-of-care Cassette for nucleic acid-based HPV diagnosis.

Boswell E[1], Barnes R[1], Awinda G[2], Nyataya J[2], Waomba K[2], Bahati F[2], Onyango C[2], Waitumbi J[2], Kariuki S[2], Onono M[2], Reboud J[1], Cooper J
[1]University Of Glasgow, [2]Kenya Medical Research Institute

Cervical cancer, nearly always caused by human papillomavirus (HPV), disproportionally affects people in low-resource settings. Nucleic acid amplification tests at the point-of-care are required to reduce this burden [1]. We have designed a simple-to-use, point-of-care cassette (Fig. 1), which incorporates sample preparation from a self-taken swab, amplification of multiple hrHPVs and an internal cellularity human control using a loop-mediated isothermal method (LAMP), and low-cost lateral flow readout.
Analytical limits of detection were determined for all three assays using synthetic DNA: between 1,000-10,000 copies/reaction for HPV16 and GAPDH, and 100-1,000 copies/reaction for HPV18. A one-step sample preparation method, consisting of resuspending cervical samples from a biobank in 0.5% Tween-20, was validated using qPCR. The prototype point-of-care diagnostic cassette was recently tested with collaborators at Kenya Medial Research Institute (KEMRI), using 150 freshly taken clinical samples, and analysis of its performance will be shared in our communication.

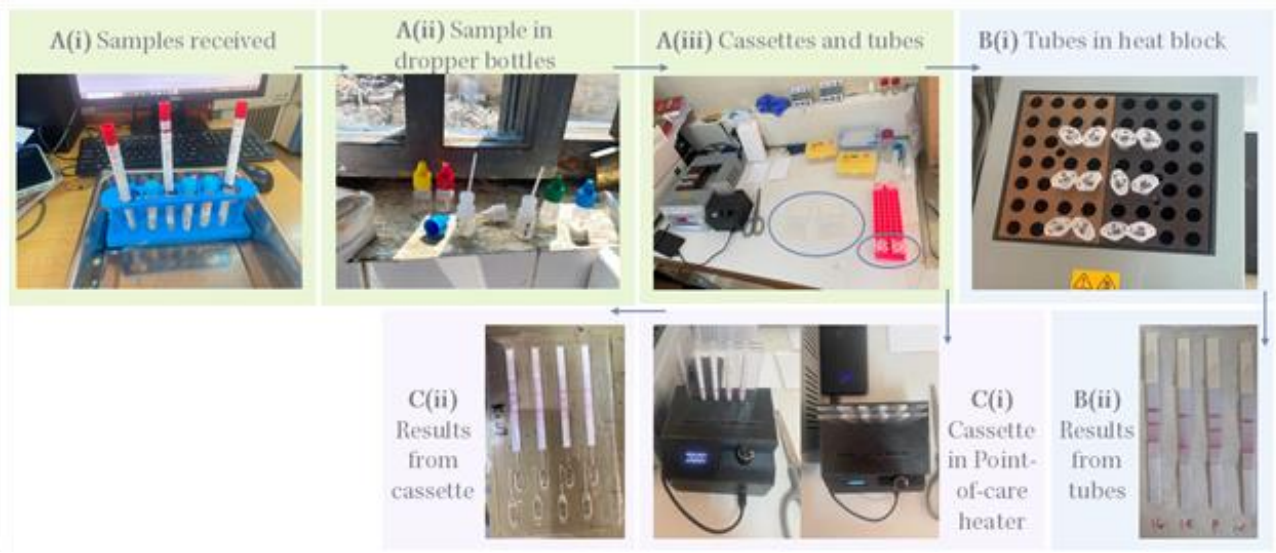

Figure 1. Testing vaginal samples for HPV using one-step sample preparation and LAMP, in cassette and tubes (controls), in Kenya.

[1] World Health Organisation, 2024, in “Target product profiles for human papillomavirus screening tests to detect cervical pre-cancer and cancer”.
[2] ICO/IARC, 2023, in “United Kingdom: Human Papillomavirus and Related Cancers”. Accessed: 24-04-2025. [Online] www.hpvcentre.net
[3] ICO/IARC, 2023, in “Kenya: Human Papillomavirus and Related Cancers”. Accessed: 24-04-2025. [Online] www.hpvcentre.net

Comparative Evaluation of Deep Learning Architectures for Automated Cell Image Classification Toward Industrial Biotech Applications

Graemer P[1], Williams J[1], Reid S[1], Childs P[1], Di Caprio G[1,2]
[1]University of Strathclyde, [2]University of Glasgow

Cell engineering is expected to play a central role in the future of regenerative medicine [1]. However, the translation of promising cell therapies remains limited by challenges in reproducibility, safety validation, and biomanufacturing scalability. One bottleneck is the lack of generalizable, automated tools for cell image classification. In this study, we evaluate a wide range of deep learning architectures for multi-class classification of cell types using the large-scale LIVECell dataset [2], which comprises over 5,000 microscopy images (FOVs are 0.875 × 0.645 mm2) containing approximately 1.6 million annotated single-cell instances across eight morphological classes. Our models include custom-built convolutional neural networks (CNNs), ResNet-style models, and state-of-the-art vision transformers (ViTs), such as Swin Transformer, and EVA-02 [3]. Each architecture was trained on both full and reduced datasets using A100 GPUs, with performance benchmarked across metrics including test accuracy, F1 score, inference latency, training time, GPU memory usage, and model complexity. ViTs and hybrid architectures achieved the best overall trade off between accuracy and computational efficiency, making them strong candidates for real time, closed loop cell classification systems. This work contributes to the foundation of next-generation bio-manufacturing pipelines, where image-based feedback could guide real-time cell manipulation and decision-making. Aligned with efforts at the Centre for the Cellular Microenvironment, this research supports the vision of automated, scalable workflows in cell and tissue engineering, replacing trial-and-error processes with dynamic, data-driven optimization. Results were generated using the ARCHIE-WeSt High Performance Computer at the University of Strathclyde.

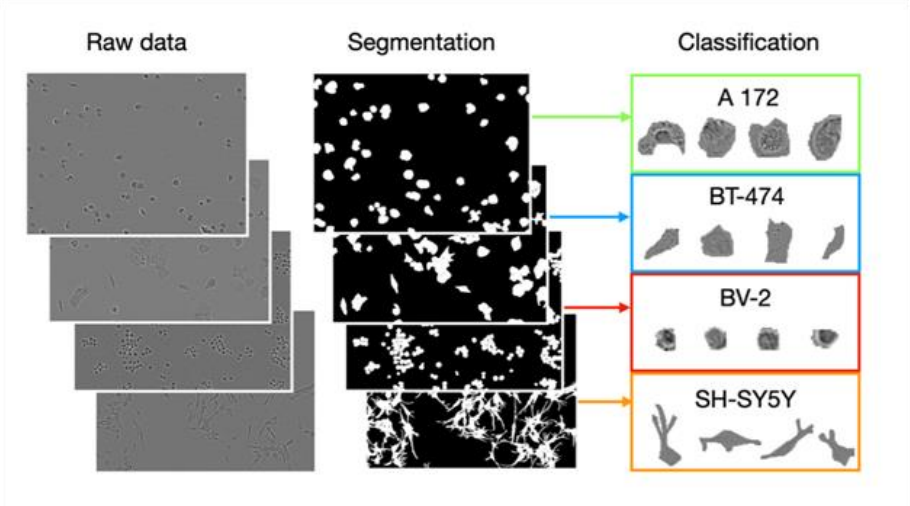

Figure. Deep learning pipeline with raw images, segmentation, and classification of four human cell lines from phase contrast microscopy data.

[1] R. Margiana, et al., 2022, Stem Cell Res Ther, vol. 13, no. 1, pp. 366.
[2] C. Edlund, et al., 2021, Nat Met, vol. 18, pp. 1038–1045.
[3] Y. Fang, et al., 2024, Image Vis, vol. 149, pp. 105171.

Machine Learning Enhanced Impedance Probe For Real-time Monitoring of Perfusion In Free Flaps Post Micro reconstructive Surgeries

Meselmani N[1], Biggs M[2]
[1]LifETIME CDT, CÚRAM – SFI Research Centre for Medical Devices, University of Galway, [2]Department of Biomedical Engineering, CÚRAM – SFI Research Centre for Medical Devices, University of Galway

Free flap perfusion monitoring poses critical challenges in micro-reconstructive surgeries, as these procedures are susceptible to failure due to postoperative vascular complications. These complications significantly increase patient morbidity and healthcare burdens [1]. Current monitoring methods rely on intermittent and subjective assessments, which have a 5% failure rate in detecting early markers of venous congestion [2, 3]. In this study, a perfusion monitoring device that utilizes electrical impedance spectroscopy (EIS) integrated with machine learning algorithms is introduced. Our approach allows continuous tissue perfusion monitoring, facilitating timely clinical interventions, thus preventing irreversible tissue damage.
Initially, a benchtop system employing an impedance analyser and a set of geometrically optimised electrodes was designed to assess the feasibility of ElS for perfusion monitoring. Cucumbers were used as tissue phantoms, distinguishing normal (hydrated) and compromised (dehydrated) perfusion states. Impedance data over a frequency sweep from 0.1 Hz to 1 MHz enabled the training of a neural network that achieved a 99% accuracy rate in differentiating between normal and dehydrated cucumber samples.
Building on these findings, a portable prototype is currently under development, integrating a minimally invasive microelectrode array patch, a precision impedance analyser, and a Raspberry Pi-based computing unit. The microelectrode array was fabricated using direct metal laser sintering (DMLS). Complete system integration is in progress, with validation studies planned for the upcoming phase.
The findings highlight the potential of EIS and machine learning to detect physiological changes and demonstrate high sensitivity to variations in water content. This indicates considerable promise for identifying early venous congestion.

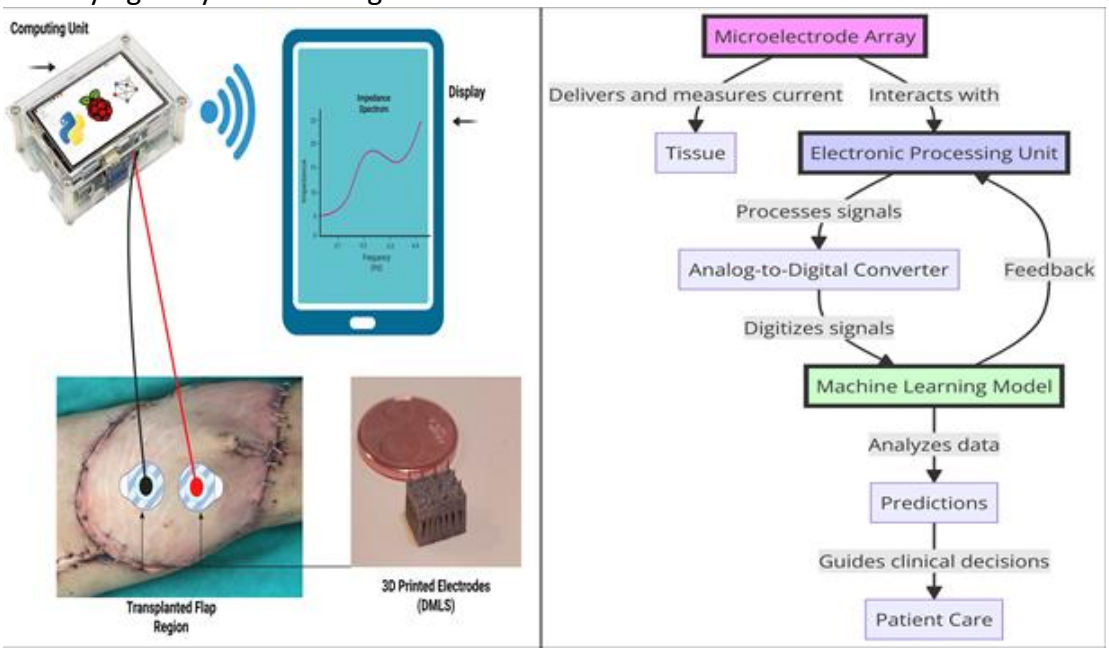

Schematic showing the prototype setup for the impedance-based monitoring of flap perfusion using 3D metal-printed electrodes.

[1] S. Knoedler et al., 2023, Front. Surg., vol. 10, pp. 1130566.
[2] F. Boissiere et al., 2021, Plast. Reconstr. Surg. Glob. Open, vol. 9, no. 1, pp. e3327.
[3] W. Wang et al., 2020, Semin Plast Surg., vol. 34, no. 4, pp. 314–320.

Evaluating nnUNet for Automated Cardiac CT Segmentation in Paediatric Congenital Heart Disease

Yu S[1], Fouad S[2], Novak J[3], Fratini A[1]
[1]Engineering for Health Research Centre, Aston University, [2]School of Computer Science and Digital Technologies, Aston University, [3]Aston Institute of Health & Neurodevelopment, Aston University

Congenital heart disease (CHD) refers to structural abnormalities of the heart and great vessels, affecting approximately one in 100 births [1]. These morphological abnormalities result in significant complications with circulation, oxygenation, and cardiac function, with diagnosis highly reliant on radiologists and clinician's available time. Medical image segmentation can be performed to isolate and extract anatomical regions of interest, producing a precise virtual 3D model. However, manual, and semi-automated segmentation approaches are labour-intensive and subject to inter and intra operator variability. Artificial intelligence (AI) driven deep learning approaches are increasingly explored for automated segmentation, yet its application for congenital heart disease, especially utilising paediatric datasets remains underexplored. The nnUNet, a state-of-the-art supervised deep learning framework was evaluated for CT segmentation in congenital heart disease [2]. Contributions of this research include refined relabelling of an open-source CHD dataset [3] to consist of exclusively 95 paediatric CT image sets, additionally six clinically relevant cardiac substructures were included (Superior and Inferior Vena Cava and four Pulmonary Veins). Five nnUNet configurations were compared: 2D, 3D - low resolution, full resolution, cascade full resolution and a GPU optimised preset (nnUNet ResEnc M). Additional experiments compared 7 with 13 structure segmentation as well as manual vs automatic data splitting. From preliminary results, 3D cascade full resolution was the best performing model (mean validation Dice Similarity Coefficient (DSC) 0.803), minimal difference (<0.01 DSC) was found between manual and automated splitting of data into training, validation, and testing sets and seven substructure segmentation outperformed 13 substructures by approximately 11%.

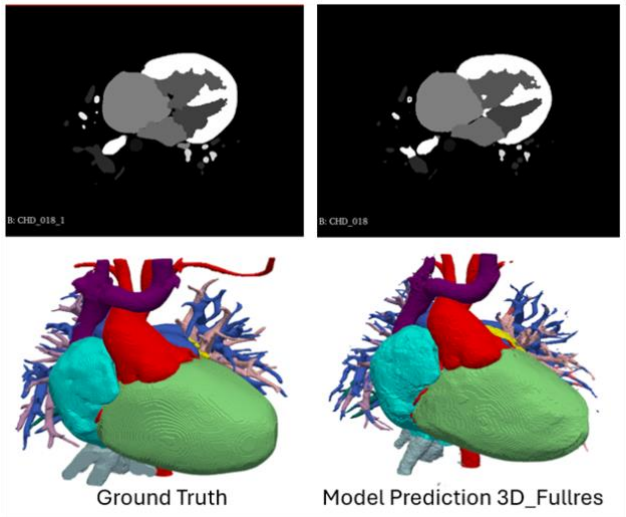

Comparison between ground truth and 3D_fullres model prediction. Top row shows axial CT slice, bottom row shows corresponding 3D visualisations

[1] Bakker, M.K., et al (2019). BMJ Open, 9(7), p.e028139.
[2] Isensee, F., et al (2020). Nature Methods, [online] 18(2), pp.203–211. doi:https://doi.org/10.1038/s41592-020-01008-z.
[3] Xu, X., et al (2020). Medical Image Computing and Computer Assisted Intervention – MICCAI 2020, pp.77–87.

Data-Driven Interactive Visualisation Platform for Paediatric Intensive Care Using the PIC Database

Alkooheji E[1], Fouad S[1], Fratini A[1], Kavakli-Thorne M[1], Angelova M[1]
[1]Aston University

Recently, the government pressured the National Health Service (NHS) to improve its productivity by at least 4% while cutting costs by at least 1% for the upcoming year [3]. Additionally, such issues negatively affect the paediatric intensive care unit (PICU) as they must make quick and critical decisions with the increasing number of patients and limited available beds. To address these issues, we have developed an interactive visual analytics tool that facilitates the exploration of multimodal data from the Paediatric Intensive Care (PIC) database [1]. Collected from the Children's Hospital of Zhejiang University School of Medicine between 2010 and 2018, the PIC database includes over 12,000 admissions, capturing detailed information on demographics, vital signs, laboratory results, medications, and clinical notes. Our tool integrates open-source Python-based data processing and visualisation libraries (Pandas, Seaborn, and Matplotlib) into an interactive timeline interface, allowing clinicians to explore and correlate variables across time and patient cohorts and allowing it to be reusable on any structured medical data. This tool draws on a structured pipeline adapted from methodologies established for MIMIC-IV, tailored for the paediatric context [2]. It presents clinicians with relevant patient data on demand, enables the identification of clinical trends, and allows informed timely decision-making. By improving the utilisation, availability and readability of sophisticated data, the solution will support better outcomes in PICUs and contribute directly to NHS goals of care modernisation and addressing system pressures [3].

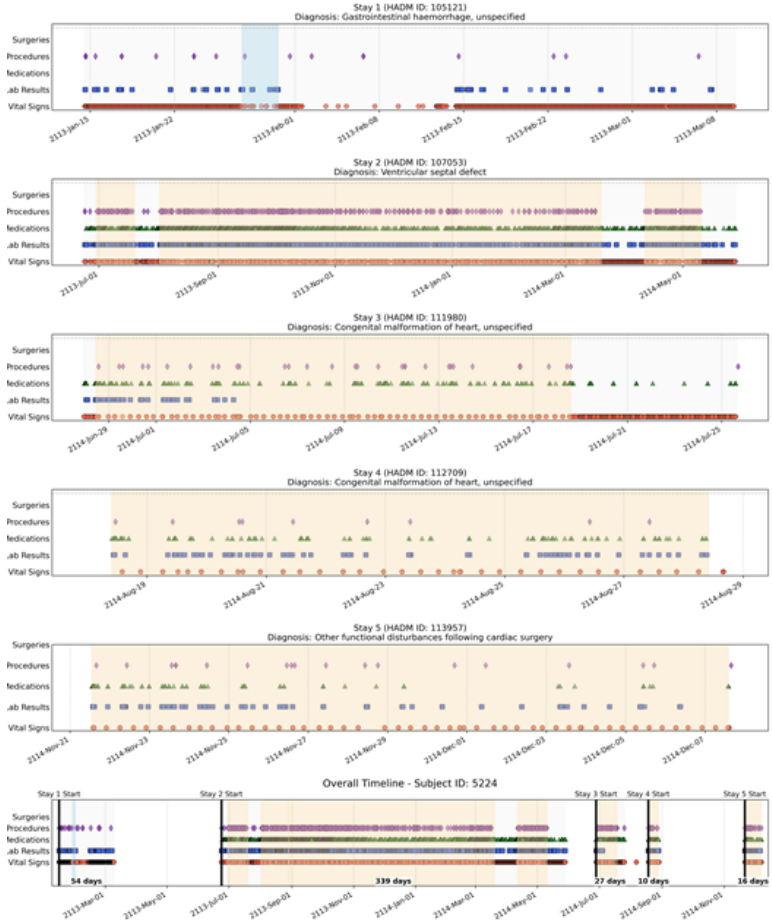

[1] Zeng, X. et al., 2020, Scientific Data, 7(1). https://doi.org/10.1038/s41597-020-0355-4
[2] Gupta, M. et al., 2022, in Proceedings of Machine Learning Research, 193, pp. 311–325.
[3] NHS England, 2025. NHS England» 2025/26 priorities and operational planning guidance. https://www.england.nhs.uk/long-read/2025-26-priorities-and-operational-planning-guidance/

Micromechanics in Human Prostate:

A Histology-Based Computational Homogenisation Approach

Chen Y[1], Anderson C[1], Ntala C[2], Ozel A[1], Reuben R[1]
[1]Heriot-watt University, [2]NHS Scotland

Human prostatic tissue exhibits complex mechanical behaviour due to its multiphasic, heterogeneous nature, involving interconnected epithelial, stromal, and luminal components. This study aims to develop a computational framework to quantify how microstructural changes, particularly in pathological conditions such as cancer, affect mechanical properties.
Representative 2D and 3D tissue microstructure models were reconstructed from high-resolution histology images. Epithelial compartments and acinar lumens were modelled as hyperelastic materials, while the collagen-fibre-rich stromal tissue was modelled using the Holzapfel-Gasser-Ogden (HGO) model to explicitly account for tension-compression asymmetry due to collagen fibres [1]. Finite-element-based homogenization with periodic boundary conditions was used to evaluate apparent mechanical properties in both 2D and 3D samples [2] (Figure. 1). Structural analysis, including fabric tensor calculation and collagen fibre orientation mapping, was performed to investigate changes associated with cancer progression.
The 2D analysis of normal prostate tissue revealed a strong correlation between the area fraction of tissue constituents and their microstructural fabric tensor. Results demonstrated significant mechanical and structural anisotropy, primarily driven by the stromal collagen network. The stromal tissue played a dominant role in defining the overall mechanical response. Both the direction and magnitude of mechanical anisotropy were closely linked to stromal anisotropy.
This work presents a histology-based computational homogenization framework to quantify the apparent mechanical behaviours of human prostatic tissues. It serves as a foundation for understanding structure-property-function relationships in glandular tissues and cancers. Ongoing research extends this framework to assess structural and mechanical changes across different prostate cancer grades using 3D histology data.

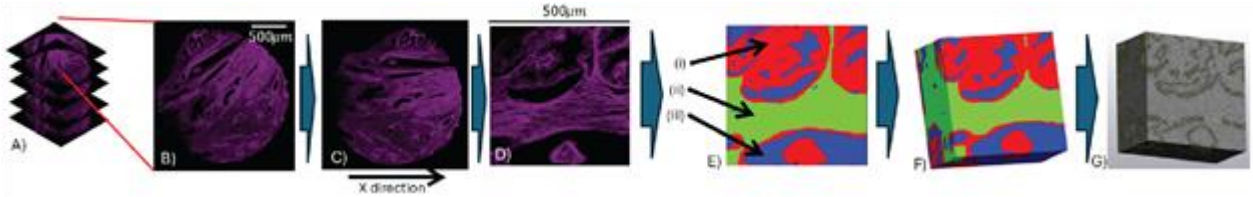

Confocal stacks were aligned (A), rotated (C), cropped (D), segmented (E), combined into 3D (F), and meshed for FEA (G).

Journal Articles:
[1] T.C. Gasser et al., J R Soc Interface, 3(6),15–35, 2005.
[2] D. H. Pahr and P. K. Zysset, Biomech Model Mechanobiol, 7(6), 463–476, 2008.

TomoSAXS enables quantification of nano- to whole-joint-scale structure and mechanics in the intervertebral disc

Parmenter A[1,2], Newham E[3], Chen J[1], Disney C[4], Snow T[4], Bosi F[1], Bay B[5], Terrill N[4], Gupta H[3], Lee P[1,2]
[1]University College London, [2]Research Complex at Harwell, [3]Queen Mary University of London, [4]Diamond Light Source, [5]Oregon State University

Collagen fibres in the annulus fibrosus (AF) of the intervertebral disc (IVD) form lamellar structures which enable load transfer and flexibility throughout the spine. This study combines synchrotron computed tomography (sCT), digital volume correlation (DVC) [1,2], and small angle X-ray scattering (SAXS) [3] to investigate nano-, micro- and whole-joint-scale biomechanics in the IVD.
In situ TomoSAXS (correlative sCT and SAXS) of fresh-frozen rat IVD was performed at Diamond Light Source. SAXS (2D maps, 9 angles) was performed at beamline I22, sCT at I13-2 (voxel size 1.6µm). 2 sets of scans were performed, first under 1N compressive preload, second after 50µm compression. Fibre analysis of sCT data (Avizo XFiber) measured fibre orientations in the AF. Deformation of fibres was quantified using DVC (iDVC). Tissue and fibre level strains (Fig.1a,b,c) were calculated through polynomial fitting of the displacement field [1,2]. TomoSAXS reconstruction using orientation data from sCT enabled the quantification of nanoscale structure and strain on a per-fibre basis (Fig.1d).
2% bulk IVD compression resulted in a mean AF tissue level compressive strain of 4.4±3.2 %, fibre strain magnitude of 2.7±2.9 %, and fibrillar strain magnitude of 1.8±1.5%. This hierarchical strain pattern likely arises due to load sharing between fibrous and matrix components, with composition varying across the IVD. Both lamellar and trans lamellar strain patterns were observed (Fig. 1b). Strain showed region specific correlations with fibre curvature, and collagen prestrain (initial D-period) was found to play a key role in fibrillar loading, showing a significant negative correlation with D-period strain ($p<0.01$).

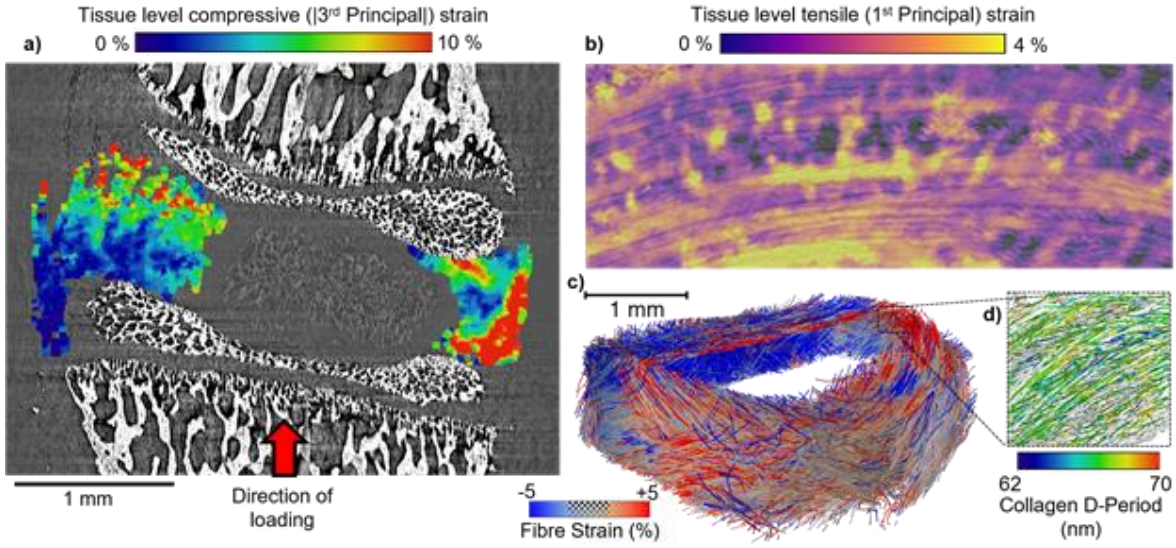

Figure: a) Compressive strain, b) anterior AF tensile strain, c) fibre strain, and d) initial collagen D-period in the IVD.

[1] A. L. Parmenter et al., 2024, bioRxiv
[2] C. M. Disney et al., 2022, Acta Biomaterialia, vol. 138, pp. 361-374
[3] W. Badar et al., 2025, Advanced Science, vol. 12, no. 1

Characterising And Simulating Posterior Vault Distraction In Crouzon Craniosynostosis - A Case Study

Franchetti-Romero V[1,2], Dong R[2], Samiepour Ardakani Y[2], Liang C[2], Paternoster G[3], Khonsari R[4], Moazen M[2]
[1]Université Paris Cité, École Nationale Supérieure d'Arts et Métiers (ENSAM) and Paris Sciences & Lettres (PSL), [2]Department of Mechanical Engineering, University College London, [3]Service de Neurochirurgie, Hôpital Necker - Enfants malades, Assistance Publique - Hôpitaux de Paris, CRMR CRANIOST, [4]Craniofacial Growth and Form Laboratory, Hopital Necker–Enfants Malades, Assistance Publique - Hopitaux de Paris, Faculte de Medecine, Universite Paris Cite

Crouzon syndrome involves early fusion of cranial joints, that restricts the brain growth, leading to skull deformities. Posterior vault distraction (PVD) is used to expand the skull and increase the intracranial volume (ICV) [1]. The aim of this study was to characterize PVD in an individual with sequential head computed tomography (CT) data and to develop a validated finite element (FE) model of PVD.
CT head scans at five time points (Figure A) were analyzed to characterize (a) osteotomy gap at several points (Figure B), (b) ICV, and (c) overall skull morphology (Figure C). A FE model was developed based on the preoperative CT (Figure D), simulating PVD by applying displacements at clinical distraction sites. A series of sensitivity analyses were carried out to the choice of elastic moduli of the ICV and osteotomies (that were identified to considerably impact the prediction of the FE model) [2]. In silico osteotomy widening and overall skull shape were compared to the clinical CT measurements.
CT analysis showed non-uniform distraction, with actual displacements across the osteotomy gap differing from the 1 mm/day distraction induced at the anatomical site that distraction was clinically fixed. Model were sensitive to the considered variable. The best agreement to clinical data (1.29% error) was achieved with a Young's modulus of 0.5 MPa for intracranial contents and 0.1 MPa for osteotomies.
The validated model developed in this study provides the foundation for further studies to advance clinical management of syndromic craniosynostosis, with future validation in larger cohorts being needed.

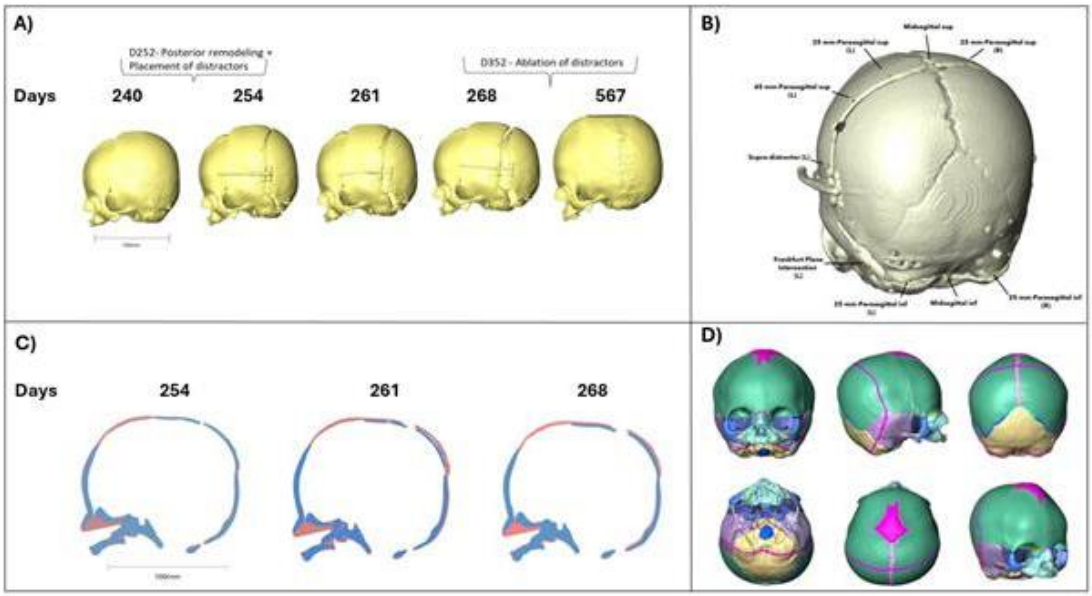

Figure: (A) CTs timepoints, (B) Osteotomy gap landmarks, (C) In-silico (pink) and in-vivo (blue) skull cross-sections, (D) In-silico model

[1] Craniosynostosis. David Johnson et al., 2011, Eur J Hum Genet., vol. 19, no. 4, pp. 369–376.
[2] Using Sensitivity Analysis to Develop a Validated Computational Model of Post-operative Calvarial Growth in Sagittal Craniosynostosis. Connor Cross et al., 2021, Front. Cell Dev. Biol, vol. 9.

From Ventricular Enlargement to White Matter Injury: A Biomechanical Perspective on Normal Pressure Hydrocephalus

Darvishi V[1], Del Giovane M[2,3], David M[2,3], Kolanko M[2,3], Sharp D[2,3], Malhotra P[2,3,4], Carswell C[2,4], Ghajari M[1]
[1]HEAD Lab, Dyson School of Design Engineering, Imperial College London, [2]Department of Brain Sciences, Imperial College London, [3]UK Dementia Research Institute Care Research and Technology Centre, Imperial College London and the University of Surrey, [4]Department of Neurology, Imperial College Healthcare NHS Trust

Normal pressure hydrocephalus (NPH), a potentially treatable cause of dementia, is marked by progressive ventricular enlargement and damage to periventricular white matter. However, the biomechanical mechanisms underlying these changes remain poorly understood. We developed a high-fidelity, anatomically detailed finite element (FE) model of the human brain incorporating key structures such as sulci, falx cerebri, septum pellucidum, and pia mater—features often omitted in prior models. Using MRI data from 30 healthy adults aged 62–82, we constructed an age-matched brain template. Ventricular expansion in NPH was simulated via a novel displacement-based approach derived from non-linear image registration between this healthy template and MRI scans from 22 NPH patients aged 54–85. This method improves upon traditional pressure-driven models by enabling anatomically realistic deformation of ventricular geometry [1],[2],[3]. The model accurately reproduced key imaging markers, including a 20.5% increase in Evans Index, a 70.8% reduction in posterior interhemispheric distance, and a 26.5% thinning of the septum pellucidum—closely matching MRI-based observations. Predicted strain patterns revealed localized mechanical stress in periventricular white matter regions that correspond with abnormalities seen in diffusion tensor imaging (DTI). DTI measures white matter abnormality, which can explain the symptoms of NPH patients. This modelling framework provides a mechanistic link between imaging biomarkers and tissue-level deformation, offering insights into disease progression. It also lays the groundwork for optimizing treatment strategies, such as surgical shunting, and exploring the broader role of biomechanics in neurodegeneration. Future work will incorporate patient-specific anatomy and axonal architecture to assess individual vulnerability to injury.

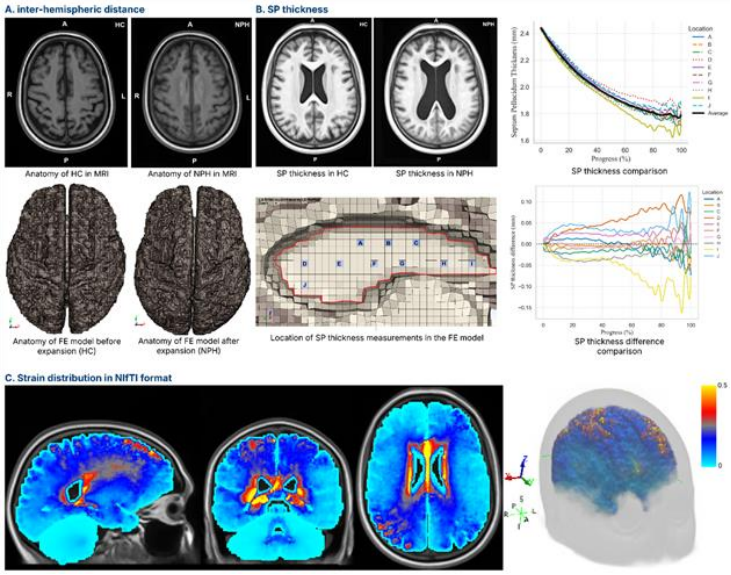

Figure: (A–B) MRI and model predict reduced inter-hemispheric distance and SP thickness. (C) Strain concentrates near ventricles in NPH.

[1] Shigenori K et al. , 2011, J neurology.[2] Dutta-Roy T et al. , 2008, J Biomech. [3] LefeverJ A et al. , 2013, J Biomech.

Patient-Specific Cervical Spine Finite Element Modeling to Advance the Understanding and Treatment of Degenerative Cervical Myelopathy

Mondal S[1], Davies B[2], Newcombe V[2], Sutcliffe M[1]
[1]Department of Engineering, University Of Cambridge, [2]Department of Medicine, University of Cambridge

Degenerative cervical myelopathy (DCM) is a common spinal disorder caused by progressive compression of the spinal cord due to degenerative changes in the cervical spine, leading to motor and sensory deficits [1]. Finite element (FE) analysis is critical for understanding DCM progression, representing individual injuries, and optimising surgical strategies. However, existing models often lack accurate representation of spinal cord anatomy, particularly the distinction between grey and white matter [1]. Patient-specific models are essential, as anatomical variability significantly influences spinal cord loading patterns and surgical outcomes. This study presents a patient-specific FE model of the cervical spine integrating CT and MRI data, combining high-resolution bone imaging with detailed soft tissue characterisation. Vertebrae and intervertebral discs were segmented from CT using MIMICS, while grey and white matter of the spinal cord were segmented from MRI using Spinal Cord Toolbox. 3D Slicer was used for image registration. In Abaqus, vertebrae were modelled as rigid bodies, and hyperelastic material properties were assigned to IVDs and spinal cord [2]. Ligaments were modelled using axial connectors with non-linear elastic properties [2]. High-quality meshing and appropriate contact definitions were implemented. The model was subjected to 1 Nm pure moments for flexion-extension with T1 fully constrained. Predicted intersegmental range of motion showed strong agreement with previous studies. Spinal cord stress-strain distribution due to the flexion-extension movement without pre-compression is shown in Fig. 1. Peak spinal cord strain occurred at points where the spinal cord narrows. This model provides a valuable tool for understanding DCM and guiding personalised treatment.

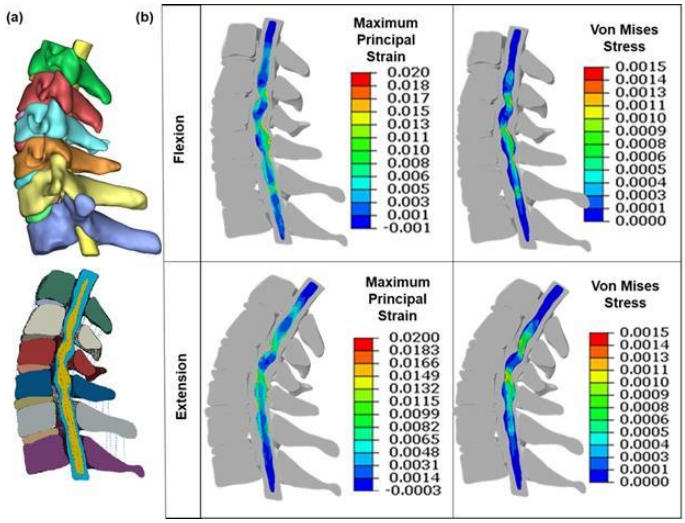

(a) Patient-specific spine model, and (b) stress-strain distribution at the spinal cord subjected to flexion-extension movement.

[1] Ben et al, 2022, Global Spine Journal, 12; 78-96.
[2] Sam et al. 2023, Brain and Spine, 3; 101743.

Synchrotron x-ray radiation induced damage in bone during in situ µCT experiments

Peña Fernández M[1], Sikorski M[1], Levin S[2], McPhee S[1], Sinclair L[3], Chen Y[1], Reinhard C[3], Wolfram U[2]
[1]Heriot-Watt University, [2]Clausthal University of Technology, [3]The University of Manchester at Harwell

In situ synchrotron radiation micro-computed tomography (SRµCT) experiments enable detailed analysis of bone microarchitecture and fracture mechanisms. However, ionising radiation can induce structural damage in bone tissue [1], complicating mechanical testing interpretation. This study investigates synchrotron X-ray radiation effects on cortical bone mechanical properties. Cortical bone specimens from ovine femur were prepared in longitudinal and transverse orientations and underwent in situ SRµCT (0.81 µm voxel size, 2250 projections, 0.2 s/projection) three-point bending tests at I13-2 (Diamond Light Source,), resulting in regions of high (notch location) and low (edge location) radiation exposure. Monte Carlo simulations [2] were used to simulate absorbed radiation dose rates, which ranged between 5 to 30 Gy/s (Figure 1a), resulting in local doses of 2.25-9 kGy at edge and 13.5-54 kGy at notch locations for one to four tomograms acquisition. Microindentation testing [3] revealed significant anisotropic responses (Figure 1b). In the transverse orientation, the highest radiation doses (54 kGy at notch) led to a 54% reduction in indentation modulus and a 73% decrease in contact hardness compared to control samples. Longitudinal orientation showed greater resistance with only 9% modulus reduction and 41% hardness decrease at equivalent doses. This radiation-induced softening near the notch may accelerate crack propagation, potentially due to ionisation changes in the non-fibrillar matrix [4]. These findings highlight the importance of considering radiation effects when interpreting SRµCT fracture experiments. Future work will integrate microstructural analysis with digital volume correlation to create a model accounting for radiation-induced damage in bone fracture mechanics at the microscale.

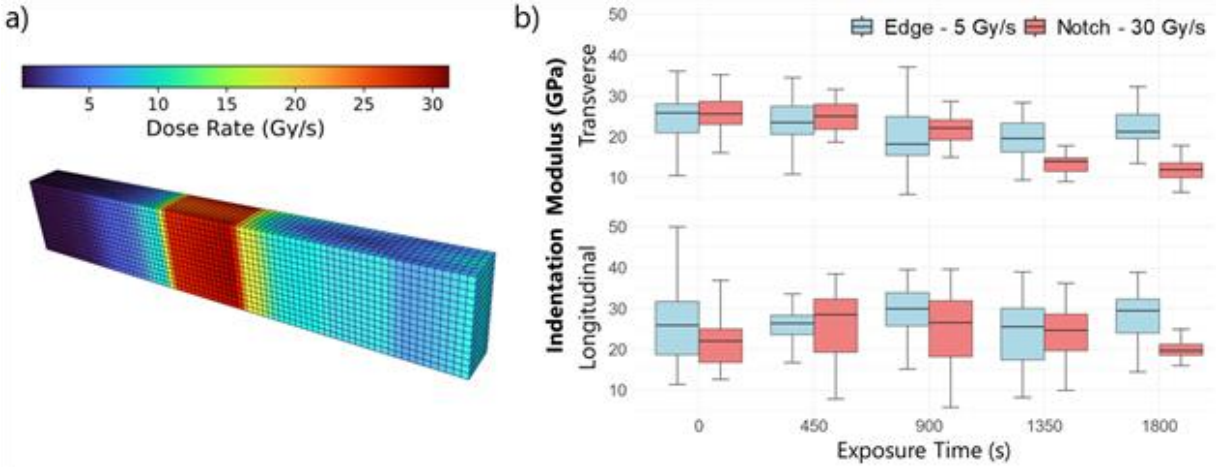

Figure 1: a) SRµCT dose rate distribution (180° rotation). b) Indentation modulus under increasing SR X-ray exposure time (n=3 samples/group).

[1] Peña Fernández et al., 2023, Acta Biomater., vol. 167, pp. 83-99.
[2] Battistoni et al., 2015, Ann. Nucl. Energy, vol. 82, pp. 10-18.
[3] Mirzaali et al., 2016, Bone, vol. 93, pp. 196-211.

Finite element modelling and validation of stent-induced growth and remodelling in aneurysmal aortas

Marimuthu S[1], Maclean C[2], Brodie R[2], Geelkerken R[3], McGinty S[1], Hill N[1]
[1]University Of Glasgow, [2]Terumo Aortic, [3]University of Twente

Biological tissues and organs constantly remodel due to stress or changes in homeostatic conditions. Following endovascular aortic repair, the aorta could grow and remodel over time to reduce the excessive stresses caused by the less compliant and oversized stent grafts (compared to the aorta). The most proximal rings of the Anaconda device (TerumoAortic, UK) are designed with high stiffness and a diameter larger than the aorta to obtain better fixation. These influence the increase in the diameter of the aorta and the reduction in the contact force between the stent graft and the aorta wall. Hence, it is necessary to understand and predict this adaptation to minimise complications such as device migration and endoleaks. This study aimed to understand the growth and remodelling (G&R) following stent graft implantation using a volumetric growth model with growth along the fibre direction. The framework was divided into pre- and post-growth phases, and the aorta geometry was assumed to be a simple cylinder with only the medial layer. The modified GOH model was used to model the aorta's hyperelastic anisotropic behaviour. To validate the framework, finite element simulation results were compared with abdominal aortic aneurysm patient data acquired at pre-operative discharge stages (Koenrades et al., 2018). Then, the growth parameters were estimated using follow-up (2 years) CT scan data. The dilation of the two proximal rings was captured, which closely matches the CT scan data, and the results from this study clearly show the reduction in aorta wall stresses due to vascular adaptation.

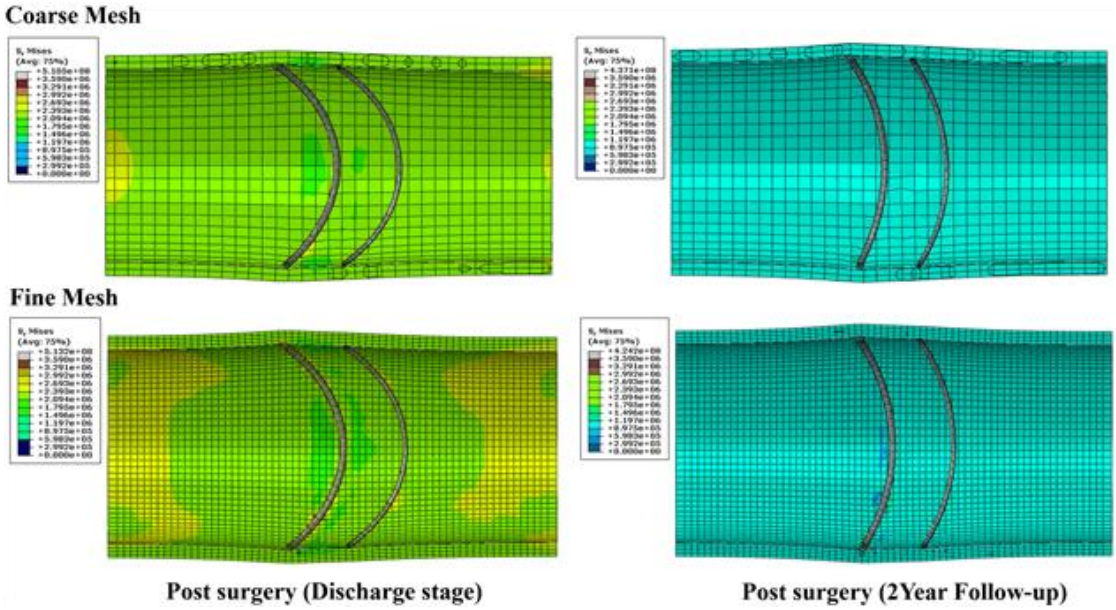

Plots showing the stent-induced von Mises stresses on the aorta. The results were validated using CT data.

Koenrades, M. A., Klein, A., Leferink, A. M., Slump, C. H., & Geelkerken, R. H. (2018). Evolution of the Proximal Sealing Rings of the Anaconda Stent-Graft After Endovascular Aneurysm Repair. Journal of Endovascular Therapy, 25(4), 480–491

Quantifying haemodynamic forces across the cerebral microvasculature using a computational modelling approach

Al-Areqi A[1,2], Coccarelli A[1,2]
[1]Department of Mechanical Engineering, Faculty of Science and Engineering, Swansea University,
[2]Zienkiewicz Institute for Modelling, Data and AI, Faculty of Science and Engineering, Swansea University

Steady blood flow to the brain is essential for maintaining its functionality by supplying it with oxygen and nutrients. Complex physiological mechanisms underlie the autoregulation of blood flow. Characterisation of these mechanisms requires profound knowledge of their multi-scale nature. Having efficient computational tools facilitates, in combination with experimental findings, a better understanding of blood flow autoregulation. With current 1D blood flow models, recovering haemodynamic quantities in arterial networks can be highly computationally demanding [1,2]. Furthermore, the degree of vascular constriction varies between different vessel types -such as arteries and arterioles- a feature that was rarely addressed by earlier models. In the current work, we introduce a computational framework to overcome these limitations. This framework comprises integrated multi-physics sub-models to represent vessel wall mechanics and haemodynamic forces of autoregulated cerebral micro-networks exhibiting spatial heterogeneous vascular contractility. Given the small vessel calibre and predominant quasi-steady blood flow within these networks, flow dynamics were modelled according to Poiseuille flow assumptions, enabling a computationally effective nonetheless consistent description of pressure-flow relationship. Results shows that the proposed computational framework offers greater efficiency while generating predictions of vessel diameter change and blood flow redistribution that are comparable to those of higher-fidelity models. Employing computational models that accurately capture the autoregulatory behaviour with computational efficiency yields deeper physiological insight into cerebral microcirculation and promotes the adaptation of computational tools within clinical applications.

[1] Epstein et al., 2015, Am J Physiol Heart Circ Physiol, vol. 309, no. 1, pp. H222-H234.
[2] Liu et al., 2024, Int J Numer Method Biomed Eng, vol. 40, no. 6, pp. e3828.

Development of a skeletonization algorithm for segmentation of disconnected and collapsed blood vessel networks

Burke O'Leary E[1], Walsh C[1], Berg M[1], Bosi G[1], Lee P[1], Shipley R[1]
[1]University College London

High-resolution imaging methods such as synchrotron computed tomography (sCT) and hierarchical phase-contrast tomography (HiP-CT [1]), combined with advanced algorithms, enable detailed segmentation of cardiac microvasculature. However, in ex-vivo tissue vessels often appear collapsed or fragmented due to the absence of physiological blood pressure, limiting the applicability of standard skeletonization algorithms for flow modelling. We present a shape-based skeletonization algorithm for disconnected and non-cylindrical vessel segmentations, enabling vascular graph construction for estimating tissue permeability - an important measure of microvascular function. The method mitigates false branching caused by non-circular vessel cross-sections and reconnects aligned endpoints that may otherwise impact permeability estimates.

Nodes are iteratively placed at local maxima of the 3D chamfer distance map (CDM) (Fig 1B) , with Gaussian-weighted spheres subtracted to avoid overlap (Fig 1C). Vessel direction is determined using principal component analysis (PCA) (Fig 1D), with centroid correction based on orthogonal re-slicing. A cone-search step connects nodes (Fig 1F), forming paths consistent with local vessel radius and direction. Boundary and internal node placement are handled separately, and edge nodes are filtered using modified CDMs. Radii are adjusted to correct for overestimation due to off-angle slicing. Seven algorithm parameters, including radius and search cone scaling factors, are optimised using quantitative and topological metrics, including one adapted from Walsh et al. [2].

Compared to standard methods [3], our approach can yield better-connected vascular networks, particularly in imaging datasets with segmentation artefacts. Its robustness to artefacts makes it well suited to ex-vivo biological imaging, including sCT.

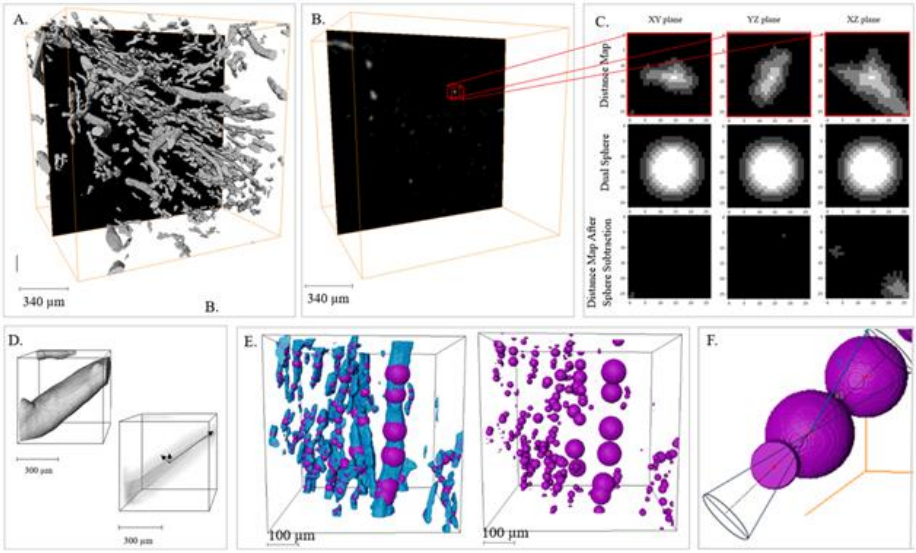

Figure: Skeletonization pipeline: segmented vessels (A), distance map (B–C), principal directions (D), nodes (E), and cone-search connectivity (F)

[1] Walsh C. L. et al., 2021, Nature Methods, vol. 18, no. 12, pp. 1532-1541.
[2] Walsh C. L. et al., 2024, Comput. Biol. Med., vol. 171, p. 108140
[3] Fouard C. et al., 2006, IEEE TMI, vol. 25 no. 10, pp. 1319-1328

Modelling diseased prosthetic valve leaflets for redo-tavi simulations

Sayeed T[1], Eren O[1], Yang S[1], Bressloff N[1]
[1]University Of Leeds

Degenerative aortic valve disease is a progressive condition where the aortic valve, which plays a vital role in blood regulation, gets damaged over time. The most common, minimally-invasive method to treat this condition is transcatheter aortic valve implantation (TAVI), where a bio-prosthetic valve is implanted within the diseased native valve via a catheter. Over time, these bio-prosthetic valves are likely to degenerate. When this happens, a common option for treatment is to deploy another bio-prosthetic valve inside the degenerated valve, termed Redo TAVI. While there is existing clinical evidence of the need for considering the calcification of the initial bio-prosthetic valve leaflets before deploying the second valve, currently the effect of these calcifications on Redo TAVI outcomes are lacking in the literature [1]. Hence, this work primarily focuses on developing a computational model that captures the calcifications on degenerated prosthetic leaflets so as to establish a framework to assess their impact on Redo TAVI. Visual assessment of excised bio-prosthetic valve leaflet images from the literature was used to design the leaflets [2, 3]. Preliminary results have used TAVI deployment simulations to successfully demonstrate superimposition of the modelled degenerated leaflets onto the deformed valve frames (Fig. 1). Currently Redo TAVI simulations are being setup to assess the impact of including such degenerated bio-prosthetic leaflets on secondary valve deployment. Ultimately, this research aims to support clinical decision making in more accurately predicting the outcome of the Redo TAVI procedure, thus avoiding complications and improving patient outcomes.

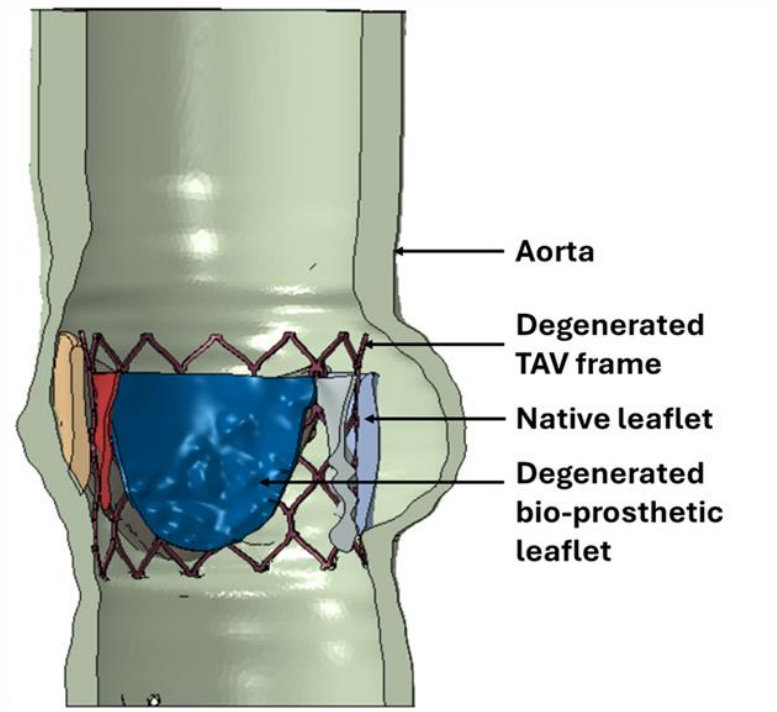

Fig. 1: cross-sectional view of the superimposed degenerated bio-prosthetic leaflets onto the deformed valve frame in a patient-specific aortic root.

[1] David M et al., EuroIntervention; 22(2024): 1390-1404.
[2] Stephanie S et al., Journal of the American College of Cardiology 82.17_Supplement (2023): B158-B158.
[3] Daniel H-V et al., The Annals of Thoracic Surgery 108.3 (2019): e173-e174.

The Mitotic Chromosome Periphery: A Fluid Coat That Mediates Chromosome Mechanics

Mendonca T[2], Tassieri M[1], Urban R[3], Lucken K[2], Coney G[2], Kad N[3], Wright A[2], Booth D[2]
[1]The University Of Glasgow, [2]The University of Nottingham, [3]The University of Kent

Mitotic chromosomes are specialised packets of condensed genetic material with dynamic mechanical properties. Each chromosome is coated by a sheath of proteins and RNA, called the mitotic chromosome periphery (MCP). The MCP is widely considered as an essential chromosome compartment where its multiple functions bestow material properties important for successful cell division. However, the details of the micromechanical properties of mitotic chromosomes, and specifically if and how the MCP contributes to these features, remain poorly understood. In this study, we present the most comprehensive characterisation of single-chromosome mechanics to date spanning a broadband frequency range, using optical tweezers and a novel microrheology technique. We extend this analysis to the first direct measurements of MCP micromechanics by manipulating levels of Ki-67, the chief organiser of this compartment, and apply a rheological model to isolate its contribution to chromosome dynamics. We report that the MCP governs high-frequency self-reorganisation dynamics and acts as a structural constraint, providing force-damping properties that mitigate mitotic stress. This work significantly advances our understanding of chromosome micromechanics and how the MCP contributes to the fundamental properties of chromosomes.

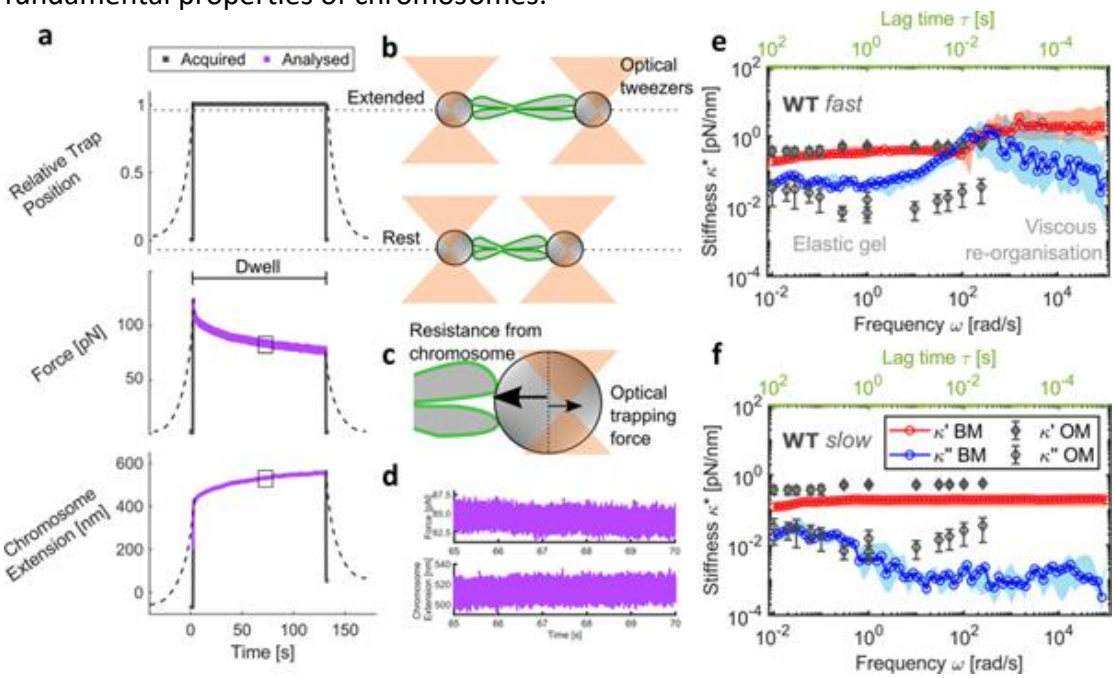

Broadband microrheology of chromosomes. a Schematic of microrheology experimental procedure. Dashed lines represent data at a force-loading rate of 0.2 µm/s and solid lines for 100 µm/s. Data in purple were analysed to provide broadband mechanical response. b Schematic representation of the tweezer and chromosome positions from (a). c Opposing forces experienced at bead handles (one shown) in the non-equilibrium state. d Zoomed-in sub-region of the analysed force at one bead and chromosome extension data. e Complex stiffness κ^* (ω) with frequency (bottom axis in black) and lag time τ (top axis in green) from broadband microrheology (BM) of WT chromosomes at 100 µm/s (median and 95% CI; n = 14 chromosomes), highlighting regions of viscous reorganization and gel-like behaviour. Data in blue are the viscous modulus κ''(ω) and in red are the elastic modulus κ'(ω). f κ^* (ω) at 0.2 µm/s force-loading rate (median and 95% CI; n = 15 chromosomes) of WT chromosomes. e and f are both overlaid with oscillatory microrheology (OM) data from Meijering et al. (2022) 40,74. Schematics shown are not to scale.

Development of Electroconductive Polymer fibres by Pressurised Gyration for Cardiac Tissue Engineering Applications.

Grano De Oro Fernandez J[1], Amarakoon M[1], Edirisinghe M[1], Matharu R[1,2]
[1]Mechanical Engineering Department, University College London, [2]Department of Civil, Environmental and Geomatic Engineering - University College London

Cardiac patches composed of non-conductive polymers offer a promising approach to repairing myocardial infarction (MI) damage. Enhancing these scaffolds with electrically conductive fibres has been shown to improve therapeutic efficacy, yet fabrication techniques remain restrictive [1]. This research focuses on developing and producing electroconductive polymer-based cardiac scaffolds that closely replicate the structure and function of natural heart tissue. Utilizing pressurized gyration (PG), fibres were created for the first time from polypyrrole (PPy) blended with polycaprolactone (PCL) in chloroform and from Poly(3,4-ethylenedioxythiophene)-poly(styrenesulfonate) (PEDOT\:PSS) combined with polyethylene oxide (PEO) in water. Fibres were generated with varying concentrations of conductive polymer (5–10% w/v) and under different applied pressures (0–0.2 MPa) [1]. Scanning electron microscopy (SEM) revealed that the resulting fibres resemble the size and morphology of cardiac connective tissues: PEDOT:PSS 5% at 0 MPa mirrored endomysium (0.38 µm), PEDOT:PSS 10% at 0 MPa reflected perimysium (1.02 µm), and PPy 7.5% at 0 MPa resembled epimysium (3.88 µm) [1]. Electrical analysis using a four-point probe indicated that the formulation with PPy 10% at 0.2 MPa achieved the most comparable conductivity to native cardiac tissue, measuring 0.22 S/m [1]. Fourier-transform infrared spectroscopy (FTIR) confirmed no residual solvent remained, attributing conductivity solely to polymeric bonding. The findings demonstrate that the developed fibres possess favourable electrical and material characteristics for cardiac repair applications. Additionally, PG is highlighted as a promising and scalable fabrication method for conductive fibres, potentially enhancing the development of next-generation cardiac patches for MI therapy [1].

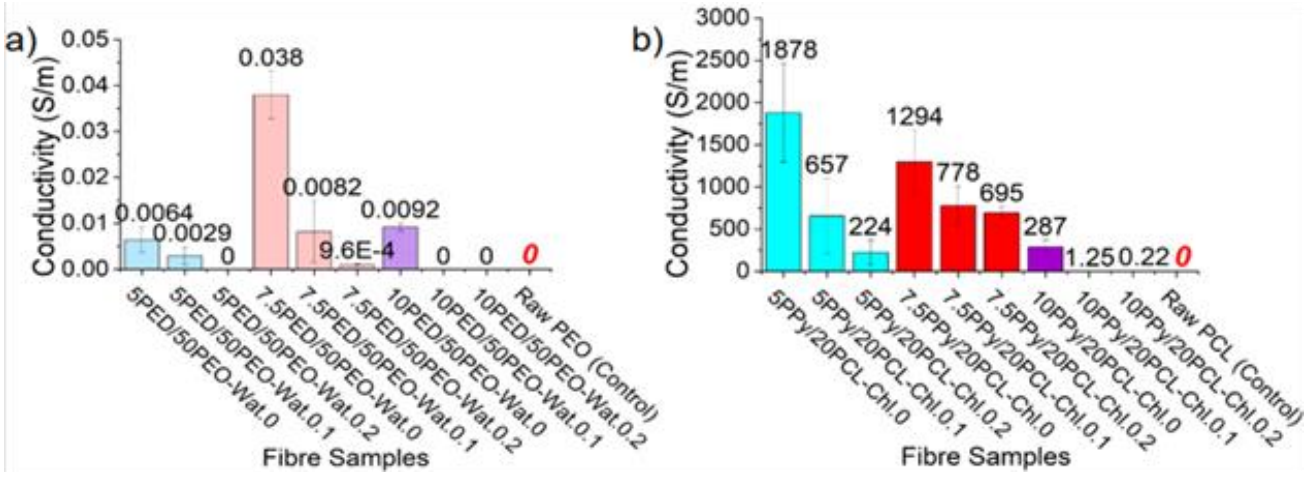

Electrical conductivity values.

a) PEDOT:PSS values for each pressure and concentration.
b) PPy values for each pressure and concentration

[1] Grano de Oro Fernandez et al., Macromolecular Materials & Engineering.

Biopolymers for Cardiac Patches Application

JIBAWI N[1], Shepherd J[2]
[1]Leicester University, [2]Leicester university

Cardiac tissue engineering offers potential as an alternate technique of to heart therapy. Electrospinning is a common method considered for production of cardiac patches however there is limited control over fibre diameter, small pore size and limited cell infiltration[1,2]. The objective is to optimize electrospinning of polyurethane(PU) patches through process control and combination with gelatin.

In order to create scaffolds appropriate for cardiac patch applications, different electrospinning solutions were evaluated in this study. These solutions were created by mixing 1,1,1,3,3,3-hexafluoroisopropanol(HFIP)and gelatin(in different concentration)with(PU). The ability to produce continuous fibres during electrospinning and the calibre of the final fibres were seen by (SEM) which was used to assess each formulation. PU-based solutions, especially those that included 3% gelatin as an addition, showed greater success rates than other formulation, which failed to produce fibrous mats and instead droplet formation.

The results show that adding gelatine to the PU + HFIP solution significantly decreased the fiber's diameter and increased porosity from 15% to 27%. Gelatin has a tendency to lower surface tension and raise the solution's charge-carrying capacity, which encourages the polymer jet to stretch more during electrospinning and produces finer fibres[3].

Successful cardiac tissue engineering requires overcoming many barriers. Major issues still remain around biocompatibility, such as immunological rejection, low cell survival rates, and ineffective cell seeding. This work focused on optimizing solutions to enhance fibre morphology and scaffold microstructure. In the future Additional components will be considered to enhance the scaffold's mechanical characteristics and electrical conductivity.

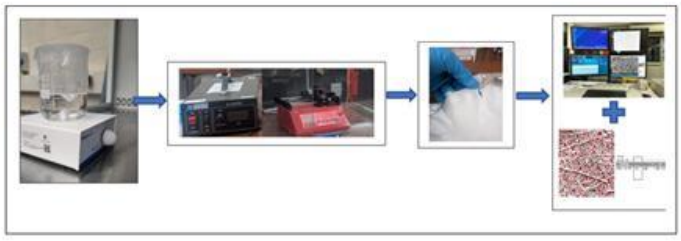

Figure (1) the process of forming cardiac scaffolds

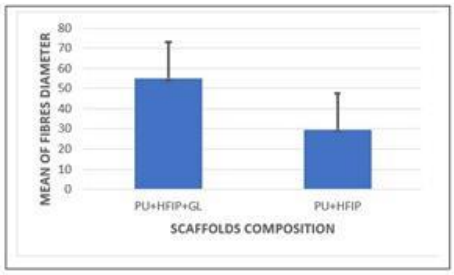

Figure (2): The difference in the fibres diameters

1. Bhullar, S.K., et al., 2025, Basic to Translational Science, vol. 10, no. 2, pp. 227-240.
2. Ghofrani, A., et al., 2022, European Polymer Journal, vol. 174, no. 111332, pp. 1-20.
3. Mani, M.P., et al., 2019, Polymers, vol. 11, no. 4, pp. 2-16.

Tissue-engineered oral mucosal models and electrical impedance spectroscopy for rapid and early diagnosis of oral cancer

Furmidge R[1,2], Colley H[1,2], Murdoch C[1,2], Matella M[2,3], Lang Z[2,4], Lin Z[2,4], Walker D[2,3]
[1]School of Clinical Dentistry, The University of Sheffield, [2]INSIGNEO Institute, The University of Sheffield, [3]School of Computer Science, The University of Sheffield, [4]School of Electrical and Electronic Engineering

Oral cancer is the 10th most common cancer in the UK, with over 3,500 deaths in the UK in the last year [1], and an estimated 188,000 deaths globally in 2022 [2]. Oral cancer is typically diagnosed after a GP or dentist assesses a suspicious lesion. If necessary, a biopsy is taken for pathological analysis, with results taking 1–2 weeks. Late diagnosis of oral cancer reduces survival from 90% to 50% [1], making early detection of oral cancer critical to reducing mortality.
Electrical Impedance Spectroscopy (EIS), a non-invasive technique measuring tissue electrical impedance via a harmless alternating current, offers a promising alternative. We hypothesised that structural and compositional variations in oral potentially malignant lesions (OPML) and cancerous tissues, recapitulated in tissue-engineered models, would yield distinct EIS spectra compared to healthy tissue, optimising the diagnostic procedure.
To create physiologically relevant in vitro models, we engineered 3D oral mucosal constructs using decellularised human skin dermis. Normal oral fibroblasts were co-cultured with various oral keratinocyte cell lines representing healthy, OPML, and cancerous phenotypes at an air-to-liquid interface. The electrical impedance of these tissue-engineered oral mucosa models was measured using a novel handheld oral EIS device. This data was then integrated with finite-element mathematical modelling and machine learning algorithms to develop a diagnostic support system which was capable of distinguishing cancer, OPML and healthy phenotypes.
These results demonstrate the feasibility of utilising tissue-engineered oral mucosa models to develop and validate a non-invasive EIS-based diagnostic tool for OPML and oral cancer.

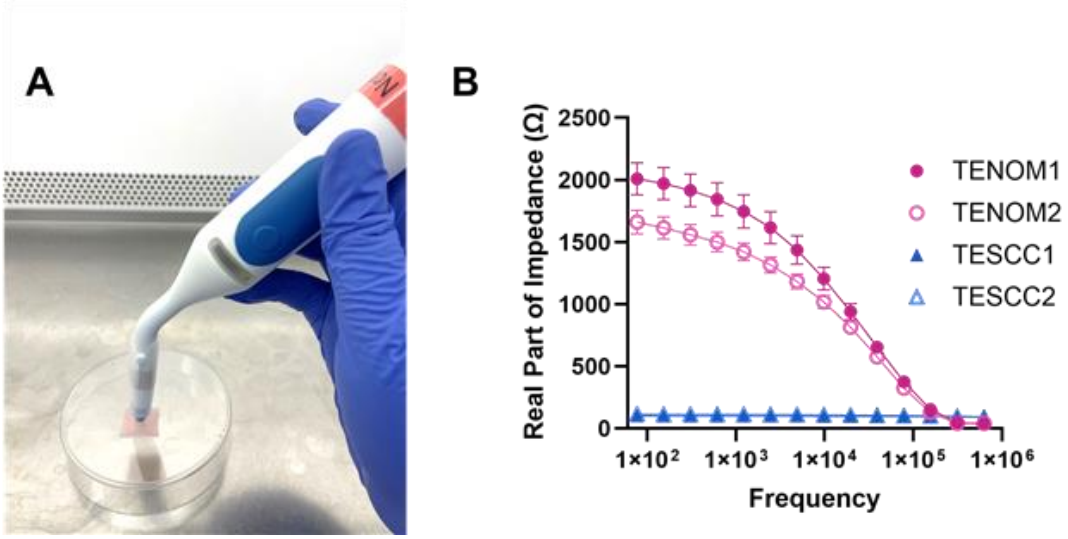

(A) Measuring tissue-engineered oral mucosa with EIS device. (B) EIS spectra for tissue-engineered normal (TENOM) and carcinoma (TESCC) models.

[1] Foundation, O.H. State of Mouth Cancer UK report 2023/2024. 2024.
[2] The Lancet Oncology (2025) 'Prioritising Oral Health in Cancer Care', The Lancet Oncology, 26(1), p. 1. doi:10.1016/s1470-2045(24)00724-1.

Combination of 3D printing with electrospinning for biomedical applications

Radacsi N[1]
[1]The University of Edinburgh

Three-dimensional (3D) printing is constantly transforming from object-oriented prototyping at a small scale to much more comprehensive manufacturing platforms and has become an attractive candidate for biomedical applications. However, many current 3D printing approaches lack the ability to produce filaments with the high resolution necessary for creating scaffolds for a range of tissues. In addition, the pore size of 3D-printed scaffolds is significantly larger than the cell size, adversely affecting cell-seeding efficiency and tissue formation. Electrospinning uses high voltage to generate nanofibers with large specific surface areas [1]. It is the most efficient method for producing nanofibers with a well-defined structure, which can mimic the physical functions of the native extracellular matrix, providing many attachment points for cell adhesion. I will present the different combination methods of 3D printing and electrospinning processes for the fabrication of biomaterials, including vascular grafts [2] and bone scaffolds [3].

[1] D. Ji, Y. Lin, et al., 2024, Nat. Rev. Meth. Prim., 2024, 4, 1.
[2] F. Fazal, F. P. W. Melchels, et al., 2024, Adv. Mat.Technol., 2400224.
[3] D. L. Yang, L. A. Stephen, et al., 2024, Macromol. Mat. Eng., 2400286

Prototype development for hyperspectral imaging of glioblastoma samples using the OpenFlexure 3D-printed microscope

Mollins A[1], Kallepalli A[1,2]
[1]Department of Biomedical Engineering, University Of Strathclyde, [2]School of Physics and Astronomy, University of Glasgow

Hyperspectral imaging has found application within AI-integrated glioblastoma diagnostics, with classifier deep learning models able to identify tumour sections of histological samples from their hyperspectral “signatures” with greater sensitivity than from RGB data [1]. However, hyperspectral imaging microscopy systems are expensive, limiting clinical translation of this methodology. OpenFlexure has produced a 3D-printed microscope with a precision motorised stage, controlled by a Raspberry Pi. This enables accessible brightfield imaging of cellular samples with minimal upfront cost [2]. While the precision motor control is an asset, the diagnostic applications of the OpenFlexure microscope are limited by its standard RGB imaging capabilities.

Our work reengineers the OpenFlexure microscope, adapting it to house a low-cost hyperspectral imager built from off-the-shelf components [3], whilst leveraging its existing motor control to realise the push-broom technique for reconstructing hyperspectral image "cubes". The reengineered system allows integration with existing classifier algorithms, enabling low-cost diagnostic-grade imaging and classification of small fixed histological samples. The prototype will be tested with biological samples and evaluated on its sensitivity, specificity and ease of use. Through this work, we are presenting and validating a proof-of-concept biomedical diagnostic imaging system with advanced spectral imaging capabilities and setting the stage for its application in resource-limited settings.

[1] Ortega et al., 2020, Sensors, vol. 20, no. 7
[2] Knapper et al., 2024, Phil. Trans. R. Soc. A. vol. 382, no. 2247
[3] Sigernes et al., 2018, Optics Express, vol. 26 no. 5

Glomeruli to Whole Organ Modelling of Blood Flow in the Human Kidney

Javanmardi Y[1], Lyu M[1], Zhou Y[1], Wang Y[1], Walsh C[1], Tafforeau P[2], Long D[1], Jafree D[1], Bellier A[3], Torii R[1], Lee P[1,4]

[1]Univercity College London, [2]European Synchrotron Radiation Facility, [3]University Grenoble Alpes, [4]Research Complex at Harwell, Oxfordshire

Renal blood flow is regulated by a complex vascular network spanning from large arteries to microscopic arterioles. However, imaging techniques limit comprehensive haemodynamic analysis of such multiscale vasculature in intact human kidneys. Here, we combined a new synchrotron X-ray imaging method, Hierarchical Phase-Contrast Tomography (HiP-CT) [1], with computational flow modelling to characterise the vasculature and simulate blood flow dynamics across scales. Using HiP-CT, we imaged an intact human kidney at local voxel sizes down to 2.6 µm, reconstructed the vascular network within high-resolution regions, and statistically inferred missing vessels to generate a complete arterial tree of ~1.6 million vessels. Flow simulations revealed an exponential relationship between flow rate and Strahler order, appearing linear on a semi-logarithmic scale, consistent with patterns observed in rat kidneys [2]. With glomeruli segmented by a deep learning model, we assessed the effect of renal artery stenosis (RAS), showing that mild stenosis (<50%) had minimal impact on glomerular filtration rate (GFR), while severe stenosis (≥70%) reduced GFR by ~85%, in line with clinical reports [3]. Additionally, pruning lower-order vessels demonstrated the risk of underestimating haemodynamic parameters if microvasculature is omitted. This integrative approach provides a powerful multiscale framework for understanding kidney function and vascular disease progression. Our findings highlight the importance of high-resolution imaging to ensure physiologically accurate haemodynamic models, supporting future in silico diagnostics and therapeutic strategies.

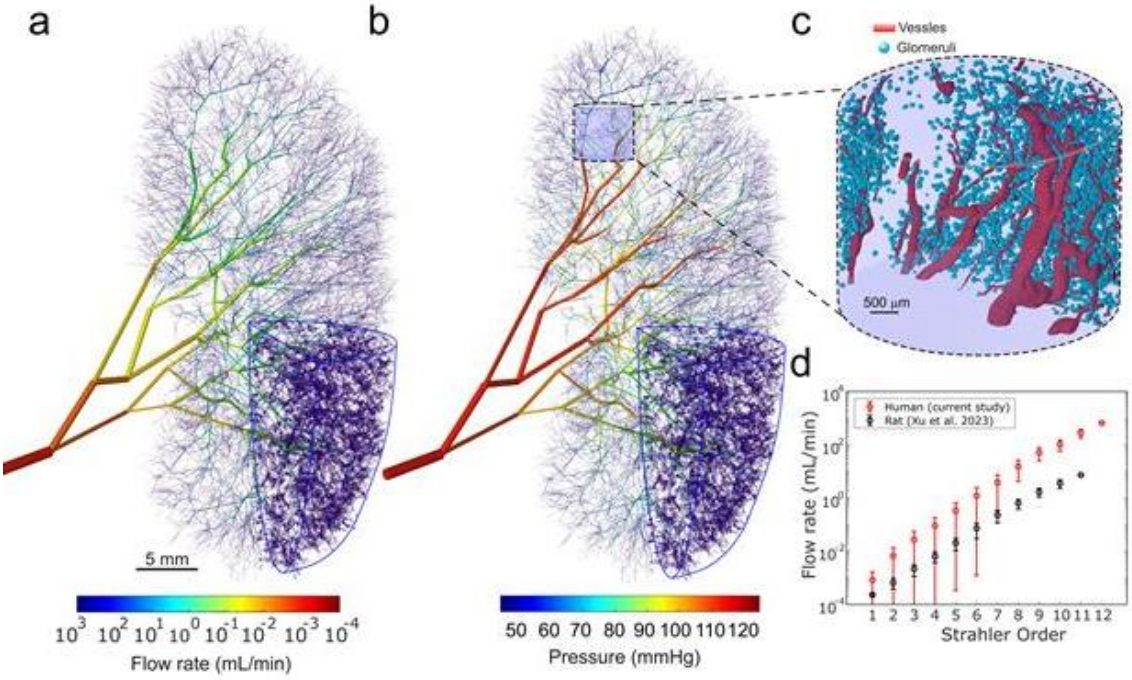

(a, b) Simulated flow and pressure; (c) glomeruli and microvasculature; (d) flow–Strahler order relationship in HiP-CT-derived vasculature.

[1] Walsh et al., 2021, Nat Methods, vol. 18, no. 12, pp. 1532–1541.
[2] Xu, P., et al., 2023, Sci Rep vol. 13, 7569.
[3] Kalra PA, et al., 2023, Nephrol Dial Transplant.; vol. 38, no.12, pp:2835–2855.

3D Prostate Reconstruction from Surface-Based Ultrasound Scans

Bennett R[1], Barrett T[2], Gnanapragasam V[2], Ho Tse Z[1]
[1]Queen Mary University Of London, [2]Cambridge University

Prostate cancer (PCa) will affect 1 in 8 men in the United Kingdom during their lifetime and has a total economic cost estimated at £650 million/year [1]. Earlier detection of PCa, in the form of risk stratification, can help reduce associated costs, while improving patient outcomes. Surface-based ultrasound (SUS)-derived prostate-specific antigen density (PSAD) presents itself as a potential risk stratification metric [2]. The problem becomes estimating the size of the prostate from SUS scans and is the focus of this work. A clinical prospective dataset of 19 patient SUS prostate scans has been collected from Cambridge University Hospital (ethics reference NRES 03/018). A size estimation pipeline has been developed that makes use of the you only look once (YOLO) [3] object detection framework in combination with the nnU-Net [4] segmentation framework. This pipeline has been tested on the transverse abdominal ultrasound scans of the dataset following a 5-fold cross-validation approach. The outputs of the YOLO network – in the form of bounding boxes – were used as extra channel inputs to the nnU-Net network (see the figure for sample results). Preliminary DICE scores were found to be in the range of 95%, with volume calculations pending. The presented pipeline was found to return exceptionally high DICE scores, with the inclusion of the second input channel for the segmentation network resulting in substantial performance gains. Work is currently underway to further develop this pipeline into a system that can be used by the NHS in a primary care setting.

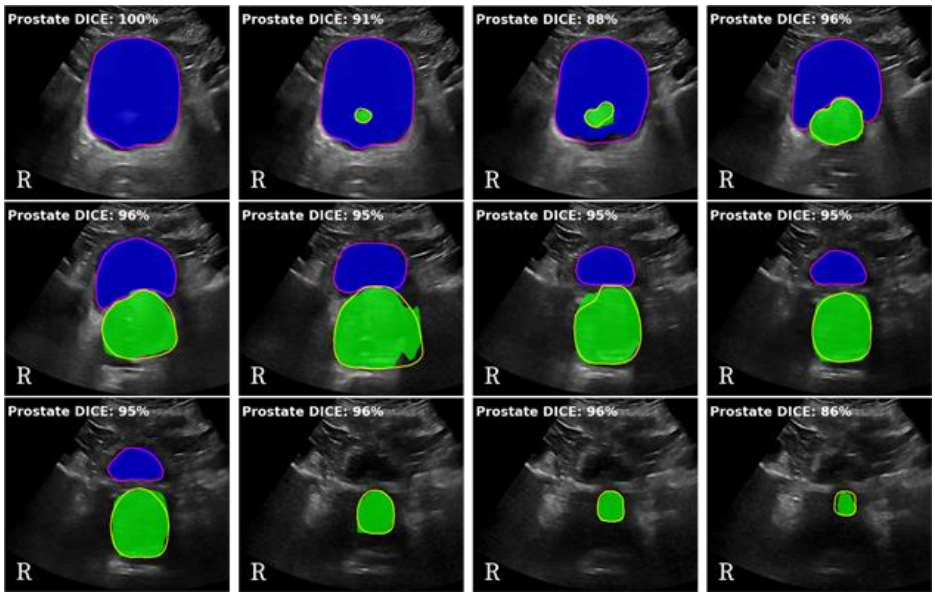

Figure showing sample results for a patient's scan, showing prostate (green) and bladder (blue) segmentations of the two-channel network.

[1] https://www.icr.ac.uk/about-us/icr-news/detail/prostate-cancer-spit-test-could-save-the-nhs-500-million-a-year, [01 May 2025].
[2] M. Ohori et al, Urology, Volume 46, Issue 5, 1995, pp. 666-671.
[3] R. Varghese et al, 2024 International Conference on Advances in Data Engineering and Intelligent Computing Systems (ADICS), 2024, doi: 10.1109/ADICS58448.2024.10533619.
[4] F. Isensee et al, Nat Methods 18, 2021, 203–211

An Open-Source Tool for Accurate Determination of Polar Moment of Inertia in Bone from micro-Computed Topography

Feechan A[1], Jaffrey H[2], Sims N[3], Williams J[1]
[1]Department of Biomedical Engineering, Wolfson Centre, University of Strathclyde, [2]Institute of Molecular, Cell and Systems Biology, College of Medical Veterinary and Life Sciences, University of Glasgow, [3]Bone Cell Biology & Disease Unit , St. Vincent's Institute of Medical Research, University of Melbourne

Bone strength is governed by both geometry and material composition. Most commercial software for microCT image analysis (e.g CTAnalyser, Bruker) calculates parameters like the polar moment of inertia (pMOI) using binarised images, without incorporating tissue mineral density (TMD). As a result, what is typically reported as pMOI is actually the polar moment of area (pMOA), which reflects geometry alone, and not mass distribution.
We developed an open-source Python-based tool that calculates pMOA and pMOI separately, using calibrated greyscale datasets. The tool performs pixel-wise integration of TMD and radial distance, providing a more biomechanically accurate estimate of torsional resistance.
The tool was tested on preclinical datasets from rat and mouse models known to affect bone microarchitecture and density, including spinal cord injury-induced osteoporosis[1], and knockout models, suppressing B-cell lymphoma 3-encoded protein[2] and phosphoinositide-3 kinase[3], alongside controls. While pMOI and pMOA were spatially correlated across all datasets (Figure 1), regions of denser bone further from the centroid contribute disproportionately to pMOI, making it sensitive to spatial heterogeneity in TMD. In models with non-uniform TMD distribution, this leads to meaningful divergence between pMOA and pMOI.
This tool highlights the importance of distinguishing between geometric and densitometric parameters. It is being further improved to enable CT-based-structural rigidity analysis, which combines geometrical data with TMD to calculate axial, bending, and torsional rigidities.

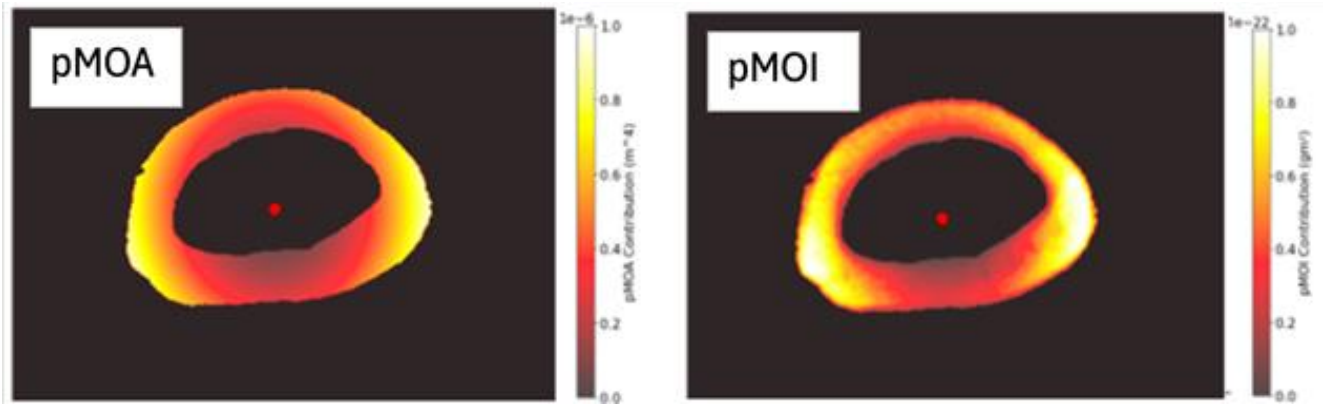

Figure 1: The spatial distribution of pMOA and pMOI in the femoral diaphysis, for a representative PI3K knockout mouse.

[1] J.A. Williams et al., 2022, J. Musculoskelet. Neuronal Interact., vol. 22, no. 2, pp. 212.
[2] H. Jaffrey et al., 2023, Arthritis Rheumatol., vol. 75,no. 12 pp.2148-2160.
[3] N. K. Y. Wee et al., 2024, J. Bone Miner. Res., vol. 39. no. 8, pp. 1174-1187.

Use of Stereo-DIC on Surgical Images to Substitute Palpation in Minimally Invasive Surgery

Nowakowska I[1], Durcan C[1], Saleh M[1], Henrywood R[2], MacPherson B[1], Reuben R[1], Chen Y[1]
[1]Heriot-watt University, [2]CMR Surgical

Although minimally invasive surgery improves post-surgery patient recovery, it reduces haptic feedback to the surgeon, increasing the risk of tissue damage and eliminating the possibility of palpation during the surgery. This study evaluates the feasibility of using stereo-DIC as a substitute for palpation to detect embedded structures such as lymph nodes, blood vessels, nerves, or cancerous tissue borders. A nodule was embedded into silicon phantoms and ex-vivo porcine liver tissue samples at depths of 0-10mm. The samples were then loaded in uniaxial tension up to 50% strain and recorded with a stereoscopic surgical laparoscope. To represent surgical loading conditions as closely as possible, the stiffness ratio between the nodule and the surrounding tissue was 7:1, representing a common stiffness ratio between healthy and cancerous tissue, and the samples were loaded up to the rupture strain of liver tissue [1]. 3D displacement results were obtained from NCorr[2] and DuoDIC[3], and strain maps were calculated by an in-house algorithm in python. We found that it was possible to locate the nodule in the surface strain maps up to an embedded depth of half a nodule diameter between the sample surface and the top of the nodule. The detection was highly influenced by the high image noise present in the laparoscope, and the propagation of this noise into both the stereo-DIC results as well as the strain maps. Future work includes customization of the correlation algorithm for the surgical conditions to improve the detection depth.

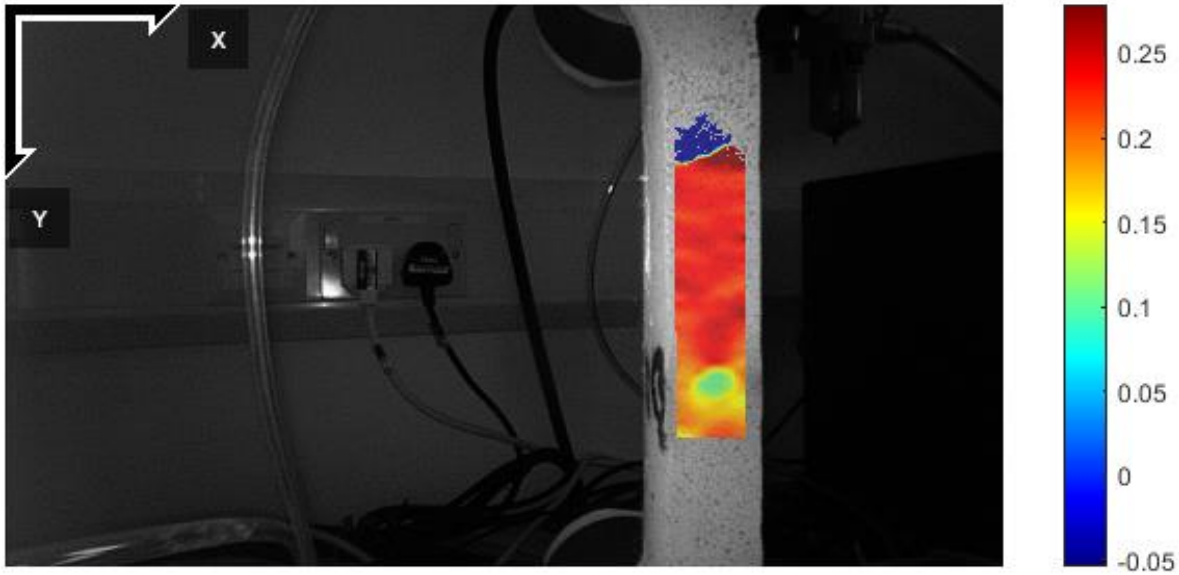

Figure 1: Strain map of nodule embedded in tissue-mimicking silicone phantom under tension

[1] Lemine, A.S. et al., 2024, Biomech Model Mechanobiol, vol. 23, pp. 373-396
[2] Blaber, J. et al., 2015, Exp Mech, vol. 55, no. 6, pp. 1105-1122
[3] Solav et al. 2022, Journal of Open Source Software, vol. 7, no. 74, pp. 4279

Real-Time Prostate Detection in Surface-Based Ultrasound Scans

Bennett R[1], Barrett T[2], Gnanapragasam V[2], Ho Tse Z[1]
[1]Queen Mary University Of London, [2]Cambridge University

Prostate cancer (PCa) will affect 1 in 8 men in the United Kingdom during their lifetime and has a total economic cost estimated at £800 million/year [1]. Earlier detection of PCa, in the form of risk stratification, can help reduce associated costs, while improving patient outcomes. Surface-based ultrasound (SUS)-derived prostate-specific antigen density (PSAD) presents itself as a potential risk stratification metric [2]. An associated difficulty with SUS-derived PSAD is locating the prostate during scanning. To address this, we propose using object detection algorithms to help guide the probe operator during scanning, ensuring a suitable scan is taken before size estimation is attempted. A clinical prospective dataset of 19 patient SUS prostate scans has been collected from Cambridge University Hospital (ethics reference NRES 03/018). Three state-of-the-art object detection frameworks – you only look once (YOLO) [3], RetinaNet, and FasterRCNN – were initially compared. RetinaNet performed marginally better in most metrics, however, only YOLO was able to operate with real-time speeds and, as a result, was tested further. On full scans, YOLO return intersection-over-union (IoU) scores of greater than 0.75, and average precision (IoU > 0.75) score of about 0.75, highlighting its robustness, with inference speeds of 23 frames-per-second (see figure for sample results). These results show that real-time prostate detection in SUS scans is possible to within a high degree of accuracy. This allows for the future development of a size estimation pipeline that does not require a highly skilled/trained clinician, enabling risk stratification deployment in primary care settings.

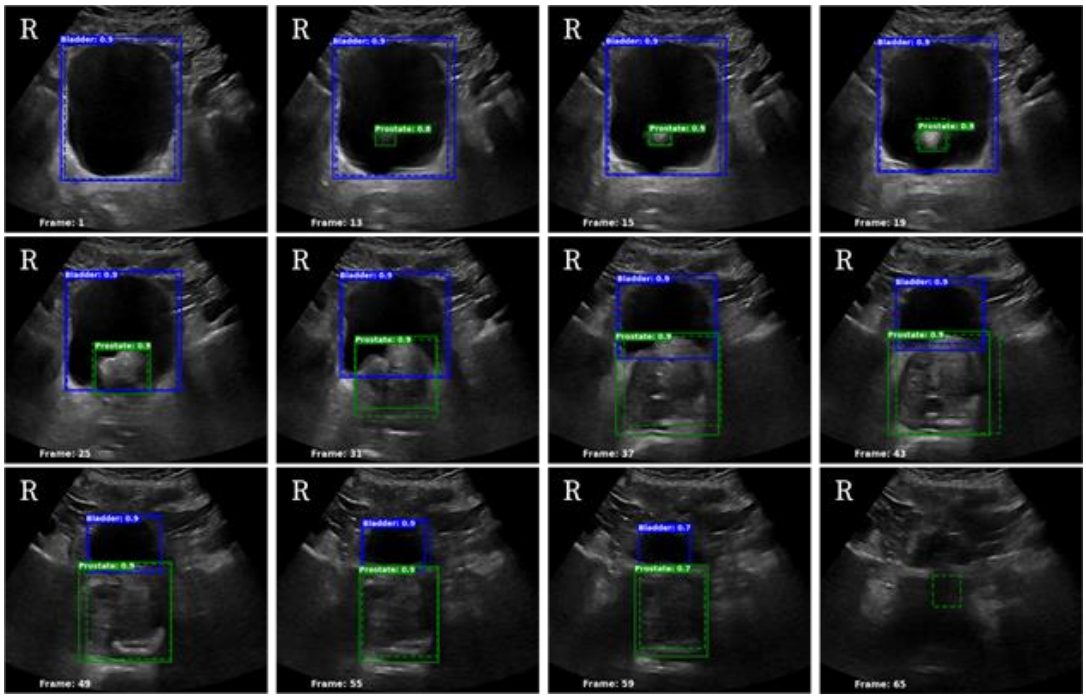

Figure showing sample results for a patient's scan, showing prostate (green) and bladder (blue) bounding boxes (solid–inferred, dashed–expert).

[1] https://www.icr.ac.uk/about-us/icr-news/detail/prostate-cancer-spit-test-could-save-the-nhs-500-million-a-year, [01 May 2025].
[2] M. Ohori et al, Urology, Volume 46, Issue 5, 1995, pp. 666-671.
[3] R. Varghese et al, 2024 International Conference on Advances in Data Engineering and Intelligent Computing Systems (ADICS), 2024, doi: 10.1109/ADICS58448.2024.10533619.

Near-infrared fluorescent glutathione capped gold nanoclusters: impact of synthesis conditions and hairpinDNA functionalization

Wang B[1], Chen Y[1], Laurand N[1]
[1]University of Strathclyde

Fluorescent imaging in the near-infrared (NIR) region has attracted significant attention in biomedical research due to its deep tissue penetration, reduced autofluorescence, and enhanced spatial resolution compared to visible light imaging. Among the various NIR fluorescent probes, gold nanoclusters(AuNCs) have emerged as a promising candidate, owing to their tunable emission properties, excellent photostability, biocompatibility and ease of surface functionalization[1,2]. This work focuses on the synthesis of NIR-fluorescent GSH-AuNCs and subsequent functionalization with hairpinDNA (hpDNA). We have investigated the influence of synthesis conditions on their fluorescence properties by adjusting pH, concentration of HAuCl4 and reaction temperature. It's found that tuning synthesis parameters enables fine control over emission wavelength. Specifically, increased pH, higher gold concentration, and elevated temperature promote the formation of GSH-AuNC emitting in NIR region. Consequently, we have successfully synthesized highly fluorescent GSH-AuNCs with emission at 825nm under 365 nm excitation and an average fluorescence lifetime of 3.6µs. The strong NIR emission, large Stokes shift and long fluorescence lifetime highlight the potential of GSH-AuNCs for applications in bioimaging and sensing. Moreover, the functionalization of GSH-AuNCs with thiolate hpDNA labelled with Cy5 has been investigated using a salting process. GSH-AuNCs emitting at 640nm were chosen as their emission spectroscopically overlaps with the absorption of Cy5 (638nm). Successful conjugation of hpDNAs to the GSH-AuNCs surface facilitated Förster resonance energy transfer, as confirmed by both steady-state and time-resolved fluorescence spectroscopy. These findings provide a strong foundation for the development of GSH-AuNCs-based platforms for future application in NIR imaging and sensing.

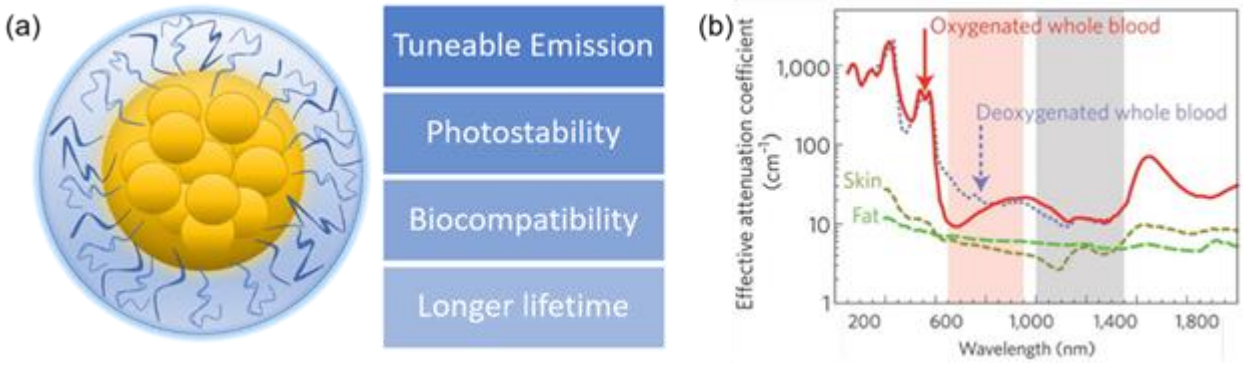

Fluorescence properties of AuNCs, plots of effective attenuation coefficient in human tissues versus wavelength in NIR(indicating low absorption and scattering).

[1] B. A. Russel, et al. J. Mater. Chem. B 2016; 4:p6876-6882.
[2] Z. Luo, et al. J. Am. Chem. Soc. 2012; 134:p16662-16670.

Development of a Transparent Patient Severity Score Using Biomarker Profiles and Age with Applications to Limited Datasets

Aimaganova A[1], Grammatopoulos D[2,3], Khovanova N[1]
[1]School of Engineering, University of Warwick, [2]Institute of Precision Diagnostics and Translational Medicine, University Hospitals Coventry and Warwickshire NHS Trust, [3]Division of Translational and Experimental Medicine, Warwick Medical School, University of Warwick

Severity scoring systems are essential for clinical decision-making and patient stratification, but often depend on vital signs, comorbidities, or organ function metrics unavailable in retrospective datasets. To address this in hospitalised patients with respiratory infection, we developed a transparent, formula-based severity score (SS) using five variables: age, albumin, interleukin-6, white cell count, and urea.
A cohort of 1,122 patients with 23 biomarker profiles from University Hospitals Coventry and Warwickshire NHS Trust was used to develop the score. Two normalisation frameworks, quantile-based and standard deviation-based, guided feature reduction, and stepwise logistic regression with multicollinearity testing and likelihood ratio analysis were used to derive the initial score. Bayesian optimisation was then applied to the SS formula coefficients to maximise the AUC. Patient location (ward vs. critical care unit) was used as a real-world severity proxy.
The final five-feature SS to discriminate between ward and CCU patients achieved an AUC of 0.90 (95% CI: 0.88-0.91) in the development set and 0.86 (95% CI: 0.80-0.90) in an independent testing set (n=237). Despite using only five features, it matched the performance of an XGBoost model trained on all 23 biomarkers plus age. SHAP analysis showed strong alignment between SS and XGBoost predictions (r = 0.67), confirming that the SS captures a comparable severity indicator while offering full transparency and biological interpretability.

This work demonstrates that a biologically grounded, statistically transparent score can support patient stratification in retrospective and data-limited settings, offering a practical alternative to opaque machine learning models for risk assessment in clinical research.

Fast Scan Cyclic Voltammetry as a Translational Tool for Neuroscience

Hashemi P[1]
[1]Imperial College, London

The pathology underlying psychiatric illnesses is unknown and as such diagnosis and treatment of the disorder remain a great challenge. In this work, experimental models using biosensors and theoretical analysis models will be presented that probe the fundamental roles of neurotransmitters such as serotonin in the development of the disease. We first describe the fabrication of carbon fiber microelectrodes (CFMs) by hand, then we describe the electrochemical technique that simultaneously identifies and quantifies neurotransmitters in real time. We apply the method in vivo in mice and in human derived cerebral spheroids. First, we find that we can reliably measure a serotonin biomarker that accompanies behavioural phenotypes of depression in mice and that this biomarker is inflammation induced. Second, we find that antidepressants with different modes of action all raise extracellular serotonin levels in mice, attesting to the potential utility of measuring serotonin for drug screening purposes. Finally, via human derived cellular models and probes for monitoring from the human periphery, we show promise for translating our findings to humans. In conclusion we find that many important facets of the pathology of mental illness can be partially explained by measuring neurotransmitters in real time using electrochemical sensors.

Fluorescent gold nanoprobes for biomarker RNA detection

Sankar A[1], , Zinuo Li[1], Hui-Rong Jiang[2], D. Li[3], D.J.S. Birch[1], Yu Chen[1]
[1]1Photophysics Group, Department of Physics, University of Strathclyde, 107 Rottenrow, Glasgow G4 0NG, U.K.University of Strathclyde, [2]2Strathclyde Institute of Pharmacy and Biomedical Sciences, University of Strathclyde, Glasgow G4 0RE, United Kingdom, [3]3Department of Biomedical Engineering, University of Strathclyde, Glasgow G4 0RE, U.K.

RNA biomarkers are widely utilized in both liquid biopsy and tissue analysis, enabling non-invasive detection and monitoring, as well as providing insights into tissue-specific gene expression profiles. In this study, we present a new approach for detecting biomarker RNAs within exosomes, cells and tissues using fluorescent gold nanoprobes. These nanoprobes comprise small gold nanorods functionalized with fluorophore-labelled DNA hairpins designed to hybridize with specific RNA sequences [1,2]. Nanoprobes targeting LINC00261, PSMA and VEGF-A were synthesized using a reported method.[3] A significant increase in fluorescence intensity was observed in the presence of targets in solution, indicating hairpin opening upon hybridization with their targets. Cancer cells with elevated levels of target RNAs treated with nanoprobes showed higher fluorescence intensities in flow cytometry and longer fluorescence lifetime in FLIM imaging compared to negative controls, confirming the nanoprobes' sensitivity to intracellular RNA. Furthermore, nano-flow cytometry showed that cancerous exosomes exhibit a higher mean fluorescence intensity upon nanoprobe treatment compared to non-cancerous exosomes, demonstrating effective RNA detection. Notably, as nanoprobe concentration increased, fluorescence intensity in cancer-derived exosomes rose, while that of non-cancerous exosomes remained low, indicating the nanoprobe's specificity. Finally, FLIM imaging of retinal pigment epithelium tissue treated nanoprobes revealed the presence of fluorescent nanoprobes and an extended fluorescence lifetime, confirming both nanoprobe uptake and RNA detection in tissue. Overall, these findings demonstrate the ability of fluorescent nanoprobes to detect target RNA in exosomes, cells and tissue, supporting their potential application in both liquid and solid biopsies for cancer detection and monitoring.

References

1. Y. Zhang, et al., Faraday Discussion. 2015; 178:p383
2. G. Wei, et al., J. Biomed. Opt. 2016; 21:p097001
3. Z. S. Mbalaha, et al. ACS Omega 2019; 4:p13740–13746

A novel microfluidic-enabled tool for enhancing the performance of electrochemical biosensors at research level

Dobrea A[1,2], Blake R[3], Macdonald D[3], Altmann Y[4], Corrigan D[3], Jimenez M[1]
[1]Biomedical Engineering Department, University of Strathclyde, [2]James Watt School of Engineering, University of Glasgow, [3]Pure and Applied Chemistry Department, University of Strathclyde, [4]School of Engineering and Physical Sciences, Heriot-Watt University

Electrochemical biosensors have transformed medical diagnostics due to their low cost, scalability, and portability. However, the translation of these sensors from the lab bench into commercial use remains limited [1]. Integration with microfluidics is widely seen as a solution to this challenge [2], yet fewer than 6% of electrochemical sensor studies feature fluidic components (Web of Science, 2020–2025). A key tool currently missing from the electrochemical biosensor developer's toolkit is an accessible platform that standardises biosensor fabrication while accommodating different detection layouts and electrode formats. To that end, we present the WAFFLE (Wee Ally for Flow Functionalisation of Low-cost Electrodes), an automated, IoT-enabled microfluidic platform featuring modular design, off-the-shelf micropumps and valves, and an intuitive user interface accessible from any Wi-Fi enabled device. The WAFFLE allows a more controlled delivery of reagents and samples to the sensing surface compared to what is typically done at research level. Using this platform, we demonstrate a 5 and 1.6-fold increase in detection sensitivity of electrochemical immunosensors for IL-6 (an inflammatory marker) and cardiac troponin I (heart attack marker) respectively and a reduction in surface monolayer variability by 37%. Furthermore, we introduce a novel data analysis method using the Monte Carlo Markov Chain (MCMC) algorithm to enhance the robustness of impedance data fitting—addressing issues of current software like local minima trapping. Together, WAFFLE and the MCMC impedance data fitting approach offer a practical path toward bridging research and the commercial deployment of electrochemical biosensors, empowering broader adoption of microfluidic solutions in laboratories.

The WAFFLE platform. (Left) Profile view. (Right) Inside of the platform featuring microvalves, micropump, and control electronics.

[1] J. Wu et al., "Device integration of electrochemical biosensors," Nat. Rev. Bioeng., vol. 1, no. 5, pp. 346–360, 2023, doi: 10.1038/s44222-023-00032-w.
[2] A. Fernández-la-Villa et al., "Microfluidics and electrochemistry: an emerging tandem for next-generation analytical microsystems," Curr. Opin. Electrochem., vol. 15, pp. 175–185, 2019, doi: 10.1016/j.coelec.2019.05.014.

User Centric Design Study for the Development of Digital Twins for Sepsis Diagnosis and Management

Chakshu N[1], Hee Yook S[2], Nithiarasu P[1]
[1]Faculty of Science and Engineering, Swansea University, [2]Faculty of Medicine, Health and Life Science, Swansea University

In the UK, 245,000 sepsis cases are identified each year, with nearly 48,000 deaths caused by this condition. It has been noted that 25% of these deaths could have been prevented through timely diagnosis and appropriate treatment [1]. Across the NHS, health and social care professionals have strongly recommended the development of diagnostic tests at different points of care [2], such as to rule out 'out' infection and 'in' infection, to better inform patient care and associated testing. This highlights the need for advanced and automatic tools to assist in closing this gap. In parallel, studies have shown that deep learning models can assess Electrocardiograms (ECG), a routinely conducted test, to screen for sepsis [3]. It has been observed that approximately 50% of patients diagnosed with sepsis exhibited signs of myocardial dysfunction evident on the ECG, including but not limited to decreased amplitude of the QRS complex and increased QRS duration [4].
Building on these and other on-ground insights, this work explores the development of digital twins powered by data driven AI and one-dimensional blood flow models, through a user centric perspective. The aim is to identify the right venues (see Figure 1) for the point of entry of digital twins into patient care, determine how they should ingress data based on existing practices, and define where and when to provide inputs to users, in order to assist in reducing misdiagnosis, lowering operational workload, and speeding up recovery through personalised care.

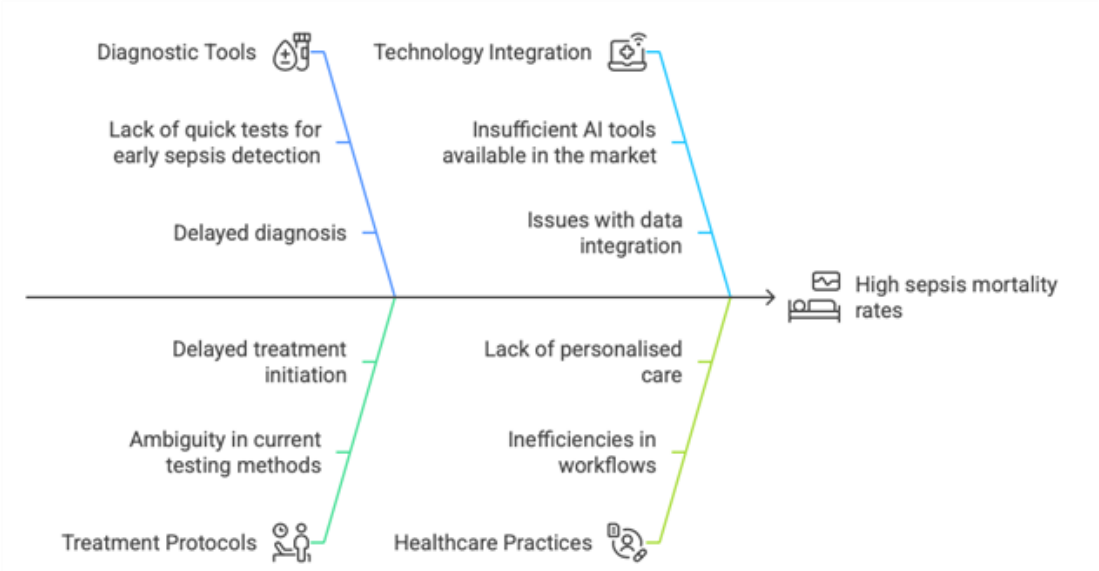

Figure1: Design study to explore where Digital Twin technology can support sepsis care by reducing mortality and accelerating treatment.

[1] UK Sepsis Trust, 2024.
[2] Winter, A. et al., 2020, Antibiotics (Basel, Switzerland), 9(11), 737.
[3] Kwon, J. M et al., 2021, Scand. journal of trauma, resuscitation and emergency medicine, 29(1), 145.
[4] Rich, M. M. et al., 2002, Cardiology, 97(4), 187–196.

3D-printed mechanically-realistic synthetic kidney models towards digital twin-assisted surgery.

Asciak L[1], Zhang K[2], Kyeremeh J[3], Cao F[2], Jiang Y[2], Kazakidi A[1], Stewart G[3], Luo X[2], Shu W[1]
[1]Department of Biomedical Engineering, University Of Strathclyde, [2]Department of Design, Manufacturing and Engineering Management, University of Strathclyde, [3]Department of Surgery, University of Cambridge, Cambridge Biomedical Campus

3D-printing of organ models is becoming increasingly popular in surgery, with applications in training, planning, rehearsal, and patient communication[1]. Recent advancements in digital health technologies, such as the introduction of digital twins (DT) in medicine, present further opportunities where these models could play an important role. By developing a mechanically-realistic, anatomically-accurate, and patient-specific physical organ model, a DT framework may be designed to assist surgeons throughout the entire perioperative process[2]. To achieve this, the first step is to develop a 3D-printed model based on patient imaging data composed of materials that closely mimic the mechanical behaviour, including elastic and viscoelastic properties, and the tactile properties of human soft tissue. In this work, we investigated an interpenetrating polymer network (IPN) hydrogel comprising poly(N-isopropylacrylamide) (pNIPAM, a thermo-responsive polymer) and sodium alginate, produced via light-based 3D-printing to create surgical kidney models. Material characterisation tests showed that by varying monomer concentrations, the mechanical properties of the IPN hydrogels could be fine-tuned to match human kidney tissue (Fig.1A,B) [3,4]. Using these hydrogels, scaled-down 3D-printed models of human kidneys were produced as a preliminary step towards fabricating surgical kidney phantoms (Fig.1C). Ongoing work involves 3D-printing optimisation of the kidney models and surgical tool-tissue interaction deformation studies using an RGB-D camera to feed data to a DT. Overall, this approach shows great promise in producing mechanically-realistic organ phantoms, potentially reducing dependency on cadavers and animals in surgery, while also contributing to the development of cutting-edge digital health technologies, such as the proposed real-time Digital Twin-Assisted Surgery (DTAS)[2].

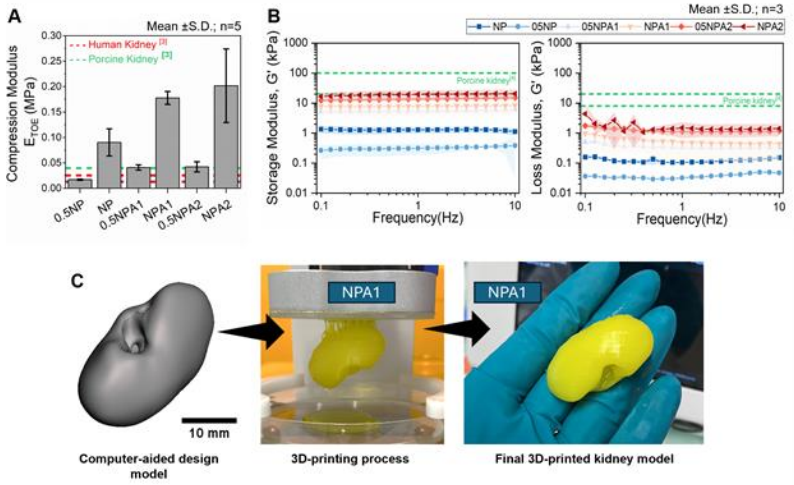

Figure 1: pNIPAM:alginate IPN hydrogels: (A) elastic and (B) viscoelastic properties, and (C) 3D-printed scaled-down kidney model.

[1] K. Qiu et al., 2018, Annu. Rev. Anal. Chem., 11(1): p.287-306. [2] L. Asciak et al., 2025, npj Digit. Med., 8(1): p.32. [3] J.G. Snedeker et al., 2005, J. Biomech., 38(5): p.1011-1021. [4] G. Nieva-Esteve et al., 2024, Mater. Adv., 5(9): p.3706-3720.

A database to fix the inconsistency in clinically reported human airway dimensions

Ola M[1], Seal M[2], Burrowes K[2], Kaul H[1]
[1]University Of Leicester, [2]Auckland Bioengineering Institute, University of Auckland

Respiratory disease causes 4 million deaths annually/worldwide. Precision medicine represents a powerful approach to treating respiratory diseases, but requires the ability to stratify a priori patient-specific response (e.g. lung function or reduction in muscle mass) to therapy. In silico models are increasingly being utilised to achieve this[1]. However, this entails developing more sophisticated computer models that accurately recapitulate patient-specific pathophysiology[2]. The starting point is creating a precise lung geometry. Despite a plethora of literature on this topic, reported airway dimensions are inconsistent. Consequently, computer predictions compromise and inhibit the clinical scale delivery of precision respiratory medicine. To address this, we systematically reviewed clinical literature on human airway wall thickness vs bronchial diameter. We analysed ~50 airway datasets for healthy and diseased patients (17). To conduct direct comparison between various datasets, we standardised the data (i.e. wall thickness) to bronchial diameter. We noted significant inconsistency in reported dimensions. For example, the tracheal thickness varied from 0.3–6.3mm and 0.52–6.99mm for healthy and diseased individuals. Unsupervised clustering divided the data into three clusters with only cluster 2 providing realistic estimates. Different data from all three clusters were simulated on a ventilation model[3], which predicts differences in model outcomes via inconsistent dimensions. Using this analysis, we have created a database where researchers can upload new datasets or confirm whether their dataset recapitulates airway dimensions accurately. We anticipate our work and database will help standardise modelling outcomes in the respiratory context and, thereby, accelerate the development and deployment of precision medicine strategies in respiratory medicine.

[1] R. Bordas et al., 2015, PLoS One, vol. 10, no. 12, pp. e0144105.
[2] S.C. George et al., 2007, Drug Discov. Today Dis. Models, vol. 4, no. 3, pp. 123–124.
[3] A.J. Swan et al., 2012, J. Theor. Biol., vol. 300, no. 1, pp. 222–231.

Effect of Supporting Surface on Chest Compressions During CPR: A Finite Element Study

Cui Z[1], Tang J[1], Jiang L[1]
[1]University of Southampton

Chest compression plays a critical role in the chain of survival during cardiopulmonary resuscitation (CPR) [1], especially in out-of-hospital settings whereby current survival rate remains below 10%. International guidelines, e.g. European Resuscitation Council [2], recommended a chest compression rate of 100–120/minute and an effective compression depth (ECD) of approximately 30% of the anterior–posterior chest dimension (below 5cm for a child, and 5-6cm for an adult) to achieve effective restoration of organ and coronary perfusion. In-silico studies using finite element analysis (FEA) have been widely adopted to aid understanding of chest mechanics during CPR [3]. However, to date, no studies have comprehensively accounted for the compliance of supporting surfaces in CPR FEA.

A theoretic FEA model is reconstructed from clinical CT data, incorporating a typical ribcage and sternum whereby the ECD is also defined (Figure 1a). Material properties corresponding to an adult and a child as well as three typical supporting surfaces i.e. ground, soft mattress, firm mattress are included in Figure 1b. A load (420N for adult and 300N for child) was applied to the sternum, mimicking a real chest compression. Figure 1c shows larger ECDs with mattress supports are obtained as compared with those from the rigid ground (up to 6% for adult, and 6.5% for child). This could be taken into consideration for future FEA studies and effectiveness of CPR deliveries. The effects of support surfaces on thoracic stress distribution will also be analysed.

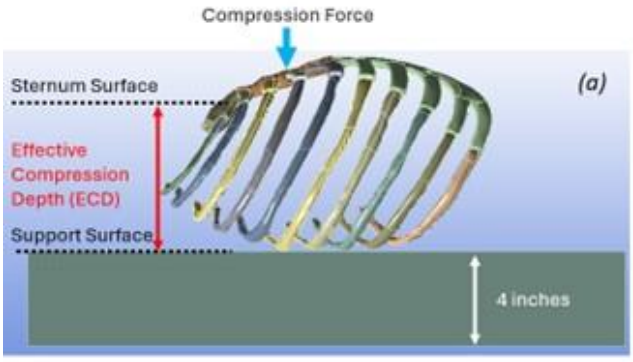

Materials	Young's Modulus	Poisson's Ratio
Adult Rib Bone (Cortical)	12 GPa	0.3
Adult Cartilage	5 MPa	0.47
Child Rib Bone (Cortical)	9 GPa	0.3
Child Cartilage	3 MPa	0.47
Soft Mattress	0.1 MPa	0.35
Firm Mattress	1.2 MPa	0.35
Rigid Ground	3 GPa	0.2

(b)

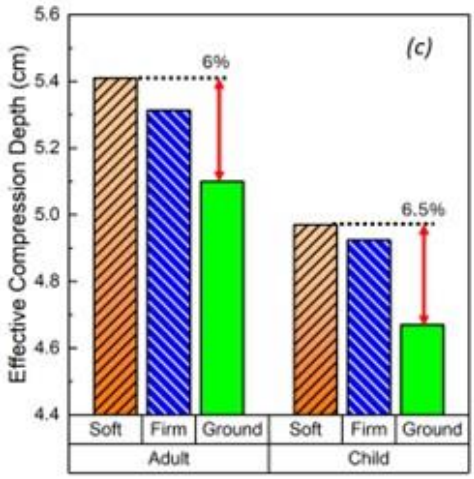

Figure 1 (a) The FE model; (b) Material properties; (c) EDs obtained across different support surfaces.

1. B. J. Bobrow et al., 2010, JAMA, vol. 304, no. 13, pp. 1447–1454.
2. T. M. Olasveengen et al., 2021, Resuscitation, vol. 161, no. 1, pp. 98–114.
3. J. H. Jeon et al., 2024, Bioeng., vol. 11, no. 5, pp. 491.

Evaluating Suture Performance in Abdominal Wall Closure: A Simulation-Based Approach

Poprawa N[1], Weragoda D[1], Makarovaite V[1]
[1]University Of Kent

This project presents the outcomes of a COMSOL Multiphysics [1] simulation evaluating sutures for the prevention of incisional hernias, focusing on stress distribution across a 3D abdominal wall model measuring 15 cm by 4 cm by 6 cm. The anatomically representative model incorporates skin (3 MPa), fascia (5 MPa), linea alba (7.73 MPa), muscles (0.19 to 2.75 MPa), fat (3.50 kPa), and peritoneum (6.79 MPa), subjected to a physiological intra-abdominal pressure of 30 mmHg (approximately 4 kPa) (Fig. A). Various suture closure methods were assessed, including interrupted and continuous patterns (Fig. B), clips, and tensioning or mass closure techniques at various levels of abdominal closure. The simulation showed that continuous sutures consistently generated higher localised stress than interrupted sutures across the same material types (Fig. C & B) when utilised in deep versus superficial layers, an unexpected result that contrasts with existing literature, which typically suggests continuous patterns distribute tension more evenly. It also demonstrated that abdominal tissue is more prone to tearing than the suture itself, aligning with observed suture failure patterns in abdominal surgeries at East Kent Hospitals NHS Trust (EKHUFT). The project delivers a proof of concept that demonstrates how finite element analysis can help identify optimal suture strategies, offering environmental benefits by reducing the need for physical experiments and material waste. It also aims to reduce future hernia incidence, improve recovery, and lower healthcare costs, estimated at near £70 million annually in the UK [2].

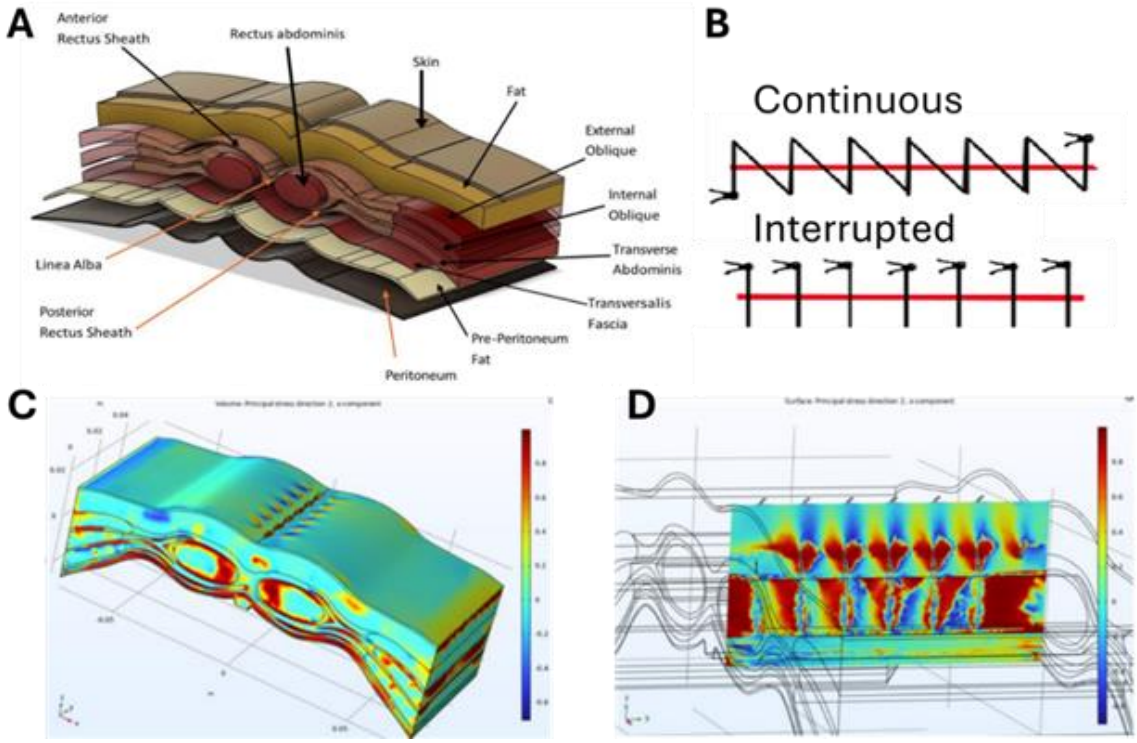

Figure: 3D abdominal wall modelling showing suture types and stress distribution using COMSOL: A)full model, B)comparisons, and C)3D and D)2D.

[1] COMSOL AB, 2024, COMSOL Multiphysics® v6.2 User's Guide, COMSOL Inc., Stockholm, Sweden.
[2] British Hernia Society, 2020, Unwarranted Variation Scenario: Getting the Complex Abdominal Wall Repair Pathway Right, British Hernia Society, July 2020.

Radar-Based Classification of Knee Osteoarthritis Rehabilitation Exercises Using Deep Learning

Cooper A[1,2], Pathmanabhan M[1], Elsayed M[1], Akaydin A[1], Ghadban N[1], Vuckovic A[2], Clarke J[3], Le Kernec J[1]
[1]BioRadar Lab, University Of Glasgow, [2]Centre for Rehabilitation Engineering, University of Glasgow, [3]Department of Orthopaedics, Golden Jubilee University National Hospital

Knee osteoarthritis (KOA) is a major contributor to pain and mobility limitation in older adults [1]. Rehabilitation exercises are a core component of conservative management [2]. This study presents a simulation-first approach for classifying KOA rehabilitation exercises using radar-derived micro-Doppler (μD) spectrograms and deep learning.

μD spectrograms were generated using a custom radar simulation pipeline driven by motion capture data from 14 participants performing four clinically relevant exercises: reverse lunges (RLN), standing knee flexions (SKF), seated knee extensions (SKX), and squats (SQT). A pre-trained ResNet-18 architecture was fine-tuned using focal loss. To evaluate model consistency and robustness, ten independently seeded models were trained using stratified sampling. Performance was assessed on an internal held-out test set and validated on a separate external dataset comprising six unseen participants (n = 60 images per class). Across ten independently trained models, internal test set performance was highly consistent with mean F1- scores ≥ 0.98 for all classes. External validation achieved mean F1-scores of 0.91–0.98 across classes and an overall accuracy of 93.63% ± 2.24%, confirming strong generalisation despite training solely on synthetic data.

The aggregated confusion matrix (Figure 1) illustrates the model's robustness and the most common misclassification patterns.

This work demonstrates the feasibility of using simulated radar data to train high-performing classification models for KOA rehabilitation. The simulator, preprocessing pipeline, and model will be released as open source to support future research. Validation on real radar data is currently underway.

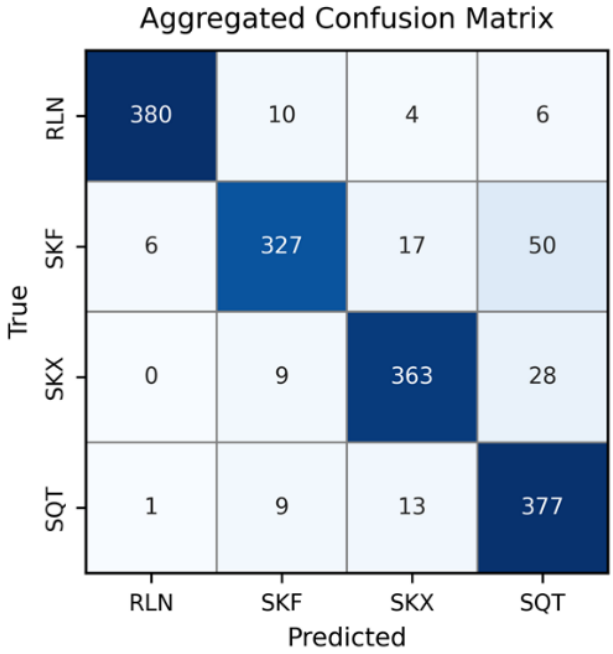

Figure: Aggregated confusion matrix across 10 models on external validation set

[1] D.J. Hunter et al., 2006, BMJ, vol. 332, no. 7542, pp. 639–642.
[2] M. Fransen et al., 2015, Br J Sports Med, vol. 49, no. 24, pp. 1554–1557

Clinically-relevant lower limb joint angle reconstruction from arbitrary 2D images of gait.

Paton A[1], Giardini M[2], Ligeti A[1], Riches P[1]
[1]University Of Strathclyde, [2]University of Dundee

Despite marker-based motion capture systems (MBS) being the gold standard for kinematic analysis, they are not in widespread clinical use, whereas markerless motion capture systems (MMS) return data unsuitable for immediate clinical application. If single-camera images of gait contain sufficient information to predict clinically meaningful joint angles (RMSE <5°), this could herald a step change in home and community-based rehabilitation monitoring. Five Raspberry Pi cameras, placed around a treadmill and time-synchronised with Vicon at 10Hz, captured six healthy participants walking for 2 minutes. Pose estimation software, OpenPose, determined 2D pixel coordinates for 25 joint centres from each frame. For each lower limb joint, coordinates were centred at the joint interest and normalised with respect to the distance between the neck and mid hip pixel values. Left and right-sided normalised joint centre coordinates of hip, knee and ankles and time-synchronised flexion/extension from 5 participants trained various regression models, which were tested using the sixth participant. The model predicting right hip angles provided values within acceptable accuracy, with a RMSE of 2.4° and 95% of data lying within ±2.3°. The other five joint models were less successful with the right ankle performing the worst with a RMSE of 15.7° and 95% of data lying within ±9.8°. There was no dependence of the accuracy of model predictions on camera angle. The developed workflow shows tremendous potential to determine lower limb joint flexion from 2d images given a larger training data set.

Walking With a Stimulated Hip: Exploring the Role of Gluteus Medius FES in Gait

KATIRCI O[1,2], Bull A[1]
[1]Department of Bioengineering, Imperial College London, UK, [2]Department of Health Sciences, Afyonkarahisar Health Sciences University

Stroke is a major global cause of mortality and long-term disability [1], often resulting in reduced muscle activation, impaired pelvic stability, asymmetric weight distribution, and difficulties in lower limb transfers. These deficits negatively affect balance, increase fall risk, and impair gait performance. External lateral pelvic correction has been shown to enhance paretic-side muscle activation and weight-bearing [2], potentially achievable through functional electrical stimulation (FES) targeting hip abductors. This feasibility study investigated the acute effects of FES applied to the gluteus medius muscle in healthy individuals, examining its impact on the activation and performance of surrounding lower extremity muscles during walking. The research aimed to establish baseline insights necessary for future clinical studies involving stroke survivors. Ten healthy participants (5♂, 5♀; age: 26.9±2.31 years) were evaluated under two conditions: walking with and without FES. Electrodes placed on the non-dominant gluteus medius delivered a 45 Hz asymmetrical biphasic waveform at a maximum current of 80 mA, sufficient to induce hip abduction without discomfort. Participants walked over force plates at self-selected speeds, while motion and force data were captured using a 10-camera VICON system and Kistler force plates, subsequently processed via Vicon Nexus, MATLAB, and FreeBody software. Statistical analyses included Shapiro-Wilk normality tests followed by paired t-tests or Wilcoxon tests, as appropriate (α=0.05). Contrary to initial hypotheses, significant or near-significant decreases in muscle force were observed in three muscles (area under the curve, UCA) on the FES-stimulated side (Table 1), suggesting participants might transfer weight to their dominant limb to avoid FES-induced sensations.

Muscle	Condition	Peak force Mean or Median (BW)	SD or Min-Max	UCA Mean or Median (BW)	SD or Min-Max	p-value Peak	p-value UCA
Gluteus Medius	Control	1.44	0.56	48.23	16.69	0.11	0.03
	FES	1.31	0.38	41.24	9.06		
Gluteus Minimus	Control	0.31	0.11-0.55	9.04	2.57	0.11	0.05
	FES	0.28	011-0.47	7.79	2.79		
Rectus Femoris	Control	4.50	1.68	96.81	41.28	0.27	1.00
	FES	4.17	1.23	96.81	44.14		
Soleus	Control	2.32	1.17	55.41	0.91-124.44	0.25	0.10
	FES	2.49	1.16	76.81	26.57-120.81		

Table 1. Significant or near-significant body weight-normalised (BW) peak and total muscle forces on the non-dominant side during walking

[1] Campbell et al., 2019, Nat Rev Dis Primers, 5:70.
[2] Hsu et al., 2017, Clin Neurophysiol, 128(10):1915-22

A biomechanical comparison of athlete agility performance under mental and physical fatigue

Docherty C[1], Childs C[1]
[1]Strathclyde University

Agility is a complex open motor skill that demands simultaneous coordination of multiple cognitive, physical, and technical constraints [1]. While the importance of agility performance is well established, evidence surrounding the underlying mechanisms, and the effect of fatigue on agility performance metrics is lacking. This study aimed to determine the impact of mental and physical fatigue on reaction time during a laboratory-based agility test.

Fourteen athletes (7 male, 7 female, aged 23.2 ± 3.6 years) participated in a randomised within-subjects crossover study. Participants attended three days of testing, separated by >48 hours. Each day consisted of identical time-synchronised pre-intervention and post-intervention testing using a D-Flow programmed agility test, Kistler force plates, and Vicon Nexus motion capture. In between testing, participants either completed a Stroop Test mental fatigue, a Wattbike physical fatigue, or a control intervention. Reaction time was defined between the start of the test and the first vertical ground reaction force (Fz) reading exceeding a ±20N threshold.

A linear mixed-effects model was used to assess the effect of time (pre and post) and condition (mental fatigue, physical fatigue, and control) on reaction time. Participant differences were included as a random intercept. There was no significant main effect of time or condition x time interaction; however, there are some differences between the conditions that approach significance. This conference presentation will delve into the nuances of the differences revealed, along with their implications for the development of agility training protocols and testing batteries in performance sport.

[1] Sheppard & Young, 2006, Journal of Sports Sciences, 24(9), 919-932.

The Assessment of Muscular and Kinematic Asymmetry Following a Transtibial Amputation

Little H[1], Murray L[2], Aranceta-Garza A[1]
[1]Centre for Medical Engineering and Technology. University of Dundee., [2]Department of Biomedical Engineering, National Centre for Prosthetics and Orthotics, University of Strathclyde.

This pilot study aimed to investigate muscle activation and joint kinematic asymmetry in individuals with transtibial amputation (TTA). We explored the relationship between neuromuscular activity using Delsys Trigno Avanti surface electromyography (sEMG) and gait mechanics using Xsens Awinda-Movella inertial measurement technology. Christensen et al., investigated movement asymmetries in transtibial amputees, particularly during high-demand tasks like step ascent. They found significantly greater asymmetries in knee and ankle mechanics compared to healthy controls [1]. Surface EMG and IMUs were used to assess the rectus and biceps femoris during functional mobility tasks, including the Timed Up and Go (TUG) test and the 2-Minute Walk Test (2MWT). On average, rectus femoris activity was 44 % lower in the amputated limb compared to the intact limb. Our results align with findings by Sarroca et al., who reported that quadriceps activation was up to 30% lower than in controls, particularly at higher walking speeds, suggesting muscular asymmetries, while hamstring activation remained relatively consistent [2]. Unlike current research suggesting hamstring activity is largely unaffected by TTA, our findings showed a 155.6% increase in hamstring activation on the amputated limb, indicating a substantial compensatory role during TUG test. Correlations suggest that increased muscle activation was often associated with greater kinematic asymmetry, implying compensatory mechanisms. While differences were noted across prosthetic foot types, the small sample size limited firm conclusions. This study offers early insights into gait asymmetry and compensatory strategies in TTA individuals, highlighting the need for further investigation.

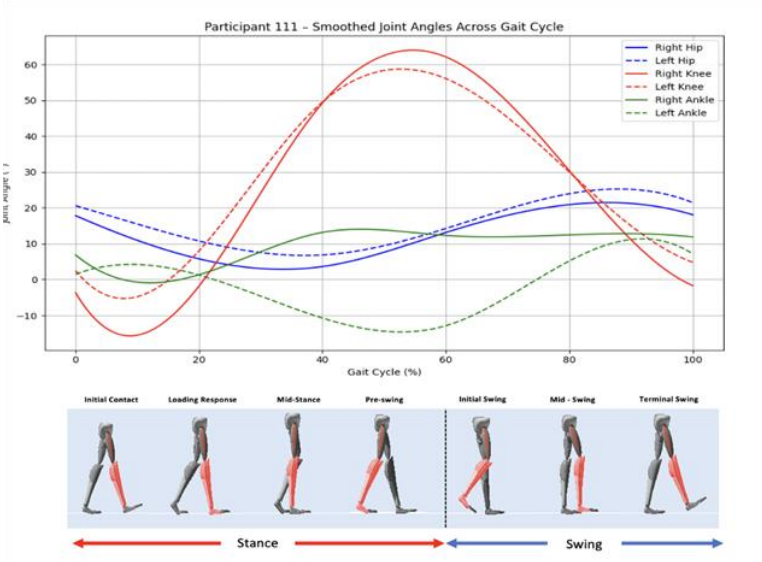

Symmetries in TUG gait: left ankle shows more dorsiflexion, right knee more extension, right hip reduced extension.

[1] Christensen et al., 2020, Movement asymmetry during low and high demand mobility tasks after dysvascular transtibial amputation, Clin Biomech, vol. 80, 105102. [2] Sarroca et al., 2021, Muscle activation during gait in unilateral transtibial amputees, J Clin Med, vol. 10, no. 14.

Near-cellular to Whole Organ Quantitative Mapping of the Human Heart Using Hierarchical Phase-Contrast Tomography

Brunet J[1], Cook A[3], Dejea I Velardo H[2], Bellier A[4], Walsh C[1], Tafforeau P[2], Lee P[1]
[1]Department of Mechanical Engineering, University College London, [2]ESRF, [3]– Institute of Cardiovascular Science, University College London, [4]– Laboratoire d'Anatomie des Alpes Françaises (LADAF)

Quantitative, multiscale mapping of the human heart is essential to understand cardiac structure-function relationships and the pathophysiology of cardiovascular diseases. While imaging below 50µm voxel size has been applied to small animal hearts and fetal specimens [1], visualizing the intact adult human heart at near-cellular resolution has remained a major challenge. Hierarchical Phase-Contrast Tomography (HiP-CT), a synchrotron X-ray technique, now enables non-destructive imaging of large soft-tissue organs at circa-10 micrometers-scale resolution across the entire volume [2]. Here, we applied HiP-CT to image a complete adult human heart at 8.01 µm isotropic voxel size. We performed detailed 3D segmentation of key cardiac systems. Cardiomyocyte orientation was calculated using an inhouse python code based on structure tensor. Vascular and neural trees were skeletonized for morphometric analysis.

Our results demonstrate that HiP-CT can resolve and quantify the architecture of the coronary arterial and venous systems, the conduction system, cardiac lymphatics, and extrinsic innervation with unprecedented resolution (Figure 1). Coronary vessels were segmented from major trunks to fine branches including the sinoatrial artery. Myocyte orientation was mapped throughout the myocardium, showing the helical structure of cardiomyocyte aggregates. The atrioventricular conduction system was traced from nodal tissue through Purkinje fibers. We further identified lymphatic pathways and lymph nodes, and visualized the trajectory of cardiac nerves from extrinsic sources into the myocardium. This study highlights the capacity of HiP-CT to resolve, segment, and analyze major functional systems within the intact human heart at multiple scales, bridging the gap between clinical imaging and cellular architecture.

Figure 1: 3D visualization of an intact adult human heart. Coronary arteries(red), veins(blue), nerves(white), lymphatics(green), conduction system(yellow), cardiomyocyte orientation(rainbow).

[1] Garcia-Canadilla et al., Circ. Cardiovasc. Imaging 11.10 (2018)
[2] Walsh et al., Nat Methods 18, 1532–1541 (2021)

Resolving micron-scale features within a whole head using HiP-CT

Urban T[1,2], Mirone A[2], Brunet J[1,2], Dejea I Velardo H[2], Bellier A[3], DIdziokas M[1], Moazen M[1], Orsine Murtas Dias K[4], Petrushkin H[4], Walsh C[1], Lee P[1], Tafforeau P[2]
[1]Department of Mechanical Engineering, University College London, [2]European Synchrotron Radiation Facility, [3]University Grenoble Alpes, Department of Anatomy (LADAF), AGEIS, CIC Inserm 1406, [4]Moorfields Eye Hospital NHS Foundation Trust

Quantifying the morphology and structure of the head at various length scales is crucial to understand patho-physiological processes and improve the diagnosis and treatment of associated diseases. A range of imaging techniques with different contrast modalities, achievable field of view, resolution, and in-vivo compatibility serve this purpose. Synchrotron-based hierarchical phase-contrast tomography (HiP CT) is one of them, offering high soft-tissue contrast and resolution with a large field of view, but no in-vivo compatibility.

So far, HiP-CT has only been applied to soft-tissue human organs. To address challenges in imaging complex samples with both hard and soft tissues, the iterative Eikonal Phase Retrieval (EPR) method was recently introduced. It accounts for the polychromatic X-ray spectrum and uses a forward model of X-ray propagation from sample to detector.
Here, we demonstrate the feasibility of using HiP-CT and EPR to image an entire skinned sheep head prepared in 70% ethanol with an isotropic voxel size of 16.5 µm, achieving high contrast for both hard and soft tissue (Panel A-H). We performed local zooms in two regions of interest. In the eye (voxel size 4.23 µm), micron-scale features such as retinal layers, the ciliary body, the vasculature in the sclera and the bundles in the optic nerve can be visualized (Panel I-N). In the coronal suture (voxel size 2.20 µm), even the collagen structures within the suture are visible (Panel R). This work highlights the potential of HiP-CT to image a complete head and hierarchically zoom without sectioning to resolve micron-scale features locally.

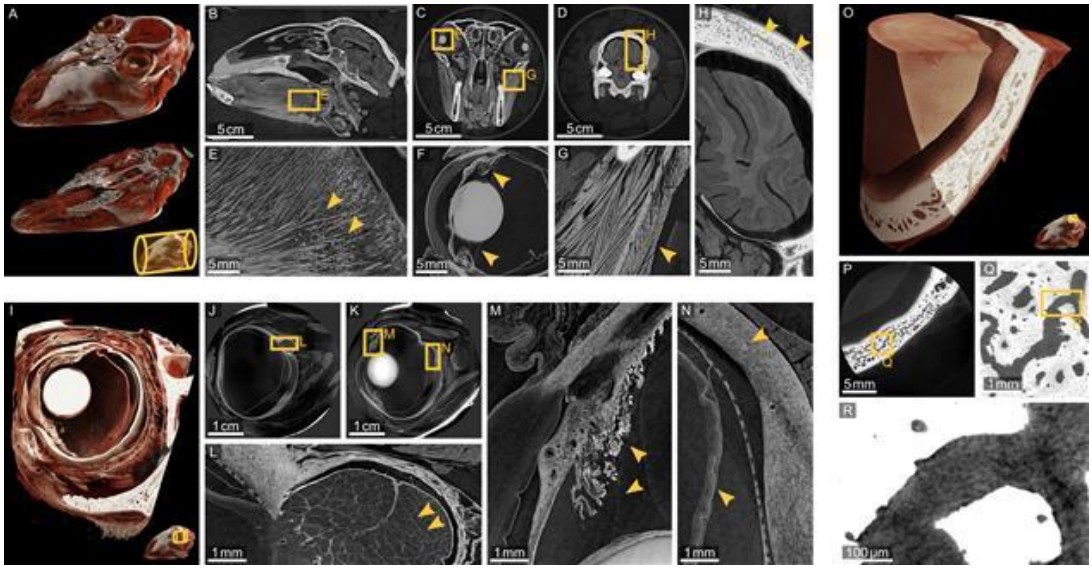

Figure: Top left, complete sheep head. Bottom left, local tomography in the eye. Right, local tomography in the coronal suture.

Towards the use of Hierarchical Phase-Contrast Tomography (HiP-CT) as a ground truth reference for validating Diffusion-weighted Magnetic Resonance Imaging (dMRI).

Wanjau E[1], Chourrout M[1], Javanmardi Y[1], Lee P[1], Walsh C[1]
[1]Department of Mechanical Engineering, University College London

Mapping white matter structure and connectivity is fundamental to understanding brain function, improving neurosurgical planning, and advancing research into neurodegenerative diseases. While dMRI is widely used to infer white matter connectivity, it provides an indirect probe of tissue microstructure based on modeling the diffusion of water. In addition, typical dMRI resolution is in the order of millimeters while white matter axons have diameters in micrometer range. These factors create uncertainties in resolving small fiber bundles and complex white matter profiles necessitating validation with complementary imaging that can directly image axons [1]. This study introduces HiP-CT [2] as a ground-truth imaging modality for characterizing white matter fiber orientation. HiP-CT is a non-targeted contrast synchrotron X-ray imaging technique that offers non-destructive, 3D imaging of whole human organs at resolutions greater than 25µm/voxel. Given HiP-CT's non-targeted contrast nature, we also investigated the influence of vessels on white matter analysis. We developed a computational pipeline that includes human-in-the-loop vascular segmentation and structure tensor analysis (STA) to quantify white matter orientation. Our results demonstrate that HiP-CT combined with STA enables non-destructive, contrast-free, micron-scale quantification of white matter fibers, overcoming key limitations of traditional validation modalities such as histology. Furthermore, vascular networks exert minimal confounding effects on fiber orientation estimates in HiP-CT as shown by high angular correlation with/without vessel masking. This work establishes HiP-CT as a powerful tool for high-resolution ground-truth validation of standard dMRI models [3-4], providing a crucial step towards more accurate mapping and understanding of the human connectome.

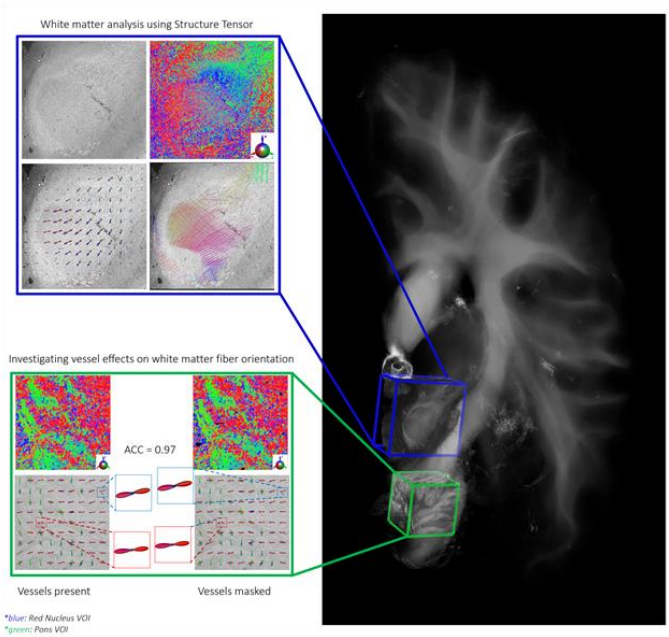

Structure Tensor Analysis pipeline for estimating white matter fiber orientation in HiP-CT. Vessels are shown to exert minimal confounding effects.

[1] A.Yendiki et al., 2022, Neuroimage, vol. 256, pp. 119146. [2] C.L.Walsh et al., 2021, Nat Methods, vol. 18, no. 12, pp. 1532–1541. [3] P.J.Basser et al., 1994, Biophys J, vol. 66, no. 1, pp. 259–267. [4] J.D.Tournier et al., 2007, Neuroimage, vol. 35, no. 4, pp. 1459–1472

Cohort analysis of the high-resolution atlases of whole ex vivo brains with hierarchical phase-contrast tomography (HiP-CT) and NextBrain

Chourrout M[1], Keenlyside A[1], Balbastre Y[2], Boettcher L[3], Brunet J[1,4], Urban T[1,4], Dejea I Velardo H[4], Tafforeau P[4], Bellier A[5], Lee P[1], Walsh C[1]
[1]Dept. of Mechanical Engineering, University College London, [2]Dept. Experimental Psychology, University College London, [3]Rollins College, [4]European Synchrotron Radiation Facility, [5]Laboratoire d'Anatomie des Alpes Françaises

Mapping neuroanatomical structures across age and disease states highlights pathological development and leads to novel therapeutic targets. Currently, this often relies on 1mm MRI scans in clinical practice [1], but the changes we need to detect are often at the mesoscopic scale (100um–10um). Other complementary techniques such as light-sheet microscopy [2] are not currently scalable to adult whole brains; furthermore, they are inherently destructive and targeted towards a few cell types or markers. Using hierarchical phase-contrast tomography, we were able to scan ex vivo intact and unlabelled brains down to 15–20 microns in a matter of a few hours [3]. By adapting tools from the MRI community [4], we can efficiently analyse this unique data, providing highly detailed, 3D modelling of the deep structures of the brain across the six donors of this study.

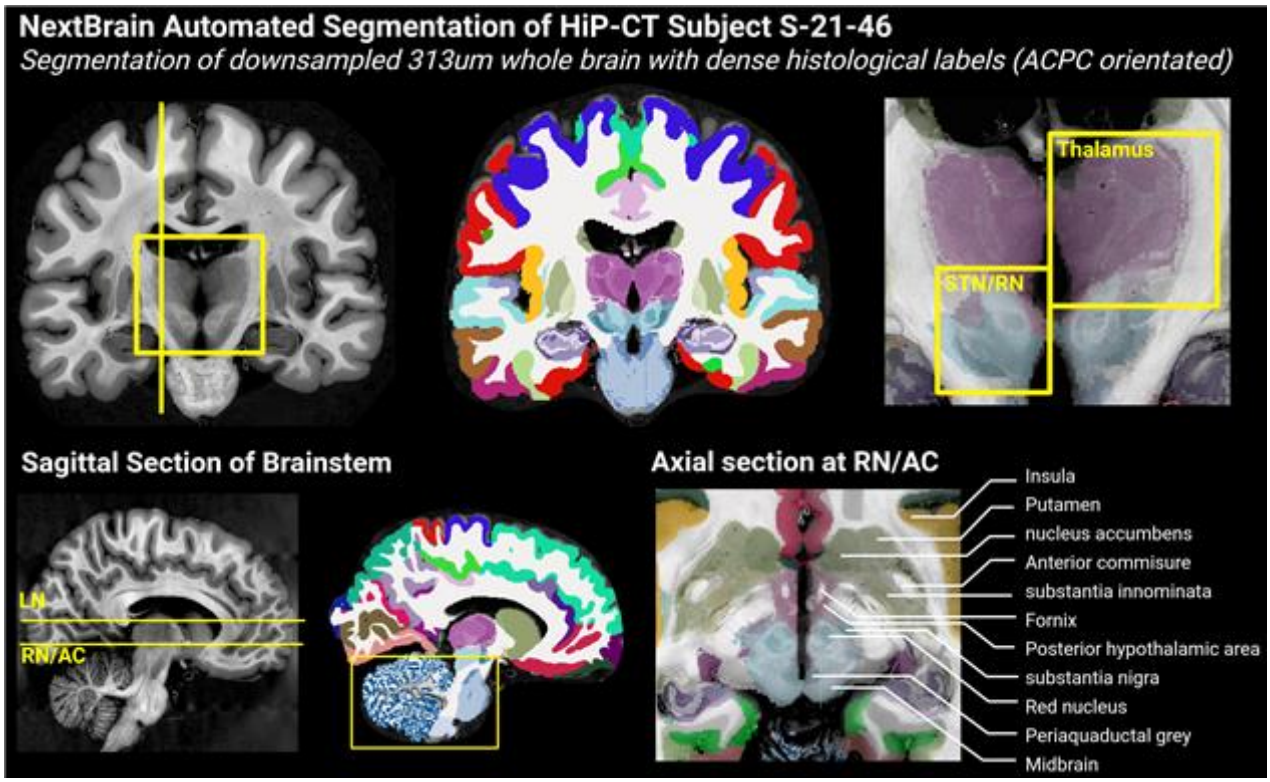

NextBrain automated segmentation of the HiP-CT of the whole brain of donor S-21-46

[1] Lerch JP et al. Nat Neurosci. 2017 Feb 23;20(3):314-326.
[2] Hillman EMC et al. Annu Rev Neurosci. 2019 Jul 8;42:295-313.
[3] Walsh CL et al. Nat Methods. 2021 Dec;18(12):1532-1541.
[4] Mancini M et al. Sci Rep. 2020 Aug 14;10(1):13839.

Establishing a Contrast-Enhanced Micro-Computed Tomography Protocol for Visualizing Rodent Growth Plates

Jayasuriya S[1], Bull A[1], Ashton D[1]
[1]Department of Bioengineering, Imperial College London

Growth plates are drivers of longitudinal growth in children and play a key role in determining bone shape and size at maturity. Disruption and injuries to the growth plate can lead to growth disturbance and secondary musculoskeletal conditions. Rodent models have been used to study the pathophysiology of growth plate injuries and evaluate potential new treatments. Changes in growth plate structure and morphology following injury have conventionally been assessed using histological methods that are destructive and experimentally challenging and yield two-dimensional analysis, or using micro-Computed Tomography (µCT), which is limited by growth plate radiolucency.

Contrast-enhanced micro-Computed Tomography (CE-µCT) has previously been used for imaging of rodent articular cartilage in models of osteoarthritis. CE-µCT using an appropriate contrast agent and growth plate infiltration approach could provide a means of non-destructive, three-dimensional imaging of rodent bone growth plates. This study presents the first protocol for CE-µCT imaging of rodent growth plates and their adjacent epiphyseal and metaphyseal bone. The development process involved testing different contrast agents, staining durations, µCT parameters, and tissue preparation strategies. This protocol offers a novel alternative for assessing growth plate injuries in rodent models while overcoming key limitations of conventional imaging methods.

Skeletonization to Assess Cardiac Vasculature Segmentation in Hierarchical Phase-Contrast Tomography

Occhipinti E[1], Javanmardi Y[1], O'Leary E[1], Lefebvre T[1], Brunet J[1,2], Bellier A[3], Cook A[4], Lee P[1], Walsh C[1]
[1]Department of Mechanical Engineering, University College London, [2]European Synchrotron Radiation Facility, [3]Laboratoire d'Anatomie des Alpes Françaises, Université Grenoble Alpes, [4]Institute of Cardiovascular Science, University College London

Hierarchical Phase-Contrast Tomography (HiP-CT) is an advanced imaging modality that enables multi-scale imaging of entire organs, achieving voxel sizes ranging from 25µm low-resolution overview scans to 1–2µm high-resolution volumes of interest [1]. This technology has been successfully used to examine a variety of organs, including the heart, enabling detailed structural and vascular analysis across scales [2]. Such high resolution presents new opportunities for vascular segmentation, from large vessels down to fine capillaries. However, to evaluate the quality and utility of such segmentations, robust and interpretable metrics are needed. Skeletonization offers a promising approach to assess and quantify vascular structures, as it reduces segmented volumes to simplified representations that preserve topological and morphological features [3]. In this study, we compare several skeletonization methods applied to HiP-CT data of the human heart (voxel size=32.04µm) including classical techniques such as the medial axis thinning algorithm and the tree-structure extraction algorithm for accurate and robust skeletons (TEASAR), as well as newer machine learning-based approaches. Using manually labelled segmentations as ground truth, we extract skeletons, identify nodes and branches, compute morphological and topological features, and assess the robustness of each skeletonization method. Our results reveal trade-offs between accuracy, computational complexity, and feature stability across techniques, with different features contributing variably to biological interpretations such as vascular branching patterns, connectivity, and structural integrity. These findings offer guidance on selecting suitable skeletonization algorithms for evaluating vascular segmentations in high-resolution volumetric datasets and support future quantitative analysis of HiP-CT, and other synchrotron and laboratory tomographic data.

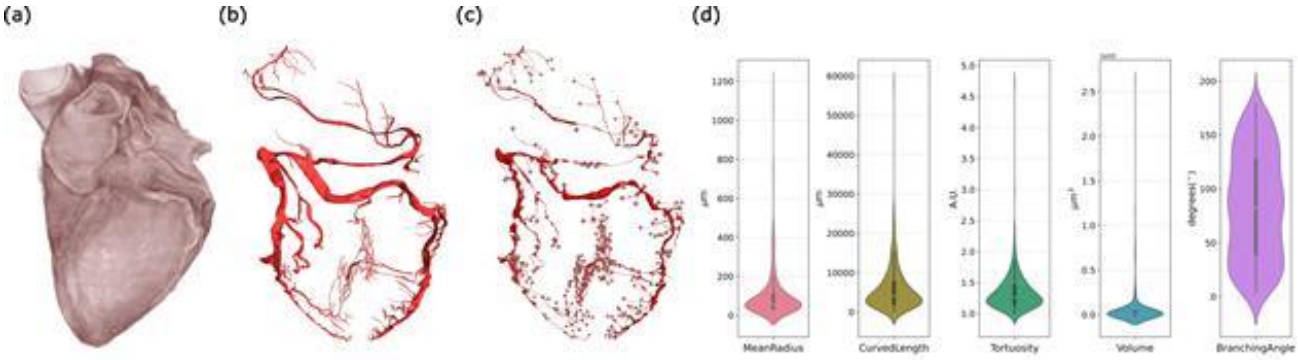

Figure: a) HiP-CT volume of the heart; b) Manual vascular segmentation; c) Skeleton and branch points; d) Segment features extracted

[1] C.L. Walsh et al., 2021, Nat Methods, vol. 18, pp. 1532-1541
[2] J. Brunet et al., 2024, Radiology, vol. 312, no. 1, pp. e232731
[3] C.L. Walsh et al., 2024, Computers in Biology and Medicine, vol. 171, p. 108140

Game development of a stability-based leaping activity for rehabilitative use

Forsyth L[1], Tawy G[2], Childs C[1]
[1]Biomedical Engineering Department, University of Strathclyde, [2]Division of Cell Matrix Biology & Regenerative Medicine, School of Biological Sciences, The University of Manchester

For stability-based rehabilitation to be successful the programme must include progressive and varied practices. Manipulating the activity and/or environment can ensure progress is achieved [1]. Virtual reality presents the opportunity to create diverse and challenging, yet controllable, environments for rehabilitation. For game development it is important to understand exercise progression for rehabilitation to be optimised for player engagement. The aim of this study was to assess performance of a virtual reality leaping game by exploring the relationship between challenge and engagement for optimal rehabilitation progression. Eleven healthy, able-bodied adults (26±4 years old) attended one testing session. The Strathclyde Cluster Model [2] and pointer calibration were applied to all participants. Movement was tracked using Vicon Tracker and live streamed to D-Flow software. The aim of the Leap Game was to avoid oncoming objects. The inputs were object velocity, size and distance. These inputs were manipulated for eight conditions. The percentage of objects hit in 30 seconds, and perceived enjoyment and difficulty were recorded as outputs. Conditions 3, 4 and 8 were the most difficult to perform ($p<0.05$) and were also perceived the most difficult ($p=0.01$). Conditions 6, 4 and 1 were reported as the most enjoyable. Increasing object size was the most difficult manipulation. Object velocity was the manipulation reported as most enjoyable. This study found that object size and distance are key variables for game difficulty, while velocity is important for enjoyment. These findings could optimise the balancing of challenge and engagement in future rehabilitative virtual reality games.

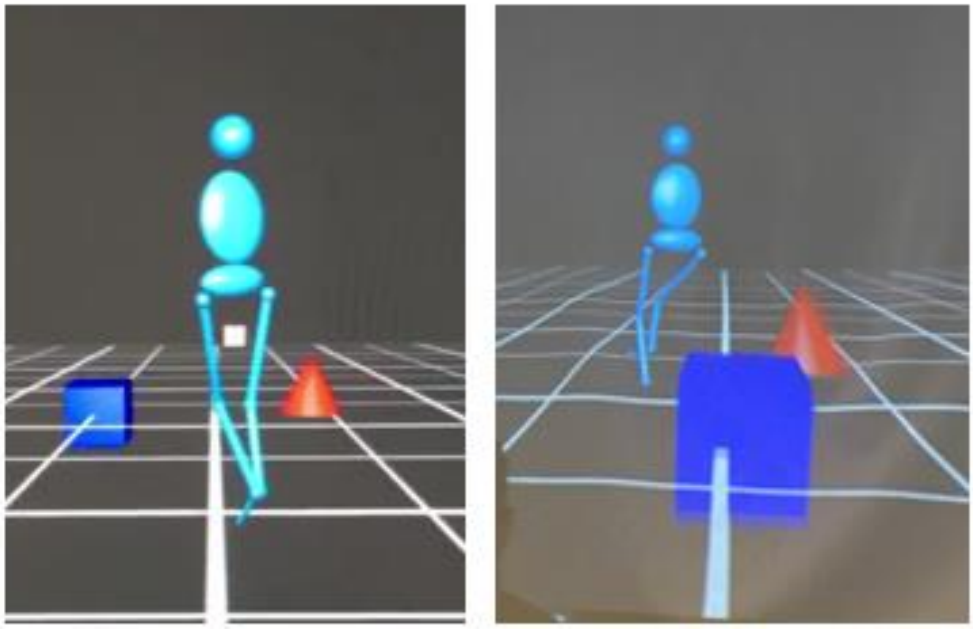

Two different levels of the Leap Game as seen by participants

[1] D Conradsson et al. 2012. Bmc Neurology, 12.
[2] LJ Millar et al. 2019. Computer Methods in Biomechanics and Biomedical Engineering. 22: 149-158.

Do sound spatialisation engines affect sound localisation abilities in normal-hearing human participants?

Domniteanu A[1], Gallacher J[2], Giardini M[3]
[1]University Of Strathclyde, [2]AA Scottish Cochlear Implant Programme, [3]University of Dundee

Detecting the direction sound provenance is indispensable to clinical hearing testing. The gaming industry developed solutions for immersive spatialization of sound in virtual environments [1], which could be used to create portable localisation tests for clinical use. It is unclear whether different implementations affect people's ability to localise sound in a virtual setting. Normal-hearing participants (n=15) were invited to six sessions. Each session, after screening through automatic Pure Tone Audiometry, participants listened to pairs of sounds through audiometry headphones and pressed a button to indicate whether the second sound came from the left or the right of the first, in a 2-alternative forced choice study [2]. Participants listened to recordings of 800Hz Pure tones virtually spatialized 1.9m away from the listener in Unreal Engine 5.3.2 (UE5) using one of the following engines: UE5 Panning, Google Resonance, Steam Audio, project Acoustics, FMOD Studio and Wwise. The angular separation between the two sounds decreased logarithmically, following the Cardiff Visual Acuity test protocol [3] and started at 10^{o}. This was repeated at 6 more azimuth positions. The smallest identified angular separation was recorded at each azimuth and Bland-Altman comparison plots were generated. Few outliers indicate the measurements are similar, although bias separates the engines into three groups. The presence of bias confirms that the spatialisation engine directly impacts the localisation abilities of people and the choice of engine must be carefully considered. A comparison to real sound and wider angular separations will help inform this decision in the future.

[1] K. Rogers et al., 2018, In proceedings of 2018 CHI Conference on Human Factors in Computing Systems, pp.1-13.
[2] F. A. A. Kingdom et al., 2016, "Psychophysics: A Practical Introduction", Second Edition. Academic Press
[3] T. O. Adoh et al., 1994, Vision research, vol. 34, no. 4, pp. 555-560.

Enhancing Myoelectric Prosthetic Response Through Sex-Differentiated Forearm EMG Analysis

Gonzalez Carmona B[1], Aranceta-Garza A[1]
[1]University Of Dundee

A myoelectric prosthesis is a type of upper-limb prosthetic device that relies on decoded surface electromyographic (sEMG) signals to differentiate muscle activity and facilitate motor control. While sex-based anatomical and physiological variations are well-documented, there is a lack of research focused on finding how these variations might affect the sEMG signals. Therefore, the aim of this research was to run a proof of concept to determine the feasibility of understanding and investigating if there were any sex-based differences in forearm sEMG signals during activities of daily living.

Twenty participants (10 male, 10 female) performed static (finger point, neutral, and pinch) and dynamic (pouring water) tasks while their sEMG signals were recorded for the muscles Extensor Digitorum, Extensor Carpi Radialis, Extensor Carpi Ulnaris, and Flexor Carpi Radialis. Signal normalisation and statistical analysis were conducted to assess intra- and inter- group differences.

Only statistical significant differences ($p=0.045$) were found for the muscle Extensor Carpi Ulnaris when neutral hand position was being examined, as well as for the pouring water task ($p=0.045$). Due to the small sample size of participants, these results cannot be extrapolated to determine whether or not there are sex-based differences in sEMG. However, differences were observed in the way to which participants would approach and perform the dynamic task. These findings highlight the need for larger-scale studies to confirm whether sex-based variations in sEMG signals impact the design and control of myoelectric prostheses. Further research could enhance personalization in prosthetic control algorithms, ensuring equitable functionality across different user groups.

Measuring effort in listening through tactile response times

Arya J[1], Simpson D[1]
[1]University Of Southampton

The most commonly used method of testing for hearing loss is Pure Tone Audiometry, which has been shown to be a poor indicator for speech comprehension in noise and thus has little ecological relevance for real-world hearing tasks. With hearing loss, listening in noise becomes more effortful and leaves fewer cognitive resources for other tasks. The aims of this study were to assess if response time with speech-in-noise stimuli used in an established hearing test for the uniformed services could be a promising indicator of effortful listening and hence to provide recommendations for follow-on studies. Fifteen participants with normal hearing were recruited. Participants listened to words with five different SNRs (Signal-to-Noise ratios) of 5, 0, -5, -9 and -12dB. Three closed sets of nine words (colours, numbers or letters) were used and each word was used twice in random order (i.e. eighteen words of each category) leading to a total of 15 test runs in each participant. Response times were measured from a touch-screen by both an accelerometer and the stimulus generating software (PsychoPy®, University of Nottingham). As expected, when SNR decreased, accuracy in word identification decreased and response times increased. This was seen in the cohort averages and also consistently in individuals. Different individuals and word sets showed a wide range of response times. The accelerometer gave more robust results than PsychoPy®. The protocol used appears promising for further investigations of effortful listening, giving insights beyond the accuracy in word identification.

Human in vitro systems to study skeletal biology and advance animal-free research.

Budyn E[1]
[1]Ecole Normale Superieure Paris-saclay

While animal models permit to work with many well-characterized individuals, results can be difficult to translate to humans. Human models offer new opportunities despite challenges such as limited number of samples, legal regulations, the need for reliable supplies, and approved facilities. Human in vitro models provide a human environment that can encompass a missing complete living organism as in animal models.

Because human tissue and cell behavior are more complicated than most mammals, advanced 3D imaging techniques such micro-CT, nano-CT, confocal fluorescent microscopy are key to understand human organoids and accurately follow the cell biology. Material characterization techniques such as nanoindentation or spectroscopies and mechanical characterizations using miniaturized testing can complement these models. Because in vitro systems are alive, in situ mechanical stimulations can drive the proper cell biology and approach in vivo conditions. Finally, mRNA analysis can be correlated to the expressed proteins in the secretome. This procedure in organ-on-chip platforms was applied to study the effects of aging and pathologies on human bone and to study the effects of regenerative medicines in the human intervertebral disc.

Acknowledgments
The author is grateful to CNRS INSIS PEPS Mécanique du future, Soleil Synchrotron 20191708, 20201633, 20230772, 20231906 awards, IsoTiComir award from the GS-SIS of University Paris-Saclay, the Anatomical Gift Association of Illinois and, the Gift of Hope Organ and Tissue Donor Network and Donor's Family.

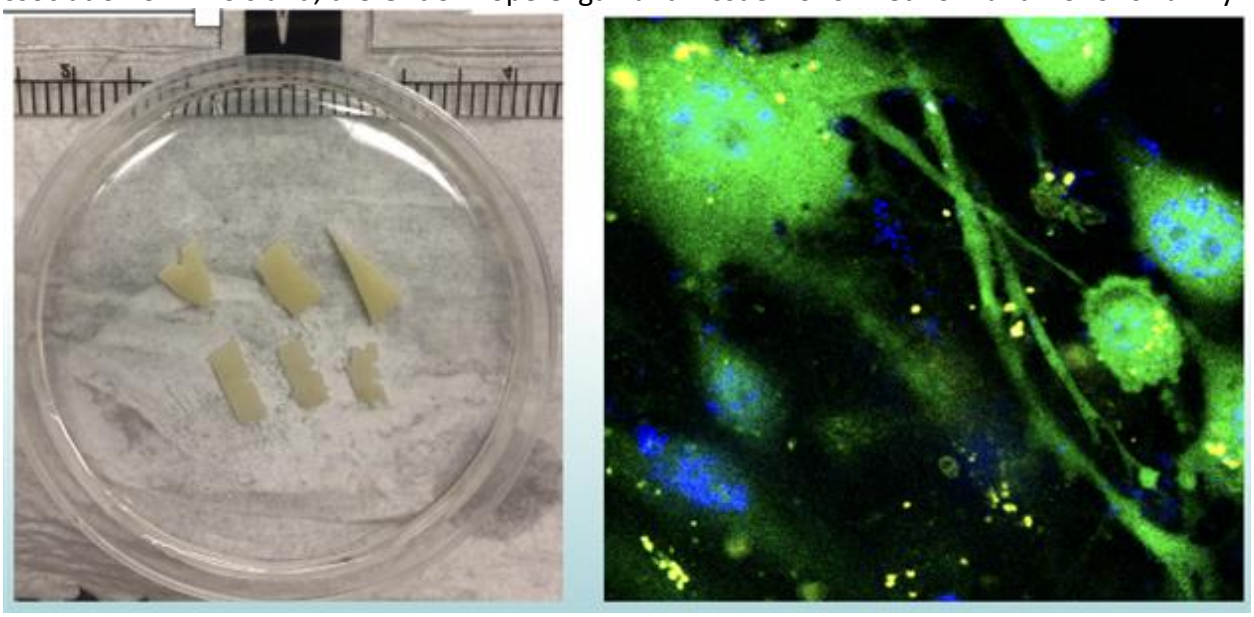

a) Different shapes for the bone-on-chip, b) stem cell derived osteocytes.

[1] E. Budyn et al., 2018, MRS Advances, vol. 3, no. 26, pp.1443-1455.
[2] E. Budyn, 2023, Tissue Engineering Part A, vol. 29, pp. 13-14.

Evaluating the use of smart glasses as a display screen for environmental control system users

Henderson G[1], Dolan M[1], Hill R[2]
[1]SMART Services, NHS Lothian, [2]Institute of Population Health, University of Liverpool

Most environmental control system set ups require a screen to be mounted in front of the user. Users report associated frustrations with screen positioning and moving of systems [1]. Using a smart glasses display (Figure 1) could potentially address these issues. Previous studies have concentrated on the impact of smart glasses on assisting users with hearing or visual difficulties rather than individuals with muscle weakness [2]. The aim of this study was to explore with service users the usability of and satisfaction with smart glasses when operating an environmental control system.

To address the above aim, established environmental control system users were set-up with smart glasses for a 3-week trial. A satisfaction questionnaire was undertaken pre and post trial. In addition, a semi-structured interview was carried out with participants to explore the impact that the smart glasses had on usability.

Four users completed the trial and it was found that users' satisfaction decreased after using the smart glasses. Some of the disadvantages discussed included the smart glasses creating a visual barrier and positioning. The main reported advantage was the use of the system in alternative positions where it is challenging to mount a standard display.

In summary, the participants in this study did not benefit from the use of smart glasses, despite this, some key advantages to using the smart glasses were identified. If the disadvantages were addressed by manufacturers there is potential that smart glasses could be an effective display for an environmental control system and support independence.

Figure 1: A mock up of how the smart glasses display would appear for the user.

[1] M. Myburg et al., 2017, Disability and Rehabilitation: Assistive Technology, vol. 12, no. 2, pp. 128-136.
[2] D. Kim et al., 2021, Applied Sciences, vol. 11, no. 11, 4956.

Comparative Analysis of Handcrafted and Deep Learning Features for Radar-Based ECG Reconstruction: Advancing Inclusive Non-Contact Cardiovascular Monitoring

Ghadban N[1], McGleish O[1], Elsayed M[1], Cooper J[1], Le Kernec J[1]
[1]University Of Glasgow

"Traditional electrocardiogram (ECG) systems necessitate the use of skin-contact electrodes, which may be unsuitable for individuals with dermatological conditions, mobility impairments, or cultural considerations. We have developed a radar-based, non-contact ECG reconstruction framework that integrates both handcrafted feature extraction and deep learning techniques. The handcrafted features encompass spectral (dominant frequency, spectral entropy), statistical (skewness, kurtosis), and physiological (heart rate variability, respiration rate) metrics, extracted using Python-based signal processing tools. Concurrently, deep learning models were trained on raw radar signals to discern complex patterns. The performance of the handcrafted features and deep learning models was evaluated both independently and in combination. Each approach demonstrated distinct strengths: handcrafted features offered interpretability and robustness, while deep learning models provided adaptability to signal variability. The combined approach resulted in superior ECG reconstruction accuracy, with enhanced correlation to ground truth ECG signals across diverse demographic profiles. Integrating handcrafted and deep learning features enhances the accuracy and inclusivity of radar-based ECG reconstruction. This hybrid framework presents a viable alternative to traditional contact-based ECG systems, particularly benefiting populations where such methods are impractical. The approach supports equitable healthcare delivery by facilitating accessible and reliable cardiovascular monitoring in diverse settings."

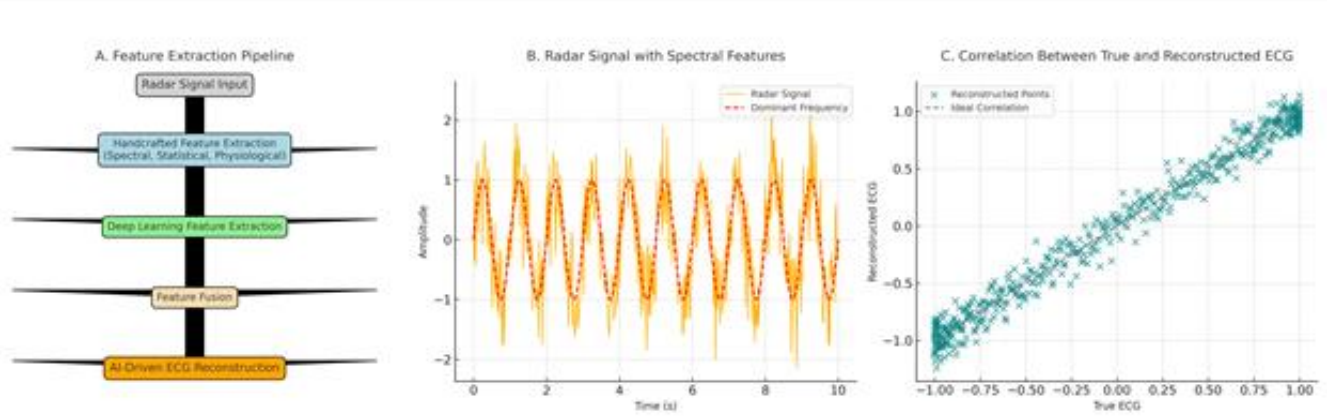

Hybrid feature extraction pipeline combining handcrafted and deep features to reconstruct ECG signals from radar with clinical accuracy.

[1] V. Gupta et al., 2021, J. Inst. Eng. (India) Ser. B, vol. 102, pp. 1049–1060.
[2] H. Malik et al., 2023, PeerJ Comput. Sci., vol. 9, p. e1364.
[3] X. Long et al., 2013, IEEE J. Biomed. Health Inform., vol. 18, no. 4, pp. 1272–1284.

Validation study of machine-learning algorithms to interpret paediatric sleep studies and diagnose sleep apnoea from retrospective PSG & CRSS data

Black S[1], Jones Y[1], Kubba H[2,5], Hamilton R[3,5], Burns P[4,5], Buchan E[4,5]
[1]Seluna Ltd, [2]Ear Nose & Throat Department, Royal Hospital for Children, NHS Greater Glasgow & Clyde , [3]Department of Clinical Physics and Bioengineering, Royal Hospital for Children, NHS Greater Glasgow & Clyde, [4]Department of Paediatric Respiratory and Sleep Medicine, Royal Hospital for Children, NHS Greater Glasgow & Clyde, [5]University of Glasgow, School of Medicine, Dentistry & Nursing

Paediatric obstructive sleep apnoea (OSA) is a prevalent but underdiagnosed condition. It is marked by intermittent upper airway obstruction during sleep, resulting in episodic oxygen deprivation and disrupted sleep. Affecting roughly 96 million children worldwide, untreated OSA leads to impaired neurodevelopment, ADHD-like symptoms, mental health decline, and an increased risk of chronic cardiac, neurological, and metabolic disorders. Current diagnostic pathways utilise inpatient polysomnography (PSG) or cardiorespiratory sleep studies (CRSS), which produce large volumes of multi-channel physiological datasets. Manual analysis of this data is labour intensive, subject to inter-rater variability, prone to human error, and time-consuming (up to 4 hours per study). Due to this bottleneck, many children receive treatment to surgically remove the tonsils, without a gold-standard diagnosis, as waiting lists continue to grow. Existing auto-scoring tools, which improve departmental efficiency, lack validation and evidence in paediatric populations and have therefore not been recommended by the 2024 NICE diagnostics guidance. Seluna have developed the first machine learning-enabled, device-agnostic Software as a Medical Device (SaMD) tailored specifically to interpret paediatric sleep studies. The SaMD applies clinically interpretable machine learning algorithms to automate data processing and support clinicians in diagnosing OSA. We report on the design and preliminary results of a 500-patient clinical validation study in collaboration with NHS Greater Glasgow & Clyde. The study evaluates model accuracy against gold-standard manual scoring, alongside assessments of model interpretability and transparency which are essential for clinical adoption. Our findings indicate the potential for AI-assisted interpretation to improve throughput and further standardise the diagnostic pathway.

Development of a Dual-Lever Rowing Ergometer and Novel Trunk Stability Metrics for Objective Assessment in SCI Rehabilitation

Regulski L[1], Carver F[1], Kalyan D[1], Benaben A[1], Bharatia C[1], Mccall R[1], Andrews B[1], Chappell M[1], Evans N[1]
[1]University Of Warwick

Conventional Functional Electrical Stimulation (FES) rowing ergometers constrain users with rigid backrests and trunk support straps, limiting trunk engagement and reducing rehabilitation effectiveness for individuals with spinal cord injury (SCI) or lower-limb amputations. We developed a novel dual-lever rowing ergometer using a Chebyshev "Lambda" linkage to enable near-linear handle motion and near-normal rowing mechanics without the need for backrest or trunk strapping, thereby promoting active trunk control. To objectively evaluate rehabilitation progress, we introduced two novel trunk stability metrics: the Trunk Stability Score (TSS), derived from trunk sway and mediolateral handle forces, and the percentage of time spent outside the stability zone, based on Zero Moment Point (ZMP) analysis. These metrics address a critical gap, as no existing dynamic postural control measures are suited to rowing applications. Pilot validation with able-bodied users demonstrated that higher TSS and lower out-of-zone time correlate with improved trunk stability, establishing both as effective relative metrics. Surface electromyography (EMG) confirmed activation of key muscle groups, including the rectus femoris, biceps brachii, and triceps brachii, supporting the system’s biomechanical effectiveness. Together, the ergometer design and novel trunk stability metrics offer a promising platform for adaptive rowing ergometry, enabling functional training with reduced support and allowing clinicians to track rehabilitation progress objectively over time.

[1] R. L. Lambach et al., 2018, J Spinal Cord Med, vol. 41, no. 1, pp. 1–9.
[2] R. S. Gibbons et al., 2014, Spinal Cord, vol. 52, no. 12, pp. 880–886.
[3] I. Danilov et al., 2016, in Proc. Joint Conf. Comput. Vision, Imaging and Graphics, pp. 160–166

Design of A Base-Model Forearm Prosthetic: A Versatile System for Partial and Near-Elbow Amputations

Carriero E[1], Trejo M[1]
[1]University Of Leicester

For many amputees, particularly those wishing to return to sports, commercial forearm prosthetics often fall short. Most models are not designed for the dynamic, repetitive movements required in physical activity, nor do they support a smooth transition to daily tasks. Discomfort, limited range of motion, excessive weight, and poor adaptability are commonly reported issues [1], often leading to prosthetic abandonment [2]. This project aims to bridge that gap by developing a multifunctional prosthetic that enables participation in sport (specifically table-tennis), promotes physical wellbeing, and supports reintegration into community life, while also addressing everyday functional needs.
To address these issues, we introduce a body-powered forearm prosthetic designed for adaptability, comfort, and user-specific functionality. It includes: a front locking ring for interchangeable attachments (such as a table tennis paddle) via a lock-and-twist mechanism; a central forearm socket with a snap-fit AAA-battery case and motor; and an adjustable extender that fits the residual forearm, adaptable to the amputation level. The design emphasises modularity, lightness, and comfort.
A questionnaire was distributed to current prosthetic users, including amateur and professional para table tennis athletes, to gather feedback on material preferences and usability. Based on this input, the prosthetic was designed using Polyetheretherketone (PEEK), a thermoplastic known for its strength-to-weight ratio, biocompatibility, flexibility, and 3D-printing capabilities.
This multi-functional design aims to offer a more adaptable solution compared to existing options, allowing for the re-integration of individuals with disabilities into sports and communities. Our approach shows potential for improving user experience, expanding functional capability and reducing abandonment.

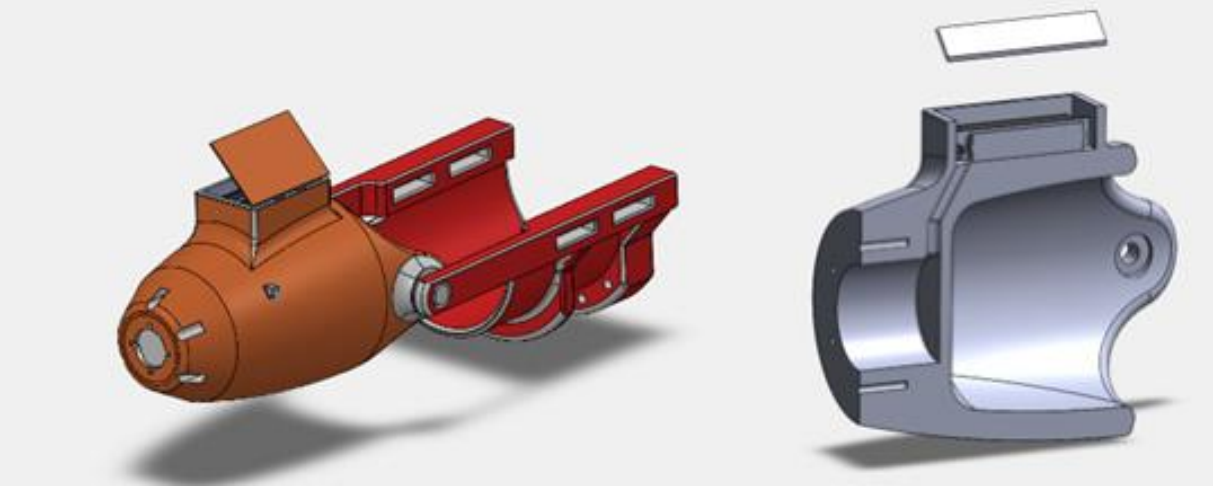

Figure 1 – Full Assembled Model and Half-Section Forearm Socket Views

[1] Resnik, L., et. al, N., 2012. Advanced upper limb prosthetic devices: implications for upper limb prosthetic rehabilitation. Arch. Phys. M. 93(4), pp.710-717.
[2] Biddiss EA, Chau TT. Upper limb prosthesis use and abandonment: A survey of the last 25 years. Prosthet. Orthot. Int. 2007;31(3):236-257. doi:10.1080/03093640600994581.

Implementation of pressure monitoring and a risk algorithm to evaluate pre- and post- interventions in the community

Hoque R[1], Caggiari S[2], Aylward-Wotton N[1], Worsley P[1]
[1]Skin Sensing Research Group, School of Health Sciences, University of Southampton, [2]School of Biomedical Sciences, University of Leeds

Individuals in the community, particularly those with mobility impairments, face high pressure ulcer risk due to prolonged immobility [1]. The 'Pressure Reduction through cOntinuous Monitoring In the community SEtting' (PROMISE) project implemented continuous pressure monitoring (CPM) technology, aiming to inform support surfaces selection and posture [2]. This study demonstrates a novel approach to analysing CPM data with a refined algorithm, evaluating pre- and post-intervention changes [3]. 17 of 105 recruited community residents underwent pre- and post- PROMISE intervention using ForesitePT (Xsensor, Canada). An intelligent algorithm [4] analysed buttock pressure data for duration/magnitude of peak pressure gradient and index. A risk algorithm [3] classified exposures (low to very high) via pressure-specific sigmoid curves linking pressure-time relationships (Fig 1A-D). Fig.1F-I depicts the percentage of monitoring time in four exposure categories, colour-coded in severity (green/low→red/very high), with respect to duration and magnitude of peak pressure gradient and peak pressure index, both pre- and post-PROMISE intervention. While some
patients (Pt1-2) maintained >80% low-risk time, others (Pt15) remained high-risk. No consistent trends emerged; Pt6 improved (orange→green) while Pt7 regressed. Patients with existing ulcers showed prolonged high-pressure exposure. This novel risk algorithm successfully quantified pressure-time risk, showing potential to support self-management of posture and awareness of situation of risk. As intervention showed mixed effectiveness across participants, the findings demonstrate the need for personalised posture management approaches. Further development is required to establish subject-specific sigmoids. This could be integrated in a novel sensing array for community monitoring use and aid targeted intervention and clinical decision making.

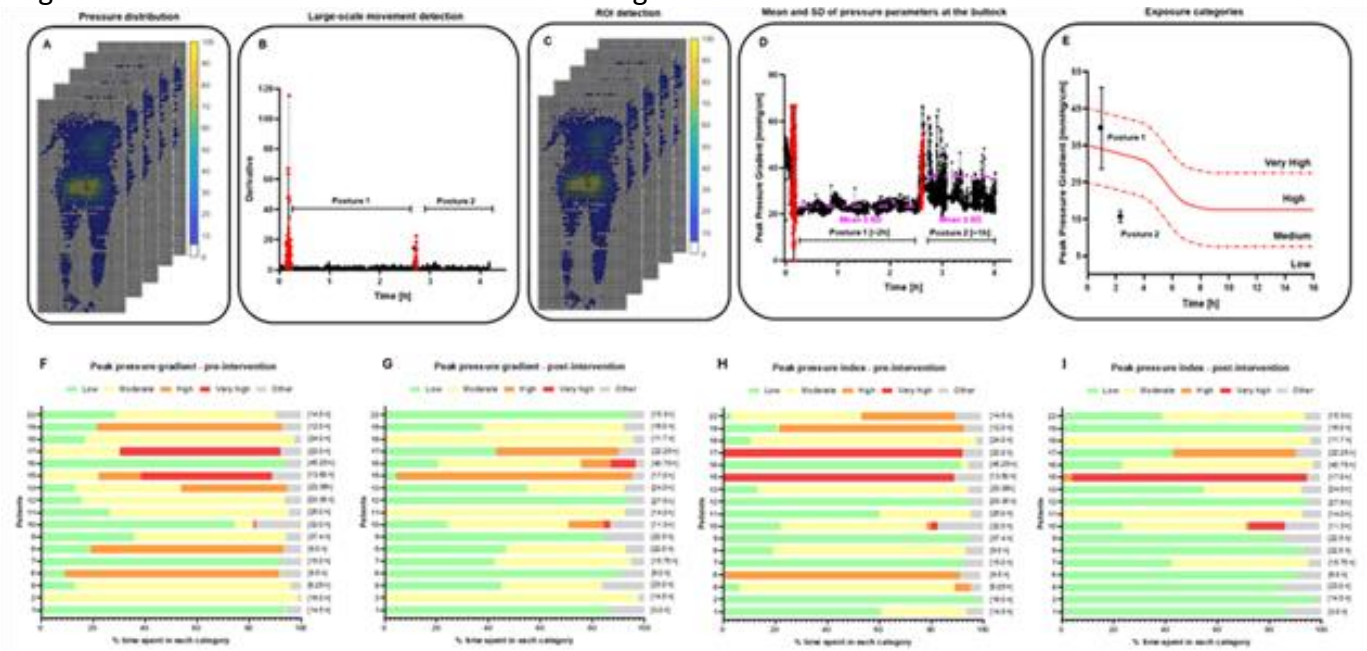

Machine Learning-based posture/mobility detection from CPM data (A-E) translated into risk stratification for pressure ulcers from a community cohort (F-I).

[1] Freiberger et al, 2020, Frontiers in Physiology. [2] PROMISE, Health Foundation. [3] Caggiari et al, 2024, JTV. [4] Caggiari et al, 2021, MEP.

Re-engineering stump skin to improve load bearing capacity

James I[1], Hayes J[1,3], Beatie-Edwards E[1], Hettiaratchy S[1,2], Masen M[3], Higgins C[1]
[1]Department of Bioengineering, Imperial College London, [2]Department of Surgery, Imperial College London, [3]Department of Mechanical Engineering, Imperial College London

The rehabilitation and reintegration of amputees, especially in activities requiring load-bearing on stump skin, remain significant challenges. Conventional prosthetic sockets often cause stump skin injury because it is not naturally adapted to withstand mechanical stress. As a result, two-thirds of amputees suffer from mechanically induced dermatoses, including pressure ulcers and blisters.

It is well accepted that skin identity is conferred by fibroblasts within the skin. We previously proposed using plantar fibroblasts as an autologous cell therapy to confer load-bearing capacity to the residual limb [1]. While effective in enhancing load bearing [2], this strategy is limited by the high costs of preparing cells as medicinal products.

Previous research has identified specific fibroblast populations that orchestrate key differences in cell-cell communication in palm, sole, and hip [3]. In our study, we seek to identify which differences contribute to load bearing, specifically factors enhancing the reprogramming capacity of plantar fibroblasts.

To assess this, we engineer 3D skin constructs with dermal and epidermal components, providing a more realistic cellular environment compared to 2D systems. Plantar fibroblasts from different donors are seeded into an Alvetex scaffold to form the dermis, and keratinocytes from a single donor form the epidermis. We perform macro- and microscale stiffness assessments and single-cell RNA-sequencing to correlate gene expression with reprogramming efficiencies.

This approach enables accurate assessment of donor-specific reprogramming potential and identifies factors driving reprogramming variability. Ultimately, these factors will be used to reprogramme skin instead of plantar fibroblasts, resulting in a cost-effective, off-the-shelf treatment option.

[1] C.J.Boyle et al.,2019, Sci Adv, vol. 5, no.10, pp. eaay0244.
[2] S. S. Lee et al., 2024, Science, vol. 385, pp. eadi1650.
[3] J. Wiedemann et al., 2023, Cell Rep., vol. 42, no. 1, pp. 111994.

Effect of Shoe-Mounted IMU Sensor Positions on Toe Clearance Estimation

Boroomand H[1], Tang J[2], Jiang L[3]
[1]University Of Southampton, [2]University Of Southampton, [3]University Of Southampton

Toe clearance during gait cycles is a critical metric for assessing tripping and fall risks [1]. Inertial Measurement Units (IMUs) mounted on shoes, mostly on the dorsal aspect (e.g., shoelaces), have been used to evaluate foot trajectories in real-world settings. Kinematic models, assuming a rigid foot segment [2], have been developed to estimate toe clearance from dorsal IMU data. However, these models often overlook foot dorsiflexion during gait cycles. Moreover, with the emergence of wearable systems that position IMUs at various shoe/insole locations for improved usability, there is no systematic study on the effect of sensor locations on toe clearance estimation.
IMUs were placed at four common shoe-mounting locations, i.e. toe, shoelace, below ankle, and heel on a HOKA shoe (Figure 1a). Data were collected from a healthy individual walking at a self-selected speed. A sensor fusion-based signal processing approach was applied to transform data to the global frame, enabling double integration to compute foot trajectories [3] (Figure 1b). The kinematic model [2] was used to estimate the toe clearance profile. Figure 1c shows that IMUs placed below the ankle and at the heel produced estimates closest to direct toe measurements, while the commonly reported shoelace-mounted sensor resulted in the largest deviation. Further investigation into model parameter tuning tailored to specific sensor placements will also be presented.

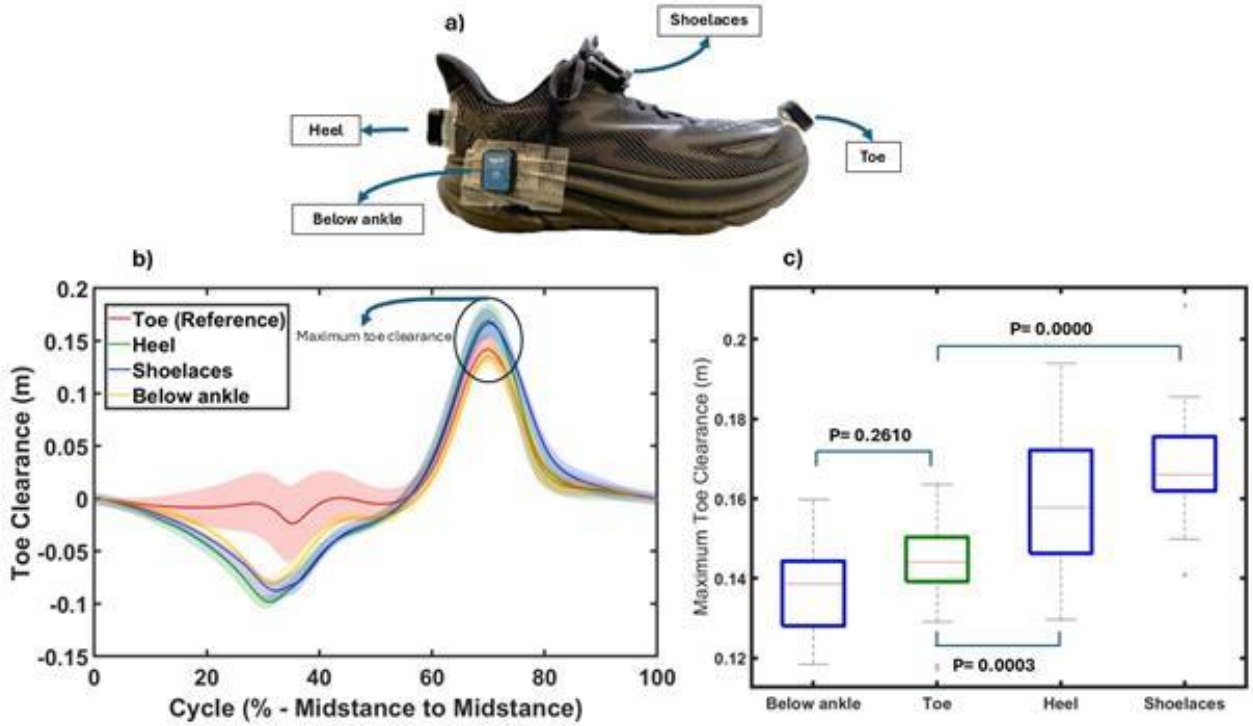

Figure 1- a) Sensor placements, b) Clearance trajectories at the toe, c) Maximum toe clearance for data from different sensors

[1] M. A. Avalos et al, 2023, Gait Posture, vol. 107, p. 189
[2] B. Mariani et al, 2012, IEEE Trans Biomed Eng, vol. 59, no. 12, pp. 3162–3168
[3] J. Hannink et al, 2017, Sensors (Basel), vol. 17, no. 9, p. 1940

Assessment of Wearable Technologies for Monitoring TKA Recovery

Forsyth L[1], Ligeti A[1], Clarke J[2], Riches P[1]
[1]University of Strathclyde, [2]The Golden Jubilee National Hospital

Approximately 100,000 total knee arthroplasty (TKA) procedures occur annually in the UK [1], placing high demand on rehabilitation services. Despite its importance, TKA rehabilitation lacks standardised protocols [2]. Wearable technologies offer a means to enhance early home-based rehabilitation through remote monitoring and assessment. This study aimed to validate MotionSense™ sensors against clinical motion capture for assessing knee ROM in a TKA population.

Ten TKA patients were recruited (Weight: 88.0±15.6kg; Height: 1.73±0.12m; BMI: 30.09±3.22kg/m², mean ± standard deviation). Data was collected preoperatively and at 1-week- and 6-weeks postoperatively. Participants completed three activities. Knee flexion was determined by Vicon PlugInGait™ (100 Hz) and by a proprietary algorithm to which MotionSense™ sensors (~50Hz) exported data in real-time. Following up-sampling to 100Hz, cross-correlation was used to time synchronise the measurements in gait cycle windows from peak flexion to peak flexion. Root mean square errors (RMSE) were calculated between technologies in each gait cycle window.

Preoperatively, participants walked at 0.56±0.14m/s, one-week postoperatively at 0.52±0.14m/s and by 6-weeks postoperatively at 0.60±0.28m/s ($p<0.05$).

Knee ROM decreased following surgery (Table 1). However, by 6 weeks postoperative, ROM increased. Preoperatively, RMSE data demonstrated excellent agreement between the MotionSense™ sensors and the Vicon system across all activities (Table 1).

MotionSense™ sensors performed accurately across all activities. At one-week post-TKA, participant ROM was reduced, resulting in higher accuracy. Wearable devices can confidently be implemented within clinical and rehabilitative environments, evidencing their ability to accurately measure sagittal knee ROM.

		Knee Angle (°)									
		Max Flexion			Min Flexion			ROM			RMSE
		Vicon	*MS*	*Δ*	*Vicon*	*MS*	*Δ*	*Vicon*	*MS*	*Δ*	
Preop	Walking	45.5 (8.8)	45.9 (8.3)	-0.5 (3.1)	7.0 (10.3)	5.8 (10.2)	1.2 (0.5)	38.5 (9.7)	40.2 (8.0)	-1.6 (3.6)	2.6 (1.0)
	Stair Ascent	53.6 (34.9)	53.2 (34.7)	-1.3(4.1)	5.3 (10.6)	6.6 (9.4)	0.4 (1.3)	48.4 (28.1)	46.6 (27.3)	1.8 (5.2)	2.1 (0.8)
	Stair Descent	39.5 (8.8)	39.7 (9.6)	-0.2 (1.6)	6.6 (8.2)	6.3 (7.6)	0.3 (0.7)	32.9 (2.2)	33.4 (4.1)	-0.5(1.9)	1.3 (0.4)
	Flexion/ Extension	99.7 (15.9)	94.5 (14.6)	5.2 (3.7)	2.7 (8.4)	4.32 (6.1)	-1.6 (3.1)	97.0 (19.8)	90.2 (17.7)	6.8 (6.2)	3.2 (1.8)
1 Week Postop	Walking	47.1 (6.2)	47.9 (4.8)	-0.9 (1.4)	15.5 (1.3)	14.3 (3.2)	1.2 (1.9)	31.6 (5.0)	33.6 (1.7)	-2.0 (3.3)	1.5 (0.5)
	Stair Ascent	51.5 (2.7)	52.5 (1.5)	-1.0 (1.1)	18.4 (0.9)	17.6 (2.7)	0.7 (1.8)	33.1 (1.7)	34.9 (1.2)	-1.8 (2.9)	1.2 (0.5)
	Stair Descent	48.3 (2.8)	47.7 (4.1)	0.6 (1.3)	14.2 (0.8)	13.9 (2.9)	0.3 (3.7)	34.1 (2.0)	33.8 (7.1)	0.3 (5.1)	0.9 (0.1)
6 Weeks Postop	Walking	56.4 (7.1)	55.5 (5.3)	1.0 (2.6)	11.9 (3.3)	13.1 (4.5)	-1.2 (1.6)	44.6 (3.9)	42.4 (0.8)	2.2 (3.3)	2.3 (0.9)
	Stair Ascent	78.9 (18.7)	76.3 (5.4)	2.6 (4.3)	13.6 (3.1)	15.9 (14.5)	-2.3 (2.8)	65.3 (17.4)	60.4 (10.7)	4.9(6.9)	2.5 (0.9)
	Stair Descent	74.9 (23.7)	71.5 (19.0)	3.4 (4.9)	12.1 (6.3)	13.2 (8.7)	-1.1 (3.1)	62.8 (22.4)	58.3 (17.4)	4.5 (7.3)	2.6 (1.9)
	Flexion/ Extension	83.2 (12.0)	77.6 (15.8)	5.6 (7.5)	12.9 (12.2)	14.6 (11.7)	-1.7 (4.6)	70.4 (15.2)	63.0 (16.8)	7.4 (11.7)	4.7 (3.4)

Preop: Preoperative; Postop: Postoperative, Min: Minimum, Max: Maximum; ROM: Range of Motion; RMSE: Root Mean Square Error; MS: MotionSense™; Δ: difference between Vicon and MotionSense™ (and pooled SD).

Table 1. Mean knee angle (SD) and Error (SD) results for the functional activities of the TKA clinical population.

[1] National Joint Registry, 2022, NJR Annu. Rep., no. 19, pp. 1–200. [2] D. F. Hamilton et al., 2020, BMJ, vol. 371, no. m3576, pp. 1–10.

Wearable Soft Sensor for Capturing Multiple Degrees of Freedom Movement

Nugraha M[1], Rossiter J[1], Conn A[1]
[1]University Of Bristol

A central challenge for wearable kinematic sensors without off-board ancillary equipment is capturing the high degree of freedom motion of joints and body posture. This research presents a soft capacitive sensor capable of multiple degrees of freedom (DOF) sensing for wearable applications. The single-common double-capacitor (SCDC) sensor has three electrodes and measures linear stretching, bending, and twisting action, by simultaneously measuring the capacitance across different electrode pairs. Analytical modelling of the sensor response to each DOF is experimentally validated measurements and can be used to tune the electrode geometry. Experimental results demonstrate how the sensor can measure simultaneous stretching and bending or simultaneous stretching and twisting and a lightweight wearable sensor is presented that can measure finger joint angles. We further investigate how multiple SCDC sensors can be integrated into a two-wire system by adopting band stop filter (BSF) circuitry to simplify the number of wires connecting to each SCDC. A wearable application for multiple SCDCs attached to the human back is proposed using BSF circuitry, which can capture numerous DOF with a single pair of wires connected to the microcontroller. The dimensional scalability and ease of fabrication of the SCDC sensor make it well suited to emerging applications in wearable posture and motion sensing, soft robotic manipulation, and locomotion.

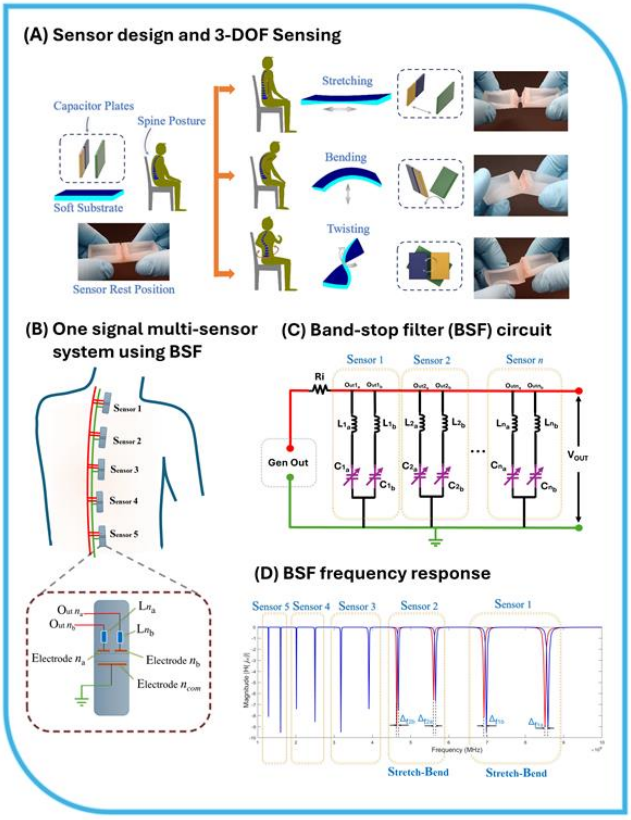

Figure 1. (A) The sensor design and principle. (B) One-signal multi-sensor system. (C) Band-stop filter (BSF) circuit. (D) Output signal.

[1] M. I. Nugraha et al., 2025, IEEE Robot. Autom. Lett., vol. 10, no. 4, pp. 3550–3557. [2] J. Kim et al., 2024, Adv. Funct. Mater., vol. 34, no. 7, pp. 1–16. [3] K. Chubb et al., 2025, Bioinspir. Biomim., vol. 20, no. 1, p. 016002.

The validity of IMU-derived kinematics after 7 hours of use for long-term monitoring of military personnel musculoskeletal health.

Smith S[1], Wisdish S[2], Osofa J[3], Farris D[2]
[1]University Of Nottingham, [2]University of Exeter, [3]Defence Science and Technology Laboratory

Wearable technology is becoming popular for real-world movement analysis due to its accessibility, relative low cost and ease of use compared to optical motion capture (OMC). Inertial measurement units (IMUs) have proven validity against OMC, however, these validations tend to be up to 1-2 hours [1], [2], with little-to-no evidence of the extended use of such systems over multiple hours, or even days. This would be useful when monitoring the musculoskeletal health of military personnel who carry out strenuous occupational and operational tasks over whole days, with the aim of reducing potential injury. This study compared the error in IMU-based motion analysis measures before and after a physically active day of use. Fifteen healthy (8F, aged 27±4 years) civilian participants wore 7 commercially available lower body IMUs for an average of 7 hours whilst completing 6 walking laps of 2.3 miles each, returning for regular lab-based tests for evaluation against OMC during planar functional movements. Comparisons were made using root mean square errors (RMSE) for validity and t-tests for errors between time stamps. Kinematic error data captured pre and post 7-hours were compared, with RMSE values ranging from 3-9.1° for knee and ankle, and between 14-19° for the hip, aligning well with the literature [2]. RMSE values were not significantly different pre and post. This shows that IMUs can collect valid kinematic data following extended periods of wear.

[1] M. Al Borno et al., J. Neuroeng. Rehabil., vol. 19, no. 1, pp. 1–11, 2022
[2] M. P. Mavor et al., Sensors (Switzerland), vol. 20, no. 15, pp. 1–14, 2020

Gaming rehabilitation for ankle injuries: a feasibility study using the DANU Sports smart sock

Nagle A[1], Jinphol A[1], Teixeira J[1], Penev V[1], Forsyth L[1]
[1]University of Strathclyde

Rehabilitation is effective at reducing risk of reinjury, which increases nine-fold following a lateral ankle sprain [1]. However, no standardised protocols exist for return to activity and completion rates remain low [2][3]. Gamification has been an effective solution to enhance rehabilitation. This study aimed to assess the feasibility of integrating the DANU Sports smart sock into a gaming system for the rehabilitation of ankle sprains. The data acquisition protocol on the DANU Bluetooth module was customised to produce real-time data. Three games were developed and integrated with this sensor data. Game control was achieved through movement capture with the IMU sensor on the lateral malleolus and the capacitive pressure sensors below the soles. Twenty healthy participants (age: 22.6±1.7; 12F/8M) tested the game functionality during a single laboratory session. Balance was assessed using the Balance Error Scoring System (BESS) before and after a period of game play. A user satisfaction survey assessed perceived motivations and engagement, as well as feedback of the overall gaming system. The DANU Sports' system was successfully integrated as a game controller. No adverse events were reported during testing. Acute effects of the balance training resulted in improved BESS scores (pre: 7.50±2.11, post: 6.65±2.29, $p<0.05$) and improved perceived stability. Participants reported high comfort and low movement restriction of the smart sock with 85% finding the games enjoyable/extremely enjoyable. The study supports the feasibility of rehabilitation gaming in a healthy population using the DANU Sports system. Further testing is warranted in a population following an ankle sprain.
Game-play and testing set-up with DANU smart sock as a controller

[1] B. Picot et al., 2024, Sports Med.-Open, vol.10, no. 1, pp.23.
[2] S.F. Bassett et al., 2007, Phys. Ther., vol. 87, no. 9, pp. 1132-1143.
[3] E.A. Wikstrom et al., 2020, Jour. of Sport Rehab., vol. 29, no. 2, pp.231-237.

Optical Fibre-Based MRI-Compatible Knee Sensor for Osteoarthritis

Ganguly P[1], Ahwal F[1], Kumar R[1], Venkatesh R[2], Ellison P[1], Chauhan M[1]
[1]University Of York, [2]Leeds Teaching Hospitals NHS Trust

Osteoarthritis (OA) is a degenerative joint condition affecting 10 million people in the UK, with 5.4 million cases of knee OA, and 350,000 new cases being diagnosed each year. The unloader knee brace is one of the current treatments available to patients, they are a quick, easy way to support your knee joint and relieve symptoms like pain and stiffness. They can also help the user heal safely and prevent future injuries. However, unloader knee braces are not patient-specific; while for some patients it is useful, for others it may increase joint stress, causing more pain and discomfort to the patient. The biomechanical effects of braces on joint loading characteristics are not well quantified.

This study aims to address these issues by assessing the long-term impact of braces on knee health, measuring the forces exerted by the knee brace over time to evaluate its effect on joint loading and cross-validating this using MRI imaging to assess joint alignment.

This study introduces a novel force sensor, leveraging optical fibre technology to make it MRI-compatible. The sensor is constructed from a coiled optical fibre embedded in a foam layer and housed within a 3D-printed ABS structure. This enables force measurement through light attenuation and amplification, which results from fibre distortion. Initial Arduino-based testing has demonstrated the sensor's ability to detect forces in the 0-7.5 N range, with future iterations targeting a larger range of force through integration of signal amplification and rigorous tensile calibration

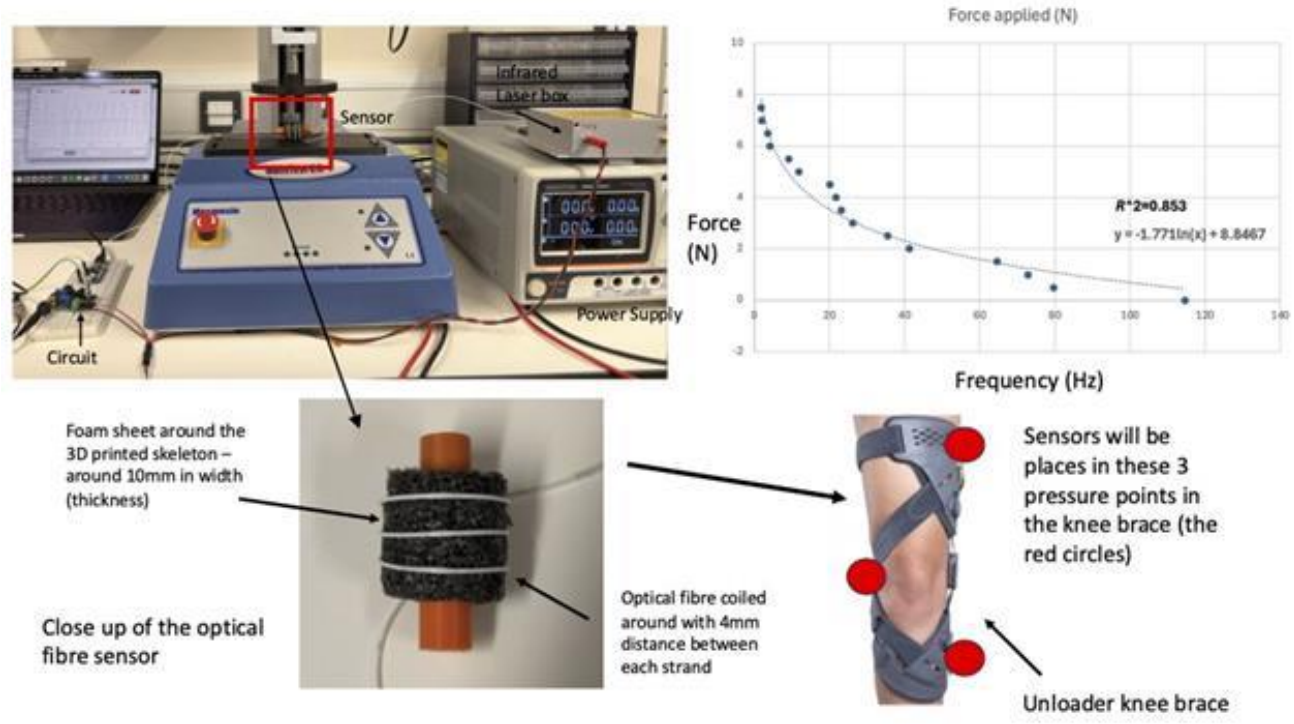

Images to show sensor set-up and placement in the knee. Graph to show the Force Applied and Force Equation.

Improving blood vessel segmentation via noise reduction using Noise2Inverse: Case study on a HiP-CT Kidney X-ray tomogram

Chen D[1], Brunet J[1], Zhou Y[1], Walsh C[1], Lee P[1], Hagen C
[1]University College London

Hierarchical Phase-Contrast Computed Tomography(HiP-CT)[1] enables 3D imaging of intact human organs at micrometre resolution, providing invaluable insights into the vascular network, among other features. However, image noise reduces the accuracy of automated segmentation, while manual segmentation is time-consuming and impractical to upscale. Therefore, a suitable image denoising technique is required. In this study, we applied Noise2Inverse(N2I)[2], a self-supervised denoising technique for CT images that does not require low-noise data for training, to a 3D HiP-CT dataset of a human kidney. The results showed that N2I, when applied with an appropriate choice of network structure and training hyperparameters, improved the images significantly compared to conventional denoising techniques such as median filtering and BM3D. Fine edge details, such as smaller blood vessel walls, were well maintained, while homogeneous areas were smoothed. Quantitative analysis showed that the signal-to-noise ratio was improved from 16.36dB to 29.92dB after denoising. Fourier ring correlation analysis also showed improvement on spatial resolution from 326µm to 55µm. By applying a well-trained automated segmentation model[3], the results showed an improvement on the Dice score: in the Figure, the Dice score for the slice was increased from 0.65 to 0.88, with 1 being perfect alignment between automated segmentation and the ground truth. This demonstrated better identification of blood vessels in the denoised slice. For the whole volume data, the Dice score was increased from 0.79 to 0.81. These findings demonstrate the potential of N2I to improve HiP-CT image quality for vascular segmentation, enabling more accurate and scalable analysis of organ microvasculature.

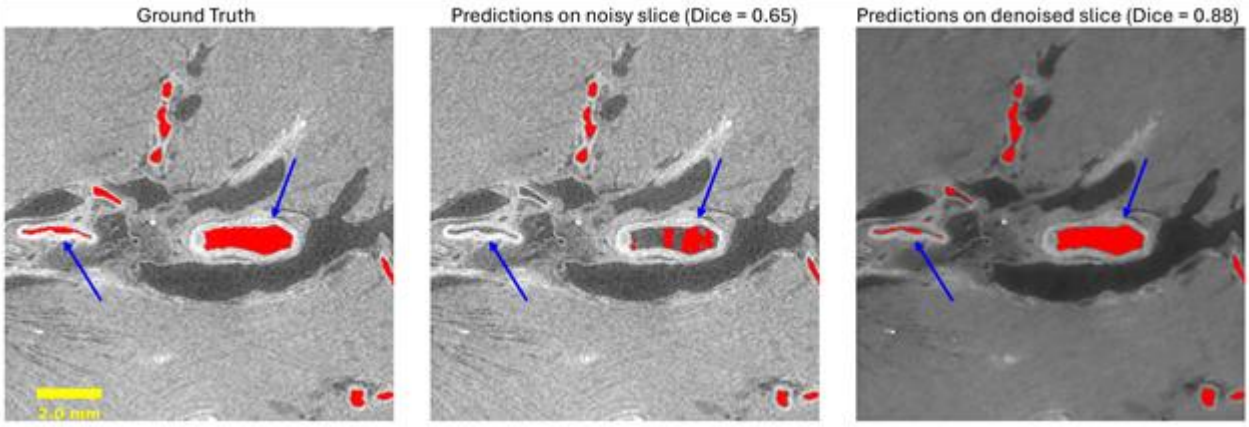

Figure: Blood vessel segmentation comparison on HiP-CT Kidney scan. Blue arrows highlight better segmented blood vessels in the denoised image.

[1] Walsh et al., 2021, Nat Methods, vol. 18, no. 12, pp. 1532–1541.
[2] Hendriksen et al., 2020, IEEE Trans.on Comp. Imaging, vol. 6, pp. 1320-1335.
[3] Yagis et al., 2024, Sci Rep, vol. 14, pp. 27258.

Early radiation therapy response assessment using multi-scale photoacoustic imaging

Lefebvre T[1,2,3], Oraiopoulou M[2,3], Bunce E[2,3], Else T[2,3], Wright L[2,3], Golinska M[2,3], Hacker L[4], Brodie C[3], Kupczak S, Cheng Y[3], Young L[3], Sweeney P[2,3], Bohndiek S[2,3]
[1]University College London, [2]University of Cambridge, [3]Cancer Research UK Cambridge Institute, [4]University of Oxford

Characterising tumour vascular response to radiation therapy (RT) is key to understanding how oxygenation and microvascular disruption influence outcomes. Tumour vasculature delivers oxygen, enhancing RT efficacy up to 3-fold[1]. In vivo visualisation of this phenotype can therefore inform on response and radioresistance[2]. Thus, we hypothesized that multi-scale photoacoustic imaging (PAI) can provide depth-resolved insights into tumour oxygenation and vascularity for RT evaluation in preclinical models. Orthotopic breast cancer xenografts (MCF7, MDA-MB-231) were implanted in BALB/C nude mice (n=46). CT-guided RT (SARRP, Xstrahl) following TG-61 calibration[3] targeted tumours while sparing healthy tissue. At 400 mm³, mice received single-dose RT (SDRT, 20 Gy), hypofractionated RT (HFRT, 25 Gy in 5 fractions), or no treatment. Tomographic and mesoscopic PAI (MSOT, RSOM,iThera) were performed 24h pre-, post-RT, and at endpoint (mean 7 days). Images were quantified for oxygen saturation (sO_2), responding fraction (RF) to gas challenge[4], and blood volume and vascular density[5]. Tumours were excised for immunohistochemistry (IHC). MDA-MB-231 tumours grew aggressively faster than MCF7 ($P<0.01$). PAI assessment revealed the higher hypoxic and radioresistant phenotype of MDA-MB-231 at baseline (RF, $P<0.01$; vascular density, $P<0.001$). RT reduced growth across groups ($P<0.001$), with HFRT MCF7 showing best response. KI67 IHC confirmed decreased proliferation post-RT ($P<0.05$). RT decreased vascular density across treated groups, especially at the ablative regimen, SDRT ($P<0.05$). Overall, MCF7 xenografts showed improved response, linked to higher pre-RT oxygenation and vascular permeability. RT-induced vascular alterations could be mapped with mesoscopic PAI. Thus, PAI effectively predicted radioresistance and shed light on the vascular response to RT.

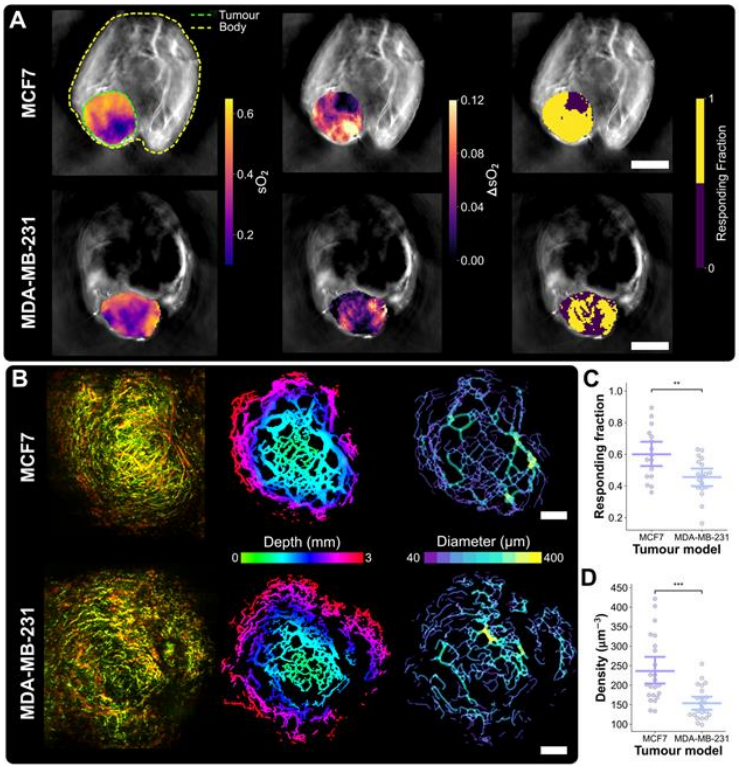

A)Tomographic and B)mesoscopic PAI reveal differences in C)oxygenation and D)vasculature between breast cancer models, underpinning radiosensitivity.

[1] M.R. Horsman et al., 2012, Nat Rev Clin Oncol, 9, 674-87.
[2] T.L. Lefebvre et al., 2022, Front Oncol, 12, 803777.
[3] C.M. Ma et al., 2001, Med Phys 28, 868-893.
[4] M.R. Tomaszewski et al., 2017, Theranostics, 7, 2900-2913.
[5] E.L. Brown et al., 2022, Photoacoustics. 20, 100357.

Enabling Co-localised Multi-scale Analysis of Hierarchical Phase-Contrast Computed Tomography of Intact Human Organs through Image Co-registration

Lefebvre T[1], Stansby D[1], Zhou Y[1], Chen D[1], Occhipinti E[1], Bellier A[3], Tafforeau P[2], Ackermann M, Lee P[1], Walsh C[1]
[1]University College London, [2]European Synchrotron Radiation Facility, [3]Laboratoire d'Anatomie des Alpes Françaises (LADAF), Université Grenoble Alpes, [4]University Clinics Aachen

The advent of synchrotron X-ray hierarchical phase-contrast computed tomography (HiP-CT)[1] has enabled the imaging of intact human organs and their anatomical substructures and functional subunits across scales. Integrating its multi-scale imaging capabilities in analysis pipelines of structures such as the vasculature opens new opportunities for learning-based strategies to capture finer features at unprecedented resolutions. To this end, we tested two co-registration techniques for aligning high-resolution volumes of interest (VOI) to whole-organ scans. Kidney, brain and heart were obtained from Hannover Biobank or LADAF. Following established protocol[2], formalin-fixed organs were progressively dehydrated to 70%EtOH, degassed, and mounted in a 70%EtOH/agar mix for stabilisation. HiP-CT acquisitions were performed at the ESRF BM05. Reconstruction and phase retrieval were performed with PyHST2, at 50µm and 13µm binned isotropic voxel sizes. Following rigid co-registration based on manually selected landmark, an affine co-registration was evaluated between images using mutual information (MI)[3] or automatically-detected scale-invariant landmarks (ORB)[4]. Alignment quality was assessed with structural similarity index (SSIM) and target registration error (TRE) of landmarks. The initial co-registration led to poor alignment of finer structures across scales. Following MI-based or ORB-based co-registration, alignment of VOIs was improved in terms of SSIM 16.8±12.4% vs. 23.7±6.6%, and TRE -18.3±13.7% vs. -41.4±2.5%, respectively. ORB-based co-registration led to the most accurate co-localisation of smaller substructures revealed at high-resolution. Leveraging label-free HiP-CT, we demonstrated semi-automated alignment strategies of hierarchical data. Scale-invariant methods show promise for improved multi-resolution co-registration, with applications scoping deep learning-based super-resolution, segmentation of functional subunits, and diagnosis of mesoscopic disease features.

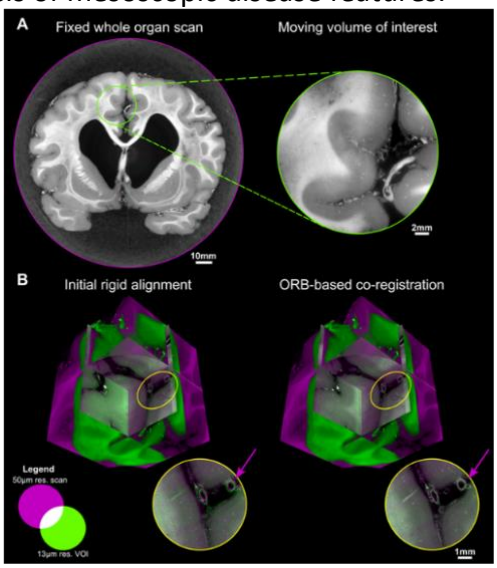

A)HiP-CT of intact human brain displaying cross-sections of whole-organ scan and high-resolution VOI. B)ORB-based co-registration shows improvement in fine alignment.

[1] Walsh et al., 2021, Nat Methods, 18, 1532–1541. [2] Brunet et al., 2023, Nat Protoc, 18, 1441–1461. [3] Maes et al., 1997, IEEE Trans Med Imaging, 16, 187-98. [4] Rublee et al., 2011, in Proceedings of ICCV, 2564-2571.

Reframing Connectomics as a Problem of Distributed Graph Networks in Synchrotron Imaging of the Human Brain

Keenlyside A[1], Chourrout M[1], Stansby D[1,2], Balbastre Y[3], Walsh C[1]
[1]Department of Mechanical Engineering, University College London, [2]Centre for Advanced Research Computing, University College London, [3]Department of Experimental Psychology, University College London

Macro- and mesoscopic models of the human structural connectome describe the connectivity of white matter fibers often used for planning deep brain stimulation. While connectome models have traditionally been developed from diffusion MRI tractography, limits to resolution require statistical inferences which leaves uncertainty around key clinical targets [1]. Hierarchical Phase-Contrast Tomography (HiP-CT) is an ex vivo propagation-based synchrotron technique for imaging whole organs at previously unseen micron-scale isotropic resolutions [2]. Though Image data is publicly available via the Human Organ Atlas (https://human-organ-atlas.esrf.fr/), the analysis of terabyte-scale volumes requires a novel approach which reframes connectomics to leverage pre-computation and data-efficient structures. Interpreting the spatial connectome as a spatial graph reduces the redundancy of streamlines by defining unique conditional paths through the network [3]. Computing graphs from skeletonised white matter in individual image chunks before hierarchically merging these sparse networks represents a scalable, distributed alternative to classical connectomics. We have developed a spatially distributed pipeline which extracts hierarchical sparse networks, thereby scaling deterministic-style tractography to terabyte-scale imaging datasets. The maximum acheivable spatial resolution of HiP-CT-based models are an order of magnitude greater than current world-leading diffusion MRI using probabilistic tractography. The use of hierarchical network structures opens up future implementation of multi-resolution and multi-modal connectomic models to bridge the gap between diffusion MRI towards ‘ground truth’ microscale connectome models. High-resolution local tractograms will further characterise surgical targets and improved accuracy in computational simulation of treatment responses. Detailed modelling of complex anatomical regions is of widespread neuroanatomical, physiological, and surgical interest.

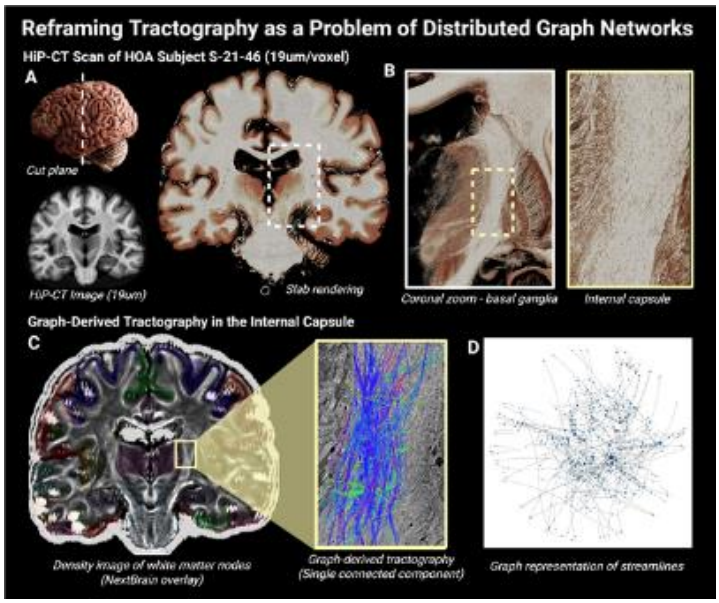

Figure.1-A: HiP-CT whole-brain volume (19um/voxel). B: Internal capsule VOIs. C: Node density and single-component graph-derived tractography. D: Graph representation streamlines.

[1] - Marchant et al. Mesoscale Brain Mapping: Bridging Scales and Modalities in Neuroimaging – A Symposium Review. Neuroinform (2024).
[2] - Walsh et al. Imaging intact human organs with local resolution of cellular structures using hierarchical phase-contrast tomography. Nat Methods (2021).
[3] – Bassett,Sporns. Network neuroscience. Nat Neurosci (2017).

Cross-modality Registration of 3D Hierarchical Phase-Contrast Tomography and 2D Histology

Zhou Y[1], Kidzeru E[2], Chen J[1], Megas S[2,3], Teichmann S[2,4], Clatworthy M[2,5], Lee P[1], Walsh C[1]
[1]Department of Mechanical Engineering, University College London, [2]Wellcome Sanger Institute, Wellcome Genome Campus, [3]Cambridge Centre for AI in Medicine, Department of Applied Mathematics and Theoretical Physics, [4]Department of Medicine & Cambridge Stem Cell Institute, University of Cambridge, [5]Molecular Immunity Unit, Department of Medicine, University of Cambridge, MRC Laboratory of Molecular Biology

Hierarchical Phase-Contrast Tomography (HiP-CT) is an emerging synchrotron-based X-ray imaging technique capable of capturing complete human organs at approximately 25 µm/voxel and zoomed regions at around 1 µm/voxel (Figure 1 (A)), thus achieving near-histological resolution [1]. This allows for bridging non-destructive 3D images with 2D histology through registration, facilitating the interpretation of detailed microscopic information throughout entire adult organs. While previous advancements of micro-CT and histology registration have shown promising alignment results of whole slices using anatomical boundaries [2], the accurate matching of tiny functional structures remains challenging due to CT low resolution constraints and non-rigid deformations during histological preparation. These problems increase computational and optimization complexities. To extend the application of HiP-CT to histology-driven studies, we performed a case study focusing on human kidneys and developed a novel protocol involving the 3D mould construction (Figure 1 (B)) to maintain anatomical orientation and minimize deformation during biopsy. Kidneys were initially scanned at the European Synchrotron Radiation Facility (ESRF) to obtain high-resolution volumetric data. Guided by the 3D mould, high-precision tissue biopsies (Figure 1 (C)) were conducted by Cellular Genetics team at the Wellcome Sanger Institute. Subsequently, histology slices were acquired from the biopsies, and glomeruli were segmented using a deep neural network. These segmented glomeruli served as landmarks for cross-modality registration between HiP-CT and histology (Figure 1 (D)). This approach presents a methodology for registering 2D histology slices into a whole-organ 3D imaging modality. It serves as a foundational step toward integrating high-resolution histological features into non-destructive, organ-scale HiP-CT imaging.

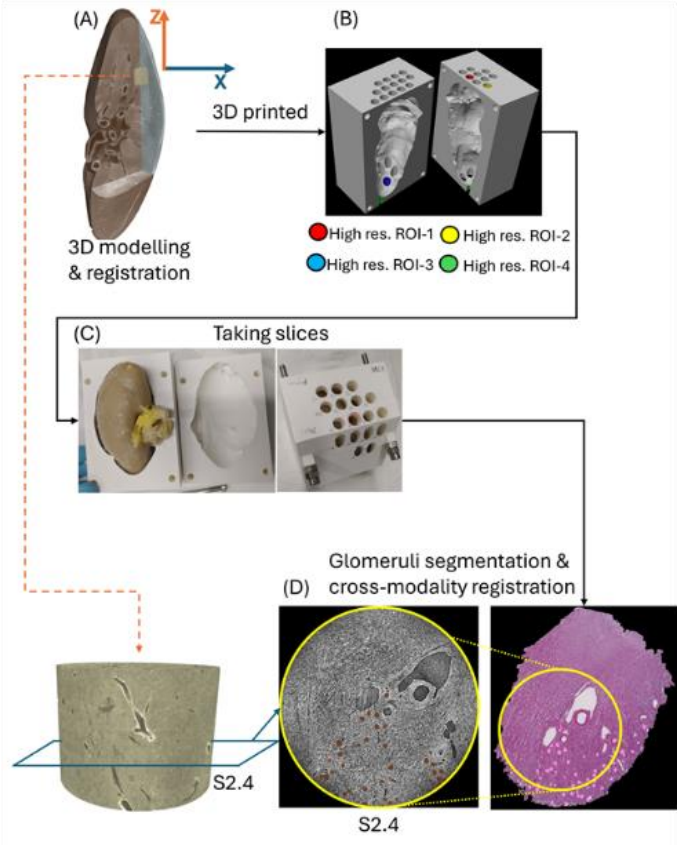

Figure 1: Protocols of cross-modality registration between 3D Hierarchical Phase-Contrast Tomography (HiP-CT) and 2D histology slices

[1] Walsh et al., 2021, Nat. Methods, vol. 18, no. 12, pp. 1532–1541
[2] Chen et al., 2024, arXiv preprint arXiv:2410.14343

Continuous Glucose Monitoring as an Educational Tool for Prediabetes

Khovanova N[1], Archavly K[1]
[1]University of Warwick

Continuous glucose monitoring (CGM) represents a significant advancement in diabetes care, offering real-time insights into glucose fluctuations in response to diet, exercise, stress, and sleep. There is growing interest in CGM's role as a preventive and educational tool for individuals with prediabetes and normoglycaemia [1,2]. As prediabetes can be improved through lifestyle changes, CGM offers a way to better understand metabolic responses and support lifestyle adjustments.

This study aimed to develop a personalised computational and behavioural approach to explore CGM's potential in promoting sustainable behavioural change and glucose regulation in prediabetes. It focused on small, self-guided modifications, such as adjusting meal choices and timing, or physical activity based on CGM feedback, leading to long-term, sustained lifestyle benefits.

As a case study example, one adult was monitored over two years; Dexcom CGM G6 was used during several 10-day periods. The participant recorded their food intake and made small adjustments to their diet and activity, without significantly impacting their everyday habits. Over time, adjustments such as increasing fibre and protein, reducing simple carbs, and avoiding closely spaced meals led to improved glucose control. Results showed steady declines in average glucose and post-meal spikes, with improvements in CGM metrics (mean glucose and time in range), and HbA1c normalised by the end of the study. This case supports CGM's value not only in monitoring but also in educating individuals with prediabetes for a sustained result. However, its use in non-diabetic populations should be guided by healthcare professionals [3] to ensure safe and effective outcomes.

[1] S. J. Zahalka et al., 2024, J. Diabetes Sci. Technol., vol. 18, no. 4, pp. 835–846, Jul. 2024
[2] N. L. Spartano et al., 2024, J. Clin. Endocrinol. Metab. vol. 110, no 4, pp. 1128–1134.
[3] A. R. Johnston et al., 2022, Diabetes Epidemiol. Manag., vol. 6, p. 100068.

Spatial variation in mechanical stimulation within 2D and 3D organ-on-a-chip models.

Ziakas G[1,2], Screen H[1,2], Hopkins T[1,2], Knight M[1,2]
[1]Centre for Predictive In Vitro Models, Queen Mary University of London, [2]Centre for Bioengineering, School of Engineering and Materials Science, Queen Mary University of London

Mechanical stimulation plays a pivotal role in the development, function and disease of tissues. Therefore, it has been proposed as an important component for organ-on-a-chip (OOAC) systems where precise control of the biomechanical environment is critical in replicating physiological conditions. The commercial Chip-S1® (Emulate) enables the application of mechanical stimulation via two vacuum channels which distort the microfluidic channels containing cells. In the present study, we characterised the 2D and 3D strain fields within this organ-chip. Mechanical stimulation was applied using a push-pull controller (Fluigent) and 2D strain was assessed by tracking membrane pore displacement between the unstrained state and at 200 - 800 mbar of negative pressure. Strain maps were also generated using digital image correlation (DIC) (MATLAB, Ncorr). For 3D strain analysis, bovine chondrocytes were encapsulated in agarose (2%), alginate (1%), or type I collagen (1.5 mg/ml) and imaged at multiple depths under strain. Results revealed heterogeneous 2D biaxial strain fields, with strain perpendicular to the axis of the channel proportional to applied pressure with a peak of 12 % strain observed in the middle of the chip at 800 mbar. Effective 3D strain transfer occurred only in collagen hydrogels, where strain was greatest closest to the membrane in the top channel but remained consistent throughout the depth of the bottom channel. Analysis of the influence of strain in biological processes is currently in progress. These findings highlight the ability to accurately apply defined mechanical strain in an OOAC platform, enabling the modelling of tissue-specific mechanical environments.

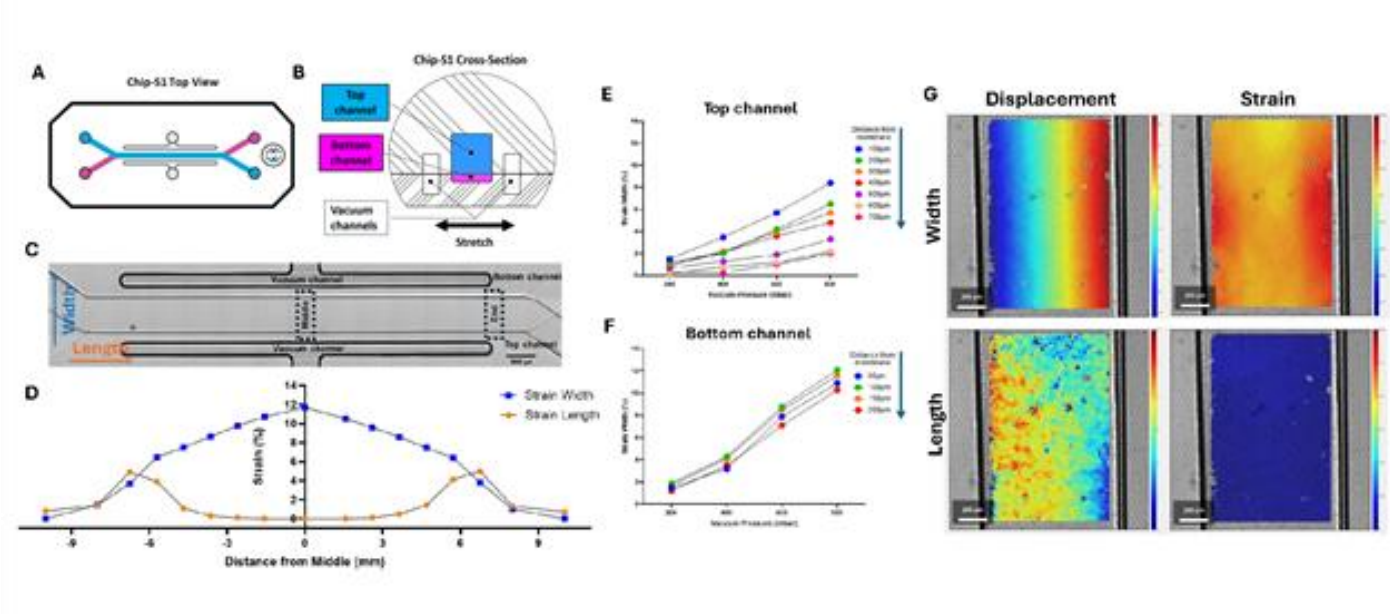

(A,B) Emulate Chip-S1®, (C) Tile scan of chip, (D) associated 2D strain fields at 800mbar, (E,F) 3D strain, (G) DIC

Engineering human stem cell-derived neuronal networks to study serotonergic neurotransmission

Bohl B[1], Prieto P[1], Murphy M[1], Hashemi P[1]
[1]Imperial College

Serotonin is a critical neurotransmitter that regulates a wide range of physiological processes, including mood, anxiety, smooth muscle function and metabolic processes. In the brain, serotonergic neurons form a complex and far-reaching network originating in the brainstem and projecting throughout the central nervous system. Due to the intricacy of this system and the limited accessibility of the human brain for direct measurements, studying serotonergic signalling and its dysregulation in various disorders such as depression remains a significant challenge. To address this, we aimed to develop a human-specific in vitro model to investigate serotonergic neurotransmission using human induced pluripotent stem cells (iPSCs)-derived serotonergic and glutamatergic neurons. We designed microfabricated microchannel devices to control neuronal network architecture and obtaining unidirectional excitatory input from glutamatergic to serotonergic neurons. We characterized synapse formation and network activity between the two cell populations and confirmed functional serotonergic signalling through electrochemical detection of extracellular serotonin using fast-scan cyclic voltammetry. This model provides a novel platform for studying human serotonergic networks and may support the development of new treatments for neuropsychiatric disorders.

Development of a modelling environment and its application to blood-brain barrier (BBB) investigation

Reid A[1], Urban M[1]
[1]University Of Strathclyde

Neurodegenerative diseases are now considered the leading cause of illness and disability worldwide, affecting 1 in 3 people. Research into effective treatments faces challenges in terms of modelling, diagnosis, and treatment of complex conditions and environments. This work focuses on the development of a modelling environment that can be applied to blood-brain barrier (BBB) investigation.

The research aims to develop a BBB model that features pulsatile flow and shear stress in a circular, vascular-like lumen by designing a small, portable, low-power, short-response-time surface acoustic wave (SAW) driven micropump as a separate device connected through tubing with the BBB model device to create a closed loop system. An acoustofluidic device for the BBB model was designed, and the research focuses on the possibility of generating a standing SAW, particularly an acoustic whispering gallery mode (WGM) in the vascular-like lumen.

The simulation results obtained from the Finite Element Analysis (FEA) software, COMSOL Multiphysics 6.2, are very promising. They clearly showed fluid flow generation inside the microchannel system for the SAW-driven micropump, and it can be used for pumping liquids through microfluidic devices. Generation of WGM was simulated in the vascular-like lumen of the BBB device, and WGM frequencies with the highest acoustic pressure level were determined, which can be applied to pattern cells in the vascular-like walls, moving them apart and safely, temporarily disrupting the BBB to allow drugs to cross this barrier. Acoustofluidic devices were successfully fabricated and are subjected to testing.

A novel blood filtration method for detection of Salmonella enterica serovar Typhi via loop-mediated isothermal amplification in a point-of-care device

Gould C[1], Ebere Akujuru E[1], Ambreen M[1,2], Wall D[1], Cooper J[1], Reboud J[1]
[1]University of Glasgow, [2]National Institute for Biotechnology and Genetic Engineering

Salmonella enterica serovar Typhi is the bacterial etiological agent that causes typhoid fever, which is a significant threat to global public health. Point-of-care diagnostics are a crucial tool in healthcare accessibility, as they allow for affordable, convenient, and rapid diagnosis. Most point-of-care typhoid diagnostics available on the market are immunoassays; however, these tests have poor sensitivity and specificity which increases the risk of inaccurate diagnosis [1]. DNA-based diagnostics are currently impractical due to low numbers of circulating bacteria as well as interference from whole blood in downstream amplification. A novel diagnostic device will utilise a blood filtration system to isolate bacteria from a high-volume (≤5 mL) sample of venous whole blood. Loop-mediated isothermal amplification (LAMP) will be used to amplify DNA due to its adaptability to point-of-care settings. The device itself will be designed with sustainability in mind due to the inclusion of biodegradable materials and device modularity. Experimental results show that the optimisation of a homemade whole blood lysis buffer does not affect Salmonella enterica serovar Typhimurium SL1344 (which serves as a model for S. Typhi) while effectively lysing whole horse blood in under 5 minutes. This, along with a bacterial lysis buffer, is currently being optimised in a custom filter. The system will allow for inexpensive DNA-based S. Typhi detection to occur in under two hours without the need for training on specialised equipment. The point-of-care utility will improve access to accurate diagnosis by facilitating clinic-based deployment in local communities.

[1] Thriemer, K., et al., 2013. A Systematic Review and Meta-Analysis of the Performance of Two Point of Care Typhoid Fever Tests, Tubex TF and Typhidot, in Endemic Countries. PLOS ONE 8, e81263.

Predicting Parkinson's Disease Severity from Gait with Federated Learning: Challenges to Overcome

Dr Chloe Hinchliffe[1], Hugo Hiden[2], Emma Packer[1], Philip Brown[3], Alison Yarnall[1,3,4], Lynn Rochester[1,3,4], Lisa Alcock[1,3], Marloes Peeters[5], Silvia Del Din[1,3,4], Paul Watson[2]
[1]Translational and Clinical Research Institute, Faculty of Medical Sciences, Newcastle University, [2]School of Computing, Newcastle University, [3]The Newcastle upon Tyne Hospitals NHS Foundation Trust, [4]National Institute for Health and Care Research (NIHR) Newcastle Biomedical Research Centre (BRC), Newcastle University and The Newcastle upon Tyne Hospitals NHS Foundation Trust, [5]School of Engineering, Newcastle University

Conventional smart home-based machine learning requires patient data to be transferred to a central server, raising privacy concerns. Federated learning (FL), which shares parameters of locally trained models instead of patient information, presents an alternative to predict Parkinson's disease severity from real-world measures of gait, as a part of the TORUS project [1]. For the CiC study [2], 55 people with Parkinson's were assessed using the Movement Disorder Society-Unified Parkinson's disease Rating (MDS-UPDRS) and wore an inertial movement unit on the lower-back for 7 days. Daily gait measures extracted using validated algorithms [3], along with patients' age, sex, and body mass index (BMI), were used to estimate the MDS-UPDRS III score in a federated system, as well as a conventional, centralised system. Random Forest (RF) and Neural Networks (NN) were tested for both systems. 53 patients had available gait data. The centralised models had mean absolute errors (MAEs) of RF=9.16 and NN=11.46. The MAEs of the server-aggregated global models were FL-RF=8.13 and FL-NN=16.00, and the mean MAEs of the local models were FL-RF=0.0 and FL-NN=12.17. However, the RF severely overfit to the local data, as seen in Figure 1. SHAP analysis of the NN showed that while the age, sex, and BMI were very important to the centralised system, lack of within-subject variation caused these importances to be extinguished for the local federated models, leading to a degradation for the global model. Therefore, this work has highlighted key challenges of using FL in a smart-home scenario.

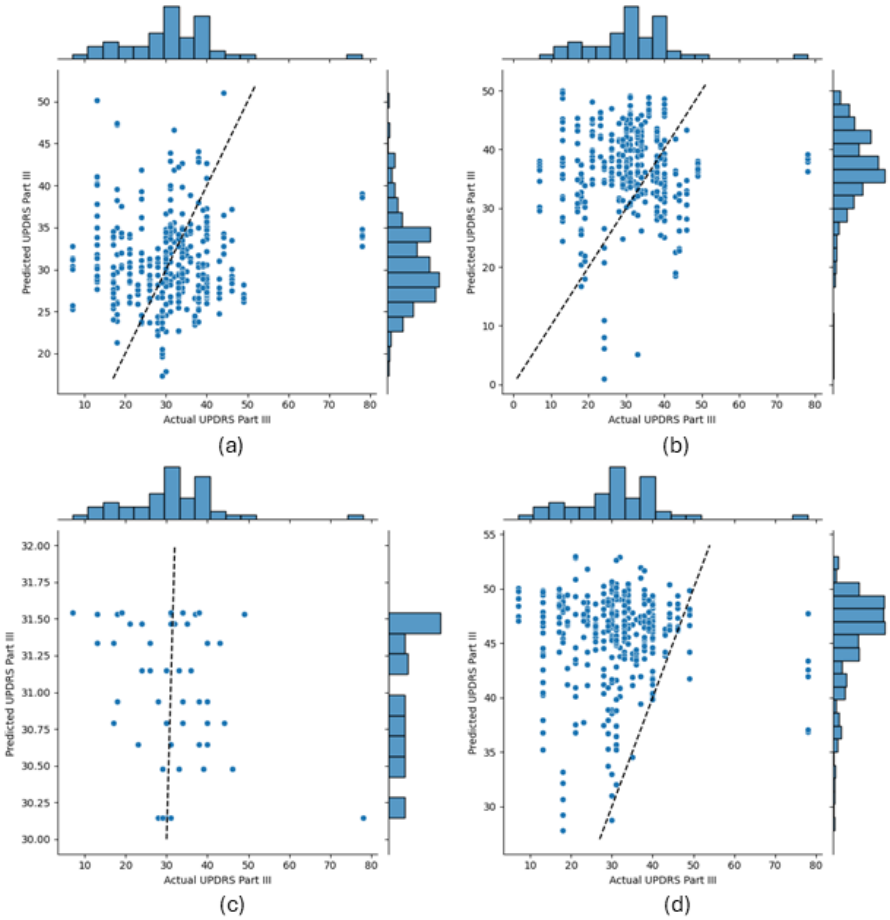

(a) Centralised RF. (b) Centralised NN. (c) Global Federated RF. (d) Global Federated NN.

[1] https://torus.ac.uk/
[2] E. Packer et al., 2023, BMJ Open, vol. 13, pp. e073388.
[3] S. Del Din et al., 2016, J Neuroeng Rehabil, vol. 13, no. 46.

Wearable-Based Activity Recognition for Older Adults: Leveraging Comfort and Flexibility in Daily Health Monitoring

Kasawala E[1], Fratini A[1], Mouli S[1]
[1]Aston University

Activities of Daily Living (ADLs) refer to the essential tasks necessary for independent living, covering both personal care and household activities. ADL monitoring has significant advantages by detecting early indicators of cognitive decline as well as physical impairments, facilitating timely and targeted interventions. Furthermore, it enables the development of personalised care plans that respond to an individual's evolving health needs, promoting proactive care to enhance overall quality of life [1]. Wearable ADL monitoring systems are often met with resistance by older adults due to discomfort and the inconvenience of continuous wear. As a result, user acceptance and overall usability remain low [2].This study presents a flexible activity recognition approach using the Bangle.js 2 smartwatch equipped with TinyML capabilities. The system is designed to adapt to different wear locations (wrist, shirt pocket, trouser pocket and ankle) to classify activities such as walking, stair ascent, stair descent and baseline idle state. By reducing dependence on fixed sensor positions, the approach promotes ease of use and supports natural integration into daily routines. The model demonstrated strong performance, achieving 92.8% accuracy in training, 90.59% in testing, and 89.72% during real-time inference across the four body placements with an average accuracy of 80% for all activities at all locations. These results suggest that consumer-grade wearables can serve as practical tools for empowering older adults to engage in continuous, personalised health monitoring. This presents a need for further research to develop a more comprehensive understanding of sensor agnostic approaches for health monitoring applications.

1.Camp, N.,et al. (2020). Technology Used to Recognize Activities of Daily Living in Community-Dwelling Older Adults. International Journal of Environmental Research and Public Health, 18. doi:https://doi.org/10.3390/ijerph18010163.

2.Fowe, I.E.et al. (2022). Understanding Older Adults' Attitudes toward Mobile and Wearable Technologies to Support Health and Cognition. Frontiers in Psychology, 13. doi:https://doi.org/10.3389/fpsyg.2022.1036092.

Habitual turning behaviour over 7 days in a participant with Parkinson's disease: A case study

Wilkinson C[1], Packer E[1], Brown P[3], Zia Ur Rehman R[2], Scott-Singer K[1], Yarnall A[1], Rochester L[1], Del Din S[1], Alcock L[1]
[1]Newcastle NIHR BRC, Translational and Clinical Research Institute, Newcastle University, [2]Janssen Research & Development, [3]The Newcastle upon Tyne Hospitals NHS, Foundation Trust, United Kingdom

Turning makes up 45% of daily living movements [1] and can be challenging task for people with Parkinson's disease (PD) [2]. Monitoring real-world mobility provides an ecological and representative assessment for evaluating health and physical function. There is emerging evidence supporting utility of turning as a sensitive measure for PD. Our understanding of turning behaviours in the real-world is less advanced; the aim was to gain better insight to allow for interpretation of data and refinement of outcomes.

Data analysis was conducted for a single participant with PD (male, 67yo, Hoehn & Yahr disease stage II, MDS-UPDRS III score 40/132) who took part in the CiC-PD study (ISRCTN Number: 13156149)[3]. The participant wore an inertial measurement unit (Axivity AX6, sampling frequency 100Hz) on the lower back for 7-days continuously. Turns were identified using a validated algorithm [4]. Turn angle, turn duration, and angular velocity for each turn were extracted. Turns were aggregated according to turn angle with a minimum turn angle of 30°.

A total of 17,452 turns were identified over 7-days (Figure 1). The number of turns decreased with increasing turn angle (more smaller turns, fewer larger turns). Turn duration increased with turn angle (i.e. smaller turns were shorter in duration). Angular velocity increased as turn angle increased (larger turns were completed faster). Further analysis will explore the clinical validity of turning behaviour and correlations with turn strategy, turn direction bias and performance in a larger cohort.

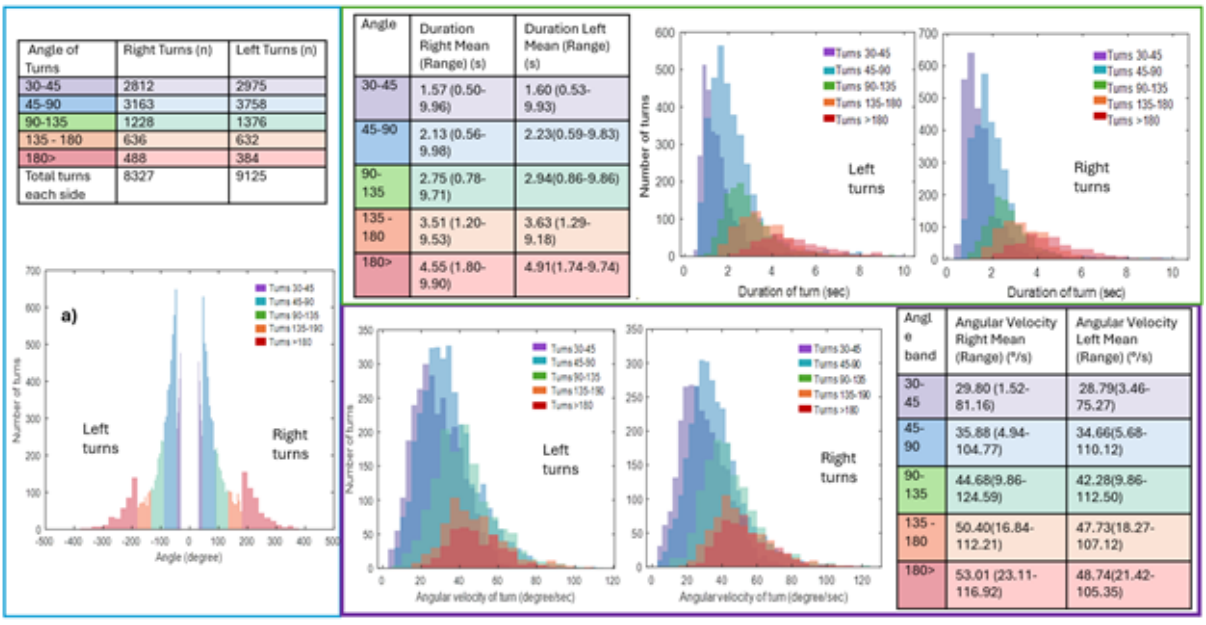

Angle of Turns	Right Turns (n)	Left Turns (n)
30-45	2812	2975
45-90	3163	3758
90-135	1228	1376
135 - 180	636	632
180>	488	384
Total turns each side	8327	9125

Angle	Duration Right Mean (Range) (s)	Duration Left Mean (Range) (s)
30-45	1.57 (0.50-9.96)	1.60 (0.53-9.93)
45-90	2.13 (0.56-9.98)	2.23(0.59-9.83)
90-135	2.75 (0.78-9.71)	2.94(0.86-9.86)
135 - 180	3.51 (1.20-9.53)	3.63 (1.29-9.18)
180>	4.55 (1.80-9.90)	4.91(1.74-9.74)

Angle band	Angular Velocity Right Mean (Range) (°/s)	Angular Velocity Left Mean (Range) (°/s)
30-45	29.80 (1.52-81.16)	28.79(3.46-75.27)
45-90	35.88 (4.94-104.77)	34.66(5.68-110.12)
90-135	44.68(9.86-124.59)	42.28(9.86-112.50)
135 - 180	50.40(16.84-112.21)	47.73(18.27-107.12)
180>	53.01 (23.11-116.92)	48.74(21.42-105.35)

Figure 1.a) Turn angle to right and left, n.0 turns. Turn duration b) or angular velocity c), mean and range

[1] B. C. Glaister et al., 2007 vol.25, no.2, pp.289-294,
[2] E. L. Stack et al., 2006 Parkinsonism & Related Disorders, vol.2, no.2, pp.87-92,
[3] E. Packer et al., 2023 BMJ Open, vol. 13, no. 9, p. e073388
[4] R. Z. U. Rehman et al., 2020 Sensors, vol.20, no.18

Investigating stride variation in curvilinear walking gait across Parkinson's disease and older adult cohorts in a supervised clinical test

Nicoll D[1], Margagliotti S[2], Payne T[3], Buckley E[4], Bandmann O[3], Bonci T[1]
[1]School of Mechanical, Aerospace and Civil Engineering & INSIGNEO Institute for in silico Medicine, The University of Sheffield, [2]Polytechnic of Turin, [3]Sheffield Institute for Translational Neuroscience, University of Sheffield, [4]Clinical Medicine, The University of Sheffield

Given the complex coordination and multisensory integration required for curvilinear walking, additional abnormalities are expected in people with Parkinson's disease (PD) [1], but it remains unclear the extent that curvilinear walking affects gait outcomes in supervised clinical tests such 6-minute walking tests (6MWT). This study therefore aims to establish if the walking strategy during curvilinear differs from straight-line walking during 6MWTs (Figure 1). Data from 16 PD (71.3±4.0 y.o., H&Y:1-3) and 8 older adults (OA) (64.9±10.9 y.o.) was collected with a multi-sensor wearable system [2]. Turns, stride duration, length and speed were extracted. Stride length and speed were normalised to participant height. Using the detected turns, the stride parameters were segmented by walking condition (straight-line vs. curvilinear) in MATLAB. Wilcoxon rank-sum tests were used to evaluate statistical differences in stride outcomes during straight and curvilinear walking for each group. Overall, 5606 and 10707 strides were detected for OA and PD, respectively. In both cohorts, about 23% of strides were detected during curvilinear walking, and had statistically longer duration, shorter length, and slower speed ($p<0.001$, Figure 1). Curvilinear walking significantly alters stride parameters of both cohorts in 6MWT. Recent work on ad-hoc pipelines to establish valid real-world outcomes using a lower-back wearable device to objectively quantify mobility changes have been tailored for patients with impaired mobility, including PD and OA [3]. These findings might suggest the need for a more tailored approach when estimating mobility outcomes if turns are detected with a single wearable device in supervised gait assessments.

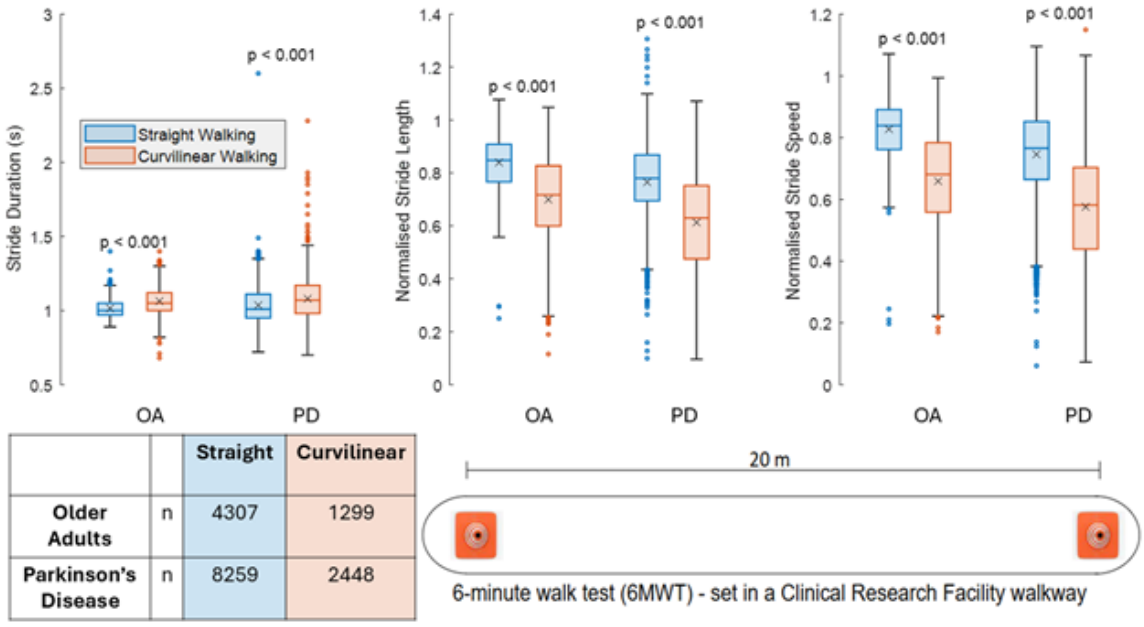

		Straight	Curvilinear
Older Adults	n	4307	1299
Parkinson's Disease	n	8259	2448

Figure 1: Box plots of stride parameters during straight and curvilinear walking and a visualisation of the 6MWT setup.

[1] M. Godi et al., 2017, Front. Neurol., vol. 8, p. 53. [2] F. Salis et al., 2023, Front. Bioeng. Biotechnol., vol. 11, p. 1143248. [3] M. E. Micó-Amigo et al., 2023, J. Neuroeng. Rehabil., vol. 20, no. 1, pp. 78–78.

Application of wearable devices in rest-activity assessment in neurodegenerative disease

Sedghi M[1], Munns S[1], Del Din S[1], Elder G[2], Taylor J[1], Alcock L[1], Lawson R[1]
[1]Translational and Clinical Research Institute, Newcastle University, [2]Northumbria Centre for Sleep Research, Northumbria University

Wearable devices are increasingly used to assess features of neurodegenerative conditions, including Parkinson's disease (PD), dementia with Lewy bodies (DLB), and idiopathic rapid eye movement sleep behaviour disorder (iRBD). Poor sleep and daytime rest-activity are common and affect the quality of life of people living with these conditions, but are challenging to measure using questionnaires, sleep diaries, and polysomnography in these groups. Wearable devices offer a real-world measurement of sleep, sedentary behaviour, and circadian rhythm without interfering with daily activities. This review aimed to understand the available technologies used to assess sleep and rest-activity in PD, DLB, and iRBD and their technical characteristics. We searched seven different databases; 81 studies met our inclusion criteria. The majority of studies included PD participants (85%), followed by iRBD (6%), Lewy body dementia (5%), Parkinson's disease dementia (4%), and DLB (1%). Actiwatch2 was the most commonly used device (n=7, 17.5%); however, 40 different wearable devices from 19 manufacturers were used across studies. The majority of these devices collected accelerometry data (n=31, 78%) while only 15% (n=6) incorporated additional sensors, such as gyroscopes (n=5, 12.5%) and magnetometers (n=3, 7.5%). Twenty-seven (67.5%) of the sensors collected triaxial data, followed by uniaxial (n=7, 17.5%) and biaxial (n=2, 5%) sensors. This systematic review highlights the heterogeneity of wearable devices and the predominance of accelerometry-based technologies over those using more comprehensive sensor combinations. Future research should focus on standardizing device specifications, integrating different sensors for more accurate outputs, further exploring iRBD and DLB, and validating wearables against clinical standards.

BioMedEng25

Poster Presentations

Abstracts

02

Poster Session, Level 2 Foyer, September 4, 2025, 12:00 - 13:00

AI-Driven Healthcare Optimization: Enhancing Early Skin Cancer Detection

Ferral B[1]
[1]Queen Mary University

Skin cancer is the most commonly diagnosed cancer in the UK. In 2022, over 900,000 suspected cases were referred to dermatology services through the NHS urgent two-week wait pathway. However, internal audits from NHS trusts show that up to 90 percent of these referrals are benign, placing considerable pressure on specialist services and delaying care for patients with malignant conditions. We are developing a mobile application using artificial intelligence to support the early triage of skin lesions in primary care. The tool enables general practitioners to upload or capture images of skin lesions and receive immediate risk predictions aligned with established clinical guidelines and the dermatological seven-point checklist. The system is designed to support clinical judgement at the point of referral. Multiple convolutional neural network models were trained and tested using publicly available datasets to assess their suitability for mobile deployment. The model based on the ResNet architecture demonstrated the highest overall performance. On a held-out balanced dataset of 391 samples, it achieved a validation accuracy of 79.5 percent. A confusion matrix illustrates strong classification performance, particularly for benign lesions, with a recall of 92 percent. This project demonstrates the feasibility of developing AI-based tools to assist referral decisions in primary care. While still under development, the approach has the potential to reduce unnecessary specialist demand and contribute to NHS goals in early diagnosis and digital innovation.

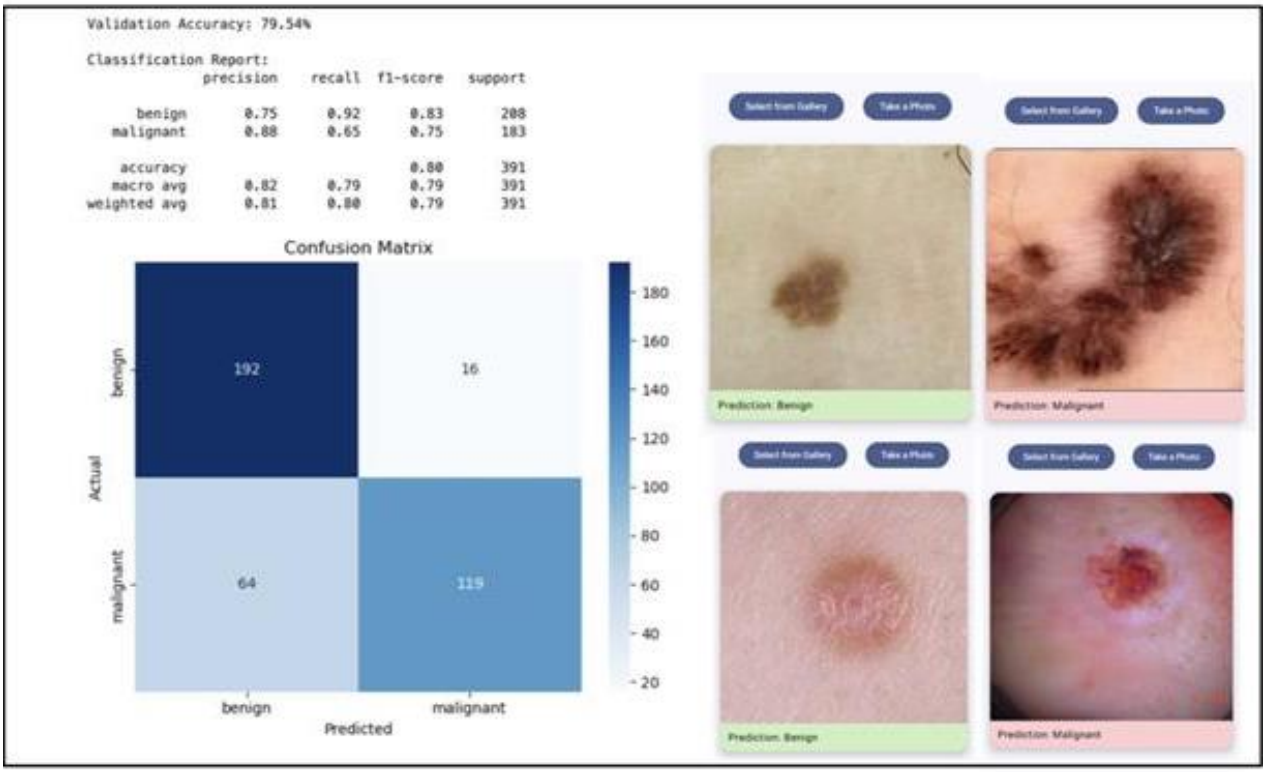

Figure 1. Functional AI app prototype showing 79.5% accuracy and user interface with predictions from an uploaded skin lesion.

04

Poster Session, Level 2 Foyer, September 4, 2025, 12:00 - 13:00

Deep Learning Interpretation of Single-Photon Sensor Array Cerebral Blood Flow Measurements

Mollins A[1], Pan M[1], Li D[1]
[1]Department of Biomedical Engineering, University Of Strathclyde

Diffuse correlation spectroscopy (DCS) is an optical measurement modality for non-invasive monitoring of cerebral microvascular haemodynamics [1]. Researchers from Edinburgh University developed ATLAS, a novel integrated single-photon avalanche diode array for real-time, high-SNR DCS measurements [2]. However, clinical application of ATLAS is hampered by the computationally slow traditional curve fitting used to extract the cerebral blood flow index (cBFI) from the sensor output autocorrelation function (ACF). DL models have been trained to extract cBFI from DCS measurements using labelled ACFs generated from analytical models used in traditional curve fitting [3]. However, the use of Monte-Carlo (MC) simulations to generate labelled datasets for model training, and the application of DL for processing ATLAS data have not been explored. Multilayer MC simulations were performed to produce large, varied, labelled datasets of ATLAS-like DCS ACFs. Long Short-Term Memory DL models were implemented and trained on these datasets using PyTorch. DL model cBFI outputs were evaluated using test ACFs from MC simulations, with the best model then tested on ACFs from experimental ATLAS measurements on an adult male head. The DL model showed significant improvements in cerebral blood flow sensitivity vs traditional fitting on the MC simulated ACFs (93% vs 69%). It had a strong linear correlation ($r = 0.984$) and a 280-fold decrease in time-to-result compared with traditional fitting when processing the experimental ATLAS ACFs. These results showed that DL models trained on data from MC simulations are a viable method of rapidly extracting cBFI, unlocking ATLAS's clinical potential for real time monitoring.

[1] Wang et al, 2024, Neuroimage, 298, 120793
[2] Gorman et al, 2024, Biomed. Opt. Exp, 15, 6499-6515
[3] Wang et al, 2024, J Biomed. Opt, 29, 015004

06

Poster Session, Level 2 Foyer, September 4, 2025, 12:00 - 13:00

Assessment of a Novel, Low-Cost Adsorption Material for the Treatment of Sepsis

Sinclair L[1], Robertson C[1], Gambrah C[2], Gourlay T[1,2]
[1]University of Strathclyde, [2]TSI Technology Ltd

Sepsis is a life-threatening condition accounting for ~20% of global deaths each year [1]. Triggered by a dysregulated response to infection characterised by uncontrolled/excessive release of cytokine signalling molecules, current treatment centres upon antibiotic administration and cytokine adsorption/removal. Adsorption/removal technologies are most effective when employed early; however, their cost often leads to delayed deployment. To address these challenges, this research assesses the capacity of a novel, low-cost material to remove pro- and anti-inflammatory cytokines, both alone and in combination. Suspensions of minimal media (sample diluent NS; Abcam, UK) and whole blood (PCV ~25%; E&O Laboratories) were spiked with IL-6 and IL-10 at levels representative of a heightened inflammatory response (~500 pg/mL). Cytokine-spiked suspensions were exposed to 1g adsorbent material for 150-min; with suspensions re-spiked with cytokines (~500 pg/mL) every 15-min. Samples were collected pre- (0-min), during (7.5-min) and post- (15-min) spiking intervals, and cytokine levels quantified using ELISA (Abcam, UK). Results indicated significant ($P \leq 0.05$) reductions in both cytokines over sampling periods – suggesting no upper limit of adsorption capacity in this instance – with significantly ($P \leq 0.05$) greater reductions demonstrated in minimal media (90.3%) versus whole blood (18.1%). Greater reductions of IL-6 versus IL-10 were demonstrated; however, reductions of cytokines alone versus in combination were statistically similar ($P > 0.05$), suggesting adsorption performance is unlikely influenced by competition with other cytokines. These findings provide proof-of-concept data to support technological development of this material with potential to replace the ‘last-resort’ approach associated with available adsorption technologies and democratize global access to effective sepsis care.
[1] K. E. Rudd et al., 2020, Lancet, vol. 395, no. 10219, pp. 200-211.

08

Poster Session, Level 2 Foyer, September 4, 2025, 12:00 - 13:00

Screening of Photosensitive Nanoparticle-Doped Elastomers for the Development of Antimicrobial Materials

Lavelle D[1], Brown R[1], Maclean M[1,2], Sandison M[1]
[1]Department of Biomedical Engineering, University of Strathclyde, [2]The Robertson Trust Laboratory for Electronic Sterilisation Technologies, Department of Electronic and Electrical Engineering, University of Strathclyde

Medical device-associated infections are a huge public health burden, and new strategies for preventing infections are urgently required. Violet-blue light photoinactivation of microorganisms [1] is an attractive surface decontamination approach, offering broad-spectrum antimicrobial activity and compatibility with mammalian cells, but lower germicidal efficacy than UV-light. We have previously shown that violet-blue (405nm) light inactivation can be significantly improved by incorporating photocatalytic nanoparticles into silicone materials, such elastomers being widely used in medical devices (catheters, stents etc) [2]. Surface etching exposes embedded nanoparticles, further improving efficacy, whilst the resulting nano-scale roughness can reduce bacterial attachment. To effectively integrate these properties into a single material, screening of a broad range of photocatalytic dopants is needed. Here, we report on antimicrobial testing of nanoparticle-doped PDMS elastomers within a custom multiwell plate device employed to increase screening throughput. TiO_2, ZnO and $SrTiO_3$ nanoparticles were incorporated into a Sylgard 184 matrix (110:1 PDMS:nanoparticle, w/w) and cured samples were etched using tetrabutylammonium fluoride. Samples were incubated with Staphylococcus aureus ($x10^5$ CFU/ml) for 1h to allow attachment. After washing, samples were exposed to 405nm light (31.5 J/cm²), incubated (37°C; 18h) in tryptone soya broth, and in situ crystal violet staining used to quantify the extent of any biofilm growth. The ZnO-doped material was the most effective for photoinactivation, with a 90% reduction in biofilm formation compared to a dark control. Together with additional bacterial attachment and physiochemical characterization data, this approach provides a route to identifying the most promising nanoparticle-doped antimicrobial elastomers for use in medical devices.

[1] R.M. Tomb et al., 2018, Photochem. Photobiol., vol. 94, no. 3, pp.445-458
[2] L. McShea et al., 2022, Mater. Res. Express, vol. 9, 085402

10

Poster Session, Level 2 Foyer, September 4, 2025, 12:00 - 13:00

A novel silk-based biomaterial approach for spinal cord injury repair

Ma H[1], Milanizadeh S[1], Viskontas M[1], Seib F[2,3,4], Bewick G[1], Huang W[1]
[1]Institute of Medical Sciences, University of Aberdeen, [2]Strathclyde Institute of Pharmacy and Biomedical Sciences, University of Strathclyde, [3]Branch Bioresources, Fraunhofer Institute for Molecular Biology and Applied Ecology, [4]Institute of Pharmacy, Department of Pharmaceutics and Biopharmaceutics

Spinal cord injury (SCI) is a serious neurological disease with limited self-recovery and a high rate of disability. However, the limited capacity for axon regeneration, coupled with the complex SCI pathophysiological environment, presents a huge challenge for current therapies. Biomaterials offer a promising approach for SCI repair, as scaffolds to bridge injury cavities. Bombyx mori silk (BmS) hydrogel can be injected into SCI sites in a minimally invasive manner [1], meeting a key requirement of biomaterials for SCI repair. BmS hydrogel possesses customizable mechanical properties that favourably supported the growth of dorsal root ganglion (DRG) explants and postnatal cortical neurons [2]. Therefore, in this study we hypothesise that BmS hydrogel injected into the lesion site of an in vivo hemisection model of SCI would be beneficial for recovery. Our results demonstrated that 3 µl of 2% BmS hydrogel at the injury site promoted significant locomotor functional recovery at weeks 2-4 compared to injury only controls ($p = 0.018$). Moreover, the injury areas of rats treated with 3 µl ($p=0.018$) and 6 µl of 2% BmS hydrogel ($p=0.027$) were significantly smaller than controls. Rats treated with 3 µl 2% BmS hydrogel had less GFAP expression ($p=0.05$), increased neuronal survival in dorsal horn ($p<0.05$), oligodendrocyte survival from rostral side to lesion in both the dorsal column and corticospinal tract ($p<0.05$), and axonal regrowth at rostral proximal were significantly enhanced ($p<0.05$). Our results suggest that silk hydrogel conferred neuroprotection after SCI and could be potentially used in combinational therapies for SCI repair.

[1] Kapoor, S. et al., (2016), Acta Biomaterialia, 31, 17-32.
[2] Varone, A., (2019), Combining Novel Biomaterial and Growth-promoting Strategies to Promote Spinal Cord Repair. University of Aberdeen.

12

Poster Session, Level 2 Foyer, September 4, 2025, 12:00 - 13:00

Developing Conductive Polymer Coatings for Monitoring and Modulating the Cell-Implant Interface

Abisoye I[1], Sandison M[2], McCormick C[3]
[1]University Of Strathclyde, [2]University of Strathclyde, [3]University of Strathclyde

Inadequate integration of implant surfaces with host tissue represents a significant problem leading to suboptimal clinical outcomes. Although surface modifications have improved biocompatibility, many implants still do not actively interact with the surrounding biological environment. Moreover, once implanted there are currently no means of monitoring the surface-host responses. Materials that can facilitate tissue integration and offer real-time feedback on cellular activity at the implant surface therefore hold great potential. Conducting Polymers represent a potentially useful material for implant coatings, with their electrical properties and potential for biofunctionalization, conferring advantages over traditional materials.[1]

In this work, protocols were established for potentioastatic electropolymerisation of Polypyrrole coatings on stainless steel. Results show that surface topography and impedance characteristics can be modulated by adjusting polymerization parameters, including monomer/dopant ratios and voltage. Moreover, inclusion of sodium salicylate as the dopant may inhibit the platelet response and dampen inflammation, particularly advantageous properties for vascular applications. Current work is focused on characterization of the biocompatibility of the coatings, with preliminary findings indicating that endothelial cells attach and remain viable after 24 hrs.

Further research is now required to better understand the surface properties with greatest influence on cell adhesion and viability, thereby allowing future optimization of biocompatibility. Likewise, the stability of the electrical properties of the coatings remains to be characterized, a key step in using the coatings as an electrochemical sensor. This will help lay the foundation for multifunctional, cell-responsive coatings capable of both monitoring and directing biological responses at the implant interface.

[1] Alison L. Marsden et al., (2018); Current Opinion in Biomedical Engineering, Vol 5, pp iii-iv

14

Poster Session, Level 2 Foyer, September 4, 2025, 12:00 - 13:00

Assessing and quantifying the relationships between spasticity, proprioception, and movement post-stroke

Usher J[1,2], Morris J[3], Aranceta-Garza A[1,2]
[1]Biomedical Engineering, School of Science and Engineering, University of Dundee, [2]Centre for Medical Engineering and Technology, University of Dundee, [3]Health Sciences, School of Health Sciences, University of Dundee

Little is known about the relationships between post-stroke impairments. For this research, the relationships between impairments were assessed from participants with stroke at 2 weeks (baseline), and at 1.5, 3 and 6-months. Data collected included spasticity, proprioception, Action Research Arm Test (ARAT), motor function, NIH stroke scale scores, lesion side and type, sex, age, and Scottish Index of Multiple Deprivation (SIMD). Furthermore, kinematics including velocity, smoothness of movement (number of velocity peaks), compensatory strategies, and joint angles were collected to assess quality of movement during ARAT performance. To date, ten participants [mean age (61±16) years, eight males, nine ischemic strokes] have completed baseline assessment. Participants with faster movements had better overall motor function and clinical outcomes along with higher total ARAT scores ($r=-0.55$, $p=0.03$, Kendall's tau). It was also observed that fewer wrist and elbow peaks, implying smoother movements, related to a higher ARAT score ($r=-0.55$, $p=0.03$; $r=-0.65$, $p=0.02$, respectively). In addition, it was found that for those with greater wrist spasticity, mean wrist and elbow velocity was lower, suggesting slower movements ($r=-0.59$, $p=0.04$; $r=-0.65$, $p=0.03$, respectively). Proprioception, age and SIMD scores did not have significant relationships with any variables at baseline, and so far, sex, side and type of lesion had no significant effect on any variable at baseline (Mann-Whitney U tests). As this research progresses, stroke recovery predictors will be determined to assist in developing highly personalised rehabilitation programs based on how changes in one impairment affect another, improving the quality of life of those affected by stroke.

Poster Session, Level 2 Foyer, September 4, 2025, 12:00 - 13:00

Development of an enhanced framework for arterial remodelling following percutaneous coronary intervention

Dal Ferro L[1], Corti A[2], Chiastra C[3], Migliavacca F[2], McGinty S[1]
[1]University Of Glasgow, [2]Politecnico di Milano, [3]Politecnico di Torino

In-stent restenosis (ISR) poses a risk for patients who have undergone stent implantation following atherosclerosis. It consists of the gradual intimal growth that follows the stenting of a patient potentially leading to the vessel's new occlusion. Computational models have been implemented in a continuous and discrete form to study ISR, incorporating various factors concurring to cause it and offering predictions on the procedure's outcomes. This work aims at presenting a patient-specific multiscale model of an atherosclerotic coronary artery including different 2D frameworks: a structural finite element module (FEM) integrated in a drug transport module and an agent-based module (ABM). The drug-eluting stent (DES) deployment module generates a deformed geometry. The drug transport module takes as input this geometry and computes the drug retention and distribution in the tissue [1]. Finally, the ABM module simulates cell and extra-cellular matrix dynamics to obtain the tissue growth and arterial remodelling [2]. The proposed work successfully reproduced how the intimal tissue regrowth is influenced by the presence of a drug released over time and inflammation. This multiscale model represents an innovative tool for the studying of ISR by presenting a cellular and tissue perspective on a patient-specific artery characterized by an atherosclerotic plaque with regions of different nature.
We will discuss various ways in which the model may be improved, and show some preliminary results.

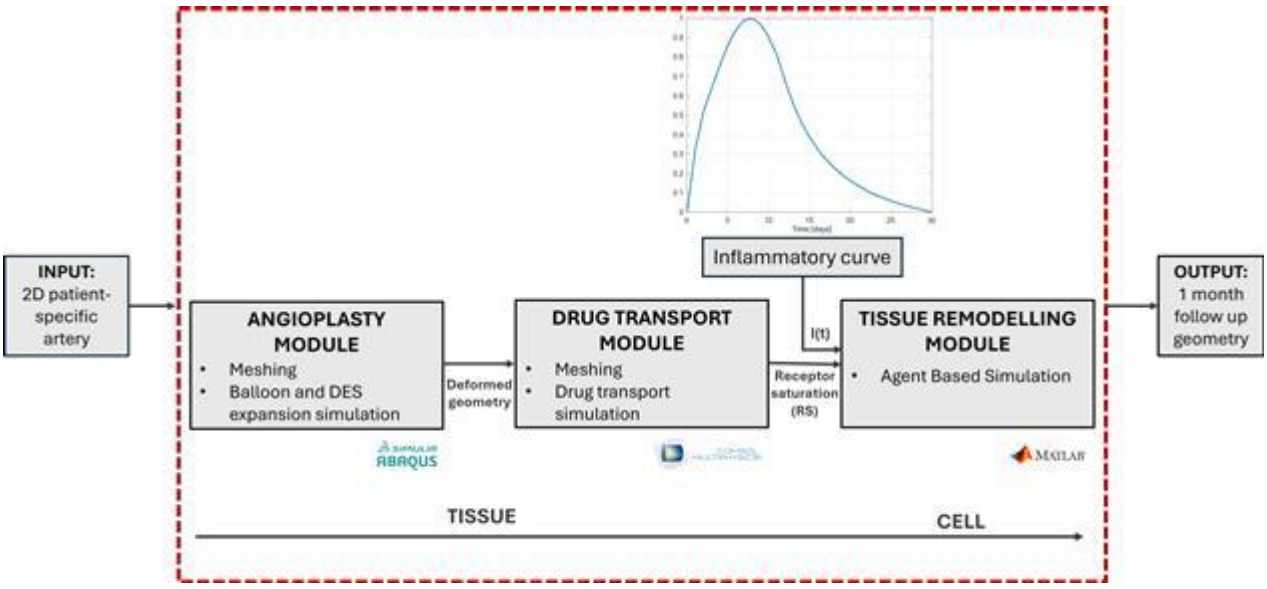

Figure: Computational framework: angioplasty module (DES deployment), drug transport module and tissue remodelling module.

[1] A. McQueen et al., 2022, J. Control. Release, vol. 349, pp. 992–1008.
[2] A. Corti et al., 2023, Comput. Methods Programs Biomed., vol. 241

Poster Session, Level 2 Foyer, September 4, 2025, 12:00 - 13:00

Microstructural and biomechanical mapping of murine vertebral endplates in osteoarthritic STR/Ort spines using synchrotron computed tomography and digital volume correlation

Henderson I[1,2], Sharma A[1,2], Parmenter A[1,2], Chen J[1,2], Pitsillides A[3], Torii R[1], Lee P[1,2]
[1]Department of Mechanical Engineering, University College London, [2]Research Complex at Harwell, [3]Comparative Biomedical Sciences, Royal Veterinary College

The vertebral endplates (VEPs) play an essential role in mechanical load and nutrient transfer in the spine. While animal studies have linked VEP microstructure and biomechanical function [1], the implications of facet joint osteoarthritis (OA) on local VEP biomechanics remain unclear. This study develops a biomechanical analysis pipeline for resolving microstructure and local biomechanical strains in loaded VEPs using synchrotron X-ray computed tomography (sCT) with digital volume correlation (DVC). Lumbar vertebra-disc-vertebra segments (L4-L5) were dissected from OA-prone STR/Ort and healthy parental CBA mice (N=3), prior to OA onset (8-10 weeks) and at advanced-OA (40+ weeks). L4-L5 segments were compressed in situ (Deben CT500) and imaged using sCT (I13-2, Diamond Light Source, 1.6µm/voxel). 3D displacement and strain fields were computed using the global DVC approach (Avizo 3D, XDVC module) in reconstructed datasets, and morphology quantified in BoneJ [2]. sCT imaging revealed high density mineralised protrusions in STR/Ort spines for the first time. Preliminary morphological analysis also indicates increased mineralisation in STR/Ort VEPs compared to CBAs at 40+ weeks ($p<0.05$). A global DVC approach enables displacement and strain field quantification across intact murine spine segments with <20nm displacement accuracy and <250µε strain precision. Further work aims to link local VEP microstructure to biomechanical strains to identify mechanical biomarkers associated with progression of OA in the spine. We envision our data can be used to validate VEP finite-element models and our approach scaled for studies involving large animals and humans. Acknowledgements: ESPRC (EP/T517793/1, EP/W524335/1), RAEng (CiET 1819/10), CZI (CZIF2022-316777), Diamond Light Source (SM29784-9).

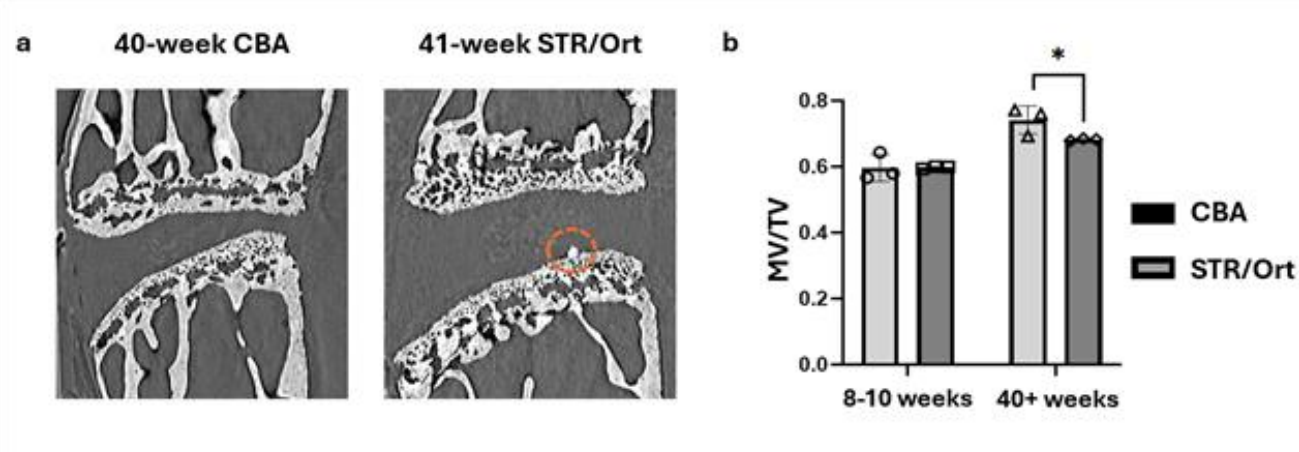

Figure:(a) Comparison of VEP microstructure, pathological mineralisation indicated (orange). (b) Increased mineral volume to tissue volume (MV/TV) with OA ($p<0.05$).

[1] M. Fainor et al., 2023, JOR Spine, vol. 6, no. 4, pp. e1287.
[2] M. Doube et al., 2010, Bone, vol. 47, no. 6, pp. 1076-1079.

20

Poster Session, Level 2 Foyer, September 4, 2025, 12:00 - 13:00

Contact forces during intraoperative varus-valgus assessment

Donald E[1], Adams C[1], Doyle C[1], Riches P[1]
[1]University Of Strathclyde

Total knee arthroplasty (TKA), used to restore damaged and osteoarthritic knees, results in instability and pain in 30% of patients [1]. Soft tissue balancing is a stage in TKA that involves making small incisions to the soft tissues of the knee, altering varus-valgus laxity and improving knee alignment affecting knee functional outcome. The procedure is subjective and there is a drive to quantify this procedure to improve patient outcomes. An a priori understanding of contact forces during this procedure is an important step in developing devices to quantify and assist the soft tissue balance process. A FE model of the native knee (Figure 1) [2] was adapted to evaluate the contact forces translated on the tibial plateau from the femoral condyles during intraoperative varus-valgus assessments. The moment required to induce separation between a femoral condyle and the tibial plateau was recorded, together with the contact force on the contralateral condyle. Lateral condyle lift-off was achieved with an 18 Nm varus moment, with a contact force of 130 N on the medial condyle in agreement with expected surgeon loads [3]. However, the application of a 70 Nm valgus moment was required to achieve lift-off on the medial condyle, an unrealistic surgeon input. At 18 Nm valgus moment, the medial and lateral condyle contact forces were ~20 N and ~200 N respectively. This model enhances our understanding of intraoperative knee joint forces and provides clear operating data for the design of devices to assist the soft tissue balance process.

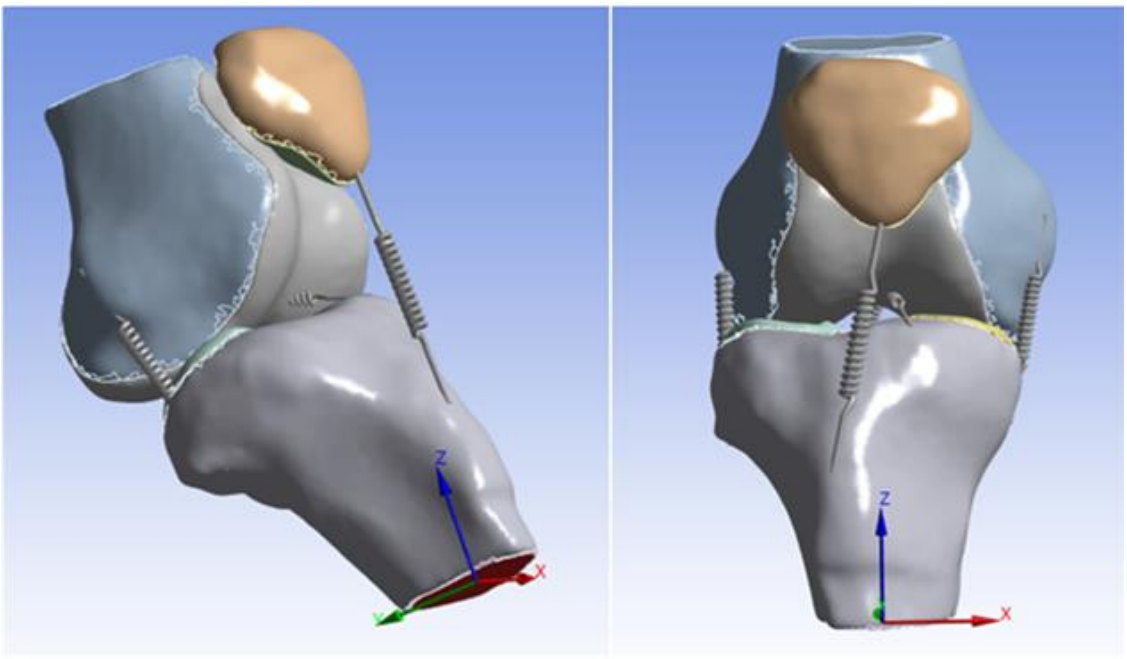

Figure: Finite element model of the native knee in full extension

[1] Bourne B.M. et al. (2010), Clin. Orthop., vol. 468, no. 1, pp. 57–63.
[2] Gu Y, & P.E. Riches (2022), Proceedings of Biomedeng22, UCL, London
[3] Clarke JV et al (2012) Proc Inst Mech Eng H., vol 229, no. 9, pp. 699-708.

22

Poster Session, Level 2 Foyer, September 4, 2025, 12:00 - 13:00

Comparison of laboratory and outdoor measurements of walking in stroke survivors

Kuntapun J[1], Johnson T[1], Kerr A[1]
[1]Department of Biomedical Engineering, University of Strathclyde

Gait assessment after stroke is typically conducted in laboratory settings that limit the number of gait cycles, require technical support, and do not reflect real-world performance. It is important to understand how the environment affects walking performance in individuals with stroke to design personalised rehabilitation interventions.

The aim of this study was to compare gait parameters of stroke individuals walking in laboratory and outdoor environments, using a commercially available accelerometer.

Three stroke participants with hemiplegia (age 46.67 ± 9.29 years, 17.33 ± 1.15 months post-stroke) and five healthy adults (age 29.60 ± 5.86 years) were asked to walk in both laboratory and outdoor settings. In the laboratory setting, participants performed two repetitions of nine walking conditions (straight, six with turns and two changes in speed). Outdoors, they walked a 400-meter course around a university campus that included multiple turns and slopes. Two small accelerometers (PAL Technologies Ltd., Glasgow, UK) were attached to the middle of both thighs to measure temporal gait parameters (stance/swing duration and symmetry).

Results from Table 1. show that stroke participants exhibited greater stance duration symmetry in outdoors environments. (0.80 ± 0.13 in the laboratory vs. 0.87 ± 0.10 outdoors) and a shorter stance duration. Furthermore, swing duration symmetry increased and swing duration was longer outdoors. In contrast, healthy participants walked faster outdoors than in the laboratory, reflected by shorter swing and stance duration. However, the findings of this study should be further investigated due to the small sample size and limited validation of thigh-mounted accelerometers.

	Stroke participants				Healthy participants			
	Laboratory		Outdoors		Laboratory		Outdoors	
	Affected side	Unaffected side	Affected side	Unaffected side	Left side	Right side	Left side	Right side
Swing duration (sec)	0.66 ± 0.06	0.58 ± 0.11	0.67 ± 0.04	0.59 ± 0.13	0.52 ± 0.06	0.52 ± 0.05	0.49 ± 0.04	0.52 ± 0.05
Stance duration (sec)	0.73 ± 0.13	0.81 ± 0.13	0.69 ± 0.22	0.78 ± 0.16	0.68 ± 0.02	0.62 ± 0.02	0.58 ± 0.05	0.55 ± 0.06
Swing duration symmetry	1.14 ± 0.10		1.17 ± 0.17		1.02 ± 0.15		1.07 ± 0.09	
Stance duration symmetry	0.80 ± 0.13		0.87 ± 0.10		0.91 ± 0.01		0.94 ± 0.06	

Table 1. Gait parameters while walking in laboratory and outdoor environments in stroke and healthy participants

24

Poster Session, Level 2 Foyer, September 4, 2025, 12:00 - 13:00

Evaluating the Failure Loads of the Meniscus Root Attachment

Dalal S[1], Jones A[1], Mengoni M[1], Wilcox R[1]
[1]University of Leeds

The meniscus is a fibrocartilaginous tissue which plays a key role in load distribution and stability in the knee. Injuries can lead to a loss of the meniscus functional abilities and the development of osteoarthritis. Current surgical repair options include the use of meniscal allografts and tissue engineered scaffolds, however the failure strength at the attachment sites is a limiting factor. The aim of this work was to develop a method to determine the failure strength at the natural meniscal root attachments to provide a benchmark for testing attachment techniques used for meniscus implantation. Porcine knees (N=8) were prepared by removing all surrounding structures leaving the menisci attached to the tibia via the three tibial roots. The menisci were sectioned centrally with the free end and tibia attached to a tensile testing machine (I3366, Instron, UK). After a preload of 10 cycles from 10 N to 50 N at 0.1 Hz each root was axially loaded at 0.5 mm/s until failure. Failure loads and approximate cross-sectional areas of the attachment sites were measured. All roots failed at the bony attachment site with failure loads shown in Figure 1. The average cross-sectional areas at the Posterior Medial (PM) root (31.7±7.2 mm²) and Anterior Lateral (AL) root (28.2±13.3 mm²) were smaller than the Anterior Medial (AM) root (36.8±14.8 mm²). The results provide baseline data on meniscal root behaviour and indicate that behaviour is not governed by the root area alone, with the bone interface and internal fibrous structure also likely contributing.

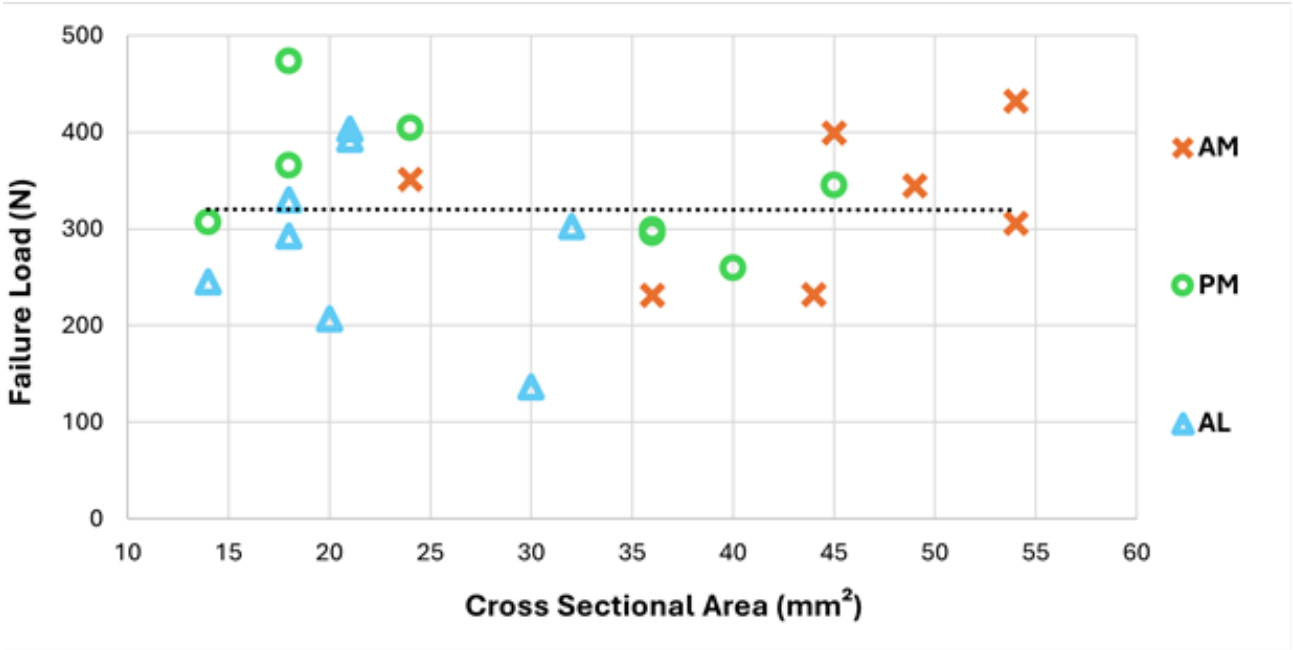

Figure 1: Failure Load vs Cross Sectional Area for Anterior Medial (AM), Posterior Medial (PM) and Anterior Lateral (AL) Roots

26

Poster Session, Level 2 Foyer, September 4, 2025, 12:00 - 13:00

Assessing Gait Biomarkers of Osteoarthritis Using Markerless Time-of-Flight Kinematic Analysis

Clarke J[1], Ellison P[1], Genever P[4], Shenker N[5], Bowes M[3], Pelah A[2,1]
[1]School Of Physics, Engineering & Technology University Of York, [2]Florida Atlantic University, [3]York And Scarborough Teaching Hospitals NHS Foundation Trust, [4]Department Of Biology, University Of York, [5]Cambridge University Hospitals NHS Foundation Trust

Early detection of osteoarthritis (OA) through non-invasive gait analysis could enable timely interventions that slow disease progression and improve patient outcomes. This study aimed to identify gait biomarkers predictive of OA in patients with a confirmed diagnosis using a Time-of-Flight (ToF) camera system and computer vision analysis relative to healthy controls. The study included 46 participants, 38 patients with clinically confirmed knee or hip OA and 8 age and sex matched controls without OA. Participants walked on a treadmill at self-selected speeds with progressive phases at 1.5, 3, and 6 km/h, while a ToF camera captured three-dimensional joint kinematics at 30 FPS. Custom algorithms extracted spatiotemporal metrics including average speed, stride length, cadence, knee range of motion, and maximum achievable speed. Previous studies have shown that OA patients may exhibit compensatory gait adaptations, including increased knee range of motion at higher walking speeds [1]. Preliminary analysis of the gathered data indicates that the OA patients exhibited increased knee range of motion at higher walking speeds compared to the healthy controls, likely reflecting quantifiable compensatory gait adaptations. These findings suggest that markerless ToF-captured gait parameters taken over a range of walking speeds could provide reliable phenotype biomarkers for OA

[1] Z. Bejek et al., 2005, Knee Surg. Sports Traumatol. Arthrosc., vol. 14, no. 7, pp. 612–622.

28

Poster Session, Level 2 Foyer, September 4, 2025, 12:00 - 13:00

Convolutional Neural Network Applied to Laser Speckle Contrast Imaging

Lu C[1], Zhang X[1], Chipperfield A[1]
[1]University of Southampton

Laser Speckle Contrast Imaging (LSCI) is a low-cost, non-invasive, non-contact optical imaging technique that has been widely used in monitoring the blood flow, growth of plants and other kinds of biomedical engineering [1]. In this paper, we used Methylcellulose Gel (MCG) & fluorescence microspheres solutions for the simulation of blood flow. With the help of a syringe pump, microscope, laser source and specially designed microfluidic channels, we have constructed a simulated blood vessel model with which we can vary the particle concentration and flow rate. Data from this experimental setup is used to test a newly developed LSCI image processing and analysis algorithm that will be introduced. By combining the processed speckle contrast images with a Convolutional Neural Network (CNN) [2], we investigate the detection of abnormal flow rates of samples and achieved classification based on the flow rate with high accuracies of ~90%. The newly developed LSCI analysis algorithm shows great potential in the estimation of blood flow rates and, potentially, variation in disease state or healing in, for example, the treatment of diabetes and burn injury. The aim is to improve the interpretability of the results of the existing LSCI analysis methods, in particular those associated with subjectivity, towards a more quantitative and automated approach.

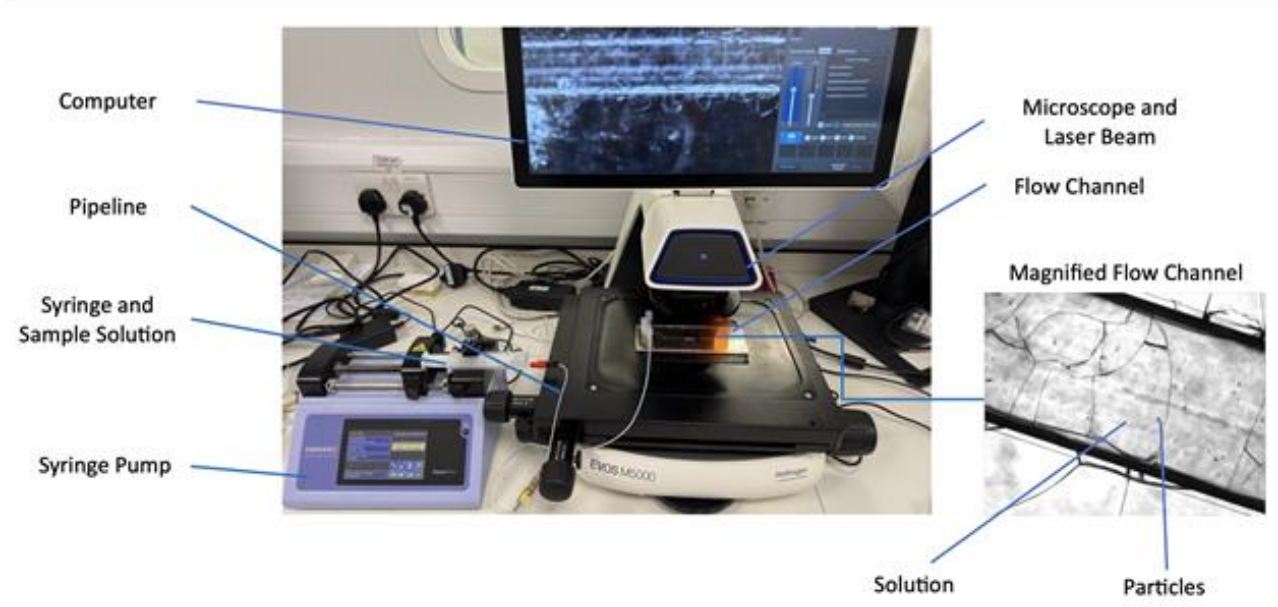

Figure: LSCI Experimental Setup (Data Acquisition Part)

[1] W. Heeman et al., "Clinical applications of laser speckle contrast imaging: a review," Journal of biomedical optics, vol. 24, no. 8, pp. 080901-080901, 2019.
[2] W. Rawat et al., "Deep convolutional neural networks for image classification: A comprehensive review," Neural computation, vol. 29, no. 9, pp. 2352-2449, 2017.

30

Poster Session, Level 2 Foyer, September 4, 2025, 12:00 - 13:00

Fluorescent imaging on chip using a custom 3D printed bio-microfluidic device

Baldwin L[1], Jones E[2], Ngamnson B[1], Carding S[2], Bewley K[3], Coombes N[3], Norris C[3], Funnell S[2,3], France L[4], Green V[1], Greenman J[1]
[1]Centre of Biomedical Sciences, University Of Hull, [2]Gut Microbes and Health Division, Quadram Institute Biosciences (QIB), [3]UK Health Security Agency (UKHSA), [4]Department of Biomedical Engineering, University of Hull

While developing a microfluidic model for studying SARS-CoV-2, it was highlighted that the ability to monitor cells/tissue on chip during the experiment was difficult using commercially available equipment. We have modified our Perspex dual-flow microfluidic device to contain an optically transparent window and be fabricated by 3D printing in a biocompatible polymer allowing the device to be fully compatible with most microscopes for on-chip imaging whilst maintaining low cost and ease of use. The resin chips were printed using a Stratasys J750 using VeroWhiteTM. Central carrier dimensions (24mm x 10mm) were maintained from previous device designs as flow and shear stress had been shown to be optimal for cell/tissue maintenance. A co-culture of HBEC-5i (endothelial) cells and CACO2 (Epithelial) cells were seeded on inserts in a simple gut-chip model. Devices were perfused with culture medium at a rate of 4µL/min for 72h. At 48h a mix of Hoechst and Rhodamine conjugated concanavalin was perfused through the device, staining the cells. On chip images under flow conditions have successfully been taken at up to x40 magnification. Post-chip analysis showed high viability retained in all cell lines (>85%), with further imaging analysis showing maintenance of both cell monolayers within the device. Ongoing studies aim to optimise the device for use with high-resolution imaging microscopes such as the DeltaVision OMX Flex allowing viable tissue to be probed and analysed in depth in real-time.

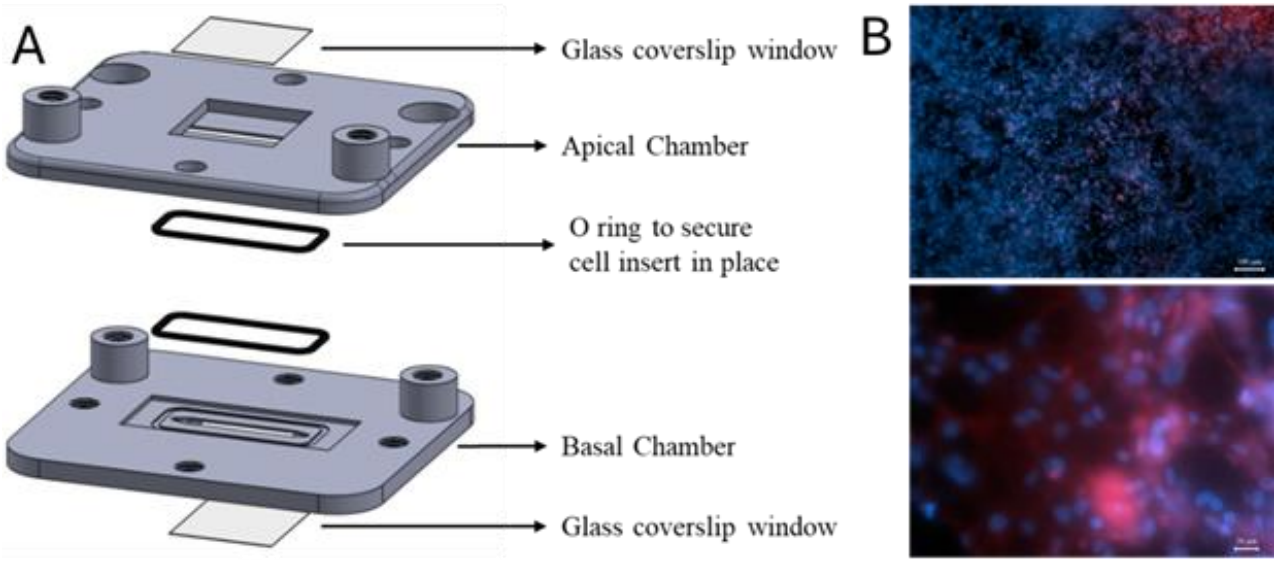

Figure 1: A) Schematic of 3D bioresin printed device B) images taken on chip at x10 and x40 magnification.

Poster Session, Level 2 Foyer, September 4, 2025, 12:00 - 13:00

Modelling Serotonin Dynamics in Human-Derived Neuronal Spheroids

Prieto Roca P[1], Bohl B[1], Hashemi P[1]
[1]Department of Bioengineering, Imperial College London

Depression is a widespread and increasingly prevalent mental health disorder characterised by prolonged periods of low mood and diminished capacity for pleasure [1]. The marked heterogeneity of depression coupled with the technical challenges of measuring the brain chemistry in vivo, has led to a lack of progress in the identification and validation of robust biomarkers, a critical barrier to accurate diagnosis and the development of targeted, personalised treatment strategies [2]. Sensors have shed enormous light on these issues. Specifically, using fast scan cyclic voltammetry at carbon fibre microelectrodes, our group has, in the past, demonstrated that serotonin is not only a principal target of antidepressant therapies [3] but also a reliable biomarker of depression phenotypes in mice [4]. Despite these advances, direct investigation of serotonin dynamics in the human brain remains out of reach due to its inaccessibility and the invasive nature of our measurement techniques. In this work, we create a novel sensing paradigm for serotonin measurements in human induced pluripotent stem cells differentiated into serotonergic neuron spheroids. We describe the sensing modality and characteristics and then experimentally and computationally model the dynamics of serotonin neurotransmission in these human derived cells. Our findings establish this new sensing model as a promising ex vivo platform for testing neuropsychopharmacological hypotheses and advancing translational models of depression.

[1] Q. Liu et al., 2020, J. Psychiatr. Res., vol. 126, pp. 134–140.
[2] J. Best et al., 2022, Serotonin and the CNS, IntechOpen.
[3] C.E. Witt et al., 2023, bioRxiv, doi:10.1101/2023.03.08.531698.
[4] M. Hersey et al., 2022, J. Neuroinflamm., vol. 19, 167.

34

Poster Session, Level 2 Foyer, September 4, 2025, 12:00 - 13:00

In-house perfluorocarbon gas core microbubbles fabrication for Nanodroplet Development in Theranostics application

Supteranon P[1], Mulvana H[1], Prentice P[1]
[1]University Of Glasgow

Microbubbles (MBs) are gas-filled contrast agents widely used to enhance ultrasound imaging, with the potential to be converted into phase-change nanodroplets (NDs) by condensing the perfluorocarbon gas core into a liquid state [1]. The objective was to evaluate the feasibility of generating stable and reproducible MBs suitable for condensation into NDs. This study presents a comparative in-house fabrication of MBs with perfluorobutane (PFB), octafluoropropane (OFP), and air cores. Lipid mixture preparation included polyethylene glycol (PEG-40-Stearate), 1,2-Distearoyl-sn-Glycero-3-Phosphocholine (DSPC), and 1,2-Distearoyl-sn-Glycero-3-Phosphoethanolamine (DSPE), all purchased from Avanti Polar Lipids. MBs were prepared via probe sonication (VXC750, 2 mm probe) at 25% amplitude, 10 seconds, followed by mechanical agitation (Vialmix®), 45 seconds. The mixture was then centrifuged at 3000 rpm, 3 minutes. The supernatant was collected and diluted (1:10) for characterization, including size distribution and concentration profiling using optical microscopy and analyzing the results via MATLAB program, confirming the successful formation of MBs and stability over 14 days. In Figure 1, the in-house fabricated MBs using OFP and PFB gases exhibit size distributions suitable for ultrasound contrast applications. OFP-MBs demonstrated a narrower and more monodisperse size profile (mean diameter = 2.15 ± 0.54 µm) compared to the broader and slightly larger distribution of PFB-MBs (mean diameter = 2.54 ± 0.95 µm). This suggests that OFP-MBs may offer greater consistency and stability. The histogram also shows a steeper drop-off in larger diameters for OFP-MBs, indicating less polydispersity. The results demonstrate the feasibility of cost-effective, small-scale MB production and highlight the potential of MB-to-ND systems.

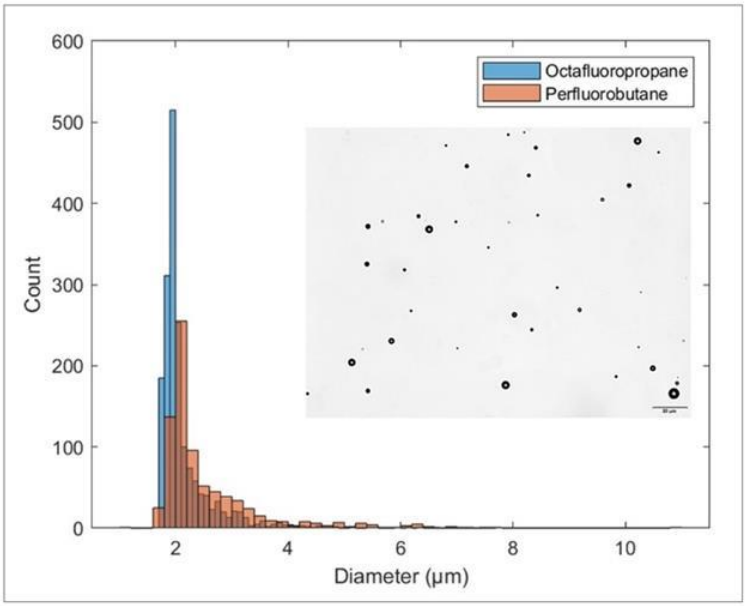

Figure 1: Size distribution of microbubbles. OFP-MB (mean diameter 2.148 ± 0.54 µm), PFB-MB (mean diameter 2.536 ± 0.95)

[1] P.S. Sheeran et al., 2017, More Than Bubbles: Creating Phase-Shift Droplets from Commercially Available Ultrasound Contrast Agents, Ultras Med Biol vol. 43(2), pp. 531-540.

36

Poster Session, Level 2 Foyer, September 4, 2025, 12:00 - 13:00

Conductive Scaffolding for Neural Tissue regeneration: 3D Bridging with Two-Photon Fabrication

Osipov V[1], Jawed A[1], Lutsyk P[1], Webb D[1], Fratini A[1]
[1]Aston University

This project aimed to develop a partially conductive microscale scaffold for use in brain tissue engineering, fabricated via two-photon polymerisation (2PP) using a PEGDA-based hydrogel infused with gold nanoparticles (AuNPs). The objective was to demonstrate whether such a scaffold could restore electrical continuity across a disrupted conductive substrate.
Gold-coated glass slides (18mm x 18mm) were prepared using physical vapour deposition and manually incised with a scalpel to simulate an interrupted conductive path. A composite solution of PEGDA, 20 nm AuNPs, and LAP photo initiator was printed directly across the incision using a 520 nm femtosecond laser at varying power levels. A custom scaffold design was developed and optimised to improve adhesion and structural integrity. Resistance measurements were taken before scratching, after the conductive path was disrupted, and following scaffold fabrication. Pre-scratch values ranged from 0-345 Ω; post-scratch, electrical conductivity was successfully interrupted, indicating a complete break in the current pathway, which was validated through subsequent electrical measurements. After scaffold printing, resistance was restored in two samples, with values ranging from 1.3 Ω to 100 Ω, confirming that the scaffold enabled electrical conduction across the gap.
This work demonstrates the successful fabrication of a PEGDA-AuNP conductive scaffold using 2PP and its ability to bridge a physical and electrical discontinuity. These findings offer proof of concept that conductive hydrogel scaffolds can be engineered at the microscale for electrical functionality, supporting further exploration of their role in neural regeneration.

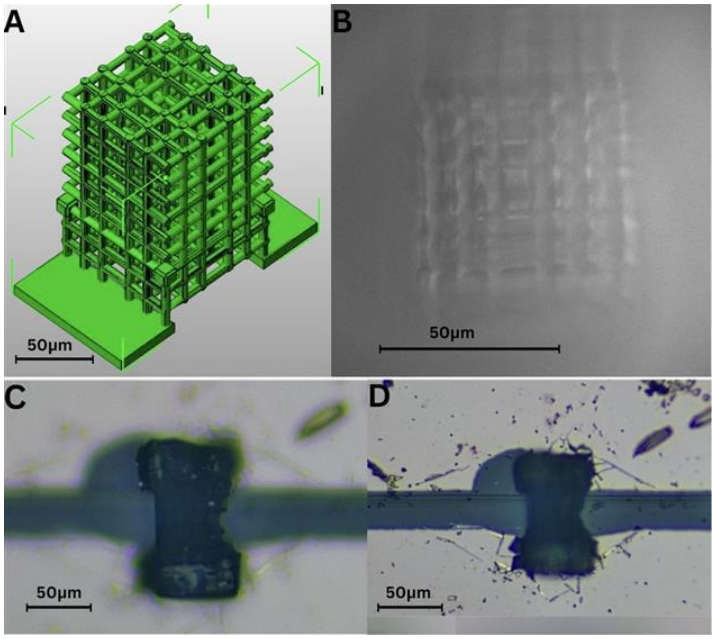

A-3D model. B-image by 2PP setup camera. C, D-photos of scaffold bridging scratched gold coated substrate at two focal depths.

38

Poster Session, Level 2 Foyer, September 4, 2025, 12:00 - 13:00

Insights of Seismocardiography in 3D Visualisation and Measurement of Physiological Characteristics

Peng F[1], Greenwald S[2], Song W[3], Tse Z[1]
[1]the School of Engineering and Materials Science, Queen Mary University of London, [2]the Blizard Institute at Barts and the London School of Medicine and Dentistry, Queen Mary University of London, [3]the School of Electrical and Computer Engineering, University of Georgia

Seismocardiography (SCG), a technique that captures the mechanical vibrations of the chest induced by cardiac activity, is gradually being applied to monitor cardiac conditions. However, physiological relevance and biomechanical origins of some SCG waveform patterns still remain unclear. In this study, we introduced a three-dimensional SCG representation to reconstruct and analyses spatial heart trajectories, using electrocardiography (ECG) as the groundtruth. Data were collected form eight healthy subjects under resting conditions (seven males and one female with mean age of 28 years, with no history of cardiovascular disease) by Raspberry Shake 3D (a 3-axis seismic sensor) and SEN0213 (a 3-lead cardiac electrical activity sensor). For the trajectory of each cardiac cycle, representative points were selected and their spatial features (Snap, Acceleration Vector Rotation Rate, Gradient, and Centre Offset Vector) were computed for further cluster analysis, and the performance was evaluated using the Silhouette Score and Calinski-Harabasz Index. Results show that a four-cluster solution was optimal for grouping representative points. Specifically, Cluster 1 is mainly located in the filling phase and rapid ejection phase. The locations of Cluster 2 primarily correspond to the atrial systole, along with the locations after the rapid filling phase. Cluster 3 primarily represents the interval between the closure of mitral valve and the opening of aortic valve, while Cluster 4 is mainly found between the closure of aortic valve and the opening of mitral valve. This indicates that the heart may follow similar patterns of movement throughout the various phases of the cardiac cycle.

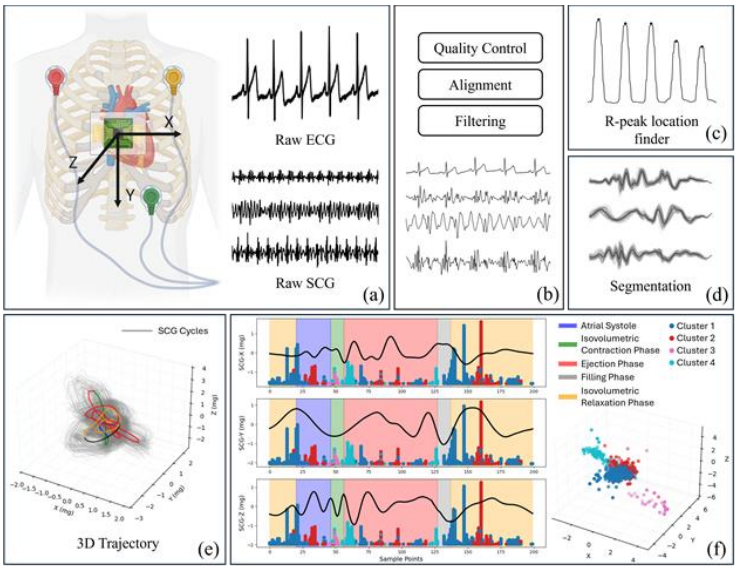

Sensor configuration and SCG signal processing workflow, including reconstructed 3D SCG trajectory, distribution of the selected points and clustering result.

Poster Session, Level 2 Foyer, September 4, 2025, 12:00 - 13:00

Concentration Polarisation in Nanofiltration of Aqueous Sucrose Solutions: a CFD approach

Puigdefabregas Nogueras A[1], Papaioannou E[2], Kazakidi A[1]
[1]University Of Strathclyde, [2]Lancaster University

Filtration of organic molecules from aqueous solutions is extensively utilised in food processing, water treatment and pharmaceutical industries [1], where efficient separation methods are critical. Pressure-driven nanofiltration (NF) processes face concentration polarisation (CP) challenges, where solute accumulation increases osmotic pressure and reduces permeate flux. The appropriate tuning of TMP and crossflow velocity (CFV) can mitigate flux decline by reducing solute back-transport. This study develops and validates a computational fluid dynamics (CFD) model to simulate concentration polarisation during nanofiltration of sucrose solutions. Experiments used a commercial polyamide-based NF membrane (NF270) in crossflow configuration at 30±2°C, with 1% w/v sucrose solution, flow rates of 500-1500ml/min and transmembrane pressures of 2-7 bar. A two-dimensional steady flow CFD model was developed using COMSOL Multiphysics, with the membrane modelled using the Brinkman equations for porous media flow. Experimental fluxes for sucrose solutions increased linearly with transmembrane pressure and were accurately predicted by the CFD model with a maximum absolute error <4%. Our model was also compared against literature data from Geraldes et al. [2], the model showed improved accuracy with a maximum error of 9.5% at high crossflow velocities, though it may not fully quantify crossflow velocity effects on concentration polarisation. The simulations demonstrated good agreement with experimental results across all tested pressures, validating the model's capability to predict flux decline due to concentration polarisation near pressure-driven flat-sheet membranes. These results contribute significantly to understanding nanofiltration processes and mass transfer mechanisms in biological systems, offering a valuable predictive tool for membrane process optimisation.

[1] Luo et al., 2018. Food and Bioprocess Technology, Vol. 11, no. 5, pp. 913–925.
[2] Geraldes et al., 2001. Journal of Membrane Science, Vol. 191, no. 1-2, pp. 109-128

42

Poster Session, Level 2 Foyer, September 4, 2025, 12:00 - 13:00

Interfacing mechanotransduction-related events in glioblastoma pathophysiology

Fowler D[1], Schulte C[1]
[1]University Of Strathclyde

The invariably lethal brain tumour, glioblastoma, exhibits well-characterised molecular and biochemical heterogeneity. Yet, glioblastoma patient prognosis remains dismal following canonical therapeutic combinations of radiotherapy and the first line chemotherapy temozolomide, reinforcing the unmet clinical need for novel druggable targets to improve patient survival. It is well established that cells sense and respond to mechanical/physical cues in their microenvironment through mechanosensing/transduction, a force-based signalling pathway that drives proteomic and phenotypic change, which might represent an additional driver of glioblastoma cell therapeutic resistance, potentially through an integrin/glycocalyx positive feedback loop [1].

Our research aims to combine bioinformatics and bioengineering techniques to identify mechanotransduction-related drivers of glioblastoma and fabricate substrates that recapitulate the largely overlooked (nano)topographical features of the altered glioblastoma-related ECM, respectively.

To dissect how mechanotransduction and integrin adhesion complex-related events are affected by glioblastoma cell/(nano)topography interaction and therapeutic treatments, we employ a combination of microscopy techniques, including, e.g., Brillouin and structured illumination. These interdisciplinary approaches allow us to interrogate changes at the cell/substrate interface and the underlying mechanotransductive-related responses and their contribution to glioblastoma pathophysiology and development of resistance to canonical therapeutic treatments.

1. Barnes JM, Kaushik S, Bainer RO, Sa JK, Woods EC, Kai F, Przybyla L, Lee M, Lee HW, Tung JC, Maller O, Barrett AS, Lu KV, Lakins JN, Hansen KC, Obernier K, Alvarez-Buylla A, Bergers G, Phillips JJ, Nam DH, Bertozzi CR, Weaver VM. A tension-mediated glycocalyx-integrin feedback loop promotes mesenchymal-like glioblastoma. Nat Cell Biol. 2018 Oct;20(10):1203-1214.

44

Poster Session, Level 2 Foyer, September 4, 2025, 12:00 - 13:00

Automated segmentation of the renal artery for digital twin assisted surgery (DTAS)

Kandangwa P[1], Kyeremeh J[1], Stewart G[2,3], Shu W[1], Kazakidi A[1]
[1]University Of Strathclyde, [2]Cambridge University Hospitals NHS Foundation Trust, [3]University of Cambridge

Radical and partial nephrectomies are essential treatments for kidney tumours but are frequently complicated by significant blood loss due to the complex and highly branched renal vasculature [1]. Minimising vascular damage and maximising resection techniques during surgery depend on precise renal artery identification and localisation. In this study, we use 3D slicer and its relevant plug ins for automatic segmentation which enables precise visualization and identification of renal artery branches. The segmentation pipeline provides comprehensive visualization of both the renal vasculature and the major abdominal organs adjacent to the kidney, while also allowing assessment of patient-specific variations in vascular complexity. By providing anatomical clarity, this framework alongside other techniques has the potential to support preoperative planning and real-time surgical decision-making.

[1] H.A. Hassouna et al., 2012, Indian J. Urol, 28, 3-8.

Poster Session, Level 2 Foyer, September 4, 2025, 12:00 - 13:00

Laser Induced Graphene (LIG) Electrodes for detection of Cryptosporidium parvum

Aziz A[1], Corrigan D[1], Mani V[1], Bartley P[2], Katzer F[2]
[1]University Of Strathclyde, [2]Moredun Research Institute

Cryptosporidium parvum is an intracellular protozoan parasite responsible for causing diarrheal illness in mammals, including humans. The main source of infection is through the ingestion of oocysts from faecal contaminated food and water. Among all Cryptosporidium species, C. parvum is potentially the most important to detect as it is zoonotic. Each year over 4000 human cryptosporidiosis cases are reported by labs in the UK. In immunocompromised people, young children, and young calves infections can persist for a longer period and can sometimes prove to be fatal [1]. With limited treatment available, early detection seems the best option to limit the occurrence of the disease in the first place. Current detection methods rely on polymerase amplification reactions (PCR), microscopy, and enzyme linked immunoassay (ELISA) [2]. These techniques despite being gold standard, are expensive, non-portable, time consuming, and require a trained operator. My research work focuses on providing a solution to these problems, by developing a point-of-care diagnostic tool. Electrochemical detection techniques are sensitive, cheap and less time consuming therefore they are a popular choice for monitoring of water borne parasites. This work combines molecular amplification techniques along with electrochemical detection. The principle is based on development of a gold-modified graphene electrode, screening of an ideal primer pair for isothermal recombinase polymerase amplification (RPA) of C. parvum, and immobilization of the primer onto the surface of electrode. Successful completion of these steps will provide a fast, easy single platform approach for the amplification and detection for the C. parvum.

Figure.1 LIG electrode design and printed version

1. Rawlins, M., 2024, Animal and Plant Health Agency: APHA Science Blog.
2. Bartley et al., 2024, Curr Res Parasitol Vector Borne Dis, 5: p. 100160.

48

Poster Session, Level 2 Foyer, September 4, 2025, 12:00 - 13:00

Accessible and Low-Cost Fabrication of High-Performance Electrochemical Microfluidic Gold Sensors Using Consumer-Grade Equipment

Gordon A[1], Corrigan D[1], Jimenez M[1]
[1]University Of Strathclyde

The development of microfluidic sensors is critical for applications in healthcare, environmental monitoring, and chemical analysis [1]. High-performance electrochemical biosensors are particularly popular in point-of-care testing due to their wide range of use, small size, low costs, and high production volume [2]. However, traditional fabrication methods rely on expensive cleanroom-based processes, hindering accessibility and scalability, while industry-contracted production can be limited to expensive large-scale runs. This study presents a low-cost, rapid, and accessible in-house approach for fabricating electrochemical microfluidic platforms using consumer-grade laser cutters. For sample processing, off-the-shelf laser systems (Snapmaker 2.0 A350T modular laser cutter) and microfluidic diagnostic tape (9969 and 9984 films, Solventum) were used to develop a microfluidic channel (Figure 1A). Sensing is then combined using laser ablation of gold-sputtered polyester (TaiDoc Technology Corporation). The developed sensors exhibited industry-competitive performance in terms of electrochemical sensitivity and reproducibility in a conductive solution (with in-house showing differential pulse voltammetry peak CoV of 5.9% versus 4.4% in commercial; Figure 1B).
The proposed approach significantly reduces manufacturing costs and improves ease of prototyping, as well as a high performing alternative to traditional lithographic or screen-printed methods. By democratizing access to sensor manufacturing, this work paves the way for broader adoption and adaptation of electrochemical sensors and microfluidic systems in research, as well as laying the foundation for translation into commercial products in resource-limited settings where conventional microfabrication tools are unavailable.

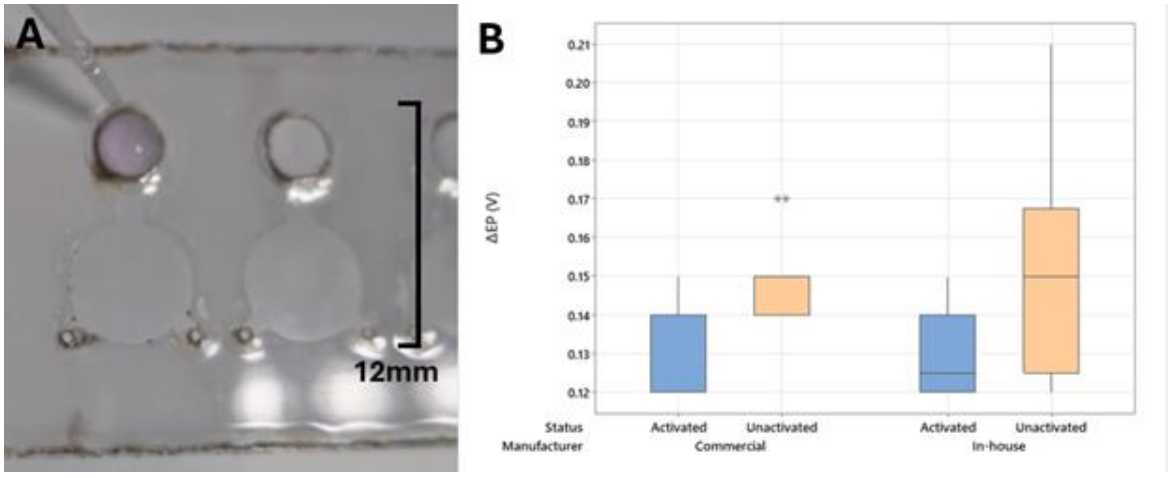

A) Microfluidic sample system using laser-cut film and tape B) Peaks of DPV of commercial versus in-house electrodes using ferriferrocyanide.

[1] N. Nesakumar et al., 2019, J. Anal. Test, 3, pp. 3–18
[2] U. Zupancic et al., 2021, Modern Techniques in Biosensors, pp. 63-93

Poster Session, Level 2 Foyer, September 4, 2025, 12:00 - 13:00

Application of gold-ablated electrochemical biosensor in diagnostics: a low-cost alternative for influenza detection

Lawson N[1], Gordon A[1], Mani V[1], O'Sullivan D[2], Corrigan D[1]
[1]University Of Strathclyde, [2]National Measurement Laboratory at the Laboratory of the Government Chemist

Avian influenza (AI) is a devastating threat to domestic poultry and wild bird populations. A single positive case results in complete slaughter of domestic flocks causing severe economic losses globally, while the opportunity for spillover of mutated and unseen strains into wildlife that lack prior immunity poses major conservation concerns [1]. Furthermore, the pathogen's plasticity and adaptability has been highlighted through its zoonotic capacity, raising concerns about future pandemics. Diagnostics present an opportunity for intervention given their effectiveness during the recent SARS-COV-2 outbreak, however traditional detection methods for AI have relied on molecular based procedures such as polymerase-chain-reaction (PCR) requiring expensive equipment and trained specialists for effective implementation [2]. Electrochemical biosensors (EB) have demonstrated their ability to combine the sensitivity of PCR with the ease-of-use and cost-effectiveness of a lateral flow [2], though the applications of in-house fabricated gold-ablated EB's specifically remains relatively unexplored compared to other methods [3]. This work demonstrates the capabilities of gold-ablated EB's in pathogen diagnostics by detecting AI and evaluating sensor performance against traditional PCR methodologies. Thiolated flu-primer sequences were immobilised on a gold-ablated electrode surface to form a self-assembled monolayer. Synthetic complementary sequences were applied to the sensor and its performance assessed by Electrochemical Impedance Spectroscopy (EIS) compared to conventional PCR gel results to highlight equivalence. This work illustrates how low-cost, in-house produced EB's comparable to commercially available systems can be achieved and utilised for pathogen diagnostics.

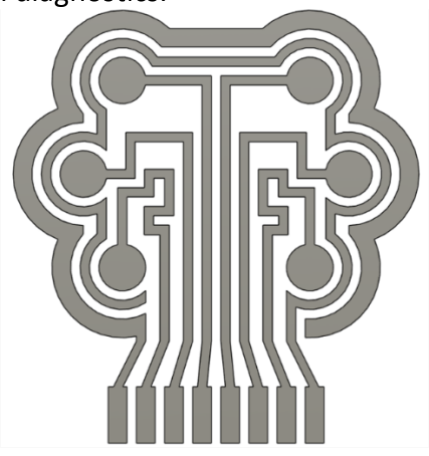

Proposed gold-ablated electrode array layout for the multiplexed detection of avian influenza

[1] A. Blagodatski, et al., 2021, Pathogens, vol. 10(5), pp. 630.
[2] P. Lasserre, B. et al., 2022, Anal Chem, vol. 94(4), pp. 2126 - 2133
[3] M. Govedarica, et al., 2025, Micromachines (Basel), vol. 16(3), pp 343

52

Poster Session, Level 2 Foyer, September 4, 2025, 12:00 - 13:00

The anti-fouling properties of electrode coatings for real-time serotonin detection using FSCV

Murphy M[1], Hashemi P[1]
[1]Imperial College London

Fast-scan cyclic voltammetry (FSCV) offers high temporal resolution and sensitivity for the detection of electroactive neurotransmitters such as serotonin. However, application in biologically relevant environments can be limited by biofouling, which arises from the non-specific adsorption of proteins, lipids, and charged macromolecules onto the electrode surface. This reduces electrochemical sensitivity and alters surface chemistry, leading to signal degradation over time.

To address this, we explore the use of lubricin - a mucin-like glycoprotein with well-characterized anti-fouling properties - as a surface modification for carbon-fibre microelectrodes. The amphiphilic structure of lubricin, consisting of a highly glycosylated central domain flanked by globular terminal regions, creates a steric and electrostatic barrier that inhibits protein and small molecule adsorption. The dense glycosylation exhibits a net negative charge, repelling similarly charged fouling agents including bovine serum albumin (BSA), media-derived supplements, and other electroactive interferents commonly encountered in biological systems.

In this study, we systematically assess the anti-fouling efficacy of lubricin-coated electrodes during FSCV-based serotonin detection across three in vitro systems of increasing biological complexity: a standard flow cell, monolayer neuronal cultures, and 3D brain spheroids. Electrodes will be challenged with fouling molecules commonly detected in blood and tissue to evaluate stability, sensitivity, and reusability of the lubricin layer under physiologically relevant conditions.

This work addresses a critical gap in the development of long-lasting and accurate neurotransmitter biosensors. Demonstrating the effectiveness of lubricin in this context paves the way for studies in more dynamic and translational systems, ensuring reliability of future findings and ultimately greater reproducibility.

54

Poster Session, Level 2 Foyer, September 4, 2025, 12:00 - 13:00

Development of a Cross-Reactive Nanophotonic Biosensor for Fluid “Fingerprinting” and Label-Free Disease Detection

Shadman S[1], McGleish O[1], Peveler W[1], Clark A[1]
[1]University Of Glasgow

Though cross-reactive sensing is a growing field with applications in water quality monitoring and beverage profiling, its use in disease diagnostics remains limited. While this approach has been applied in gas biosensing, there is a clear gap in non-targeted, cross-reactive detection of disease biomarkers in liquid samples, where a holistic biosensor generating unique chemical fingerprints could support early detection of known and unknown markers. Nanophotonic structures, intrinsically sensitive to changes in refractive index (RI), can be fabricated as sensor arrays and modified with various non-binding surface chemistries, enabling segregation of complex mixtures at the nanoscale interface. This produces characteristic optical response patterns.

Here, we present a nanophotonic biosensor which utilises silicon nanopillar arrays as its resonant sensory elements. Compared to our recent work on cross-reactive sensor arrays based on gold nanostructures, Si offers potential advantages in mechanical durability, reusability and compatibility with CMOS processes. Initial optical characterisation confirmed distinct spectral responses to varying liquid environments. Future work will assess the stability of silane-functionalised Si under acidic conditions, where gold–thiol systems typically degrade. Surface functionalisation will utilise silane molecules with orthogonal functional groups, enabling selective and cross-reactive analyte binding, producing a unique pattern of responses across the different elements of the sensory array. We aim to distinguish subtle biochemical variations in biofluids and correlate these with disease states. If successful, this platform may provide an accessible, scalable alternative to chromatographic methods for early-stage disease diagnosis.

Poster Session, Level 2 Foyer, September 4, 2025, 12:00 - 13:00

Acoustic response of individual optically trapped lipid-shelled microbubbles to pulsed ultrasound

Campbell P[1], Josey J[1], Conneely M[2]
[1]Carnegie Physics Laboratory, University of Dundee, [2]Ten Bio Ltd, James Hutton Institute

The acoustic response of lipid-shelled microbubbles is of direct importance to clinicians and medical physicists alike, especially in assessing the performance of a dispersed bolus during therapeutic or diagnostic insonation protocols. The non-linear radial response of microbubbles to pressure change, together with their facility for 'cross-talk' via secondary Bjerknes forces when multiple microbubbles are present serves to complicate the bubble ensemble's dynamics. Moreover, interpretation of the overall acoustic emission response has the additional complication that any well-defined incident [ultrasound] beam will also be scattered by the insonated microbubbles. Reliable and robust acoustic measurements are thus needed to characterise microbubble behaviour. Initial attempts to undertake such a characterisation on an individual bubble basis have met with considerable success [1] however, with some constraints on the system architecture. For the present experiments, we have extended our previous protocol using optical trapping to place individual microbubbles at well-defined displacements from targets [2], ensuring that each bubble is acoustically isolated from any nearest neighbours, and thus that any acoustic emissions arising from a pulsed ultrasonic stimulus can be characterised with optimal integrity. To that end we used a [NPL-calibrated] fibre-optic hydrophone to sense the cavitation noise response of individual commercial lipid-shelled ultrasound contrast agent microbubbles (SonoVue) that were optically tweezed to distinct displacements from the hydrophone plane. We report on the acoustic signatures arising as a function of both microbubble diameter and their respective displacement to the hydrophone.

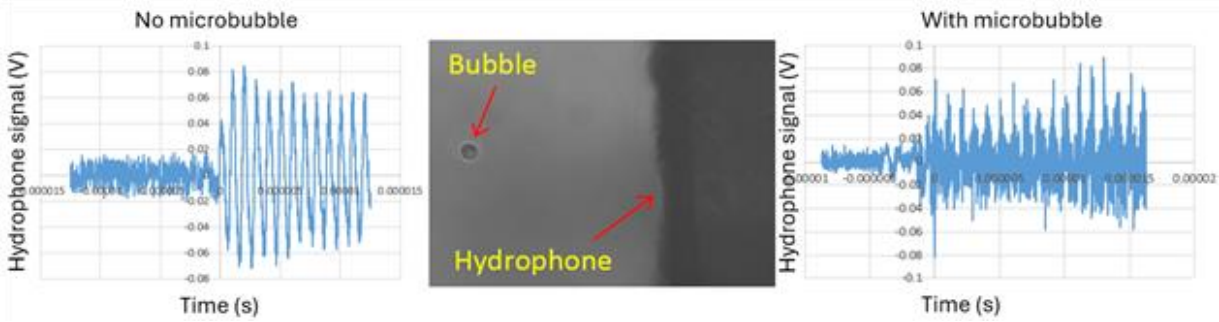

Measured hydrophone response to sinusoidal 1MHz ultrasound (no microbubbles). Photomicrograph: microbubble trapped at hydrophone. Acoustic response with trapped microbubble.

[1] Absolute measurement of ultrasonic backscatter from single microbubbles
Vassilis Sboros et al.
Ultrasound in Medicine and Biology, V31, No 8, pp 1063-1072 (2005)
[2] Membrane disruption by optically controlled microbubble cavitation
Paul Prentice, Alfred Cuschieri, Kishan Dholakia, Mark Prausnitz & Paul Campbell
Nature Physics, V1, pp107–110 (2005)

Poster Session, Level 2 Foyer, September 4, 2025, 12:00 - 13:00

Fluctuation Dynamics of Quiescent Optically Trapped Lipid-Shelled Microbubbles

Campbell P[1], Comanici R[1], Prentice P[2], Conneely M[3]
[1]Carnegie Physics Laboratory, University of Dundee, [2]School of Engineering, University of Glasgow, [3]Ten Bio Ltd, James Hutton Institute

Lipid-shelled microbubbles have theranostic potential, serving both as contrast agents in ultrasound diagnostic imaging, and as vectors for targeted drug delivery. Such applications rely on ultrasonic stimulus to drive the microbubbles' cavitation response, a regime in which a wealth of high-quality observational data exists, as well as refined physical models based on the Rayleigh-Plesset equation. In contrast, the behaviour of quiescent microbubbles in bulk fluids has received much less attention, particularly on microsecond timescales where thermally driven fluctuations might be expected to dominate. For the present experiments, we extended our earlier approach using optical trapping with high-speed imaging [1] to exercise independent spatial control over multiple commercially available microbubbles (Sonovue). A machine-learning algorithm was applied to the observational data to extract accurately calibrated radial data in an automated fashion. Radial fluctuations were observed over periods typically of 15µs duration at sub-micrometer spatial resolution and exhibited peak-to-peak amplitudes of circa 10% of the average radius whilst showing statistically significant correlation between the trapped microbubbles over a range of initial displacements. We propose that convective gradients in the ambient fluid lead to local temperature inhomogeneities that likely drive thermal capillary waves in the microbubbles' lipid shells. The role of local heating from the laser trapping environment was also considered, with initial calculations indicating that this source contribution plays a much less significant role than the presence of longer-range bulk convection in the ambient fluid. Our results also suggest a novel pathway towards non-contact probing of local thermal gradients using microbubbles as sensors.

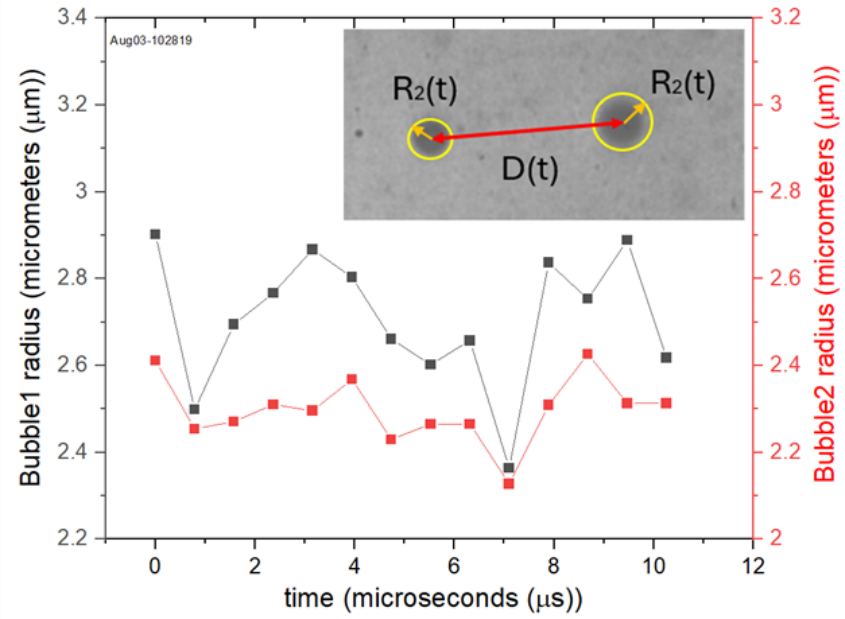

Temporal radial fluctuation of two optically trapped microbubbles as shown on inset, with parameters assessed by the machine learning algorithm.

[1] Paul Prentice, Alfred Cuschieri, Kishan Dholakia, Mark Prausnitz & Paul Campbell.
Membrane disruption by optically controlled microbubble cavitation
Nature Physics V1, pages107–110 (2005)

60

Poster Session, Level 2 Foyer, September 4, 2025, 12:00 - 13:00

Comparative Analysis of Maleimide and NHS-Ester JQ1-Trastuzumab Conjugates using Orthogonal Analytics

Jolliffe S[1], Armstrong G[1], Taladriz Sender A[1], Burley G[1], Jamieson C[1], Rattray Z[1]
[1]University Of Strathclyde

Antibody-drug conjugates (ADCs) are targeted biopharmaceuticals composed of a monoclonal antibody (mAb) covalently linked to a cytotoxic payload, designed to selectively deliver potent drugs to diseased cells while minimising systemic toxicity.[1] Currently, 13 ADCs are approved for clinical use, with over 100 in development indicating the rapid evolution of this field which is lead by advancements in linker chemistry, payload design, and target selection.[2] These structural components, alongside the inherent properties of the antibody, critically influence the physicochemical stability and overall performance of the ADC. Key Critical Quality Attributes (CQAs), such as drug-to-antibody ratio (DAR), aggregation state, and the presence of free linker-payload, serve as indicators of stability, with downstream consequences on therapeutic efficacy and safety.[1]

In this study, we explored the impact of linker chemistry on ADC properties by conjugating the bromodomain inhibitor JQ1 to the HER2-targeting monoclonal antibody Trastuzumab, using both maleimide and NHS-ester-based stochastic conjugation strategies. The resulting ADCs were characterised by Hydrophobic Interaction Chromatography (HIC) to assess DAR and relative hydrophobicity, Analytical Size Exclusion Chromatography (aSEC) to evaluate aggregation, and Reversed-Phase Mass Spectrometry (RPMS) for detailed mass analysis. By comparing the conjugation outcomes, we aimed to investigate how different linker types influence drug loading, conjugate heterogeneity, and overall biophysical profile, providing insight into the design considerations required for stable and efficacious ADCs.

[1]McCombs, J. R.; Owen, S. C. Antibody Drug Conjugates: Design and Selection of Linker, Payload and Conjugation Chemistry. AAPS J. 2015, 17 (2), 339–351. https://doi.org/10.1208/s12248-014-9710-8.
[2]Bargh, J. D.; Isidro-Llobet, A.; Parker, J. S.; Spring, D. R. Cleavable Linkers in Antibody–Drug Conjugates. Chem. Soc. Rev. 2019, 48 (16), 4361–4374. https://doi.org/10.1039/C8CS00676H.

62

Poster Session, Level 2 Foyer, September 4, 2025, 12:00 - 13:00

Reducing MRI Artefact Susceptibility Using Additively Manufactured Porous Titanium Implants.

El-Dessouky F[1]
[1]University Of Birmingham

Titanium implants, though MRI-safe, can degrade image quality by producing susceptibility artefacts that obscure critical anatomical structures. These artefacts are particularly problematic near fixation points, where they can mask post-operative complications such as microbleeds or infections. Ti-6Al-4V (Ti64) is commonly used in medical implants due to its strength to weight ratio, biocompatibility, corrosion resistance and low infection rates. However, its weak paramagnetic nature contributes to these MRI artefacts, which are worsened at increased magnetic field strengths and sensitive sequences, such as, fast gradient echo, now commonly used in modern MRI systems. Advances in additive manufacturing enable highly precise fabrication of complex lattice-structured Ti64 implants. These structures are engineered to significantly reduce implant mass, lowering the effective magnetic permeability, offering a novel strategy to mitigate MRI induced artefacts through design optimisation rather than MRI sequence modification. An artifact prediction tool was developed to simulate static magnetic field distortions and generate artificial MRI slices, by incorporating MRI threshold and skewing parameters. This allows for early-stage visualisation and evaluation of artefact patterns for different implant designs. Preliminary results (Figure 1) demonstrate a reduction in artefact volume as magnetic permeability decreases. Where a magnetic permeability of 1 represents a fully permeable medium, Magnetic permeability of 1.0005 (100%) and 1.0000005 (1%) have artefacts with the sizes 14,611mm3 and 157mm3, respectively. This approach supports the development of implants that are both mechanically robust and more MRI-compatible, enhancing surgical planning, postoperative monitoring, and overall patient outcomes.

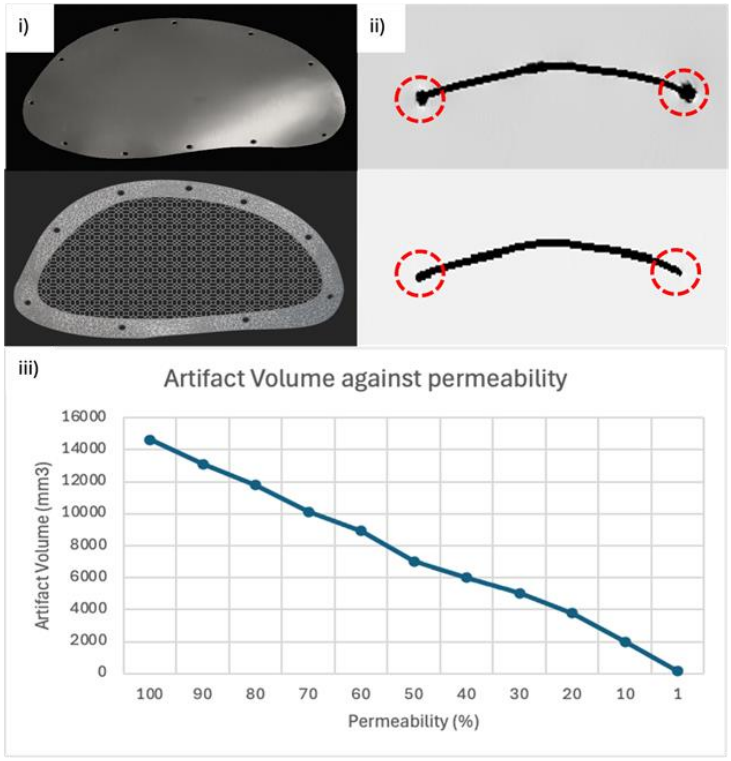

i) Cranial plate designs. ii) Artificial MRI slice capturing artefacts using MATLAB. iii) Plot comparing artefact volume against magnetic permeability.

64

Poster Session, Level 2 Foyer, September 4, 2025, 12:00 - 13:00

Investigation of Human Plasma Protein Tolerance to 405 nm Light Pathogen Reduction Treatment

Griffin D[1,2], Blore S[2], MacGregor S[1], Anderson J[1], Atreya C[3], Maclean M[1,2]
[1]The Robertson Trust Laboratory for Electronic Sterilisation Technologies (ROLEST), University of Strathclyde, [2]Department of Biomedical Engineering, University of Strathclyde, [3]Office of Blood Research and Review, Center for Biologics Evaluation and Research (CBER), Food and Drug Administration

The presence of pathogenic contaminants in blood transfusion products can pose a risk to recipients' health. Pathogen-reduction technologies (PRTs) proactively mitigate this risk by reducing or inactivating the pathogen burden in the product, however, current commercially-available PRTs require the addition of photosensitizing chemicals, proprietary irradiation bags and/or employ potentially harmful ultraviolet wavelengths. Violet-blue 405-nm light in the visible spectrum offers a safer, non-ultraviolet light-based alternative, facilitating in situ treatment of pre-bagged products without need for chemical photosensitizers. Its broad-spectrum efficacy for pathogen reduction of platelets and plasma has been demonstrated against bacteria, viruses, yeast and parasites, with antimicrobial treatments being achieved at doses compatible with the blood products themselves [1,2,3]. For practical deployment, it is important to understand the upper treatment threshold, beyond which significant changes are induced in plasma proteins. To investigate this, pre-bagged human plasma (100 mL) was treated with increasing 405-nm light doses up to 4.15 kJ/cm², applied over 72-h. Plasma samples (n=3) were removed at defined dose intervals between 58 J/cm² and 4.15 kJ/cm², and analysed using SDS-PAGE, Advanced Oxidation Protein Products assay, and Fibrinogen ELISA to evaluate plasma protein integrity upon increasing treatment doses. Results indicate no significant changes in levels of AOPP (indicative of oxidative stress) or fibrinogen concentration to at least 2.8 kJ/cm² ($p>0.05$): >50 times the dose required to achieve significant antimicrobial efficacy. These results help identify a compatible upper-treatment threshold range for 405-nm light-based PRT in pre-bagged plasma, however, further work is required for in-depth analysis of protein functionality.

[1] C.F. Stewart et al., 2024, AMB Expr, 14, 66.
[2] C.F. Stewart et al., 2022, Photochem Photobiol, 98, 504-512.
[3] J.W. Jackson et al., 2024, Sci Rep, 14, 31540.

66

Poster Session, Level 2 Foyer, September 4, 2025, 12:00 - 13:00

A Simulator for Testing CPR Devices

Ning L[1], Li X[1], Tse Z[1]
[1]Queen Mary University Of London

Cardiac arrest (CA) remains a critical global health challenge, with survival rates stagnating around 8-10% despite medical advancements. Effective cardiopulmonary resuscitation (CPR) is vital for maintaining circulation, yet achieving optimal compression depth, rate, and force is challenging. To address this, we developed a novel CPR simulator for testing mechanical and automated CPR devices. The simulator features a modular design with an inflatable heart model (compliance: 1.5–2.0 mL/mmHg) and adjustable chest stiffness (3–8 kN/m), replicating physiological deformation and hemodynamic responses. Real-time sensors monitor compression depth (4–6 cm), force (30–60 kg), and intrathoracic pressure (−4 to +12 mmHg), while a pneumatic system simulates blood flow (1.2–3.5 L/min).
Experimental results demonstrated clinically relevant performance, with stroke volumes of 22–42 mL per cycle and coronary perfusion pressure (CPP) exceeding 15 mmHg, correlating with improved survival outcomes. The simulator's heart models (3D-printed and commercial) exhibited diastole/systole ratios (1.20 and 1.11, respectively) comparable to human hearts (1.13), validating anatomical fidelity. MRI-based analysis confirmed consistent compression mechanics and intrathoracic pressure dynamics.
This system provides a repeatable, controlled environment for evaluating CPR devices, bridging gaps between bench testing and clinical applications. Future work will focus on enhancing compliance variability and incorporating patient-specific features. The simulator represents a significant advancement in CPR device optimization, offering a robust platform for improving resuscitation technologies and outcomes.

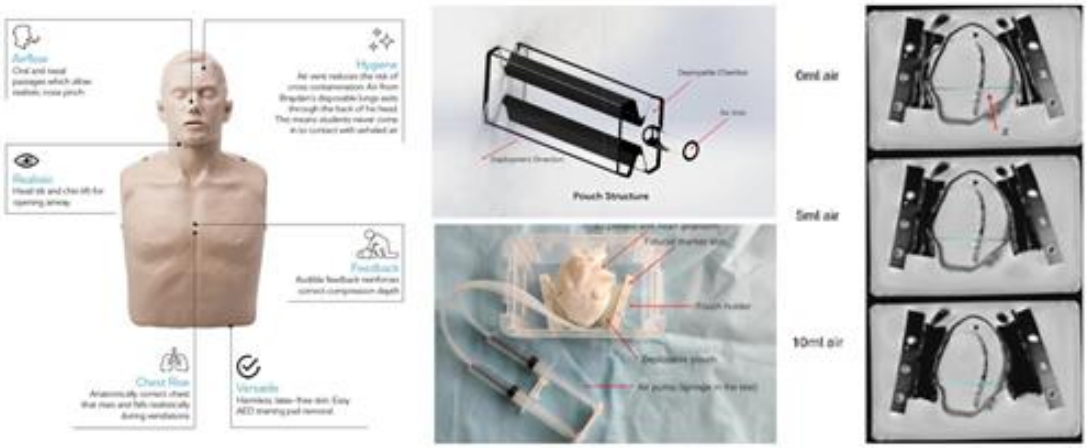

The design, test results of the CPR simulator

H. Tomita et al "Changes in Cross-Sectional Area and Transverse Diameter of the Heart on Inspiratory and Expiratory Chest CT: Correlation with Changes in Lung Size and Influence on Cardiothoracic Ratio Measurement," PLoS One
E. T. Roche et al., "Soft robotic sleeve supports heart function," vol. 9, no. 373,

68

Poster Session, Level 2 Foyer, September 4, 2025, 12:00 - 13:00

Investigating the Effects of Immune Cells on Cancer Biopsies Maintained in Bespoke Microfluidic Devices

Dorey J[1], Baldwin L[1], Green V, Greenman J[1]
[1]University Of Hull

This project seeks to model the interaction of the immune system and renal tumours, by maintaining patient derived tumour samples and peripheral blood mononuclear cells (PBMC) in a microfluidic device. A peristaltic pump was developed to circulate PBMC, from a central reservoir, through the microfluidic device providing multiple opportunities to interact with the tumour sample, before returning to a reservoir.

An Arduino-controlled peristaltic pump inspired by Davis (2021), was designed and 3D printed. A reservoir system devised from 7mL bijou vials and a custom rocking device, maintained cells uniformly distributed in media. A T cell line (Jurkats) or PBMC were circulated from the reservoir, through the device, repeatedly at various flow rates for 72 hours before their viability was measured. The Davis pump achieved stable flow rates from 1-1000µL/min, however resulted in the destruction of 90% of cells passing through the mechanism at each circulation. This device was redesigned to utilise an eccentrically offset ring pump, to replace the peristaltic mechanism, resulting in improved viability of cells passing through the mechanism. It was further modified to add cooling to the motor, including air vents and a heat sink. Jurkat cells were circulated through the device 32 times across 72 hours and maintained a mean viability 94.6% of non-circulated cells (SD=3.82, n=9). Future work will establish culture conditions for maintaining PBMC flow through the system. The device will then be used with a microfluidic chip to introduce PBMC to fresh, human renal cancer samples to show the model application.

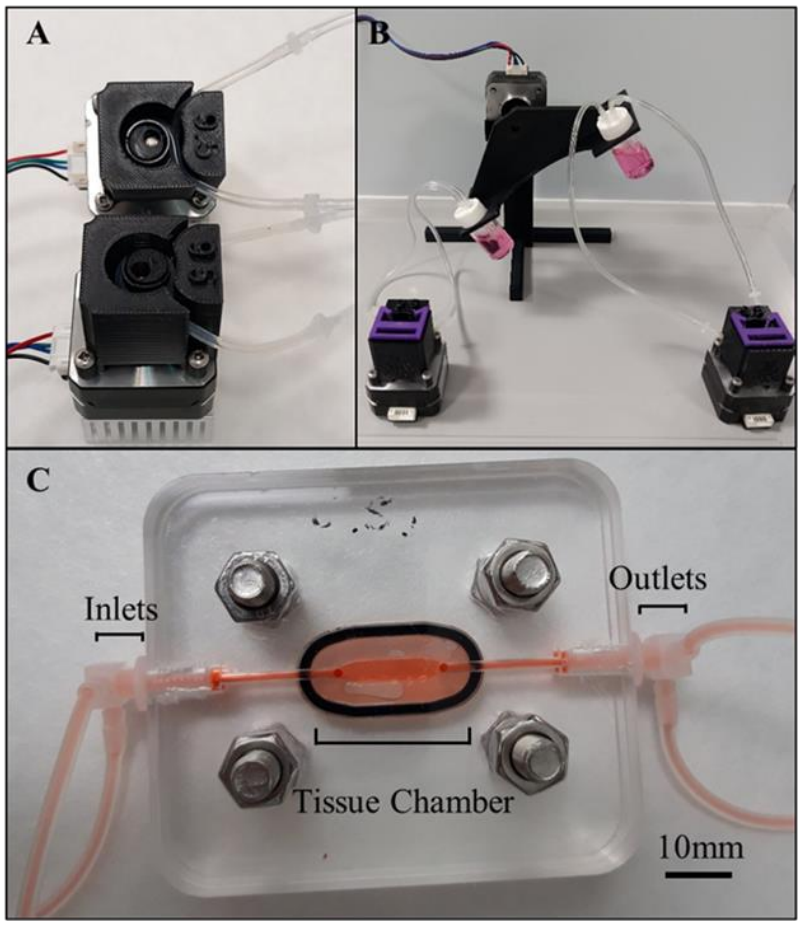

Figure 1 A) Microfluidic eccentric ring pump. B) Pump circulating from reservoirs, mounted on a rocking platform C) Microfluidic chip

[1] J.J. Davis et al., 2021, Analytica Chimica Acta, 1151, 338230 (2021)

Poster Session, Level 2 Foyer, September 4, 2025, 12:00 - 13:00

Racing to Detection: High-speed microfluidic sorting for bacterial detection in urine

Jordan K[1], Vezza V[2], Hannah S[2], Corrigan D[1], Jimenez M[1]
[1]University Of Strathclyde, [2]Microplate Dx

Urinary tract infections (UTIs) are one of the most common life-threatening infections, with a mortality rate up to 40% [1]. A delayed UTI diagnosis and hence, delayed accurate treatment can increase the risk of complications such as pyelonephritis and sepsis. The current gold standard for diagnosis is a urine culture which can take up to 3 business days to receive a result, with broad-spectrum antibiotics being prescribed in the meantime. As the severity of these infections, and their consequences, are increased by the time taken to receive an accurate diagnosis an alternative rapid diagnosis technique is urgently needed. In this work, we investigate the potential of inertial microfluidics as an avenue for culture-free, high-throughput enrichment of UTI-causing bacteria from urine [2]. To mimic the heterogeneous distribution of particles typically found in urine samples, we first created polyacrylamide hydrogels, ranging from 1.72 to 338.7 μm^2 in diameter. We tailored the hydrogel manufacturing to have an average area of ~ 4 μm^2, matching the area of UTI-causing bacteria E. Coli [3]. The hydrogels were then passed into a spiral inertial device, with Reynolds numbers (Re) ranging from 17 to 532. It was found that despite their large size variation, the hydrogels could be tightly focused in the device, allowing a 2.5X enrichment rate at Re=346. To the best of our knowledge, this is the first time inertial devices are used to enrich with such high speed highly heterogeneous and small particles providing a unique avenue for more rapid UTI-causing pathogen detection.

[1] CY. Hsiao, et al., 2020, ATM, 8, 7
[2] W. Lee, et al., 2020, MDPI, 11,9, 839
[3] R. Prats, et al., 1989, J.Bacteriol, 171, 7

Poster Session, Level 2 Foyer, September 4, 2025, 12:00 - 13:00

Developing Skin-on-a-chip (SOC) and a bioreactor to recreate environmental conditions linked to Raynaud's disease onset

Wu Z[1], Del Galdo F[2,3], Pensabene V[1,4]
[1]School of Electronic & Electrical Engineering, University of Leeds, [2]Leeds Institute of Rheumatic and Musculoskeletal Medicine, [3]Leeds Teaching Hospitals Trust, [4]Faculty of Medicine and Health, Leeds Institute of Medical Research at St James' University Hospital

Raynaud's phenomenon (RP) is a complex disease affecting up to 20% of the world's adult population, whose pathogenesis is not yet understood. It causes vasospastic attacks in the blood vessels of the body's extremities[1]. In the primary form, the symptoms are mostly cold fingers and toes, changing colour, and being triggered by cold exposure or stress. In the most severe form, called "Secondary Raynaud's", it occurs in combination with rheumatic, autoimmune diseases, such as lupus and scleroderma, and it represents one of the first symptoms of this disease[2]. In this study, we aim to develop a microfluidic skin-on-a-chip to investigate the biological mechanisms of Raynaud's disease and use a bioreactor to induce a controlled temperature drop during in vitro culture and observe cell-specific responses. The bioreactor was used to lower the temperature from 37 °C to the target temperature. The temporal and spatial dynamic of the temperature gradient in the microfluidic device was first simulated by Finite Element modelling and then confirmed by infrared imaging and in situ measurement of the temperature. The co-culture of human endothelial cells and dermal fibroblasts was optimised in the SOC, and as a first proof of concept, the on-chip response of individual cell types to a cold shock was recorded. While viability and cell morphology of HDF are not affected, shrinkage of the endothelial cell layer was observed. Based on this initial assessment, the platform is now ready for further investigation of cellular and molecular responses to cold shock in RP and scleroderma patients.

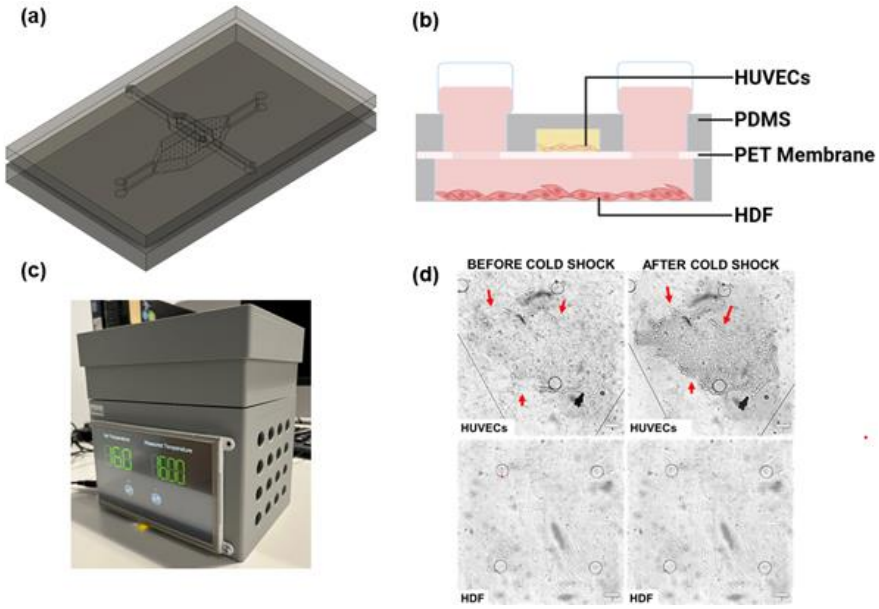

Figure 1.(a,b)Schematic of the SOC and cell types organisation ; (c)The bioreactor; (d)Results of cold exposure experiments: HUVECs and fibroblasts.

[1] A. L. Herrick, 2012, "The pathogenesis, diagnosis and treatment of Raynaud phenomenon," Nature Reviews Rheumatology, vol. 8, no. 8, pp. 469–479.
[2] M. Hughes et al., 2016, "Raynaud's phenomenon," Best Practice & Research Clinical Rheumatology, vol. 30, no. 1, pp. 112–132.

74

Poster Session, Level 2 Foyer, September 4, 2025, 12:00 - 13:00

Engineering a Microfluidic Bone Marrow Model with Integrated Mechanical Stimulation

Johnson-Love O[1,2], Paterson K[1,4], Ginesi R[3], Rodgers C[3], Manes L[5], Paoletti P[5], Dalby M[3], Salmeron-Sanchez M[3], Childs P[2], Zagnoni M[1,4]
[1]Department of Electronic and Electrical Engineering, University of Strathclyde, [2]Centre for Cellular Microenvironment, Department of Biomedical Engineering, University of Strathclyde, [3]Centre for Cellular Microenvironment, University of Glasgow, [4]ScreenIn3D, [5]School of Engineering, University of Liverpool

Disease modelling has traditionally relied on animal models; however, advances in regenerative medicine and bioengineering have driven the development of lab-on-a-chip systems as powerful alternatives. Microfluidic technologies enable the recreation of complex tissue environments, creating new platforms for targeted treatment testing and diagnostics [1]. Here, we present a novel microfluidic model of the bone marrow niche, integrated with mechanical stimulation via piezoelectric actuators. The platform delivers controlled vibration at 1 kHz and 30 nm amplitude, allowing investigation of cell mechanosensitivity under defined conditions [2]. To ensure precise vibration transmission, Finite Element Analysis (FEA) modelling optimised the design, while Laser Doppler Vibrometry (LDV) validated the vibration performance on the glass slide supporting the piezo actuator. A 3D-printed cantilever was used to hold the slide, enhancing the reliability of the vibration delivery. Cells were cultured in microwells to form 2D monolayers (fibronectin/poly-D-lysine) or 3D spheroids (Synperonic coatings) [3]. Initial experiments demonstrate that 2D cultures respond to vibration, while 3D spheroids in media alone show limited mechanotransduction, highlighting the need for improved mechanical coupling. Ongoing work incorporates a 3D hydrogel matrix to transmit vibration more effectively to spheroids and better mimic the in vivo microenvironment. This staged approach (progressing from 2D, to 3D free-floating, to hydrogel-embedded cultures) aims to create a more physiologically relevant model. Future studies will compare mechanosensitive responses across these culture conditions. This platform advances bone marrow niche modelling and provides a versatile tool for studying cell-matrix interactions under mechanical stimulation, with broader applications in disease modelling and therapeutic testing.

[1] Sontheimer-Phelps et al., 2019, Nat Rev Cancer, 19(2):65-81
[2] Robertson S. et al., 2018, Philos Trans A Math Phys Eng Sci, 376(2120): 20170290
[3] Paterson K. et al., 2022, IEEE OJEMB, 2022, 3, 86-95

Poster Session, Level 2 Foyer, September 4, 2025, 12:00 - 13:00

Engineering diverse microenvironments in organ-chip platforms: a toolkit of spatial patterning techniques

Stewart C[1,2], Davern J[1,3], Midha S[1,2], Hopkins T[1,2], Connelly J[1,3], Screen H[1,2], Knight M[1,2]
[1]Centre for Predictive in vitro Models, Queen Mary University of London, [2]Centre for Bioengineering, School of Engineering and Materials Science, Queen Mary University of London, [3]Centre for Cell Biology and Cutaneous Research, Faculty of Medicine and Dentistry, Queen Mary University of London

Organ-on-a-chip technologies have advanced in vitro modelling by enhancing physiological relevance. However, replicating the intricate microenvironments of native tissues within organ-chips requires tools and techniques to spatially pattern appropriate biomaterials [1]. Here, we present a suite of translatable micromanufacturing approaches, namely digital light processing (DLP) printing, extrusion-based bioprinting, and grayscale photomask patterning; developed and optimised to engineer spatially heterogenous tissue environments in organ-chip platforms. Gelatin polymers, functionalised with methacryloyl (Gel-MA), norbornene (Gel-NB) and thiol (Gel-SH) groups, were crosslinked using thiol-ene chemistry with multi-arm polyethylene glycol (PEG)-NB or PEG-SH under UV light (λ 365-405 nm). Rapid crosslinking occurred (<30 seconds) with tuneable hydrogel stiffness (0.4-18 kPa) modulated by adjusting reactant composition, macromer concentration, and crosslinker molar ratios. Human mesenchymal stem cell-laden hydrogels were successfully bioprinted into open-chamber organ chips (CN-Bio PhysioMimix®), where hydrogel stiffness gradients were created by precise UV light patterning. DLP printing is also compatible with open-chamber chips, where multi-directional stiffness gradients were created through 3D photomasking. Ongoing studies focus on fabricating architectural properties which guide cell alignment and differentiation. In closed-chip systems (Emulate Inc, Chip-S1®, MIMETAS OrganoPlate®), displacement techniques with ligand-tethered hydrogels successfully produced defined biochemical gradients mimicking tissue interfaces [2]. Grayscale photomask patterning further introduced stiffness gradients for additional biophysical cues. The multi-channel OrganoPlate platform also enabled the formation of adjacent 3D cellular environments to replicate complex tissue boundaries. Together, these approaches provide a powerful toolkit to spatially manipulate biochemical and mechanical cues within organ-on-a-chip systems, offering new capabilities to reproducibly fabricate complex tissue interfaces in vitro.

[1] C. Bosmans et al., 2024, Trends Biotechnol., 42, 6, 739-59.
[2] T. Hopkins et al., 2025, J. Tissue Eng., 16.

Poster Session, Level 2 Foyer, September 4, 2025, 12:00 - 13:00

A Hydraulic Robot for MRI-guided Prostate Therapy

Li X[1], Tse Z[1]
[1]Queen Mary University of London

Approximately 288,300 new diagnoses and more than 34,700 associated deaths were reported in the United States in 2023. Magnetic resonance imaging (MRI) is particularly well-suited for tumour detection, offering several key advantages such as excellent soft tissue contrast, high temporal and spatial resolution, multiplanar imaging capability, and real-time tracking of both tissues and instruments [1]. This study presents a compact design for the confined MR scanner bore with 4 DOFs, including pitch, roll, and offsets along the X-Y plane. A coaxial guide is positioned between the two support points, allowing for the manual insertion of a needle into the prostate. The robot's computer-aided design (CAD) drawing is shown in Figure (a). The robot comprises two 2-DOF hydraulic motors with a cylindrical structure measuring 25 mm in diameter and 13.9 mm in length. All components are fabricated using resin-based 3D printing to ensure MRI compatibility. Hydraulic actuation, employing incompressible fluids such as water or oil as the transmission medium, offers superior response times and higher power density than alternative actuation methods [2]. O-rings are mounted in specially designed grooves to address water leakage, and silicone lubricants are applied to minimize friction between the O-ring and the contact surfaces. The motor offers a theoretical maximum linear stroke of 43.5 mm and a rotational range of up to 101°. The resulting decoupled linear and rotational movements of each motor shaft can be independently actuated by three micro-syringe pumps. The diagram of the control system is shown in Figure (b).

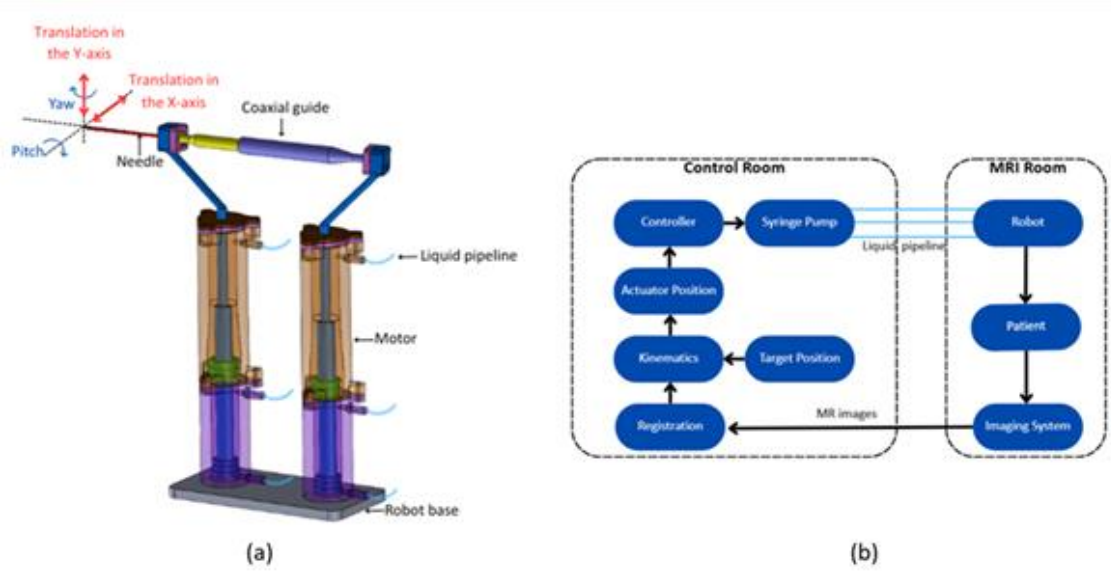

Figure: (a) CAD drawing of the robot. (b) Diagram of the control system.

[1]H. Liang et al., “Parallel Driven Robot for MRI-Guided Prostate Therapy,” IEEEASME Trans. Mechatron., vol. 30, no. 2, pp. 1557–1566, Apr. 2025.

[2]Y. Qiu et al., “MRI-Compatible Hydraulic Drive Needle Insertion Robot,” in 2021 6th IEEE International Conference on Advanced Robotics and Mechatronics (ICARM), pp. 86–92, Jul. 2021.

Poster Session, Level 2 Foyer, September 4, 2025, 12:00 - 13:00

Cellular Responses to Orthogonal Environmental Gradients in a Modular Microfluidic Platform

Dunn G[1]
[1]Univeristy Of Strathclyde

Understanding cellular responses to complex environmental stimuli is essential for advancing both fundamental biological knowledge and applications such as prosthetic neuronal–electrode interfaces. This study investigates the phenotypic outcomes of cellular monolayers and two-dimensional cultures subjected to controlled linear gradient environments within a novel modular microfluidic platform. Initial experiments calibrate individual linear gradients—topographical cues , electric field gradients, and low-velocity fluid flow—to determine the maximum phenotypic response potential of each cell type in isolation. Based on this calibration, two orthogonal environmental stimuli are then applied simultaneously to the same culture, with each gradient set to an independently optimized magnitude capable of eliciting an equivalent maximal response when applied alone. This design enables direct comparison of competing influences on phenotype expression within a single cell population. Resultant cellular phenotypes are quantitatively analyzed to assess how cells prioritize or integrate multiple concurrent cues. These findings provide new insight into the hierarchical organization of cellular environmental responses and support predictive modeling in engineered microenvironments.

Vedaraman S, et.al. Anisometric Microstructures to Determine Minimal Critical Physical Cues Required for Neurite Alignment. Adv Healthc Mater. 2021
Colin D. McCaig, Ann M. Rajnicek, et.al.
Controlling Cell Behavior Electrically: Current Views and Future Potential
Colin D. McCaig, Ann M. Rajnicek, et.al.
Physiological Reviews 2005

Poster Session, Level 2 Foyer, September 4, 2025, 12:00 - 13:00

Development of electrospun hollow fibers for muscle tissue engineering

Kruth M[1], Mouthuy P[1], Ye C[2], Hulley P[1]
[1]Nuffield Department of Orthopaedics, Rheumatology and Musculoskeletal Sciences, University of Oxford,
[2]Department of Engineering Science, University of Oxford

Muscle tissue engineering holds great promise for developing human in vitro models that could replace animals in research, with numerous potential applications in drug development, drug screening, and the study of developmental or pathophysiological processes. Such models enable testing of novel pharmaceutical compounds in human-relevant systems to identify potential toxicities and determine efficacy prior to clinical introduction. However, accurately mimicking the complexity and heterogeneity of native muscle tissue remains challenging, limiting clinical applicability and widespread adoption. A major hurdle in muscle tissue engineering is the diffusion limit, which restricts gas and nutrient exchange in thicker engineered tissues. Specifically, muscle's high metabolic demands require efficient oxygen and nutrient supply, yet passive diffusion typically only reaches depths of 100–200 µm [1]. This causes necrosis in cells beyond the diffusion range and thus restricts the size and functionality of in vitro tissues. Electrospun hollow fibres (eHFs) could offer promise for three-dimensional muscle tissue culture, as these could mimic the tissue's vasculature by providing enhanced nutrient and gas transport via a semi-permeable porous membrane [2]. Additionally, eHFs could serve as a scaffold for growing muscle tissue by mimicking the extracellular matrix (ECM) and providing anchorage points for cells [3]. This project investigates the production of eHFs from polycaprolactone (PCL) using a dissolvable fibre collector.

[1] T. Rademakers et al., 2019, J. Tissue Eng. Regen. Med., vol. 13, no. 10, pp. 1815–1829.
[2] H. Eghbali et al, 2016, Int. J. Artif. Organs, vol. 39, no. 1, pp. 1–15.
[3] I. Jun et al, 2018, Int. J. Mol. Sci., vol. 19, no. 3, p. 745.

Poster Session, Level 2 Foyer, September 4, 2025, 12:00 - 13:00

Effects of exercise-assisting mobile application (Osteoarthritis-Rehabilitation Assistant [O-RA]) on rehabilitation outcomes in the elderly: a randomized controlled parallel clinical trial

Pattanakuhar S[1,2], Sornmayura P[2], Klaphajone J[2]
[1]Department Of Biomedical Engineering, University Of Strathclyde, [2]Department of Rehabilitation Medicine, Faculty of Medicine, Chiang Mai University

Exercise is a first-line conservative treatment for knee osteoarthritis (OA) [1]. Using a mobile application may improve compliance with the exercise program [2]. However, results may be different among application types. This study aimed to evaluate the effects of O-RA application, which provides real-time motion analysis of body position during exercise via a mobile application, on exercise program compliance and correctness in elderly individuals. This assessor-blind, parallel-design randomized controlled trial recruited forty elderly participants without knee OA symptoms or diagnosis from an outpatient clinic in a tertiary care hospital in Thailand. Participants were randomized into two groups: the O-RA application (intervention) group and the standard treatment (control) group. Both groups received 15-minute exercise instruction from a physical therapist on four types of exercises and were asked to perform them daily at home for one week. The intervention group used the O-RA application to facilitate the exercise program, while the control group performed exercises independently. The control group demonstrated significantly higher exercise compliance compared to the intervention group ($p<0.05$, independent t-test). No statistically significant difference was found in exercise correctness between groups. Application difficulty-of-use and satisfaction scores were 47 and 59 out of 100, respectively. Major challenges included application instability and usability issues. In elderly individuals without knee OA symptoms or diagnosis, the O-RA application acted as a barrier rather than a facilitator for lower extremity exercise programs. Future development should focus on improving application stability and user-friendliness to enhance usability and achieve its intended purpose of exercise assistance.

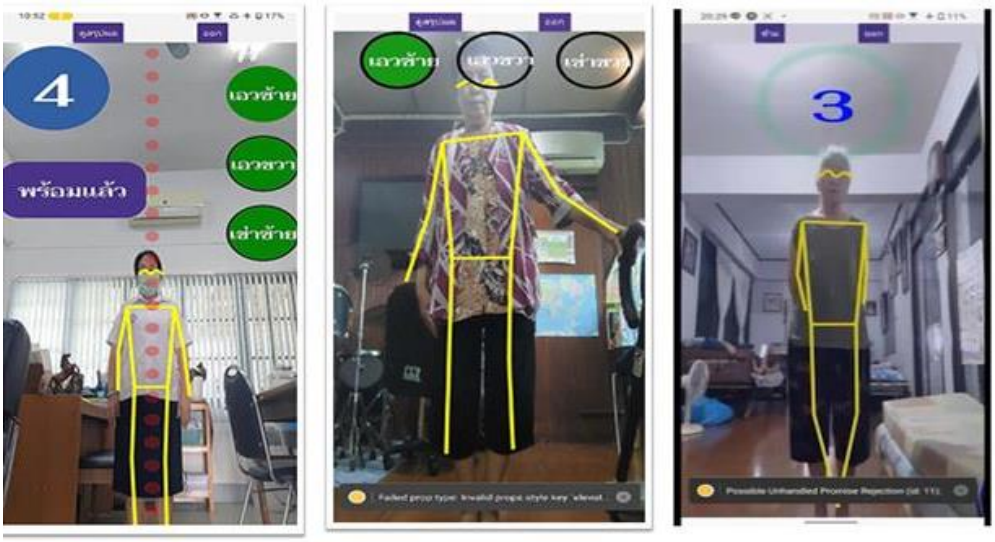

User interfaces of the real-time motion analysis integrated mobile application (Osteoarthritis Rehabilitation Assistant [O-RA])

[1] Zacharias A, et al., 2014, Osteoarthritis Cartilage, 22, 1752-73.
[2] Thiengwittayaporn S, et al., 2021, Arch Orthop Trauma Surg, 28, 1–10.

86

Poster Session, Level 2 Foyer, September 4, 2025, 12:00 - 13:00

Is Mismatch Negativity a marker of Central Neuropathic Pain Intensity in Spinal Cord Injury: A Home-Based Pilot Study

Dheerendra P[1], Ramu N[1], Solankey O[1], Nawaz R[2], Diggin S[3], Purcell M[4], McCaughey E[4], Vuckovic A[1]
[1]University Of Glasgow, [2]University of Essex, [3]Cumulus Neuroscience, [4]Queen Elizabeth National Spinal Injuries Unit

Cross-sectional studies have shown that pain intensity affects brain activity as measured by electroencephalography (EEG) in people with neuropathic pain (NP). However, more studies are needed to establish if mismatch negativity (MMN) is a biomarker of NP. We aim to determine whether the change in MMN is predictive of change in central neuropathic pain intensity due to medication. In this longitudinal study, ten people with spinal cord injury-related NP recorded their response to MMN experiment using home-based self-guided EEG set-up for ten days both before and after taking medications over a period of several weeks. Results: Wilcoxon signed rank test showed that there was no statistically significant change in amplitude and latency of neither duration deviant MMN (d-MMN) nor frequency deviant MMN (f-MMN) due to medication. Linear Regression analysis showed that the changes in amplitude and latency of d-MMN and f-MMN was not related to changes in self-reported pain intensity. So the changes in d-MMN and f-MMN was not predictive of alterations in self-reported pain intensity due to medications. Thus duration-deviant or frequency-deviant Mismatch Negativity was not able to detect self reported Neuropathic Pain intensity. We conclude that MMN may not be a surrogate or pharmacodynamic marker of Central Neuropathic Pain in Spinal Cord Injury.

Poster Session, Level 2 Foyer, September 4, 2025, 12:00 - 13:00

Design and Evaluation of a Compact EEG Acquisition Platform for Wearable Applications

Saleh M[1], Soman R[2], Seirafi M[2], Casson A[1]
[1]University of Manchester, [2]Alpha Brain Technologies

Wearable EEG devices enable flexible, non-invasive brain signal monitoring during daily activities [1]. With recent advancements in artificial intelligence (AI) and low-power wireless technologies, these devices are becoming more effective for continuous, personalized monitoring and management of neurological conditions [2]. Epilepsy, in particular, can benefit from wearable EEG systems for real-time seizure prediction and timely intervention [3].
This work presents the design and evaluation of a compact, low-power EEG acquisition platform optimized for wearable applications. The prototype (35 × 25 mm) (see Fig. 1 (1)) integrates a Bluetooth low energy (BLE)-enabled microcontroller, an inertial measurement unit (IMU), a memory chip, and a multi-channel highly sensitive EEG Analog Front End (AFE). Power consumption, measured at 4.2 V using a Keithley 2450 source meter, averaged 36.8 mA, supporting 9.5 hours of continuous operation with a 350 mAh LiPo battery (Fig. 1 (3)). The 8 Gbit memory enables continuous operation for over 30.5 hours.
Signal accuracy was assessed using a waveform generator and attenuator to provide sinusoidal inputs (10 µVpp–40 mVpp at 5 Hz, except 25 mVpp at 10 Hz; Fig. 1 (2)). Results are averages from repeated tests on 5-second signals at a PGA of 1 and a 250 Hz sampling rate. The platform accurately captured low-amplitude signals, matching the input waveforms, as shown in the statistical analysis (Fig. 1 (4)).
These results demonstrate the platform's suitability for real-world EEG monitoring, balancing compactness, efficiency, and signal accuracy. Future work will deploy on-edge Machine Learning (ML)-based models for enhanced real-time signal processing.

(1)

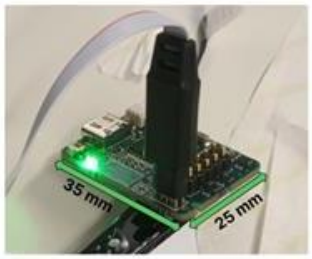

(2)

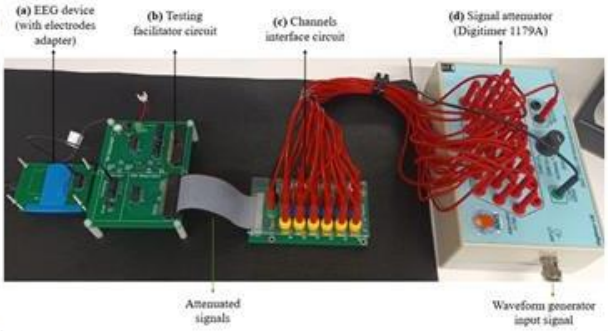

(3)

Parameter	Result
Average (mA)	36.8
STD (mA)	1.5
Minimum (mA)	36.2
Maximum (mA)	55.7
Dynamic Range (mA)	19.6
Estimated Battery Life	9.5 hours with a 350 mAh LiPo battery

(4)

Input Signal	Mean (µV)	STD (µV)	Vpp (µV)	RMS (µV)
40 mVpp	-14.2	14271.0	40395.4	14265.0
25 mVpp	12.9	8780.6	24881.2	8777.1
7 mVpp	-7.8	2487.0	7041.6	2486.0
100 µVpp	0.1	33.9	110.9	33.9
50 µVpp	-0.1	17.0	57.7	17.0
20 µVpp	0.0	6.9	27.9	6.9
10 µVpp	0.0	3.8	18.4	3.8

Fig. 1: (1) Prototype device, (2) experimental setup, (3) power consumption results, and (4) signal measurement performance results.

[1] G. Yilmaz et al., 2024, Sensors, vol. 24, no. 6, p. 1867, 2024.
[2] A. Abd-Alrazaq et al., 2023, J. Med. Internet Res., vol. 25, p. e48754.
[3] A. A. Ein Shoka et al., 2023, Multimed. Tools Appl., vol. 82, no. 27, pp. 42021–42051.

01

Poster Session, Level 2 Foyer, September 5, 2025, 12:00 - 13:00

Entropy-Based EEG Analysis for Differentiating Psychogenic Non-Epileptic and Epileptic Seizures

Shokouh Alaei H[1], Abasolo D[1], Kouchaki S[2]
[1]Centre for Biomedical Engineering, School of Engineering, University Of Surrey, [2]Centre for Vision, Speech and Signal Processing (CVSSP), School of Computer Science and Electronic Engineering, University of Surrey

Accurately distinguishing psychogenic non-epileptic seizures (PNES) from epileptic seizures (ES) is essential to avoid misdiagnosis and ensure appropriate treatment, yet it remains a significant clinical challenge. This study analysed electroencephalogram (EEG) data recorded during preictal and interictal states using entropy-based features to classify PNES and ES patients. Sample Entropy, Spectral Entropy, Permutation Entropy, Fuzzy Entropy, and Dispersion Entropy were computed from 5-second EEG windows across 17 channels. For interictal data, a two-stage feature selection strategy was applied, combining Mann-Whitney U tests and mutual information analysis, followed by permutation importance-based selection. This additional screening addressed the lower discriminative power and higher noise observed in interictal features. For preictal data, feature selection was performed solely using permutation importance, as clearer separation between PNES and ES was observed. Classification models were trained under a leave-one-subject-out cross-validation framework, with hyperparameters and thresholds tuned through nested 10-fold validation. Naive Bayes applied to selected preictal entropy features achieved a balanced accuracy of 72.35%. For interictal data, Light Gradient-Boosting Machine yielded 64.93% balanced accuracy. Entropy-based analysis revealed distinct patterns between PNES and ES across brain states. In the preictal period, entropy values were consistently higher in ES across all scalp regions, suggesting greater signal complexity preceding epileptic seizures. Sample Entropy, capturing local temporal irregularity, was the most frequently selected feature. In the interictal state, PNES showed increased entropy in posterior regions but reduced values in frontal and parietal areas. These findings support entropy-based EEG analysis as a non-invasive tool for improving the classification of PNES and ES.

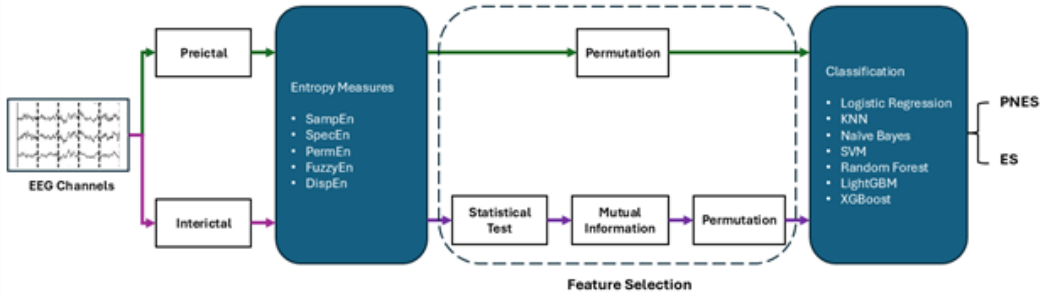

Block diagram of the proposed pipeline for classifying PNES and ES using entropy features, feature selection, and machine learning models.

03

Poster Session, Level 2 Foyer, September 5, 2025, 12:00 - 13:00

Assessment of Triage Data Variables for Predicting Acuity Classification: A Correlational Analysis of Chief Complaints and Physiological Parameters

Jacob A[1], Mouli S[1], Angelova M[1], Fratini A[1]
[1]Aston University

Emergency departments (EDs) are the first point of contact between patients and clinical personnel when a patient enters emergency care, regardless of the time of day or year. Patient processing is initiated with demographic data acquisition and chief complaints documentation. A standardised process is then followed where physiological data is obtained such as blood pressure, heart rate, respiration rate, blood saturation level, capillary refill time, and mental state [1]. In addition, symptom evaluation is conducted to assign each patient an acuity/severity score. Inconsistencies within vital signs, as well as the chief complaint contribute to stratifying patients according to a 5-point acuity classification system, based on the Manchester Triage System, level 1 determining critical conditions requiring immediate intervention [2]. Assignment of the score is reliant on the nurse's experience, emotional state, and stress levels, which increases subjectivity and bias. Failure to assign the correct scores can negatively contribute to the patient's diagnosis and compromise clinical outcomes potentially causing harm and death. By using automated techniques and statistically analysing previously existing ED visits, predictions can be made about the correlation between chief complaints, physiological data, diagnosis, and disposition. Initial results using MIMIC-IV-ED dataset [3] show that only 3.45% of visits were assigned as the highest priority, with altered mental state as being the top complaint associated with the score. This analysis can contribute to increasing patient care, reduce waiting times, reduce workload, and improve resource management in a demanding environment. This principle can be further adopted to varying age groups and departments.

[1] Mattioli, V., (2018), Congenital heart disease: the nursing care handbook: Springer, pp. 81-95.

[2] Hopman, A et al., (2025), European Journal of Pediatrics, 184(5), pp. 294.
[3] Johnson, A et al., (2023). MIMIC-IV-ED (version 2.2). PhysioNet.

05

Poster Session, Level 2 Foyer, September 5, 2025, 12:00 - 13:00

The Production of Type I Recombinant Human Collagen for Medical Device Applications

Fricker C[1], Wright C[1], Arora H[1]
[1]Swansea University

Collagen is the most abundant structural protein in the human body and is highly desirable for medical engineering applications such as scaffolds, wound dressings, and hydrogels [1]. Of the 28 known human collagen types, type I is the most prevalent, found in almost all connective tissues. Traditionally, collagen is extracted from animal tissues, raising concerns about immune response, scaffold rejection, disease transmission, and ethical or religious considerations. Recombinant human collagen (rhCol) offers a safer, more sustainable alternative for both fundamental cell studies and medical device fabrication.
In this work, both heterotrimeric rhCol(I) and single-chain rhCol(I)α1 were produced using a yeast-based expression system to explore their individual properties and applications. The collagen extracts were rigorously characterized using SDS-PAGE, circular dichroism (CD), Fourier-transform infrared spectroscopy (FTIR), atomic force microscopy (AFM), and hydroxyproline analysis. Characterization confirmed the production of correctly sized collagen molecules, comparable to bovine collagen standards. AFM imaging showed that rhCol(I) was capable of self-assembling into fibrils and fibres (Figure), a critical feature for extracellular matrix (ECM) scaffolding. The recombinant collagens were processed into electrospun mats, hydrogels, and lyophilized sponges, with mechanical properties enhanced through chemical crosslinking. This work demonstrates that precision fermentation provides a viable route to produce functional collagen, addressing ethical and safety concerns of animal-derived sources. Comprehensive characterization confirms its suitability for biomedical use across structural, biochemical, and mechanical parameters. Future research will focus on expanding the method to produce additional proteins, such as lysyl oxidase, to enable native enzymatic crosslinking of recombinant collagens.

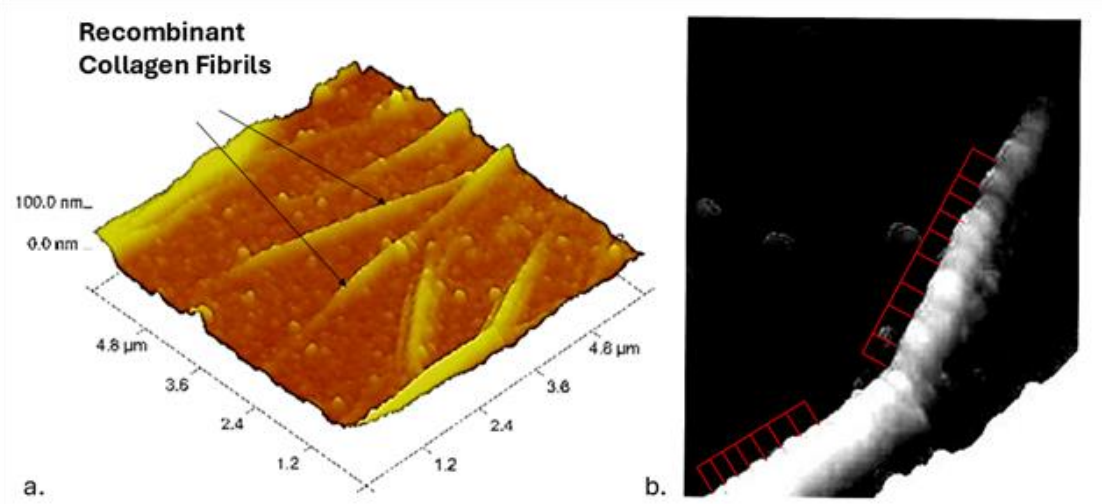

Figure: (a) AFM image of recombinant human collagen fibrils. (b) Magnified view highlighting the characteristic D-periodicity of the fibrils.

[1] J. P. Widdowson et al., 2019, Nanofiber Membranes for Medical, Environmental, and Energy Applications, 1st ed. CRC Press.

07

Poster Session, Level 2 Foyer, September 5, 2025, 12:00 - 13:00

Accelerating cytocompatible hydrogel discovery: assessment of multiplexing approaches to increase screening throughput

Sinclair L[1], Zagnoni M[1], Mosedale C[2], Sandison M[1]
[1]University of Strathclyde, [2]Matrix Bio Ltd

Hydrogels are critical components of advanced cell culture models, where they mimic the extracellular matrix and impart structural and functional properties to tissue models. Commonly used hydrogels can be associated with limitations, including having undefined composition, limited support of cell attachment and lack of ability to tailor mechanical properties. This research develops a well-defined workflow for multiplexed combinatorial hydrogel screening to accelerate the discovery of defined hydrogels tailored for tissue-specific culture models. Within microwell plates, a comprehensive hydrogel test library was established, comprising 64 formulations of photocurable hydrogels (for 3D printing compatibility), selected to produce a range of stiffnesses and cell-adhesive ligand incorporation. The base hydrogels were commonly used PEGDA (1kDa, 6kDa, 20kDa) and PhotoAlginate, used at a range of concentrations (2-20%), cross-linking densities (1-2x light dose) and cell-adhesive dopants (1-10% GelMA, 1-3% PhotoHA). Hydrogels (all materials from CELLINK, Sweden) were cured using LAP and 405nm light. For each formulation, mechanical properties (elastic modulus, peak force) were established (Biomomentum Mach-1 Mechanical Tester), with formulations spanning a range of moduli from 0.10±0.036-1107±199 kPa (mean±SD) and trends across different formulation parameters established. A subset of these formulations were screened for their ability to support cell growth using human dermal fibroblasts, cultured in 3D for seven days, with growth quantified using fluorescence imaging. Our findings, and the optimised methodology, will contribute towards the development of a robust, closed-loop hydrogel discovery workflow, where multiplexed data generation feeds into machine learning-guided computational tools for automated analysis of hydrogel composition-structure-property relationships in an accelerated, data-driven manner.

09

Poster Session, Level 2 Foyer, September 5, 2025, 12:00 - 13:00

Development of TiO2-doped polymers for enhanced optical decontamination of urinary catheters

Maclean M[1,2], Teixeira J[1], Selkirk J[1], Brown R[1], Sandison M[1]
[1]Department of Biomedical Engineering, University of Strathclyde, [2]The Robertson Trust Laboratory for Electronic Sterilisation Technologies, University of Strathclyde

Catheter-associated urinary tract infections are a significant healthcare issue, particularly for patients requiring longer-term catheterisation (>30 days). The high risk is due to the physical location and insertion site of catheters, meaning these elastomer-based devices can become readily colonised by microorganisms which form difficult-to-treat biofilms. Clinical improvements would be achieved by development of strategies to inhibit bacterial attachment and biofilm formation on catheter surfaces. Photodynamic inactivation using 405-nm violet-blue light has received significant interest as an antimicrobial strategy, with recent work highlighting enhanced light decontamination of elastomeric material (PDMS) by doping with photosensitive titanium dioxide (TiO2) nanoparticles [1]. To investigate the applicability of this towards use in catheters, where both lumen and outer surface require decontamination, tailoring the optical properties of the elastomer is critical. This study therefore conducted optical and antimicrobial characterisation of PDMS doped with TiO2-nanoparticles, at 1:5 to 1:800 PDMS:TiO2 ratios and differing material thicknesses. Results demonstrated increased light transmission through the doped elastomer with reducing TiO2 concentrations, ranging from <2% (1:5) to >35% (1:800) transmission. PDMS thickness (0.5-2 mm) also had a significant influence on the transmitted light ($p<0.001$). Doped and non-doped surfaces were then seeded with Staphylococcus aureus bacterial contamination, and 405nm light treatment (15-30 J/cm2) demonstrated significantly enhanced decontamination efficacy compared to non-doped PDMS (35-45%, dependent on TiO2 concentration; $p=0.008$). Significant decontamination was also achieved on the underside of doped materials, with results highlighting the importance of achieving a balance between the concentration of photocatalyst dopant and the corresponding light transmission through the elastomer.

[1] L. McShea et al., 2022, Mater Res Express, 9, 085402

11

Poster Session, Level 2 Foyer, September 5, 2025, 12:00 - 13:00

Visualising and modelling the tissues surrounding the follicles of flight feathers in Wood Pigeons (Columba palumbus)

Whitehouse-Lloyd H[1]
[1]University Of Liverpool

Flight in volatile bird is attributed to flight feathers, numbering 20 on each wing. During flight, these feathers experience cyclic torsional and tensile forces [1]. Flight feathers are anchored into the wing via follicles and are supported by surrounding tissues. Whilst the greater anatomy of the wing has been studied and reported on, the composition, structure and mechanical capabilities of these surrounding tissues has lacked consideration. Despite the small amount of information available, a few reports provide insights into the possible nature of these tissues. Ostmann et al. [2] presented histological sections of feather follicles and reported collections of contractile elements, interfacing with the feather shafts via tendinous tissue. Hieronymus [3], Bribiesca-Contreras and Sellers [4], used Micro-CT imaging techniques to reveal the internal assembly of the wing and the interfaces between the skeleton, muscle and covert feathers. Using similar techniques on dissected samples of Wood Pigeon flight feathers, the surrounding interfacial tissues have been visualised and modelled in 3D, to allow analysis of the tissues interfacing between the various structures of the wing.

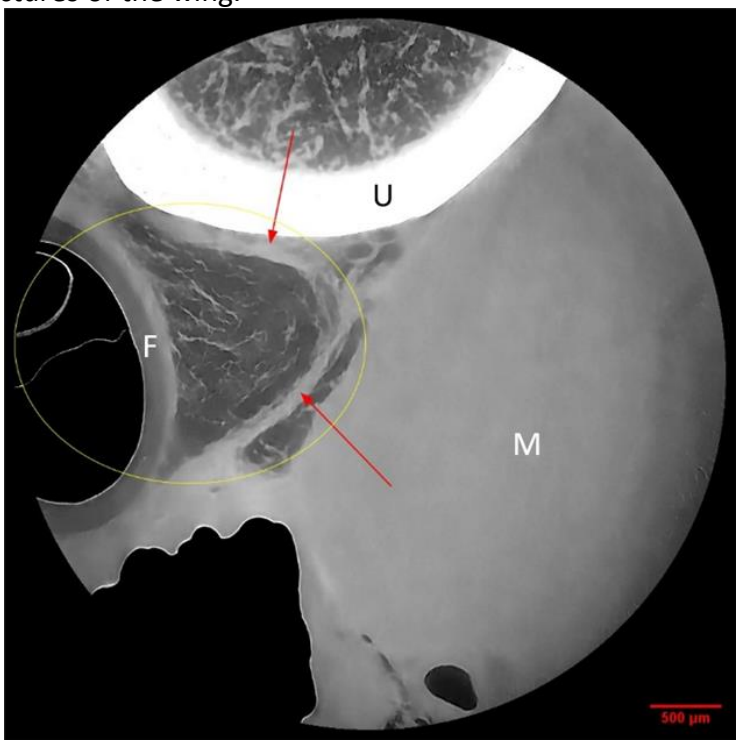

Figure 1: µCT image of Wood Pigeon wing. Ulna (U), Feather (F), Musculature (M), Region of Interest (Yellow Circle/Red Arrows).

1. C.J. Pennycuick, 2008, Modelling the Flying Bird, 1st Edition, Volume 5, Elsevier Inc
2. O. Ostmann et al., 1963, Poultry Science, vol 42, no. 4, pp 958-969
3. T.L. Hieronymus, 2016, Journal of Anatomy, vol 229, no. 5, pp 631-656
4. F. Bribiesca-Contreras et al., 2017, PeerJ, 5:e3039

13

Poster Session, Level 2 Foyer, September 5, 2025, 12:00 - 13:00

In vitro development and characterization of a ‘heart valve for all’

Kerr M[1], Seed E[1], Wheatley D[2], Reid S[1], McCormick C[1]
[1]Department of Biomedical Engineering, University of Strathclyde, [2]Department of Mathematics and Statistics, University of Strathclyde

Valvular heart disease is increasing globally, partly driven by the prevalence of rheumatic heart disease (RHD) within many low-income countries. RHD remains the most prevalent form of heart disease worldwide, with an estimated 40.5 million cases and 306,000 deaths in 2019 [1].

The Wheatley Heart Valve (WHV) is a patented polymeric heart valve. It is designed to promote blood washout in the aortic root during diastole, helping clear debris and potentially reducing the need for anticoagulants. The flat-sheet nature of the leaflets opens relatively low-cost manufacturing routes, thereby potentially removing a barrier to adoption globally [2,3].

In this study, we investigated polycarbonate urethane (PCU) for the leaflets, with several different grades and manufacturing techniques being explored. PCU films (50–200 µm thick) were produced using flat sheet casting and spin-coating, with aromatic grades offering better processability compared to aliphatic grades.

Uniaxial tensile testing was conducted to evaluate the mechanical properties of the leaflets. and the materials were laser cut, with samples taken in perpendicular directions to assess material isotropy. The leaflets produced by flat sheet casting and spin coating displayed isotropic mechanical behaviour, with Young’s Modulus in the range 41.88 to 77.21 MPa. Surface contact angle measurements showed the different polymer leaflets to be hydrophobic, with application of a thin diamond-like carbon (DLC) coating providing a small reduction in the contact angle, indicating slightly more hydrophilic-like properties.

These findings represent an important step towards development of heart valves with increased durability and enhanced haemocompatibility.

1. S. Coffey. et al. Nature Reviews Cardiology 2021.
2. S. McKee, et al. J Biomech Eng, 143(8), 2021
3. H. Oliveira, et al. Int J Numer Method Biomed Eng, 2024
4. S. F. Melo, et al. Biomater. Sci., 12, 2149-2164, 2024

15

Poster Session, Level 2 Foyer, September 5, 2025, 12:00 - 13:00

Reliability of Digital Mobility Outcomes in Postural Cortical Atrophy: A Rare Dementia Subtype

Kirk C[1], Bancroft M[2], Kaski D[2], Rohrer J[2], Del Din S[1,3], Yong K[2], Mc Ardle R[1,3]
[1]Newcastle University, [2]Dementia Research Centre, UCL , [3]National Institute for Health and Care Research (NIHR) Newcastle Biomedical Research Centre (BRC)

Posterior cortical atrophy (PCA) is a rare and often misdiagnosed dementia syndrome (1). Digital mobility outcomes (DMOs), derived from wearable devices, may support more accurate identification of PCA given that that DMOs differ across other dementia subtypes (2). Prior to clinical application, this study aimed to establish the minimum number of trials (in-lab) and days (real-world) necessary to reliably characterise DMOs in PCA. Sixteen participants (age: 72±11 years, 8M/8F) were recruited from the UCL Dementia Research Centre and wore a wearable device (Axivity AX6), across ten lab-based six-meter straight walks and seven-days in the real-world. DMOs were estimated with a previously validated pipeline (3). Mixed effects determined for each DMO, the minimal number of laboratory trials and real-world days that had intra-class correlation coefficient (ICC) of > 0.80 (5). Pace DMOs required 1-2 laboratory trials, while rhythm DMOs required 7-8 trials. Variability and asymmetry DMOs were not reliable. In the real-world, volume and pattern DMOs were stable between 3 and 7 days. Pace and rhythm DMOs required 1 to 7 days, excluding maximum walking speed from longer WBs (Table 1). In the laboratory, we recommend at least eight 6-metre walking trials to reliably capture pace and rhythm DMOs. Variability and asymmetry DMOs were less reliable, likely due to trial-to-trial gait fluctuations. In real-world settings, a minimum of seven days of data collection is recommended for stable DMO estimates, including step count—the most studied DMO in dementia (6). However, maximum walking speed from longer walking bouts is not reliable.

Laboratory Digital mobility outcome	**Minimum number of trials for ICC > 0.8**
Pace	
Walking speed (metres/second)	1 trial
Step length (metres)	2 trials
Rhythm	
Step time (seconds)	7 trials
Stance time (seconds)	8 trials
Swing time (seconds)	7 trials
Variability	
Step velocity variability (metres/second)	4 trials
Step length variability (metres)	4 trials
Step time variability (seconds)	/
Stance time variability (seconds)	/
Swing time variability (seconds)	/
Asymmetry	
Step time asymmetry (seconds)	/
Stance time asymmetry (seconds)	/
Swing time asymmetry (seconds)	/
Postural control	
Step length asymmetry (metres)	/
Rea-world Digital mobility outcome	**Minimum number of days for ICC > 0.8**
Volume of walking activity	
Number of steps (steps/day)	7 days
Walking duration (minutes/day)	5 days
Pattern of walking activity	
Number of WBs (number/day)	3 days
Number of WBs > 10 seconds (number/day)	3 days
Number of WBs > 30 seconds (number/day)	3 days
Number of WBs > 60 seconds (number/day)	4 days
WB duration (seconds)	4 days
Maximum WB duration (seconds)	5 days
WB duration variability (COV %)	7 days
Pace of gait	
Walking speed in shorter (10-30s) walking bouts (metres/second)	2 days
Walking speed in longer (>30s) walking bouts (metres/second)	7 days
Maximum walking speed in walking bouts > 10s (metres/second)	5 days
Maximum walking speed in longer (>30s) walking bouts (metres/second)	/
Step length in shorter (10-30s) walking bouts (metres)	1 days
Step length in longer (>30s) walking bouts (metres)	4 days
Rhythm of gait	
Step duration in all walking bouts (seconds)	4 days
Step duration in longer (>30s) WB (seconds)	3 days

Minimum number of trials and days required for ICCs > 0.8 for DMOs estimated from laboratory and real-world assessment:

1. Yong KXX, et al. Curr Treat Options Neurol. 2023
2. Mc Ardle R, et al. Alzheimers Dement. 2019
3. Del Din S, et al. J NeuroEngineering Rehabil. 2016
4. J. Buekers, et al. MDS 2024. Movement Disorders; 2024
5. Mc Ardle R, et al. J Med Internet Res. 2023

17

Poster Session, Level 2 Foyer, September 5, 2025, 12:00 - 13:00

Innovative Nanoindentation Device for Soft Materials in Humid Environment

Salam F[1], Vassalli M[1]
[1]University Of Glasgow

Measuring the mechanics of soft (biological)materials, such as gels, tissues, and cells, is essential for various biomedical applications. Recent advancements in mechanobiology highlight the need for devices with high sensitivity (<kPa) and spatial resolution of 1-100µm. The de-facto standard for the microscale mechanical characterization of soft materials is Atomic Force Microscopy(AFM). While this technique meets required specifications, it faces limitations in terms of throughput, usability, and integrability.

To address this, we propose a novel indentation platform based on self-sensing cantilevers for precise and efficient mechanical characterization of soft (bio)materials. This approach builds on the extensive knowledge and calibration frameworks developed for AFM while integrating the usability and flexibility of other indentation platforms like micromanipulators and non-AFM nano-indenters. The proposed platform incorporates self-sensing cantilevers, eliminating the bulky laser detection system of standard AFMs. This force sensor offers sensitivity comparable to AFM cantilevers while providing a more versatile geometry. The prototype, developed in collaboration with the nanotechnology company Schaefer SEE, integrates a recently developed self-sensing cantilever based on tri-layer technology, which operates in a conductive medium, addressing limitations of previous self-sensing sensors on the market.

The system’s performance is validated on reference soft materials, such as tissue-mimicking gels, and benchmarked against alternative sensor technologies. The platform features rapid cantilever swapping, low-latency communication protocols, and flexible embedded hardware, enabling real-time data acquisition and streamlined operation. By integrating AFM-level precision with nanoindentation usability, this platform simplifies mechanical characterization, improves reproducibility, and provides a versatile tool for studying single-cell mechanics, tissue engineering, and disease diagnostics.

19

Poster Session, Level 2 Foyer, September 5, 2025, 12:00 - 13:00

External Fixator Mechanics - A Quantitative Investigation of the Influences of Pin, Rod and Distance Factors on Fracture Micromotion.

Edwards J[1], Chappell M[1], Kumar V[2], Dharmrajan A[3], Upadhyay P[4]
[1]School of Engineering, University Of Warwick, [2]Manchester Royal Infirmary, [3]Queen Elizabeth Grammar School, [4]George Eliot Hospital

Fracture micromotion refers to controlled, subtle, interfragmentary motion between fracture ends, and is an important predictor of fracture union [1]. Optimal micromotion for bone bridging and callus formation ideally lies between 2-10% [2]. Excessive localised movement beyond these boundaries results in a high strain environment which exceeds the deformation tolerance of healing bone and inhibits callus formation. Thus, close control over micromotion is important as it modulates fracture healing. A fixator's mechanical stiffness strongly influences its control over micromotion [2]. Additionally, alterations to structural components such as pins and rods influence fixator stiffness. Consequently, variations in a fixator's structural parameters indirectly affect its ability to restrict micromotion, although the exact nature of these relationships is unclear. This study examined the impacts of pin-to-pin separation, rod-to-bone separation, and the number of connecting rods on a fixator's control of fracture site micromotion. Mechanical tests were performed on fixator constructs with a Zwick-Roell Z250 machine and a videoXtens digital camera within Warwick Manufacturing Group's Materials Engineering Centre. Constructs incorporated realistic synthetic Sawbones as surrogates for cadaveric bones. Results revealed that the addition of two transverse rods enhanced the fixator's control over localised micromotion more than any other modification. In fact, it reduced the micromotion at the superficial, intermediate and deep sections of the fracture site by 8%, 34% and 7% respectively. Conversely, the construct with the highest rod-to-bone separation (60 mm, as opposed to the 40 mm baseline) permitted 99%, 102% and 88% more micromotion than the standard construct at the aforementioned positions.

[1] X. Jia et al., "How Does the Stress in the Fixation Device Change during Different Stages of Bone Healing in the Treatment of Fractures?", 2024, Orthopaedic Surgery, 16(11), pp.2821-2833.
[2] G. Vicenti et al., "Micromotion in the fracture healing of closed distal metaphyseal tibial fractures.", 2014, Injury, 45(6), pp.s27-s35.

21

Poster Session, Level 2 Foyer, September 5, 2025, 12:00 - 13:00

Teager-Kaiser Energy Operator method for gait event detection during free-living ambulation

Johnson T[1], Kuntapun J[1], Childs C[1], Kerr A[1]
[1]University Of Strathclyde

Measuring free-living gait parameters with wearable sensors has the potential to support personalised rehabilitation [1]. There are challenges to meet the accuracy of laboratory based measurements [2], particularly in disabled populations. The aim of this study is to test the validity of a novel temporal gait measurement technique that uses the Teager-Kaiser Energy Operator (TKEO) previously developed for Huntington's disease populations [3]. The TKEO technique combines the first and second derivatives of the acceleration signal [4] to detect the timing of two gait events (initial contact (IC) and foot off (FO)). It is hypothesised that the TKEO technique will perform to the standards set out by previous work, with acceptable error for stance and swing time calculation [3]. A validation study was carried out with healthy participants (n=2, age =26+/-2) performing 6 different walks at two speeds while wearing a physical activity monitor (Pal Technologies, Glasgow, Uk) validated for thigh location and a laboratory grade measurement device (Delys, Boston, USA). There was a high level of agreement between the two systems for stance and swing time calculations (limits of agreement), see bland-Altman plots (figure 1). The high level of agreement justifies the use of this novel TKEO technique but needs to be tested with larger clinical samples before it can be exploited for rehabilitation purposes. Future plans include additional validation between the TKEO technique with a motion capture system (Vicon, Oxford, UK), and validation for stroke-affected free-living gait measurement with the TKEO technique.

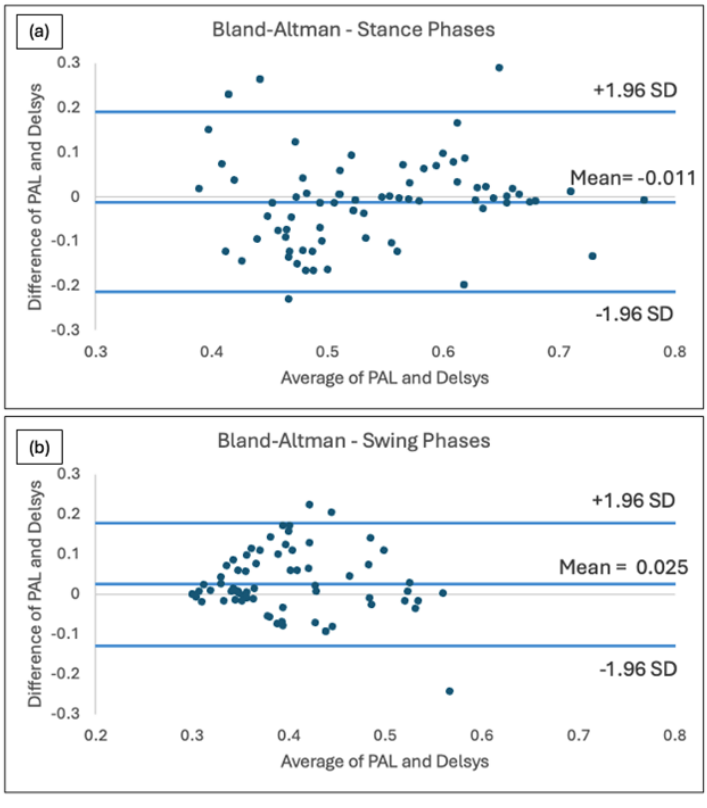

Figure 1 – Bland-Altman plots featuring system comparisons for (a) stance time calculation and (b) swing time calculation.

1.Harris, N.R. and D. Sthapit. 2016 IEEE Sensors Applications Symposium (SAS). 2016.
2.Mc Ardle, R., et al. Sensors, 2021. 21, DOI: 10.3390/s21030813.
3.Lozano-García, M., et al., IEEE Neural Systems and Rehabilitation Engineering, 2024. 32: p. 2239-2249.
4.Flood et al, 2020. IEEE Biomedical Engineering, 67(3): p. 658-666.

23

Poster Session, Level 2 Foyer, September 5, 2025, 12:00 - 13:00

Developing novel quantitative approaches to image cell and tissue elastic properties

Cunningham R[1], Bagnaninchi P[1]
[1]Centre for Regenerative Medicine, University Of Edinburgh

The mechanical properties of a cell orchestrate a wide range of critical biological processes. Despite this central regulatory role in cellular function, there are few methods available to easily quantify simple mechanical properties, such as elasticity, within a cell [1]. Current methods for quantifying cellular elasticity, such as atomic force microscopy and optical tweezers, require complex steps involving physical contact and manipulation of cells, limiting ease-of-use and practical application.

In contrast, we are leveraging recent findings in optical coherence elastography [2] to develop a microscopic approach to measure and image the elastic properties of cells and their microenvironment. First, we demonstrated its feasibility in silico at the microscopic scale. Then, we generated well characterised optical phantoms mirroring the simulated microstructures. Gel (GelMa, PEGDA) mechanical properties were modulated with a bioengineering platform (Primo, Alvelole) and imaged with a DIC microscope. Finally, after reconstructing the phase [3], we showed that a debiased passive elastography algorithm was able to retrieve the elastic profile of the optical phantoms. We use a range of microstructured optical phantoms to assess potential and limitations of our novel approach.

[1]Wu PH, et al. A comparison of methods to assess cell mechanical properties.NatMethods.2018;15(7):491-498.
[2]Mason JH, et al. Debiased ambient vibrations optical coherence elastography to profile cell, organoid and tissue mechanical properties.CommunBiol.2023;6(1):543.
[3]Koos K, et al. DIC image reconstruction using an energy minimization framework to visualize optical path length distribution.SciRep.2016;6:30420.

25

Poster Session, Level 2 Foyer, September 5, 2025, 12:00 - 13:00

Impact of Endoplasmic Reticulum Stress on Cell Biomechanics via Molecular Crowding

Behr L[1], Monnier S[2], Overby D[1]
[1]Imperial College London, [2]Institut Lumière Matière

The mechanical properties of cells influence cellular function in health and disease. One key factor influencing cellular mechanics is macromolecular crowding, where densely packed biomolecules within the cytoplasm influence cellular mechanical properties such as membrane curvature [1].
We hypothesise that the endoplasmic reticulum (ER), as one of the largest organelles, plays a key role in cytoplasmic crowding. To test this hypothesis, we induce ER-stress with thapsigargin, which is known to increase ER volume, and we measure the osmotically inactive volume fraction (phi) within the cell. To measure phi, we measured cell volume (V) over a range of osmolarities (P; 300-3000 mOsm) using Fluorescence eXclusion microscopy (FXm) [2], and applied the Boyle van't Hoff law (BvH)[3]. Experiments used HeLa cells (N=36 for both thapsigargin and vehicle-treated controls)
The relationship between V/Vo and Po/P followed the linear prediction of the BvH law, where Vo and Po represent the volume and osmolarity under isotonic baseline conditions. Following treatment with thapsigargin (5µM, 5 hrs), cell volume increased but not significantly by 8.5% (p=0.1). However, the osmotically inactive volume increased by 16% (p=0.004).
These experiments support the notion that ER stress may lead to macromolecular crowding within the cell. Ongoing studies are investigating the changes in ER volume and cell stiffness.

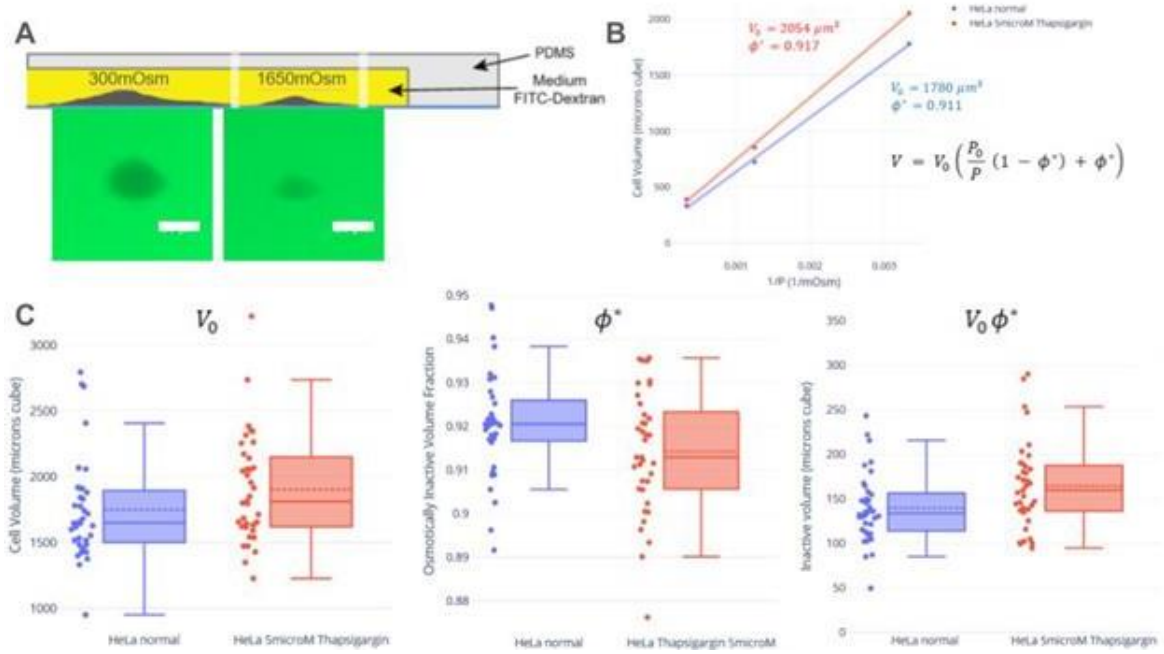

Figure: ER Stress Increases Osmotically Inactive Volume in HeLa Cells Measured by Fluorescence Exclusion Microscopy

[1] Stachowiak et al., 2012, Nature Cell Bio, 14, 944-949.
[2] Cadart et al., 2017, Methods in Cell Biology, 139, 103–120.
[3] Katkov II, 2011, Cryobiology, 62(3), 232-241.

27

Poster Session, Level 2 Foyer, September 5, 2025, 12:00 - 13:00

Mapping the Micromechanical Properties of Brittle Bones: A Comparative Study of High-Speed and Quasi-Static Nanoindentation for Osteogenesis Imperfecta Murine

Byrne A[1], Bohns F[1], Canty-Laird E[1], Akhtar R[1]
[1]University of Liverpool

Osteogenesis imperfecta (OI) is a genetic connective tissue disorder characterised by bone fragility and frequent fractures. The osteogenesis imperfecta murine (oim) model produces homotrimeric type I collagen, leading to impaired matrix organisation and a brittle bone phenotype [1]. This study investigated the application of high-speed nanoindentation (HSN) for mapping micromechanical properties in femoral bone from wild-type (WT) and oim mice. HSN enables rapid acquisition of spatially resolved maps of elastic modulus (E) and hardness (H), offering advantages over conventional quasi-static nanoindentation (QSN) for high-throughput testing [2]. HSN yielded higher E and H values than QSN, likely due to reduced sensitivity to viscoelastic effects. Genotype differences were more clearly resolved under HSN, with oim heterozygotes showing significantly elevated stiffness and hardness relative to WT. In contrast, oim homozygotes exhibited reduced stiffness, potentially due to cortical thinning and porosity. Correlation between E and H was strongest under QSN; HSN data showed greater scatter. Spatial alignment of mechanical maps with backscattered electron (BSE) images revealed regions of low E and H corresponding to osteocyte lacunae. While Ca/P ratios remained stable across genotypes, BSE imaging showed bright, irregular bands in oim homozygous bone, suggestive of local calcium enrichment not fully captured by semi-quantitative energy-dispersive X-ray spectroscopy (EDS). These findings support the view that bone fragility in oim arises primarily from disrupted matrix organisation [3]. This study establishes HSN as a powerful technique for evaluating microscale mechanical heterogeneity in preclinical models of brittle bone disease, with implications for matrix-targeted therapies.

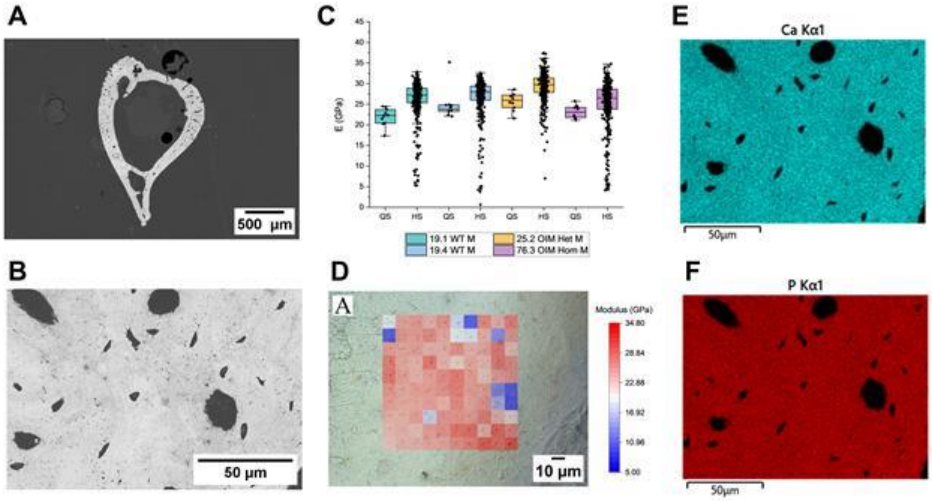

Representative BSE, EDS and HSN maps showing porosity, calcium distribution and spatial variation in modulus within oim homozygous cortical bone.

[1] K. J. Lee et al., 2022, Dis. Model. Mech., vol. 15, no. 9, pp. dmm049428.
[2] E. Rossi et al., 2023, Curr. Opin. Solid State Mater. Sci., vol. 27, no. 5, pp. 101107.
[3] A. Carriero et al., 2014, J. Bone Miner. Res., vol. 29, no. 6, pp. 1392–1401.

31

Poster Session, Level 2 Foyer, September 5, 2025, 12:00 - 13:00

Using Hierarchical Phase-Contrast Tomography to Map Blood Vasculature in the Human Kidney

Nandanwar S[1], Rahmani S[1], Walsh C[1], Long D[2], Jafree D[2,3], Lee P[1], Tafforeau P[4], Jacob J[5], Bellier A[6], Ackermann M[7,8], Dejea I Velardo H[4], Urban T[4], Brunet J[4], Jonigk D[9,10], Shipley R[1]

[1]Department of Mechanical Engineering, University College London, [2] UCL Great Ormond Street Institute of Child Health,, [3]UCL MB/PhD Programme, Faculty of Medical Science, [4]European Synchrotron Radiation Facility, [5]Satsuma Lab, Centre for Medical Image Computing, UCL, [6]Department of Anatomy (LADAF), Grenoble Alpes University, [7]Institute of Anatomy, University Medical Center of the Johannes Gutenberg University Mainz, [8]Institute of Pathology and Department of Molecular Pathology, Helios University Clinic Wuppertal, University of Witten-Herdecke, [9]Institute of Pathology, RWTH Aachen Medical University, [10]German Center for Lung Research (DZL), Biomedical Research in Endstage and Obstructive Lung Disease Hannover (BREATH)

The patterning of the renal vasculature is crucial for kidney filtration and reabsorption. Structural changes in the vasculature are commonly observed in renal pathologies such as hypertension and diabetes, which can impair kidney function. This highlights the need for advanced techniques that allow for detailed, three-dimensional imaging and quantification of blood vessels within intact organs. It has not previously been possible to capture the entire vascular network of the adult human kidney. We hypothesised that Hierarchical Phase-Contrast Tomography (HiP-CT), a synchrotron X-ray imaging technique with exceptional resolution, would address this need.

By combining label-free HiP-CT with network topology analysis, we mapped vessels from the main renal artery through interlobular branches. Although human and rodent vascular topologies are broadly comparable, humans exhibit a more rapid decline in vessel radius from hilum to cortex and deviate from Murray's Law governing diameter-branching relationships. Regional analyses across hilum, cortex, medulla, and intermedullary regions revealed how structural differences in the vasculature correspond to the unique functional roles of each kidney region. We are now applying the same HiP-CT pipeline to kidneys from young and aged mice to characterise age-dependent vascular remodelling. Topological indicators and fractal indices will be extracted to quantify complexity of the networks. Collectively, these findings demonstrate that HiP-CT is a powerful imaging tool that bridges anatomical scales, offering valuable insights into the unique vasculature of the kidney. This technique has broad implications for renal physiology and tissue engineering, with the potential to improve our understanding and treatment of renal diseases.

Poster Session, Level 2 Foyer, September 5, 2025, 12:00 - 13:00

Machine Learning in PSA and Machine Vision in MRI Prostate Cancer Screening: A Comprehensive Literature Review

Basude D[1], Bennett R[1], Tse Z[1]
[1]Queen Mary University Of London

Currently, there is no effective screening method for detecting prostate cancer. Previously, this has relied on Prostate-Specific Antigen (PSA) testing and Magnetic Resonance Imaging (MRI), both of which face limitations in specificity and accessibility respectively. This review explores literature from the last 5 years to assess how integrating Artificial Intelligence (AI) with PSA and MRI influences the sensitivity and specificity of detection of prostate cancer (Figure 1). By integrating PSA kinetics, density, and clinical variables, machine learning models can improve risk stratification—reducing unnecessary biopsies by up to 50% while maintaining high sensitivity for clinically significant cancers. Recent advances in ensemble learning and explainable AI improves PSA's reliability (from 50.6% to 74.7% [1]), enabling personalised screening protocols without sole reliance on invasive follow-ups. MRI remains the gold standard for lesion detection. However, combining MRI with machine vision offers superior spatial resolution (89% PI-RADS concordance [2]) and the ability to identify radiomic biomarkers predictive of tumour aggressiveness. AI-enhanced MRI reduces inter-reader variability in PI-RADS scoring and decreases false-positive rates by optimising biopsy decisions. The future lies in hybrid approaches, where machine learning-refined PSA screening triages patients for MRI, balancing cost-efficiency with diagnostic precision. While PSA-based AI models show promise for large-scale, low-resource settings, MRI-guided machine vision delivers unmatched localization and risk assessment. Multi-modal models that combine PSA levels with MRI radiomics improve risk stratification, guide treatment planning, and streamline clinical workflows. However, challenges such as data standardization, model complexity and the need for large-scale validation remain.

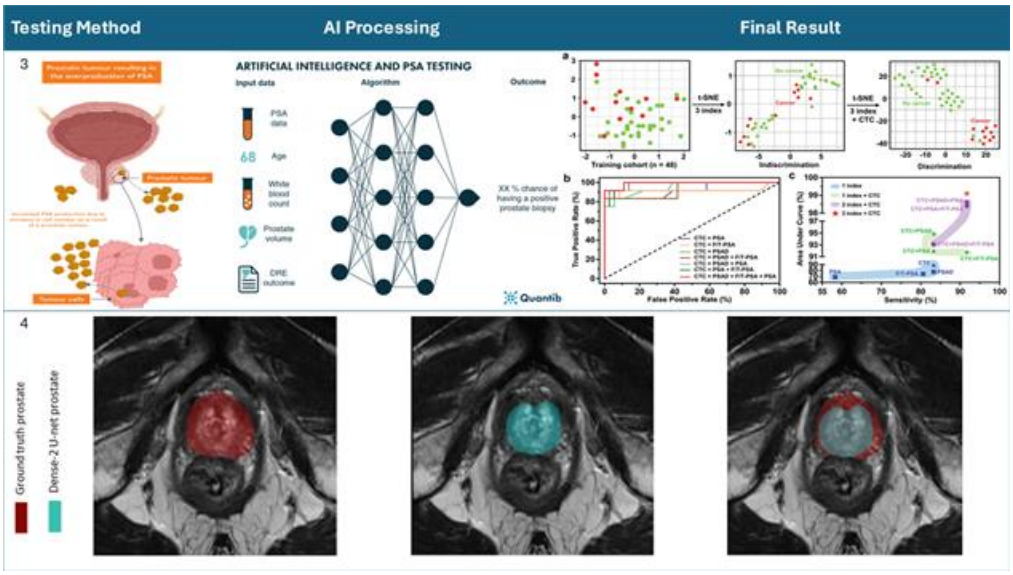

Figure 1: Application of AI to PSA [3] and MRI [4] testing

[1] N. Martelin et al., 2024, The Prostate, vol. 84, no. 9, pp.842–849.
[2] N. Sushentsev et al., 2022, Insights Imaging, vol. 13, no. 59.
[3] B. Wang et al., 2021, Researchgate, vol. 33, no. 40.
[4] N. Aldoj et al., 2020, Sci Rep, vol. 10, no. 14315.

35

Poster Session, Level 2 Foyer, September 5, 2025, 12:00 - 13:00

Hypoxia and Vascular Phenotypes in TNBC Xenografts: A Platform for Imaging-Based Evaluation Using Size-Fractionated Microbubbles

Rengganis A[1,2], Campbell K[1,2], Blyth K[1,2], Brown E[1,2], Bloom A[1,2], Nixon C[2], Cadden B[2], Mulvana H[3], Lewis D[1,2]
[1]University Of Glasgow, [2]Cancer Research UK – Scotland Institute, [3]James Watt School of Engineering, University of Glasgow

Triple-negative breast cancer (TNBC) is a heterogeneous, aggressive disease with limited targeted therapies. Vascular phenotype and hypoxia differences among TNBC subtypes may inform imaging-based monitoring [1,2]. Markers like CD31, α-SMA, CAIX, and VEGF characterize vascular pathology, but their in vivo imaging correlates remain unclear. Ultrasound contrast agents (UCAs), especially microbubbles, present a non-invasive means to evaluate tumour vasculature. We investigated how microbubble size distribution affects acoustic imaging and its validation against vascular features. Xenograft tumours from MDA-MB-231 (highly invasive) and MDA-MB-468 (less invasive) TNBC lines were established in female mice (n=4/group). Histological analysis using H&E and immunohistochemistry for CD31, α-SMA, CAIX, and VEGF was conducted. Vessel and hypoxia features were quantified with HALO v3.6 image analysis. Unpaired t-tests were used for statistical comparison. Microbubble size fractionation via low g-force centrifugation was performed to optimize imaging for future in vivo work [3]. Vessel density did not differ significantly, but MDA-MB-231 tumours showed smaller vessels (mean 27.1 µm vs. 34.8 µm, $p<0.05$), lower α-SMA coverage (0.12 mm2 vs. 0.29 mm2, $p<0.05$), greater hypoxia (CAIX: 45.2% vs. 28.0%, $p=0.08$), and higher VEGF area (0.15 mm2 vs. 0.09 mm2, $p=0.60$), indicating vessel immaturity and reduced perfusion. Size-fractionation of SonoVue (Bracco S.A.) microbubbles revealed two populations: <1.5 µm and >2 µm. These findings underscore vascular and hypoxic distinctions between TNBC models and support the use of contrast-enhanced ultrasound to define acoustic signatures of vascular dysfunction.

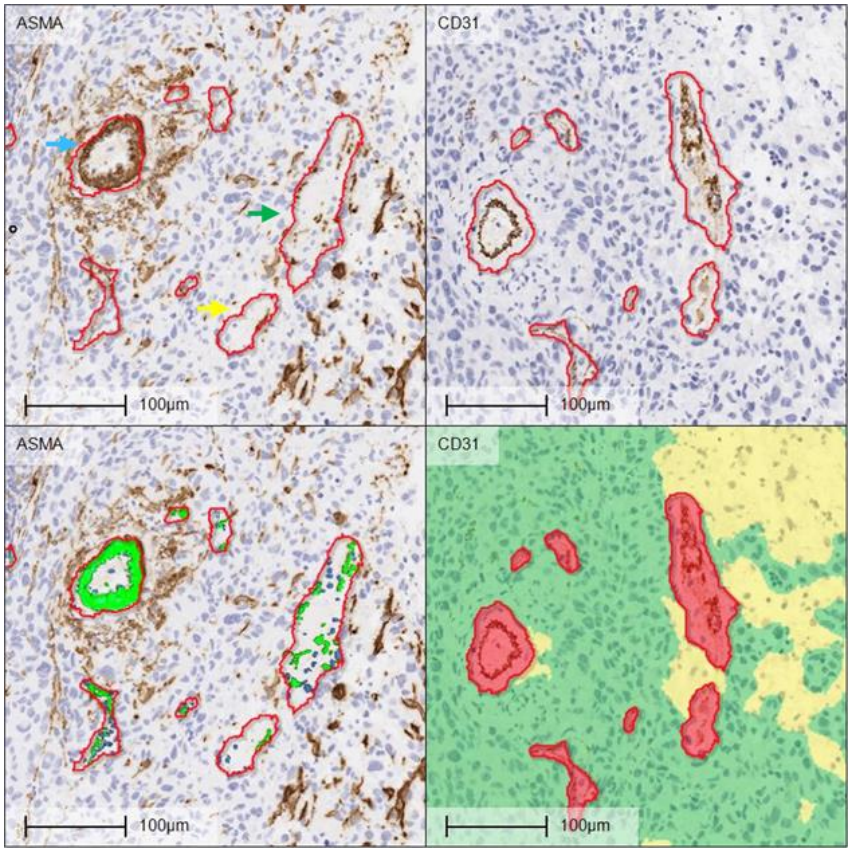

Representative vessels showing mature (blue), partially mature (green), and immature (yellow) phenotypes based on CD31 and α-SMA staining

[1] J.C. Forster et al., 2017, Hypoxia (Auckl)., vol. 5, pp. 21–32.
[2] G.L. Semenza, 2016, Biochim. Biophys. Acta Mol. Cell Res., vol. 1863, pp. 382–391.
[3] J.A. Feshitan et al., 2009, J. Colloid Interface Sci., vol. 329, no. 2, pp. 316–324.

37

Poster Session, Level 2 Foyer, September 5, 2025, 12:00 - 13:00

Dynamics underlying auditory working memory

Dheerendra P[1,2], Griffiths T[2,3]
[1]University Of Glasgow, [2]Newcastle University, [3]University College London

We aim to understand the dynamics underlying auditory working memory for maintaining 'simple' tones. We recorded MEG in 17 subjects while they maintained one of the two presented tones (or ignore both in the control condition). After 12s, subjects compared the pitch of a test tone with the maintained tone. Analysis of evoked responses showed persistent activity throughout maintenance compared to the pre-stimulus silent baseline but only at the start of maintenance when compared to the control condition. The evoked response during maintenance was source localised against baseline to bilateral auditory cortex. Analysis of induced responses showed suppressed alpha in the left auditory cortex, enhanced theta in medial prefrontal cortex (mPFC), and enhanced beta in cerebellum. In a second experiment, 19 new subjects were presented with a tone and a Gabor patch and a retro-cue indicating whether to maintain auditory or visual information for 12s. Analysis of the induced responses in auditory condition yielded similar results. Connectivity analysis showed that the theta activity in mPFC was phase-locked to left hippocampus and left auditory cortex. The beta activity in cerebellum was phase-locked to left IFG and correlated to subject's task accuracy. Using MVPA, a LDA classifier trained to decode the contents of AWM using beta PLV with right cerebellum as features identified right Anterior Cingulate Gyrus. Further, the decoder performance at Right STG & MTG was correlated to subject's task accuracy. Our data clearly shows a network of brain areas consistent with previous fMRI and ECoG experiments [1, 2].

[1] Kumar, S., et al., 2016. A brain system for auditory working memory. Journal of Neuroscience, 36(16), pp.4492-4505.

[2] Kumar, S., et al., 2021. Oscillatory correlates of auditory working memory examined with human electrocorticography. Neuropsychologia, 150, p.107691.

39

Poster Session, Level 2 Foyer, September 5, 2025, 12:00 - 13:00

Two-phase Modeling of RBC and CFL Dynamics in Idealised and Subject-Specific Microvessels

Wisitponchai T[1], Wu J[1], Kazakidi A[1]
[1]University Of Strathclyde

Modeling blood flow in realistic microvessels remains challenging, limiting insight into how flow relates to vascular health and disease [1]. We addressed these challenges by developing a two-phase blood flow model, which includes a red blood cell (RBC) phase and a cell-free layer (CFL), to investigate computationally blood distribution and mechanical responses. The model was implemented in a symmetrical 3D Y-shaped bifurcation and a non-planar mouse testicular bifurcation. With a parent diameter of 20 µm, the geometries were meshed using polyhedral and prismatic elements in Star-CCM+, and the two phases were simulated using the Eulerian Multiphase (EMP) method, with different rheological properties. The results indicated that a symmetrical annular CFL was formed due to drag and lift forces at the RBC-CFL interface, driven by high slip velocity near the vessel walls. These forces diminished at the bifurcation junctions but intensified downstream, shifting the RBC phase toward the centreline and promoting the CFL phase formation. Although asymmetry developed near the bifurcation, the CFL symmetry was gradually recovered at a long distance downstream of the bifurcation. These findings align with experimental data [2]. These findings were confirmed in the anatomically-realistic testicular bifurcation, where the curved segment upstream of the bifurcation, the wide bifurcation angle, and the shape of the bifurcation caused asymmetric lift and drag forces, resulting in asymmetric CFL and RBC phase distributions. Further downstream, despite the curved vessels, flow re-established into more symmetric patterns. Future studies could couple RBC dynamics with oxygen diffusion models to assess impacts on tissue perfusion.

[1] Alexy et al, “Physical properties of blood and their relationship to clinical conditions”, Front Physiol, 13:906768, 2022.
[2] Ng, Y.C., et al., 2016. American Journal of Physiology-Heart and Circulatory Physiology, 311(2):H487-H497.

41

Poster Session, Level 2 Foyer, September 5, 2025, 12:00 - 13:00

Thermal Dynamics within Lower Limb Prosthetic Sockets: A Computational Modeling Approach

Alhamam H[1], Masouros S[1], Bull A[1]
[1]Imperial College London

Thermal discomfort within prosthetic sockets is a commonly reported issue among lower limb amputees. It arises due to impaired thermoregulation and negatively affects long-term device use and the user's quality of life [1]. Prosthetic materials with poor thermal conductivity are thought to contribute to this disruption [2]. However, to date, little is known about how thermoregulation is altered in amputated limbs, particularly at the skin–socket interface. This study introduces a computational model developed to understand thermal behaviour at this interface and serve as a predictive tool to inform future socket designs. A finite-element model of a transfemoral limb was developed, combining simplified MRI-informed geometry with a liner–socket interface. The isolated-segment model was implemented in COMSOL Multiphysics using layered tissue domains representing skin, fat, muscle, and prosthetic components. The Pennes bioheat equation was applied to simulate internal heat transfer, including metabolic heat generation and blood perfusion. Passive heat loss through convection and radiation was applied to replicate environmental exchange. Tissue and material properties were defined from the literature. Simulations were performed under steady-state, resting physiological conditions, and resulting thermal distributions were noted. Heat accumulation was most pronounced over large muscle regions, following a proximal-to-distal gradient that aligns with previously reported experimental results [3]. These findings confirm the model as a reliable baseline for incorporating active thermoregulatory mechanisms, including sweating and activity-related responses. The model is intended to support the development of prosthetic sockets that enhance thermal comfort and reduce complication risks across varying environmental and material configurations.

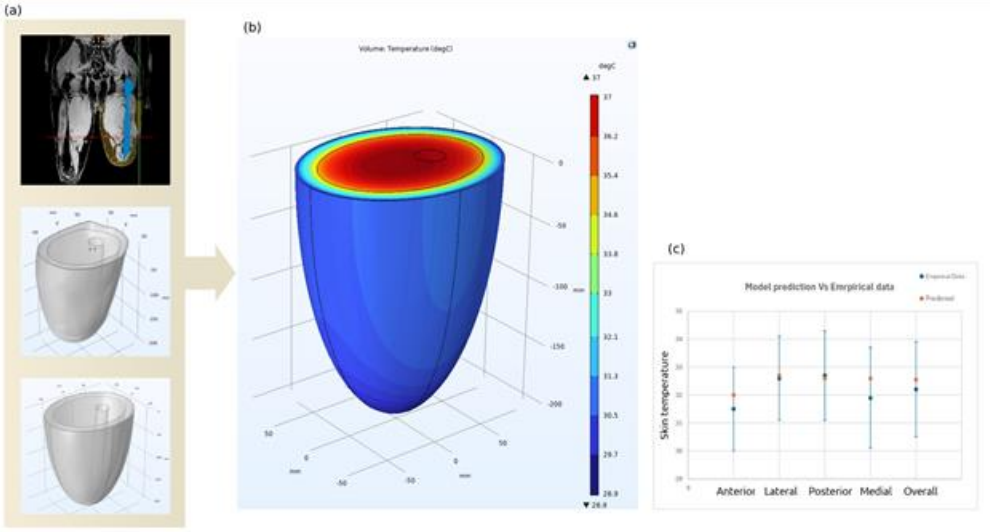

Figure: (a) Geometry extraction, (b) Predicted temperature distribution, and (c) Model prediction compared to empirical skin temperature data.

[1] K. Ghoseiri et al., 2014, J Rehabil Res Dev, vol. 51, no. 6, pp. 855–868.
[2] G. K. Klute et al., 2007, Prosthet Orthot Int, vol. 31, no. 3, pp. 292–299.
[3] R. N. Harden et al., 2008, Pain Pract, vol. 8, no. 5, pp. 342–347.

Poster Session, Level 2 Foyer, September 5, 2025, 12:00 - 13:00

Visualisation of 3T MRI Scanner Magnetic Field Based on QR Code Tracking

Li H[1], Acosta E[1], Tse Z[1]
[1]Queen Mary University Of London

Medical imaging technology has become essential for health care, early diagnosis, and image-guided intervention. Standard medical imaging modalities include X-ray, computed tomography (CT), ultrasound and magnetic resonance imaging (MRI). MRI as a non-invasive medical examination has been widely used, benefiting from its superior soft tissue contrast and anatomic detail [1]. Based on the physical principle of the MRI modality, a high-quality image can be obtained through an intense magnetic field. However, the strong magnetic field has a potential safety hazard to its working environment. The ferromagnetic material may accelerate toward the MRI scanner in such a strong magnetic field, and other potential hazards include applied torque and radiofrequency (RF) energy. 5 Gauss (0.5 mt) is considered a threshold for the implanted device when accessing the magnetic field [2]. It is valuable to provide a notification to those in the MRI environment to prevent potential damage. Smartphones, as easily reachable devices integrated with magnetometers, cameras and built-in displays, make them valuable for the 5 Gauss line visualisation. Open Source Computer Vision Library (OpenCV) is an open-source computer vision and image processing library. It provides the feature of identifying the QR code's information, and by combining it with computer vision technology, we were able to obtain the relative position between the QR code and the smartphone camera. By matching the relative position and the magnetic field collected by the smartphone, we were able to reconstruct and visualise the magnetic field distribution through the smartphone.

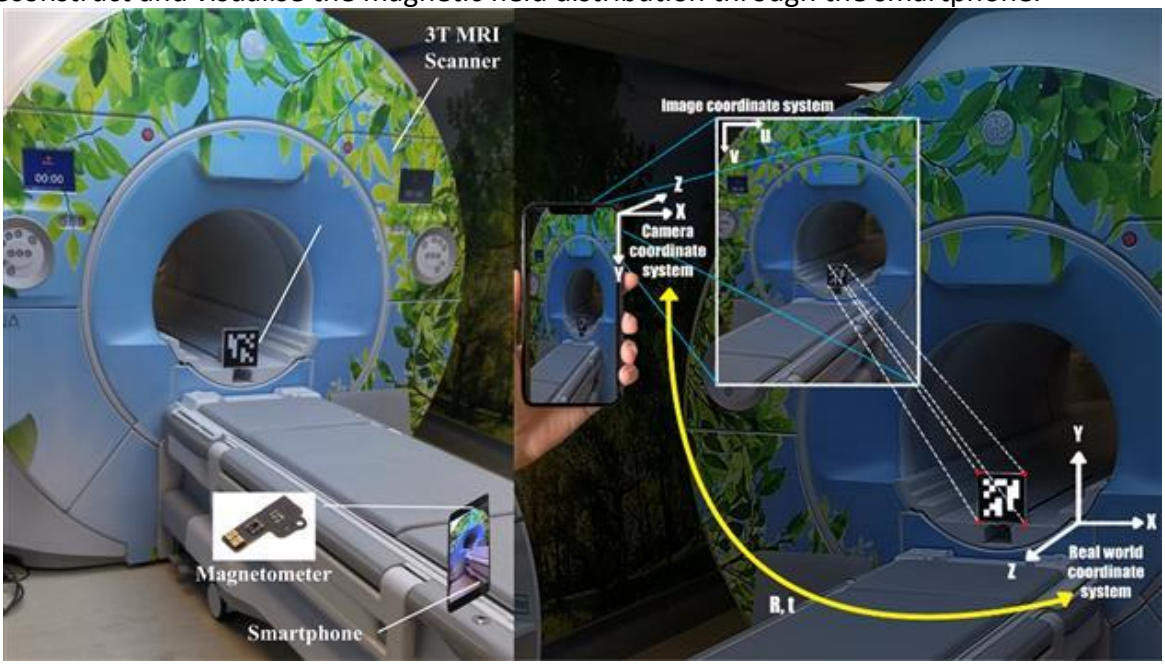

[1] E. Bercovich and M. C. Javitt, Rambam Maimonides Med. J., vol. 9, no. 4, p. e0034, Oct. 2018, doi: 10.5041/RMMJ.10355.
[2] M. C. Steckner, D. Grainger, and G. Charles-Edwards, Magn. Reson. Med., vol. 92, no. 5, pp. 2237–2245, Nov. 2024, doi: 10.1002/mrm.30153.

45

Poster Session, Level 2 Foyer, September 5, 2025, 12:00 - 13:00

Monitoring Early-Stage Beta Amyloid Aggregation and Inhibition via Fluorescence Spectroscopy

Alshammari S[1]
[1]University Of Strathclyde, [2]Northern Border University

Beta-amyloid (Ab), a peptide fragment derived from amyloid precursor protein, consists of 39-43 amino acids. Its aggregation plays a central role in the pathogenesis of Alzheimer's disease (AD), with extracellular Ab oligomers and plaques serving as key pathological hallmarks. Early molecular detection of Ab oligomers is crucial for timely diagnosis and therapeutic intervention. Fluorescence spectroscopy is a powerful tool for probing Ab aggregation kinetics and amyloid formation. In this study, steady-state and time-resolved fluorescence spectroscopy have been employed to monitor early-stage aggregation of Ab40 and Ab42. An increase in the intrinsic fluorescence intensity of the beta-amyloid's single tyrosine (Tyr) residue was observed during aggregation. Fluorescence lifetime analysis revealed three decay components, with notable changes in pre-exponential factors, suggesting that time-resolved Tyr fluorescence may serve as a sensitive indicator of early Ab aggregation. Moreover, we investigated the effects of hen egg white Lysozyme (HEWL) and lysozyme-encapsulated gold nanoclusters (Lyz-AuNCs) [1,2] on Aβ40 aggregations. Persistently low Thioflavin T (ThT) fluorescence in the presence of HEWL or Lyz-AuNCs indicated effective inhibition of amyloid fibril formation. Notably, Lyz-AuNCs showed lower aggregation-inducing potential than HEWL. Additionally, the fluorescence intensity of Lyz-AuNCs decreased linearly with increasing Aβ40 concentration. Lifetime measurement and Stern-Volmer analysis confirmed static quenching, indicating binding between Aβ40 and Lyz-AuNCs. The combined capability to inhibit amyloid fibril formation and exhibit intrinsic fluorescence makes Lyz-AuNCs a promising dual-function agent for both AD therapy and real-time fluorescence-based monitoring of Aβ accumulation and neuroinflammation.

1. N. Alkudaisi, et al., J. Mater. Chem. B 2019; 7(7): 1167-75

2. N. Alkudaisi, et al., J. Photochem. Photobiol. B 2019; 197:111540

Poster Session, Level 2 Foyer, September 5, 2025, 12:00 - 13:00

Low-cost Label Free Point of Care Biosensor: A Novel Approach for E. coli Biorecognition

Collins L[1], Henriquez F[2], Walker D[3], Corrigan D[1]
[1]University of Strathclyde, Centre for Advanced Measurement Science and Health Translation, Pure and Applied Chemistry, [2]Department of Civil and Environmental Engineering, University of Strathclyde, [3]Strathclyde Institute of Pharmacy and Biomedical Sciences, University of Strathclyde

Urinary tract infections (UTI) affect approximately 50% of females within their lifetime – making it among the most common infections worldwide [1]. Related healthcare management is a substantial expenditure, both in terms of diagnostics and the prescription of antibiotics for treatment. The main causative pathogen of UTI is uropathogenic Escherichia coli (UPEC), representing over 80% of cases [2]. Notably, increasing prevalence of antimicrobial resistance (AMR) among such bacteria complicates treatment of UTIs and therefore prognosis for patients is often more severe, exacerbating the economic, physical and mental impact. This phenomenon is amplified by the widespread exposure and incorrect prescription of antibiotics. Traditional, lab-based methodologies for UTI diagnostics require technical expertise, are costly and time consuming, causing delayed intervention and treatment, thereby risking progression of infection; and are therefore insufficient and inefficient. Consequently, development of a point-of-care (POC) device for rapid detection of UPEC is critical for minimising spread of multidrug resistant (MDR) uropathogenic bacteria; preventing further complications of infection; and reducing the overall cost of infection management. In this work, we are developing next generation biorecognition elements for UPEC, aiming to combine enhanced receptor specificity with the precision of electrochemistry. This poster will present initial progress with preliminary data demonstrating the potential for incorporation of established and new receptors for E. coli into a cost-effective impedimetric, label-free gold biosensor.

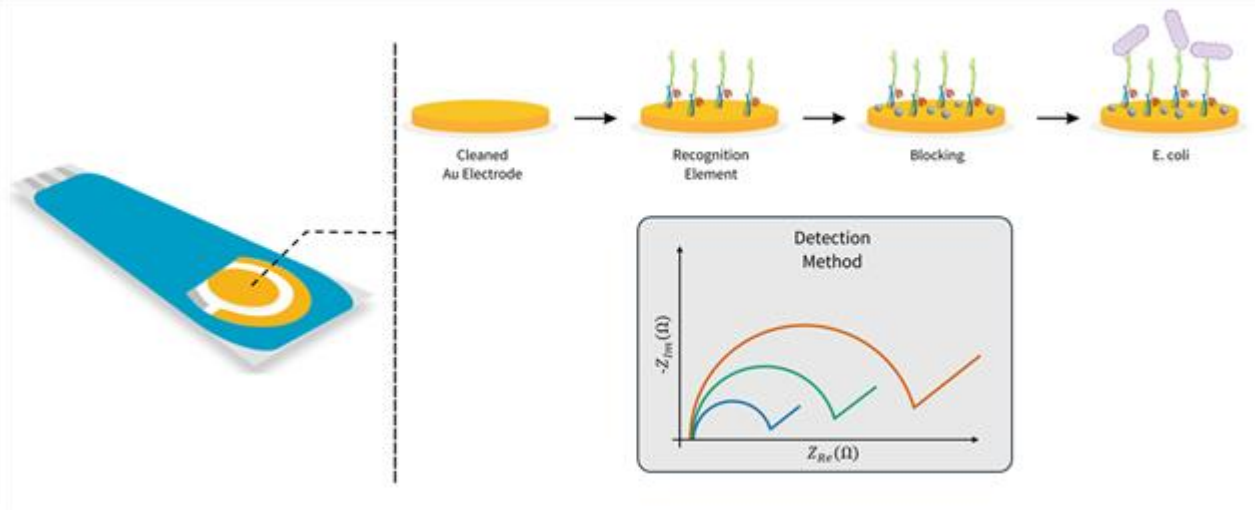

Figure: Schematic of the electrochemical biosensor fabrication process and detection of E. coli.

[1] Medina M et al., 2019, Ther Adv Urol., vol.11, pp 3-7.
[2] Kumar G et al., 2023, J Taibah Univ Med Sci., vol.18, no.6, pp 1527-1535.

Poster Session, Level 2 Foyer, September 5, 2025, 12:00 - 13:00

Analyzing non-faradic and faradaic electrochemical impedance spectroscopy for biosensor electrode functionalization

Koçoğlu S[1], McGleish O[2], Aslan Y[3], Reboud J[4], Cooper J[5]
[1]University Of Glasgow / Division of Biomedical Engineering, [2]University of Glasgow / Division of Biomedical Engineering, [3]Middle East Technical University / Department of Electrical and Electronics Engineering, [4]University of Glasgow / Division of Biomedical Engineering, [5]University of Glasgow / Division of Biomedical Engineering

The COVID-19 pandemic has underscored the critical global need for early detection of pathogens in human and animal health.Traditional molecular detection methods, such as Polymerase Chain Reaction(PCR) and Loop-Mediated Isothermal Amplification(LAMP), are commonly utilized due to their high levels of sensitivity, specificity, reproducibility, and reliability.However, these techniques often necessitate expensive reagents, complex equipment, and high-level biological expertise, which restricts their use and accessibility in areas with limited resources. Consequently, there is a continuing demand for alternative diagnostic methods that are affordable, easy to operate, and do not necessitate specialised tools or skills. Point-of-care(POC) technologies meet this demand, and electrochemical biosensors are particularly noteworthy because of their low cost, swift response times, high specificity, label-free and ease of use. These biosensors are capable of identifying various biomarkers like DNA, RNA, proteins, antibodies, or aptamers, depending on the target analyte.However, their preparation is often complex and with limited adaptability. Here we assess the performance of faradaic and non-faradaic Electrochemical Impedance Spectroscopy(EIS) techniques to evaluate the immobilisation of capture molecules on the surface.Experiments were performed using lithographically patterned gold electrodes of different electrode sizes(1, 2 and 4mm), and all were successfully coated with Bovine Serum Albumin(BSA), as a model protein. Remarkably, larger electrodes showed significant increase in impedance during non-faradaic EIS. Among the sizes evaluated, the 1 mm electrode exhibited the highest sensitivity for both EIS methods. Based on these results, the smaller electrode is suggested for future research focused on biomolecule detection due to its improved sensitivity and lower sample volume requirements.

Gold electrodes with dimensions of 4mm, 2mm and 1mm fabricated using photolithography technique

Poster Session, Level 2 Foyer, September 5, 2025, 12:00 - 13:00

Reversible Photothermal Control of DNA-Mediated Gold Nanoparticle Assemblies for Photonic PCR

Li Y[1], Reboud J[1], Cooper J[1]
[1]James Watt School of Engineering, University of Glasgow

Polymerase chain reaction (PCR) remains the gold standard for DNA amplification, including in medical diagnostics, yet traditional thermocyclers are often bulky and time-consuming, resulting in limitation in access and affordability. Photonic PCR, leveraging the plasmonic photothermal properties of gold nanoparticles (AuNPs), offers rapid, volumetric heating and holds promise for portable and faster amplification [1].
In this study, we developed a self-regulating system wherein AuNPs functionalized with thiolated single-stranded DNA (ssDNA) probes assemble via linker-mediated hybridization [2]. Upon illumination, plasmonic heating induces denaturation of the DNA duplexes, leading to disassembly of the nanoparticle aggregates [3]. This increases interparticle distances, reduces plasmonic coupling, and lowers local temperatures, theoretically allowing for rehybridization and autonomous cycling between assembly and disassembly.
We characterized the thermal stability of ssDNA–AuNP conjugates through temperature-dependent UV–vis absorbance and fluorescence measurements. The kinetics of linker DNA-induced aggregation were also investigated, revealing that linker length significantly influences assembly rates and stability. Sharp, reproducible and reversible melting transitions for DNA–AuNP networks were achieved using temperature cycling with an LED (against a control heater based on a Peltier element), compatible with PCR processing. However, repeated cycling resulted in partial degradation, likely due to the instability of Au–S bonds. Additionally, under photothermal excitation, the aggregates exhibited melting transitions similar to those under Peltier heating, suggesting that collective heating dominates over localized effects.
Future work will focus on enhancing spatial heat confinement to realize efficient, self-cycling photonic PCR systems for next-generation molecular diagnostics.

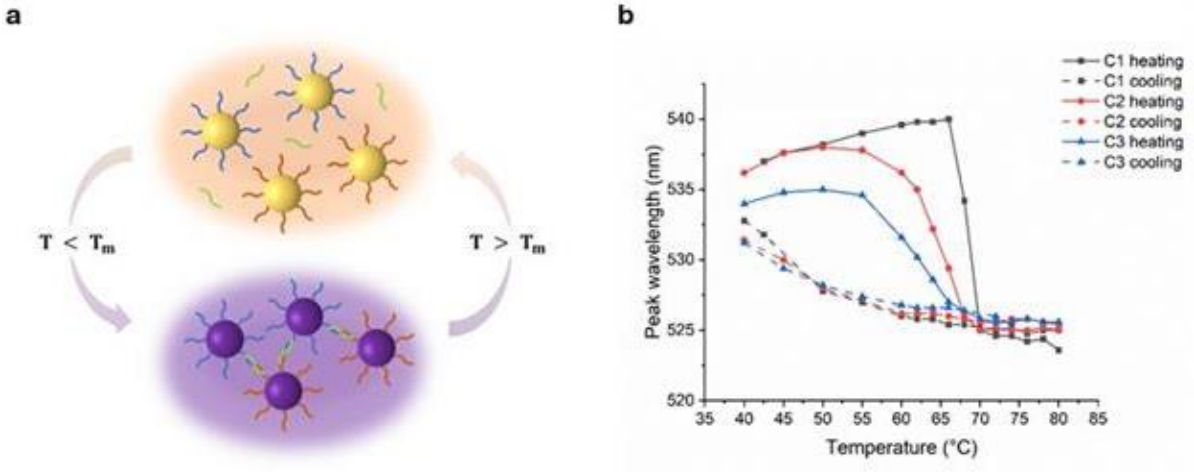

Figure 1 a) Schematic of reversible, heat-driven DNA-AuNPs assembly system. b) Peak wavelength shifts during thermal cycling.

[1] J. Cheong et al., 2020, Nat. Biomed. Eng., vol. 4, no. 12, pp. 1159–1167.
[2] X. Xia et al., 2020, Sci. Adv., vol. 6, no. 21, p. eaaz6921.
[3] M. Reismann et al., 2008, Small, vol. 4, no. 5, pp. 607–610.

Poster Session, Level 2 Foyer, September 5, 2025, 12:00 - 13:00

Development of a CRISPR/Cas-based biosensor for multiplexed RNA detection in living cells

Ostyk-Narbutt B[1], Reboud J[1], Cooper J[1]
[1]University Of Glasgow

Molecular biomarkers indicate both normal and abnormal conditions in human health, and as such, are significant in diagnosis and therapy. RNA molecules, particularly, are more sensitive, specific, affordable, and informative in comparison to other nucleic acids, making them a promising biomarker in studying disease progression [1]. For example, in regenerative medicine, detecting mRNA molecules secreted during tissue regeneration aids in therapeutic monitoring. Various methods exist for RNA detection, including RNA sequencing as the gold standard, as well as traditional fluorescent in situ hybridization techniques. However, these are limited by multiple factors, such as the fixing of cells, hindering the ability to study complex RNA dynamics in real-time. As such, this research focuses on the development of a tool for multiplexed RNA detection in vivo. CRISPR/Cas systems are powerful methods for nucleic acid detection, mainly due to their programmability and specificity, allowing their integration into synthetic genetic networks. Many CRISPR/Cas-based reporter systems rely on the generation of a fluorescent signal, which is then measured, corresponding to the detection of the target [2]. New RNA biosensing applications using such systems have been developed in vitro, such as via the reprogramming of tracrRNAs [3]. A large part of the early research will involve work with cell-free gene expression, as it provides a simplified and controlled way to develop and test CRISPR/Cas-based RNA sensors before moving to more complex in vivo systems. With further exploration of the programmability of CRISPR/Cas systems, this research aims to enable specific and multiplexed RNA biosensing in living cells.

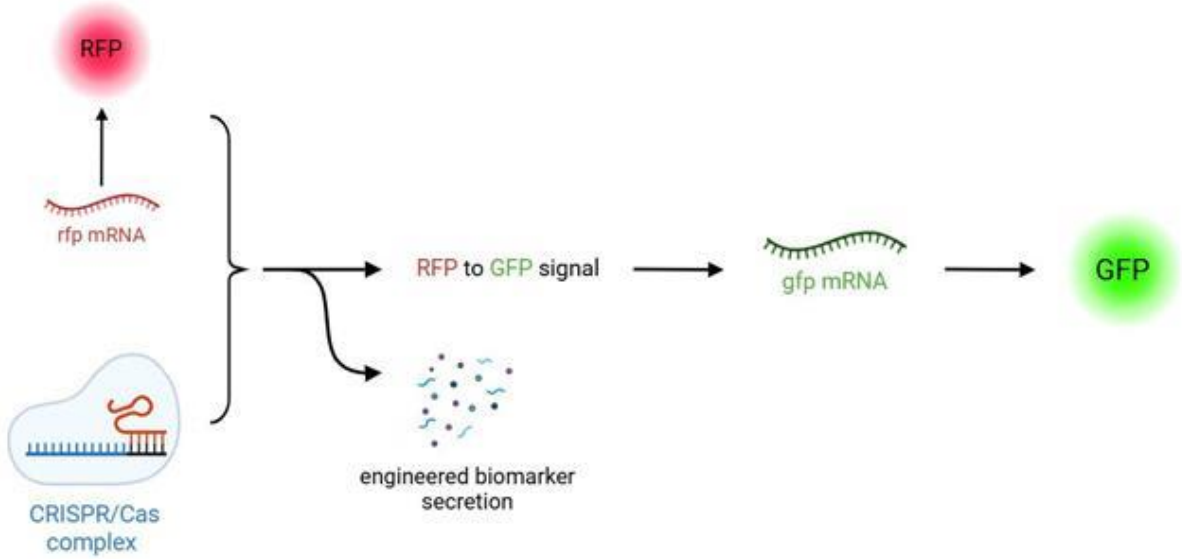

A synthetic genetic network demonstrating the designed outcomes from the interaction of a CRISPR/Cas complex and rfp mRNA target.

[1] X. Xi et al., 2017, Non-Coding RNA, vol. 3, no. 1, pp. 9.
[2] G. Jiang et al., 2024, Trends Biotechnol., vol. 42, no. 12, pp. 1601–1614.
[3] Y. Liu et al., 2022, Nat. Commun., vol. 13, pp. 1937.

55

Poster Session, Level 2 Foyer, September 5, 2025, 12:00 - 13:00

Verification and Validation of bio-signal acquisition systems for Swallowing Detection: Comparing two prototypes against a gold standard.

Uthayasooriyan N[1]
[1]King's College London

This study explores the verification and validation of two bio-signal (EMG and sound) acquisition systems designed for evaluating swallowing activity: one prototype developed for in-house studies only, the other (MotemaSens) with commercial intent. The two systems are evaluated against a gold standard (BIOPAC) to assess their performance in capturing electromyographic and acoustic data relevant to swallowing.

Both devices underwent bench tests for signal verification using known electrical inputs to evaluate gain accuracy, frequency response, and signal fidelity. MotemaSens consistently measured a 130 Hz input as 129.9 Hz across all amplitudes, displayed nearly identical gain across both EMG channels, and exhibited minimal crosstalk with correlation values between 0.009 and 0.3; while the in-house device showed slightly less accuracy, reporting values between 133 Hz and 135 Hz for a 130 Hz input, channel-to-channel gain differences that could be corrected through calibration, and crosstalk when channel 1 is connected and channel 2 is disconnected (r = 0.987).

In addition to the bench top tests, swallowing tasks were recorded in separate sessions for each system and the resulting EMG and microphone signals were compared against those obtained from the BIOPAC system. Although variability between trials limits strict signal alignment, both test systems successfully identified characteristic swallow-related features in time and frequency domains.

This work highlights the distinct yet complementary roles of verification and validation in biomedical device development, and raises a critical question: can a device that performs successfully in real-world use still be considered useful, even if it falls short in technical verification?

Poster Session, Level 2 Foyer, September 5, 2025, 12:00 - 13:00

Reversing the CRISPR/Cas process in isothermal DNA amplification for multiplex HPV detection

Zeng Z[1], Reboud J[1], Cooper J[1]
[1]University Of Glasgow

Early detection of high-risk human papillomavirus (HPV) is critical for early cervical cancer diagnosis and prevention of cancer progression.[1] While isothermal nucleic acid amplification tests (INAATs) offer an attractive alternative to polymerase chain reaction (PCR) in point-of-care applications, integrating CRISPR-based technologies enhances both specificity and sensitivity.[2] Conventional CRISPR-assisted INAATs typically rely on pre-amplification followed by Cas12a-mediated detection.[3] Here, we present an inverse workflow in which CRISPR/Cas12a cleavage precedes amplification to make the most of the tool's advantages in enhancing specificity, thus opening up large multiplexing capabilities. (Figure 1a) Target DNA is first cleaved by CRISPR/Cas12a, and loop amplification primers are designed to bind specifically to the resulting cleavage sites. Specifically, the terminal-specific primer (TSP) hybridises to the newly generated free 5' terminal and initiates hairpin-based amplification, which is further extended by auxiliary primers (P1/P2), enabling an exponential amplification mechanism analogous to LAMP. The amplification plot indicates this assay can detect $3.6x10^5$ copies/reaction of HPV16. (Figure 1b). This upstream use of CRISPR enhances target specificity and offers flexibility for multiplex detection in later assay stages. (Figure 1c) However, current limitations arise from suboptimal Cas12a cleavage efficiency, which constrains the assay's detection sensitivity. Future improvements will explore Cas protein variants with higher cleavage efficiency to improve assay performance.

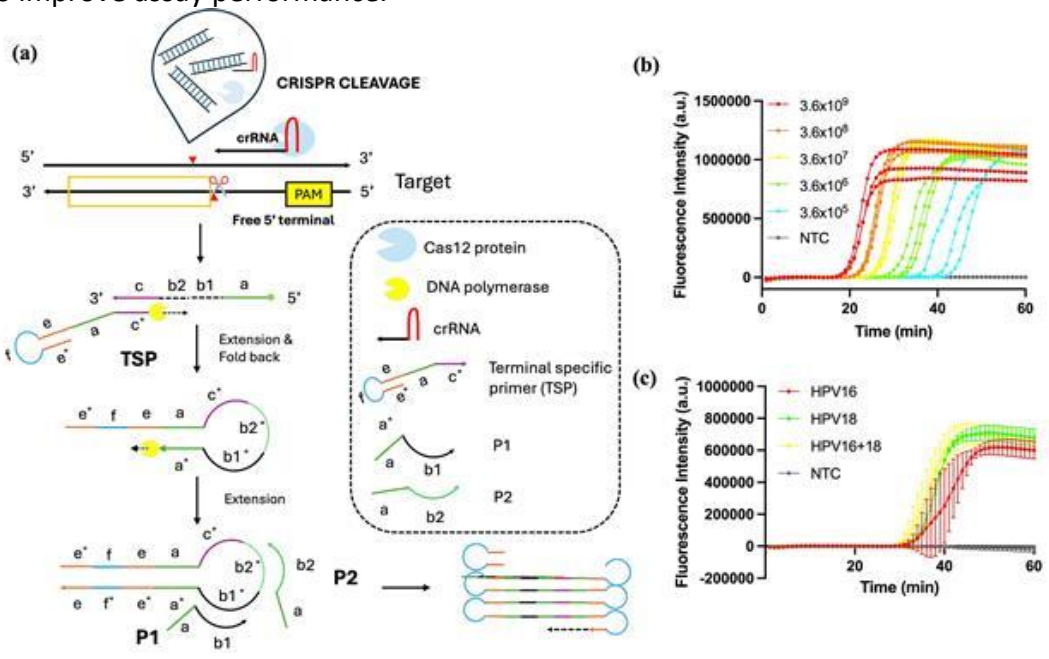

Figure1. (a). Schematic of the CRISPR/Cas12a-based loop amplification; (b). LOD of the HPV16 assay; (c). Multiplex HPV16 and 18 detections.

(1) Perkins, R. B. et al., JAMA 2023, 330 (6), 547.
(2) Lei, X. et al., Talanta 2024, 271, 125663.
(3) Pataer, P. et al., Sensors and Actuators B: Chemical 2024, 403, 135124.

59

Poster Session, Level 2 Foyer, September 5, 2025, 12:00 - 13:00

Investigating broad-spectrum antimicrobial efficacy of antibiotic-loaded PLGA coatings

Eccles S[1], Sherwood E[1], Maclean M[1], McCormick C
[1]University Of Strathclyde

Antibiotic-loaded poly(lactic-co-glycolic acid) (PLGA) coatings are a promising solution for prevention of the severe ongoing healthcare challenge that is medical device infection [1]. It is critically important that drug loading be optimised in these coatings, to ensure that local drug concentrations achieved at the implant-tissue interface are effective against pathogens, yet not toxic to patients' own cells. This study investigates the antimicrobial efficacy of a range of PLGA:antibiotic coatings (using different antibiotic types and ratios), as a first step in determining broad-spectrum efficacy of different coating compositions. The minimum inhibitory compositions will also be identified as it is critical that coatings for clinical use do not contain sub-lethal concentrations of antimicrobials, as this could encourage the development of antimicrobial resistance. Glass coverslips and medical grade 316L stainless steel 'coupons' were coated in 10% w/v solutions of PLGA (50:50 lactide:glycolide, Mw=30,000-60,000) and antibiotics, at PLGA:antibiotic ratios ranging from 50:50 to 99:1. A modified disc diffusion method, involving coated samples (n=3) being incubated on seeded agar plates, was used to assess efficacy against a panel of Gram-positive and Gram-negative bacterial species, including S. aureus and P. aeruginosa. Results demonstrate successful inhibition of bacteria, with higher inhibition from higher drug-loading coatings. Efficacy was also affected by the type of antibiotic, with rifampicin demonstrating greater efficacy against Gram-positive than Gram-negative species. This work highlights the need for consideration of the coating composition to ensure appropriate antibiotic types/levels are utilised to ensure broad-spectrum efficacy.

[2] Fraser et al., 2025, in Proceedings of IEEE Engineering in Medicine and Biology Conference (EMBC) 2025, awaiting publication, accepted May 2025.

61

Poster Session, Level 2 Foyer, September 5, 2025, 12:00 - 13:00

Towards Assessing Patient Eligibility for Optical Neural Interfaces: A Simulation Approach

Sajida H[1], Kallepalli A[1,2]
[1]Department of Biomedical Engineering, University of Strathclyde , [2]School of Physics and Astronomy, University of Glasgow

Optical neural interfaces (ONIs) offer a promising, non-invasive alternative to electrical neural interfaces, especially those based on functional near-infrared spectroscopy (fNIRS), but their performance is affected by biological factors such as skin pigmentation and hair texture, leading to potential exclusion of diverse populations [1]. This project aimed to investigate how varying wavelengths, melanin concentrations, and incidence angles affect light penetration in tissues of the head, using Monte Carlo simulations. Monte Carlo simulations [2] were done on a six-layer slab mode (epidermis, dermis [3], skull, Cerebral Spinal fluid, grey matter and white matter), across six concentrations of melanin on the Fitzpatrick scale, across wavelengths spanning 500- 1000 nm and angles 90°, 60°, 45°, 30°. Results demonstrated that higher melanin concentrations significantly attenuate photon penetration, particularly at lower wavelengths, and that oblique incidence angles further limit light delivery to deeper tissues. Wavelengths in the longer NIR range improved penetration depth across all melanin types. This study highlights the importance of wavelength selection, angle of incidence when developing ONIs to ensure equitable performance across diverse patient populations. The framework developed here could inform better eligibility assessments and promote equitable neurotechnology applications across diverse populations.

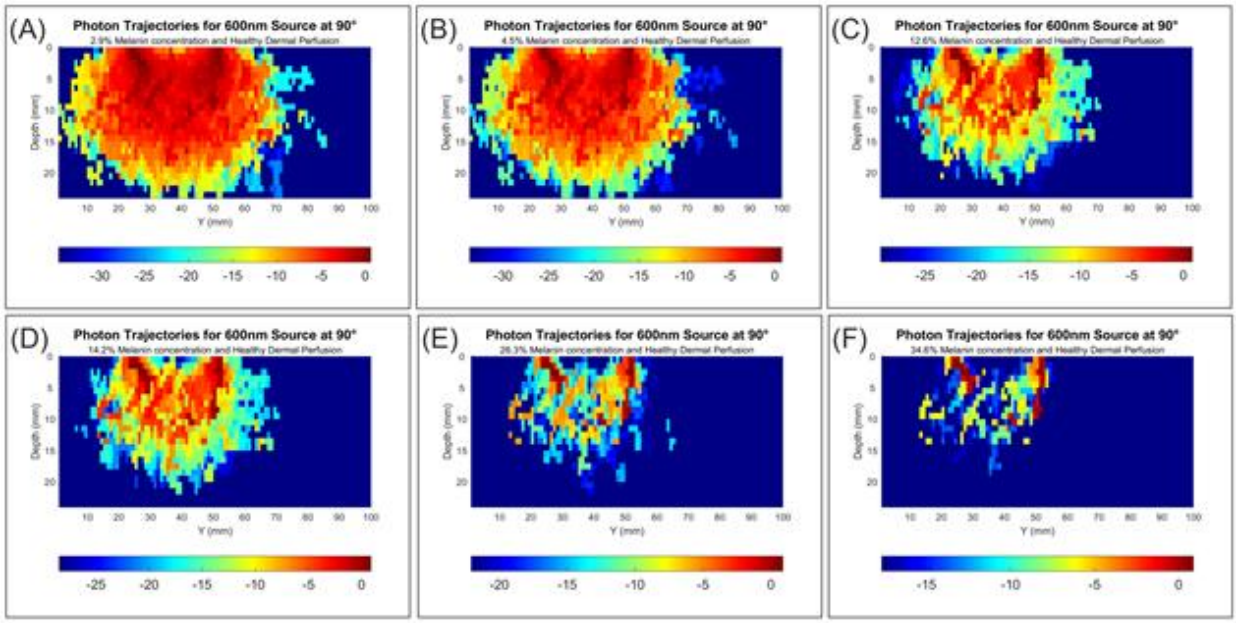

Cross-section of flux distributions of photon trajectories at 600nm and 90° incidence angle. Panels A-F show increasing Fitzpatrick scale pigmentation.

[1] J. Kwasa et al., May 2023, Frontiers in Neuroscience,vol. 17,
[2] Fang, Q. & Boas, D. A. (2009), Optics Express, vol. 17
[3] Meglinski, I.V. and Matcher, S.J., Nov (2002), Physiol Meas, vol. 23(4), pp.741–753.

63

Poster Session, Level 2 Foyer, September 5, 2025, 12:00 - 13:00

Design of an External Insulin Pod Featuring Optimized Delivery, Advanced Storage Capabilities, and Wireless Charging Integration.

Grano De Oro Fernandez J[1], Cano Ferrer X[1], Hussain I[1], Kong W[1], Thukral V[1], Muk-Pavic E[1], Huang J[1]
[1]Mechanical Engineering Department, University College London

Diabetes remains a widespread and pressing global health issue, largely driven by modern sedentary habits and lifestyle choices. This growing concern has spurred significant innovation in treatment strategies around the world \[1]. Among these advancements, insulin pumps have gained prominence for their ability to automate insulin delivery and help regulate blood glucose levels with high accuracy, offering a valuable solution for tailored diabetes management. However, despite improvements in pump design, several limitations persist — notably issues like device overheating and battery wear over time \[1]. This project focuses on refining the performance of a well-known insulin delivery system, the Omnipod Dash, by addressing its current shortcomings through strategic enhancements. Building on the existing platform, the aim is to incorporate advanced functionalities to improve overall reliability and efficiency, contributing to the evolution of more effective, user-friendly diabetes care technologies.

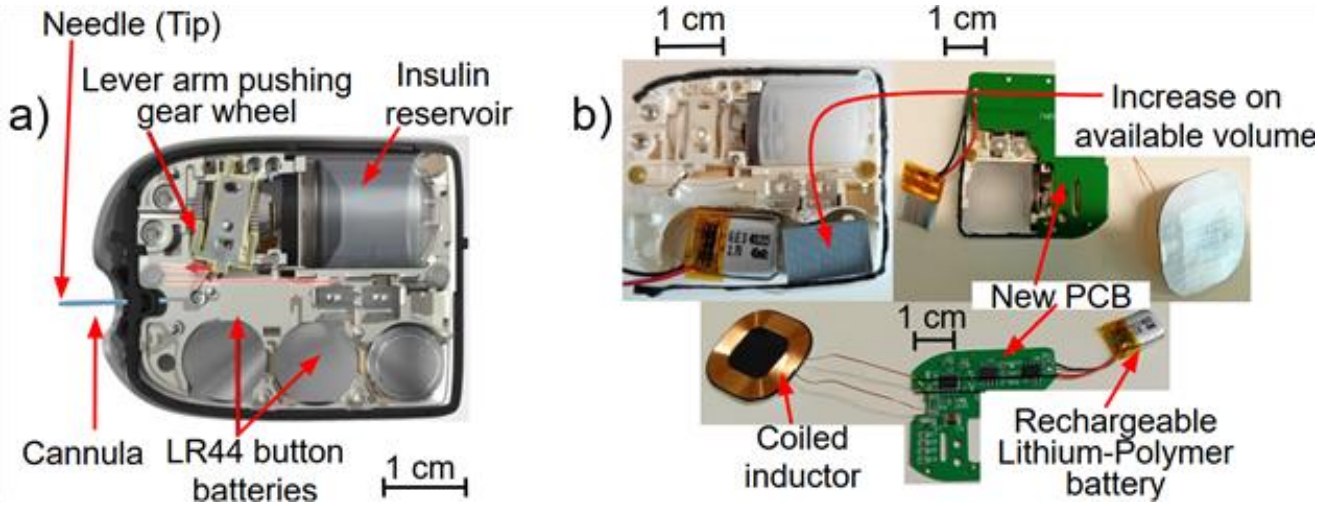

Diagram of the updates in the battery replacement and insulin capacity enhancement. a) Initial device. b) Updated insulin pod.

[1] Berget C, et al., A Clinical Overview of Insulin Pump Therapy for the Management of Diabetes: Past, Present, and Future of Intensive Therapy.

[2] Ly T. T., et al.,“Novel bluetooth-enabled tubeless insulin pump: Innovating pump therapy for patients in the Digital age,” Journal of Diabetes Science and Technology.

65

Poster Session, Level 2 Foyer, September 5, 2025, 12:00 - 13:00

Accuracy Assessment of Low-Cost IMU and Optical Tracking Systems compared to EM for Multimodal Image-Guided Interventions

Martinez Acosta E[1], Tse Z[1]
[1]Queen Mary University Of London

Accurate tracking of surgical instruments and ultrasound probes is essential for image-guided procedures such as liver biopsies and prostate volume estimation. While electromagnetic (EM) tracking systems are highly accurate, their cost is often prohibitive. This study evaluates two low-cost alternatives: Witmotion IMU and ArUco marker. A robotic arm (Uarm Swift Pro, 0.2mm repeatability) and a 3D-printed testbed (0.1mm layer thickness) simulated instrument poses (±90° rotations, ±10 cm translations), shown in figure 1. Results show ArUco markers achieve sub-millimeter positional accuracy (0.15–0.20mm RMSE) under ideal conditions, while the IMU demonstrates angular tracking with a median RMSE of 2.89°. Despite EM tracking's advantage in challenging orientations (0.35° RMSE at 0°), both alternatives offer significant cost reductions. The measured accuracies suggest potential for several clinical applications, (1) In CT-guided liver biopsies, positional errors up to 6.5 mm and angular deviations up to 6.64° still yielded 97.8% diagnostic success[1], (2) Most prostate cancer cases show a negative correlation between prostate size and both incidence and outcome, therefore, the importance of having an accurate and accessible tool for prostate volume estimation[2]. The tracking systems evaluated in this study can potentially enable such measurements through ultrasound probe tracking combined with reconstruction techniques. While environmental factors like lighting (ArUco) and magnetic interference (IMU) require mitigation, these systems may demonstrate sufficient baseline accuracy for procedures where EM tracker costs are prohibitive. Future work will explore hybrid tracking architectures and validate performance in tissue-simulating phantoms, with particular focus on 3D-volume reconstruction applications requiring both positional and angular precision.

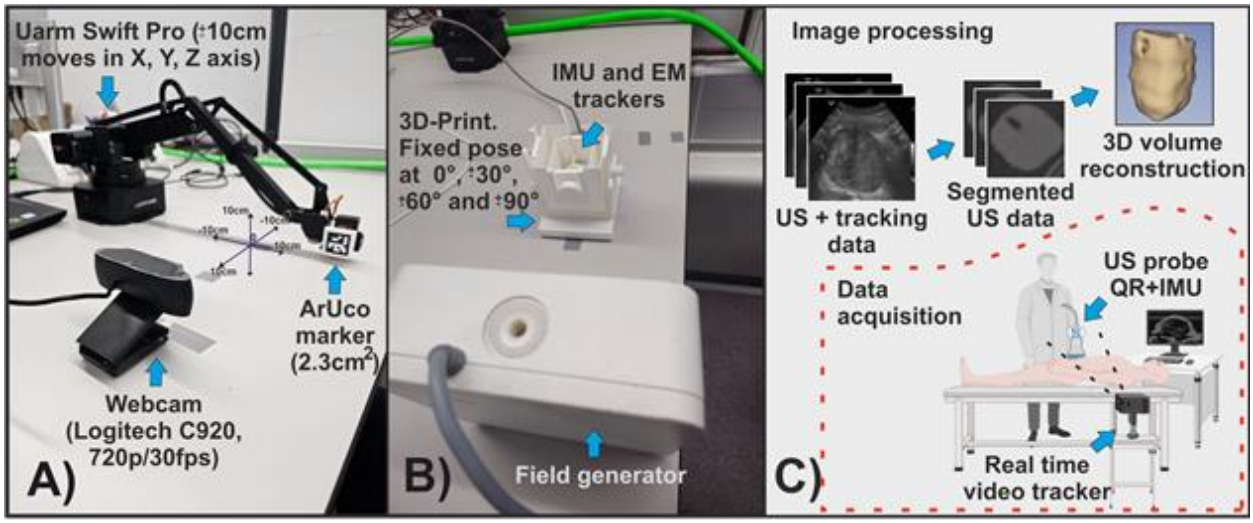

A)Marker tracked in X, Y, Z axis. B)Pose tracking of roll, pitch, yaw. C)Clinical application of the low-cost tracking system.

[1] P. Schullian et al., 2011, Comput. Aided Surg., vol. 16, no. 4, pp. 181–187.
[2] J. R. Yamashiro et al., 2021, Res. Rep. Urol., pp. 749–757.

67

Poster Session, Level 2 Foyer, September 5, 2025, 12:00 - 13:00

A Novel, FSCV-Enabled Microfluidic Chip for Serotonin Detection

Adan N[1]
[1]Imperial College London

Depression is the leading global cause of disability, a crisis only exacerbated in the post-COVID era. Yet, clinical diagnosis remains reliant on subjective questionnaires, and treatment often follows a trial-and-error process using selective serotonin reuptake inhibitors, which frequently show limited efficacy. A critical barrier to progress is the lack of objective biomarkers and reliable tools for antidepressant screening, resulting in stalled pharmaceutical innovation. Serotonin remains a key biomarker in depression research, but its rapid signalling and inaccessibility to direct sampling have hindered its clinical translation. Fast-Scan Cyclic Voltammetry (FSCV), a technique optimised for high-temporal-resolution measurements in animal models, offers new potential when adapted for human-relevant platforms. Using FSCV, the Hashemi lab have answered some important questions about serotonin roles as a biomarker in depression. Now our group wants to translate this finding to human derived models. In recent (unpublished) work, the Hashemi lab have created human derived cerebral spheroids that can release and uptake serotonin as measured with FSCV. The project aims to fabricate a microfluidic chip featuring a gated trap for organoid capture and real-time serotonin detection using carbon fibre microelectrodes. Proof-of-concept FSCV data demonstrates on-chip serotonin sensing, with signal profiles comparable to macro flow cells. While intra-tissue insertion is still under development, future designs aim for reusable, upscaled configurations. This work lays the groundwork for on chip investigations of serotonin human derived systems.

Moncrieff J, Cooper RE, Stockmann T, et al. The serotonin theory of depression: a systematic umbrella review of theevidence. Mol Psychiatry 2022.
Hersey M, Reneaux M, Berger SN, et al. A tale of two transmitters: serotonin and histamine as in vivo biomarkers of chronic stress in mice. J Neuroinflammation 2022;19(1):167

69

Poster Session, Level 2 Foyer, September 5, 2025, 12:00 - 13:00

Investigating the role of Circulating Tumour Cell Softness in Inertial Microfluidic Devices

Hay R[1], Krüger T[1], Papautsky I[2], Zhou J[3], Owen B[1]
[1]University Of Edinburgh, [2]University of Illinois Chicago, [3]Rush University

Circulating tumour cells (CTCs) are cells that break away from the primary tumour, enter the bloodstream and may initiate metastasis. CTCs also act as an early biomarker for cancer detection, having the potential to improve survival rates; however, their rarity in blood makes identification challenging. Inertial microfluidic devices have shown potential in separating a lysed blood sample of CTCs and white blood cells (WBCs), utilizing cell size, with larger cells (CTCs) migrating to the target stream faster [1]. However, the clinical application, such as cell analysis and disease diagnostics, remains limited by a lack of understanding of the underlying physics and the role of cell softness, preventing full separation. In this work we use computer simulations to investigate how the softness of CTCs, a property that can vary depending on the type and stage of cancer, impacts the separation efficiency. Here we show that the softness of the CTC influences not only its own migration behaviour but also the migration behaviour of WBCs into the target stream. Softer CTCs travel farther downstream before entering the target stream, with a higher axial and lower lateral velocity. Additionally, when a stiffer CTC is present, WBCs tend to enter the target stream farther upstream compared to simulations involving soft CTCs. This study highlights the importance of considering cell softness in the design of inertial microfluidic devices for optimised CTC separation in clinical applications.

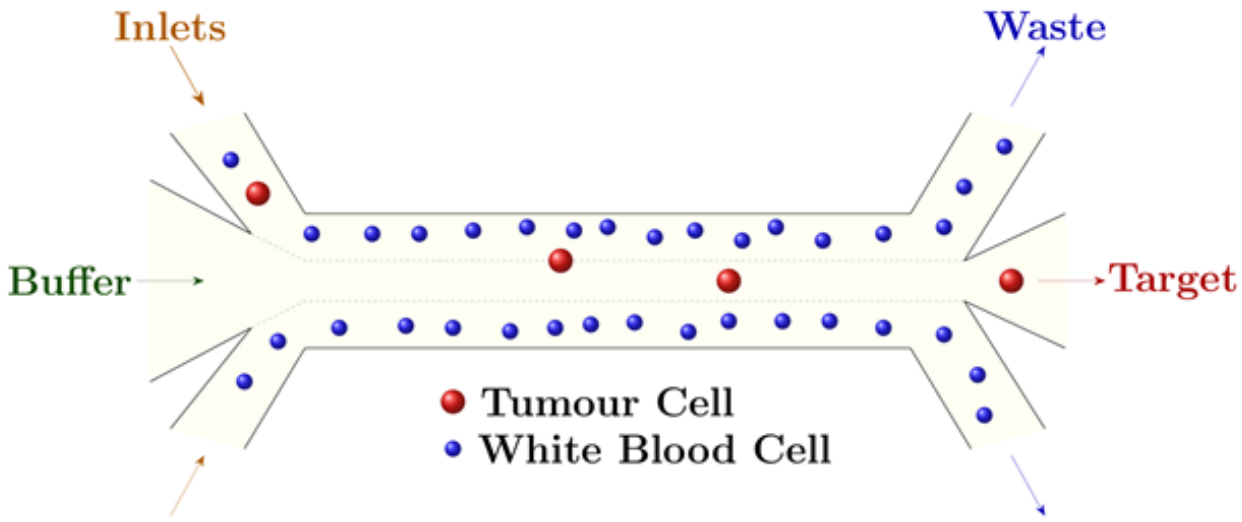

Figure: Inertial Microfluidic Device: blood sample inserted through inlets, CTCs leave via target stream and WBCs leave via waste streams.

[1] Jian Zhou et al., 2019, Microsyst Nanoeng, vol 5, no. 1, pp. 8

Poster Session, Level 2 Foyer, September 5, 2025, 12:00 - 13:00

Development of a Microfluidic Spheroid Platform to model Uterine Fibroids: A Pilot Study

Salvini L[1,2], Paterson K[3], Mellin R[3], Hill C[1,2], Sandison M[4], Zagnoni M[3,5], Hapangama D[1,2]
[1]Department of Women's and Children's Health, Institute of Life Course and Medical Sciences, University of Liverpool, Member of Liverpool Health Partners, [2]Liverpool Women's Hospital NHS Foundation Trust, Member of Liverpool Health Partners, [3]ScreenIn3D Limited, [4]Department of Biomedical Engineering, University of Strathclyde, Wolfson Centre, [5]Department of Electronic and Electrical Engineering, Centre for Microsystems & Photonics, University of Strathclyde

Uterine fibroids are benign smooth muscle tumours of the uterus affecting up to 70% of women of reproductive age [1]. They can cause heavy menstrual bleeding, symptoms related to pressure on adjacent organs, and infertility, significantly impacting quality of life. Despite their prevalence, the mechanisms underpinning fibroid growth and symptom variability remain unclear [2]. Current treatment options are limited, with hysterectomy as the gold standard—a procedure that permanently eliminates an individual's fertility potential. There is a critical need for physiologically relevant in vitro models to investigate fibroid biology and support preclinical drug testing and personalised medicine for this patient population. This pilot study developed a microfluidic-based 3D culture platform to grow spheroids from patient-derived fibroid tissue. Primary fibroid cells from six patients formed viable spheroids across all samples, with patient-to-patient variability observed in spheroid size and morphology. A positive correlation was noted between seeding density and spheroid area. Immunofluorescence confirmed the presence of smooth muscle cells (Calponin-positive) and immune cells (CD45-positive), while endothelial cells (CD31-positive) were not detected within the spheroids. To assess drug permeability and cytotoxicity, spheroids were exposed to three agents—Cisplatin, Staurosporine, and Puromycin—at a concentration of 10 µM. All drugs infiltrated the 3D structures and induced apoptosis, demonstrating the model's potential for therapeutic screening. This microfluidic spheroid model offers a miniaturised platform for studying fibroid pathophysiology and testing fertility-preserving treatments in a controlled, patient-specific context. Further optimisation and expansion of this platform could enhance understanding of fibroid heterogeneity and support the development of targeted interventions.

1. Stewart EA, Laughlin-Tommaso SK, Catherino WH, Lalitkumar S, Gupta D, Vollenhoven B. Uterine fibroids. Nat Rev Dis Primers. 2016 Jun 23;2(1):1–18.

2. Giuliani E, As-Sanie S, Marsh EE. Epidemiology and management of uterine fibroids. International Journal of Gynecology & Obstetrics. 2020;149(1):3–9.

73

Poster Session, Level 2 Foyer, September 5, 2025, 12:00 - 13:00

Development and Characterisation of an on-chip Glioma outgrowth model

Daoud J[1], Chapman C[1]
[1]Queen Mary University Of London

Tumour recurrence in high-grade gliomas, such as glioblastoma, is widespread due to the challenges associated with complete surgical removal. 95% of tumours recur within 2 cm of the surgical resection margin [1]. Current clinical measurement techniques do not accurately capture cell state during the critical stages of adjuvant therapies. The development of an on-chip model for glioma recurrence has the potential to facilitate fundamental understanding at a cellular level, as well as form the foundation of a patient specific predictive model. The aim of this work was to develop the foundation of an on-chip neural model for measuring glioma interactions with healthy neural tissue. After developing a single channel multi-well microfluidic system, 9L/lacZ (rat glioma) cells were combined with healthy primary rat astrocytes to form an initial measure of cancer incurrence. Quantitative image analysis demonstrated significantly increased initial outgrowth of glioma cells from the tumour spheroid and a sustained increase in spheroid volume. These findings align with existing results suggesting that astrocytes can add to a supportive environment for glioma cells and promote growth. Overall, this work supports the use of on-chip platforms to investigate cancer cell invasion, and offers a simple model which permits the addition of further complexities in the future.

[1] - De Bonis, P., Anile, C., Pompucci, A. et al. (2013). The influence of surgery on recurrence pattern of glioblastoma. Clinical neurology and neurosurgery, 115(1), 37-43.

Poster Session, Level 2 Foyer, September 5, 2025, 12:00 - 13:00

Reconfigurable Acoustofluidic Devices

Shaw D[1], Reid A[1], Witte K[1], Fazio M[1], McKinlay M[2], Nunez C[2], Gibson D[3]
[1]University Of Strathclyde, [2]University of Glasgow, [3]University of the West of Scotland

Acoustofluidic devices using Surface Acoustic Waves (SAWs) offer precise microparticle control [1]. Traditional SAW devices are limited to single frequencies and modes due to fixed Interdigitated Transducers (IDTs) and substrate properties [2]. This restricts their use in diverse acoustofluidic applications. This work presents the first reconfigurable acoustofluidic platform using Flexible Printed Circuit Board- Interdigitated Transducers (FPCB-IDTs) on c-axis tilted Zinc Oxide (ZnO), enabling user-selected SAW parameters for varied microfluidic tasks. C-axis tilted ZnO thin films, enabling dual-SAW-mode (Rayleigh and Shear-Horizontal) generation, are fabricated on glass via Glancing Angle Deposition. Modular FPCB IDTs (400, 320 and 200µm wavelengths) enable frequency selection (Figure (a)). IDT performance is measured via Vector Network Analyser. C-axis tilted ZnO films (α = 80°) were interfaced with FPCB-IDTs. S11 analysis identified detectible reflection minima specific to the ZnO devices. These signals occurring at frequencies indicative of Rayleigh mode SAWs (7.9MHz for 400µm, 9.8MHz for 320µm, 15.7MHz for 200µm) yielding a consistent phase velocity ~3145m/s and Shear horizontal mode (14.5MHz for 400µm, 18.5MHz for 320µm, 28.6MHz for 200µm) with a phase velocity ~5810m/s (Figure (b)). These velocities agree well with theoretical predictions. These findings validate frequency selectable SAW generation on tilted ZnO, paving the way for versatile acoustofluidic applications and contributing to the development of next-generation lab-on-a-chip technologies.

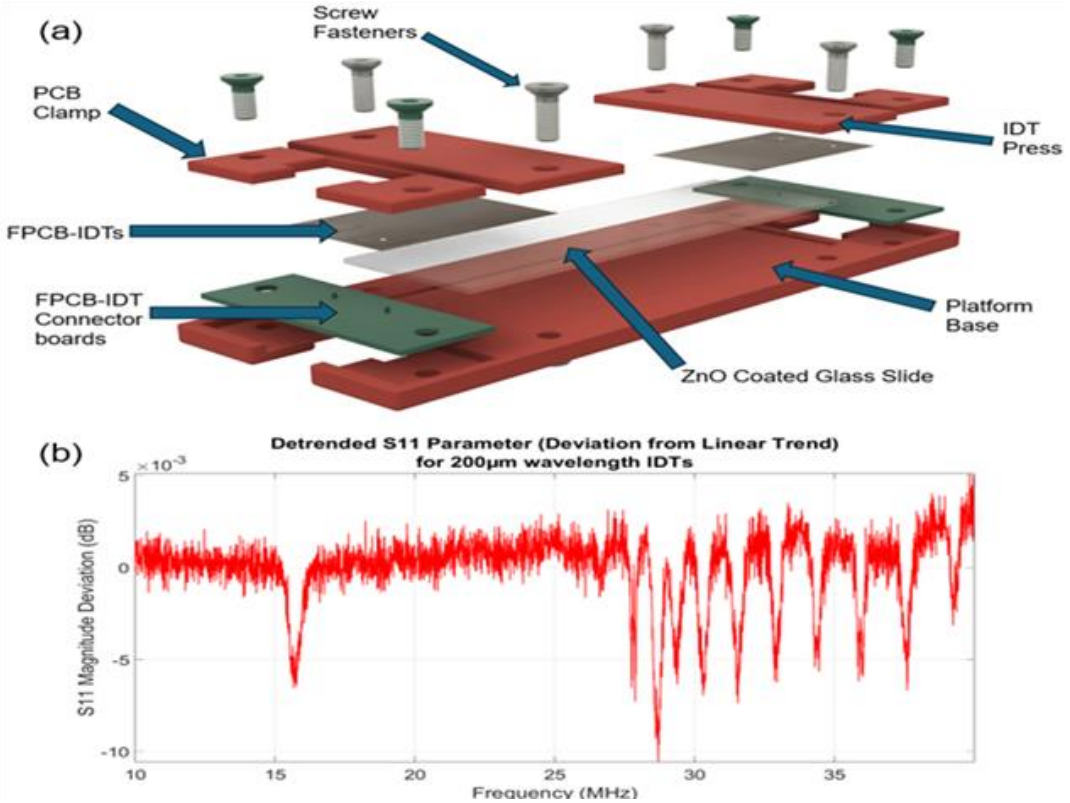

Figure: (a) Exploded view of Reconfigurable Acoustofluidic Platform. (b) Experimental S11 reflection minima (detrended) for a 200µm wavelength FPCB-IDTs

[1] WU, M. et al. 2019. Acoustofluidic separation of cells and particles. Microsyst Nanoeng, 5, 32.
[2] DU, X.et al. 2009. Microfluidic pumps employing surface acoustic waves generated in ZnO thin films. Journal of Applied Physics, 105, 024508.

77

Poster Session, Level 2 Foyer, September 5, 2025, 12:00 - 13:00

Towards an ISO standard for pin-lock prosthetic suspension systems: Considering realistic and imperfect use.

Clark A[1], Favier C[1], Bull A[1]
[1]Imperial College London

Pin-lock suspension systems are a high-volume prosthetic component, being a popular choice by clinicians for providing a simple, secure, and stable connection between the prosthesis and residuum in modern liner-based prostheses [1]. While load-bearing prosthetic devices (such as sockets, knees, and feet) are evaluated through international standards ISO 10328 and 22675 on prosthesis structural testing, suspension systems are not subject to such standards as they are outside the loading path. In addition, no standard currently exists for evaluating their general wear during their lifetime, and how this wear may affect performance and function. This is vital to understand, as it is well documented how prosthesis wear at the interface can result in common skin problems, [2], compensatory movements, and musculoskeletal conditions [3]. To address this, this project introduces methods for simulating a typical lifecycle of pin-lock devices, particularly wear of the locking mechanism and misalignment of the pin, with the aim of understanding how this wear affects function. 10,000 engagement/disengagement cycles were selected based on previous literature to represent a 5-year prosthesis lifetime (equivalent to 5+ don/doffs per day). Mechanism wear was evaluated for a shuttle lock (3rd Generation Genesis A, Bulldog Tools) and a custom smooth lock. Misalignment wear was evaluated with a 20mm pin offset against the interface guide for a selection of popular materials (PLA, PETG, PC-Blend, and Onyx®). Results demonstrated minor egging and material wear with perfect use, whereas misalignment showed significant material wear, suggesting such methods could be applied to other, yet untested, prosthetic components.

[1] K. Friel, 2005, JAAOS, vol. 13, no. 5, pp. 326-335.
[2] M. S. Keszler et al., 2019. Physical Medicine and Rehabilitation Clinics, vol. 30, no. 2, pp. 423-437.
[3] A. D. Knight et al., 2021. Adv. Wound Care, vol. 10, no. 12, pp. 671-684.

79

Poster Session, Level 2 Foyer, September 5, 2025, 12:00 - 13:00

Physiological Tension Preserves Langerhans Cell Naïve Morphology and Functionality in Human Ex Vivo Skin Explants

Hickerson R[1], Grusso D[1], Tsutsumi S[1], Campbell P[2], Conneely M[1]
[1]Ten Bio Ltd, James Hutton Institute, [2]Carnegie Physics Laboratory, University of Dundee

As the demand for human-relevant test systems grows, driven largely by ethical imperatives and the poor clinical translation of animal models, ex vivo human skin has emerged as a promising solution. Yet, upon excision, skin rapidly loses its in vivo mechanical tension, leading to contraction, altered microarchitecture, and impaired immune function. To address this, we developed a culture platform that restores physiological tension to full-thickness human skin, preserving its native structure and extending functional viability. The integrity of this new explant platform has already proven useful for preclinical assessment of chemexfoliation agents [1]. Here, we demonstrate that this same tensioned culture platform significantly enhances the retention and functionality of Langerhans cells (LCs), a key resident immune population. Using an optimized whole-tissue clearing and imaging protocol (iDISCO), LCs were visualized and quantified across extended timepoints. Tensioned skin retained significantly more langerin-positive cells than untensioned controls after 7 days and preserved dendritic morphology, the signature association with an immunocompetent state. Importantly, LC responsiveness to the contact sensitizer oxazolone was maintained over time, confirming the model's suitability for immunotoxicological testing. The explant model's generality and reproducibility make it a powerful tool for studying skin immunobiology, evaluating allergenicity, and screening immunomodulators or therapeutics. To summarise, by preserving skin's biomechanical context, this platform offers a more faithful representation of human in vivo responses than standard culture systems, supporting regulatory demand and translational applications.

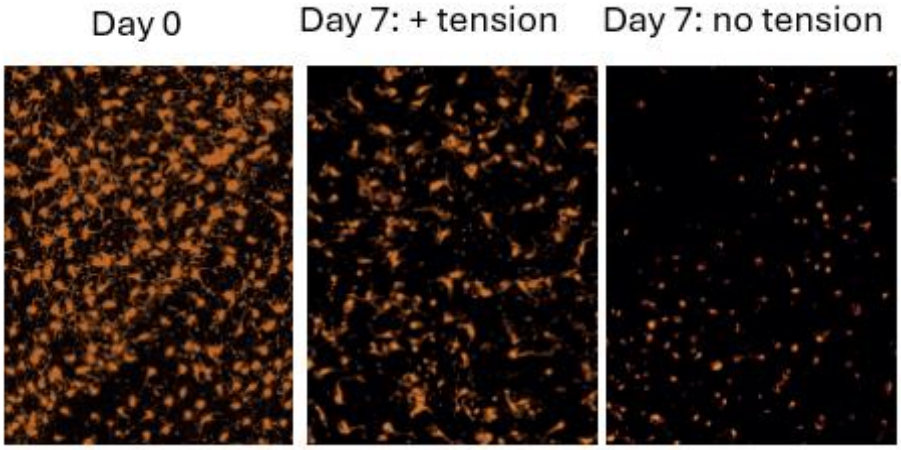

Langerhans Cells were stained (anti-langerin)

in skin cultured with and without tension for periods up to 7 days.

[1] A tensioned human skin explant model used for preliminary assessment of chemexfoliant-stimulated bioeffects
MJ Conneely, Jin Namkoong, F Allison, K Tsutsumi, D Grussu, R Willis, K Henderson, PA Campbell, J Wu, & RP Hickerson
Journal of Investigative Dermatology: Innovations 5 (1), 100305 (2025)

81

Poster Session, Level 2 Foyer, September 5, 2025, 12:00 - 13:00

Development of a Human Cerebral Microvascular Model to Investigate the Biomechanical Influence of Clotting on Angiogenesis

Eastham S[1], Wu J[1], Carswell H[1], McConnell G[1]
[1]University Of Strathclyde

With over 100,000 people admitted to hospital each year, ischaemic stroke is a leading cause of death and disability in the UK. However, only 10% of patients are eligible for surgical intervention, causing clinicians to rely on thrombolytics to dissolve clots [1]. Angiogenesis, the formation of new blood vessels from existing vasculature, is a key restorative process post-stroke, yet angiogenic mechanisms in the ischaemic brain remain under-researched [2]. Elucidating angiogenic effects on blood-brain barrier (BBB) permeability in response to clot stiffness could clarify the potentially dual nature of angiogenesis. However, experiments conducted in rodent models are difficult to translate from bench to clinic, necessitating the development of novel human models [3]. Hydrogels are a popular biomaterial for engineering 3-dimensional tissue analogues due to their high water content, structural similarity to the native extracellular matrix, and customisable polymer organisation. It is hypothesised that in this study, the clot analogue's high stiffness will drive angiogenesis beyond a restorative function and impede neural recovery. This research aims to (i) measure rodent clot mechanics for stiffness-matching purposes, (ii) model the BBB in vitro using human umbilical vein endothelial cells (HUVECs), astrocytes, and pericytes encapsulated within a tissue-matched collagen hydrogel, (iii) introduce a clot analogue using fibrin hydrogels, and (iv) investigate changes in microvessel permeability. Results from this study could support investigation into anti-angiogenic therapeutic strategies and the quick removal of clots. Additionally, confirmation of a dynamic in vitro human BBB model would promote further investigations to confirm the model's efficacy and reduce animal use.

[1] A. Patel, et al., 2020, Age and Ageing, vol. 49, no. 2, pp. 270—276.
[2] J.F. Arenillas, et al., 2007, Curr Treat Options Cardio Med 9, pp. 205–212.
[3] J.M. Wasielewska, et al., 2020, Alzheimer's Disease: Drug Discovery, chap. 7, pp. 117—134. Exon Publications eBooks.

Poster Session, Level 2 Foyer, September 5, 2025, 12:00 - 13:00

Assessing attenuation curve compliance in off-the-shelf sound spatialisation methods for sound localisation testing

Domniteanu A[1], Gallacher J[2], Giardini M[3]
[1]University Of Strathclyde, [2]AA Scottish Cochlear Implant Programme, [3]University of Dundee

Powerful sound spatialisation engines offer immersive gaming experiences [1,2] but it is unclear if they are suited for clinical sound localisation testing [3]. We assessed if the attenuation of sound from off-the-shelf sound spatialisation engines was consistent. Unreal Engine (UE5) was used to virtually record 250Hz, 4KHz and 8KHz pure tones played through a virtual speaker. Recordings were taken at 0.001m, 0.05m, 1m, 2m, 3m, 4m, 5m, 10m and 15m. The audio was spatialized using: built-in (UE5 Panning), plugins (Steam Audio, Google Resonance, Project Acoustics) and middleware (Wwise, FMOD Studio). We applied distance-based attenuation only, in a 0.1cm – 25m range. Inverse square law attenuation was applied for all implementations, except for Google Resonance, where logarithmic attenuation was used. We captured audio using Audacity and loopback on a Behringer U-PHORIA UMC404HD audio interface at 96kHz. The average power of the signals was calculated at each distance and attenuation functions were plotted. The attenuation of the three pure tones was then compared for each implementation. UE5 Panning and Wwise showed no difference in attenuation. FMOD attenuated the 8kHz signal slightly faster compared to the others. The three plugin implementations attenuated the three signals at different rates, suggesting built-in frequency dependence that may affect sound localisation assessment in unexpected ways, especially when using complex signals (Speech). We expected no attenuation differences between the three signals. The presence of this difference is undesirable and is evidence of an uncontrollable simulation parameter. The effects of this phenomenon on human perception must be investigated.

[1] K. Rogers et al., 2018, In proceedings of 2018 CHI Conference on Human Factors in Computing Systems, pp.1-13.
[2] R.W. Lindeman et al., 2012, In proceedings of 2012 ISMAR - ARTS, MEDIA, AND HUMANITIES. pp. 93-94
[3] Kitterick PT et al., 2011, Cochlear Implants Int., vol.12, no.3, pp. 164-169.

Poster Session, Level 2 Foyer, September 5, 2025, 12:00 - 13:00

Engineering a Head-Mounted Device for Real-Time Navigation Assistance for the Visually Impaired

Al Maraashli M[1], Youseffi D[1], Rasheed M[1], Sefat D[1]
[1]University Of Bradford

People with visual impairments face daily challenges in navigation and spatial awareness. Often relying on white canes or guide dogs to help them. This work designed and manufactured a special device (Figure 1) worn on the head that uses Time-of-Flight (ToF) sensors to find obstacles nearby instantly, giving haptic feedback to the person using it. The device uses three ToF sensors that are angled to cover a wide field of view of which makes it possible to spot obstacles as far as 4 meters away.
The sensors gather depth information which then is handled by a microprocessor. It is translated into haptic feedback using small coin vibration motors. The strength of the vibrations increases as obstacles get closer, making sure the response feels natural for users. A lightweight 3D-printed frame protects and covers the sensors, motors, and electronics, ensuring it is comfortable and easy to carry for users and it runs on a rechargeable lithium-polymer battery that allows several hours of nonstop usage.
Testing results showed high accuracy, staying within ±1 cm error margin. This confirms the system works well for finding obstacles. If compared to other visual aid devices, the device lets the user to be hands-free and quickly aware of objects close by, hence reducing dependency on physical navigation tools. Future works may include AI-based object recognition and machine learning to make it more adaptable.
This work shows the potential use of assistive technology, giving new solution to help improve independent movement for people with poor vision.

Figure 1: Head-Mounted Device for Real-Time Navigation Assistance for the Visually Impaired.

References

Lee, T. (2022). Time-of-Flight Sensor Overview | Mouser. [online] Mouser.co.uk. Available at: https://www.mouser.co.uk/applications/time-of-flight-sensor-overview/.
World Health Organization (2023). Blindness and vision impairment. [online] World Health Organization. Available at: https://www.who.int/news-room/fact-sheets/detail/blindness-and-visual-impairment.

87

Poster Session, Level 2 Foyer, September 5, 2025, 12:00 - 13:00

Smart Monitoring of Respiratory Health: An IoT Wearable Approach

Jia Z[1]
[1]Queen Mary University Of London

Chronic respiratory diseases (CRDs), such as asthma and chronic obstructive pulmonary disease (COPD), are among the leading causes of morbidity and mortality worldwide, contributing to over 3 million deaths annually according to the World Health Organization [1]. In the UK, CRDs are the third most common cause of death and present a growing challenge due to aging populations, environmental factors, and increasing prevalence. These conditions place a significant and sustained burden on healthcare systems, requiring frequent clinical monitoring and long-term management strategies. To address these challenges, this research proposes an IoT-based wearable system designed for continuous respiratory monitoring using widely accessible smartphone technology. The system utilizes inertial measurement units (IMUs), specifically accelerometers and gyroscopes, to capture thoracic movement associated with breathing and heart rate. Advanced signal processing techniques, including low-pass filtering and infinite impulse response (IIR) filtering, are applied to mitigate motion artifacts and enhance signal clarity. A personalized calibration mechanism is incorporated to address variability in breathing patterns due to individual physiological differences such as gender and body type. The device is intended to support early diagnosis, real-time symptom tracking, and rehabilitation, enabling patients to manage their respiratory conditions more effectively from home. By reducing the dependence on hospital-based monitoring and offering a scalable, cost-efficient solution, this system has the potential to alleviate clinical workloads and improve long-term health outcomes for individuals with chronic respiratory diseases.

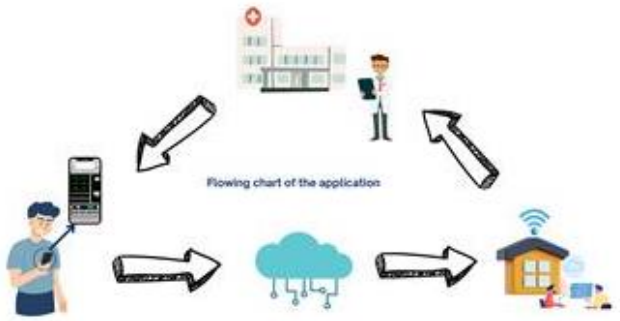

[1] "Global Burden of Chronic Respiratory Diseases," Journal of Aerosol Medicine and Pulmonary Drug Delivery, vol. 33, no. 4, pp. 171-177, 2020, doi: 10.1089/jamp.2019.1576.

BioMedEng25

University of Strathclyde, Glasgow

4th-5th September 2025